Brachypodium distachyon as a model to understand resistance to wheat root diseases

Miguel Ângelo Costa e Silva dos Santos

Doctor of Philosophy (PhD)

University of East Anglia (UEA)

Department of Crop Genetics, John Innes Centre

May 2021

Abstract

The cultivation of wheat is an ever-increasing priority for the sustainability of food production worldwide, yet wheat is susceptible to various pathogens leading to considerable yield loss. Numerous studies have been performed to combine sources of resistance to these diseases without affecting yield. Most studies, however, are performed on visual infection phenotypes on aerial parts of plants, with considerable lack of disease studies on underground soil-borne diseases, like take-all and *Fusarium* root rot (FRR). Most wheat cultivars are considered susceptible to these diseases, with low differential in response. This factor combined with the high incidence of gene redundancy due to wheat's hexaploid genome, have resulted in a lack of knowledge on the genetic basis of resistance to root diseases of wheat.

The purpose of this project was to further examine the model plant *Brachypodium distachyon* (*Bd*) to understand resistance to root diseases and identify potential resistance / susceptibility genes that play a significant role in response to FRR and take-all. The use of different *Bd* accessions lines, part of the recently re-sequenced *Bd* pangenome were used to examine responses to both diseases. A QTL analysis was performed in parent accessions of already developed *Bd* populations with promising resistance differential to FRR and *Fusarium* overall seedling death, demonstrating a novel source of resistance originating from chromosome 1 of *Bd*.

A series of RNA-seq experiments were also conducted to characterize the response of susceptible line Bd21, to low concentrations of deoxynivalenol (DON) and reactive oxygen species (ROS). The results enabled definition of DON and DON-mediated ROS expression profiles within the plant in a non-toxic background. A characterisation of candidate genes involved in response to FRR and take-all was also performed, making use of *Brachypodium* T-DNA mutant lines, along with wheat Kronos TILLING mutant lines, establishing a model-to-crop system between *Bd* and wheat.

Acknowledgements

The funding for this project was provided under the CerealPath doctoral programme from the European Union's Horizon 2020 research and innovation programme under the Marie Skłodowska-Curie grant agreement No. 674964. The host institution included the John Innes Centre, the University of East Anglia and University College Dublin.

I would like to thank my supervisor Paul Nicholson, for all the guidance and moral support provide through the entire PhD project. If it was not for his patience and sense of humour, along with his high knowledge of current practices in science, this project would have able to reach the level that it did. I would also like to thank the other members of my supervisory team, James Brown and Marianna Pasquariello, which provided invaluable knowledge for the understanding of complex and challenging scientific problems this project came across. Thirdly, I would like to thank Harriet Benbow, Alexandre Perochon and Fiona Doohan for hosting me during my placement in Dublin, and all the valuable help in the bioinformatic analyses of the different RNAseq data of *Brachypodium* and wheat response to DON and ROS.

I would also like to thank Andrew Steed and Lola González Penadés for their continuous assistance during the development of this thesis, especially in the role they played in the production of Kronos double mutants and the wheat RNA-seq data to low concentrations of DON, respectively. Other contributions to these projects were provided by Rachel Goddard in the analyses of the QTL data; Jan Bettgenhaeuser, Phon Green and Mathew Moscou in providing the Luc1xJer1, Luc1xFoz1 and ABR6xBd21 populations and its corresponding genetic and physical maps; Vanessa McMillan and Kim Hammond-Kosack for the two additional isolates of take-all; Philippe Vain and Vera Thole for the *Brachypodium* T-DNA mutants; Paul Brett for the metabolomic analyses of the 9- and 13-HODE metabolites; and finally to the John Innes horticultural services and scientific computing team for the maintenance of plant material and bioinformatic resources.

Lastly, I would like to thank the remaining members of the Nicholson and Brown groups, my CerealPath colleagues, my friends, and my family, to the continuous friendship and moral support provided during the development of this PhD. Special thanks go to my *Brachypodium* comrades in arms, recently made Doctor John Haidoulis and Doctor Elizabeth Bankes-Jones, for always being there in the worst and best moments of our *Brachypodium* saga. Another special thanks goes to my close CerealPath colleagues: Doctor Cyrielle Ndougonna, a remarkable friend which I shared most of my PhD happiest and most difficult moments; a person who provided immeasurable help during the development of my work, and a work companion throughout most of my CerealPath journey. To Doctor Ngonidzashe “Ngoni” Kangara, a friend that was able to dispel most of the dark moments and situations with a funny remark or an optimistic view. Doctor Silvia Zanini, a powerful force of humour and sarcasm that was most welcome during our little trips abroad. Doctor Karolina Slominska-Durdasiak, a contrasting force to Zanini, providing reason and discipline to our little mischiefs. And last of all, but not the least, to Doctor Markus Kolodziej, “mother duck”, for being able to organise and guide us during our CerealPath commitments and travels from beginning to end.

Abbreviations

ABC	ATP-binding cassette
ANOVA	analysis of variance
ATP	adenosine triphosphate
AUDPC	area under the disease progression curve
Bd	*Brachypodium distachyon*
BLAST	basic local alignment search tool
bp	base pair(s)
Brachypan	*Brachypodium distachyon* pan-genome
cDNA	complementary DNA
CIM	composite interval mapping
cm	centimetre(s)
DON-3-G	DON-3-O-glucoside
DEG	differential expressed gene(s)
dH_2O	deionised water
DNA	deoxyribonucleic acid
DON	deoxynivalenol
dpi	day(s) post inoculation
dps	day(s) post stratification
EDTA	ethylenediaminetetraacetic acid
EMS	ethyl methanesulfonate
Fc	*Fusarium culmorum*
FCR	*Fusarium* crown rot
Fg	*Fusarium graminearum*
FHB	*Fusarium* head blight
FRR	*Fusarium* root rot
Gbp	giga base pair(s)
Ggt	*Gaeumannomyces graminis* var. *tritici*
GO	gene ontology
GST	glutathione S-transferase
h	hour(s)
H_2O_2	hydrogen peroxide
HODE	hydroxyoctadecadienoic acid
Hz	hertz
JA	jasmonic acid
JA-Ile	jasmonoyl-isoleucine

KASP	kompetitive allele specific PCR
L	litre(s)
LC-MS	liquid chromatography – mass spectrometry
LOX	lipoxygenase
LRR	leucine rich repeat
M	molar(s)
MBF	multiprotein bridging factor
Mbp	mega base pair(s)
mg	milligram(s)
min	minute(s)
mL	millilitre(s)
mM	millimolar(s)
mRNA	messenger RNA
nM	nanomolar(s)
$O_2^{\cdot -}$	superoxide
PAMP	pathogen-associated molecular pattern
PCD	programmed cell death
PCR	polymerase chain reaction
PDA	potato dextrose agar
pH	potential of hydrogen
QTL	quantitative trait locus
REML	linear mixed model
RNA	ribonucleic acid
RNA-seq	RNA sequencing
ROS	reactive oxygen species
rRNA	ribosomal RNA
s	second(s)
SA	salicylic acid
SDS	sodium dodecyl sulfate
SIM	simple interval mapping
SNP	single-nucleotide polymorphism
TAB	Take-all inoculum build-up
TAD	Take-all decline
TILLING	targeted induced local lesions in genomes
Tris-HCl	trisaminomethane hydrochloride
tRNA	transfer RNA

U	area under the LC-MS peak measurement
UDP	uridine diphosphate
UGT	UDP-glucosyltransferases
v/v	volume per volume
VIGS	virus induced gene silencing
w/v	weight by volume
wt	wild type
x g	times gravity
%	percentage
°C	degree(s) centigrade
µL	microlitre(s)
µM	micromolar(s)

Contents

List of Tables

List of Figures

Chapter 1. General Introduction

1.1 Importance and genetic background of wheat

Cereal crops are one of the most important food supplies in the world, where maize, rice and wheat represent the largest food source for the human population. Wheat alone can reach a yearly average production of about 582.7 million tons from 213.8 million hectares where the prediction for the year 2020 has already exceeded the average amount by summing up to 761.5 million tons (From the statistics of Food and Agriculture Organization: http://www.fao.org/worldfoodsituation/csdb/). This demonstrates the global increase in demand for wheat and the need to protect it against devastating environmental and biological stresses, such as viral, bacterial and fungal diseases and herbivores. Wheat can be separated in two main categories, one is bread wheat or common wheat (*Triticum aestivum*), the most produced wheat category, being used in the production of most bread and biscuit based products. The second is durum wheat (*Triticum turgidum* ssp. *durum*) which is mainly used in the production of pasta. The main difference between the two is the nature of their genomes as durum wheat is tetraploid (AB genome) and bread wheat is hexaploid (ABD genome). When compared, for example, to model plant system *Arabidopsis thaliana* with a genome size around 0.13 Gbp (https://www.arabidopsis.org), or even the human genome with a size around 3 Gbp (https://www.genome.gov), the genomes of both species of wheat are considerably bigger, with *Triticum aestivum* having a total genome size around 17 Gbp (Brenchley et al. 2012), followed by *Triticum turgidum* with a genome size around 12 Gbp. Both types of wheat originated from the same region referred to as the Fertile Crescent and were created through hybridisation events that occurred between their common ancestors. The first hybridisation event occurred between *Triticum urartu* (the ancestor of the AA genome) and a close relative of *Aegilops speltoides*, believed now to be extinct, as the ancestor of the BB genome. This produced the tetraploid *Triticum turgidum* (AABB), which is commonly referred as emmer wheat. The wild emmer wheat (*Triticum turgidum* ssp. *dicoccoides*) underwent a further hybridization event around 30 000 years ago with *Aegilops tauschii* (the ancestor of the DD

genome), resulting in the hexaploid ancestor of bread wheat *Triticum aestivum* (AABBDD). Both the wild emmer wheat and ancestor of bread wheat were subsequently domesticated by humans around 10 000 years ago, to produce the contemporary tetraploids *Triticum turgidum* ssp. *dicoccum* and durum wheat *Triticum turgidum* ssp. *durum* (ancestors of *Triticum turgidum* ssp. *dicoccoides)* and all the different cultivars of hexaploid bread wheat commonly used nowadays (Heslop-Harrison 2001). Although originating from different species, the similarity between their individual ABD chromosome sets (homoeologous genomes) is very close. It has been predicted that around 95% to 99% from the coding regions of each sub genome are similar between each other, where normally one gene is represented with two to three copies depending on the ploidy of the wheat species (Krasileva et al. 2013). So far most of the gene copies are commonly reported as redundant to each other, but during the domestication event these three copies could have evolved to work in distinct ways, specializing to a specific environment or condition, working with each other to make a dose gradient effect, or suffering an entire sub functionalization (Borrill, Adamski, and Uauy 2015). The overall genome is also rich in repetitive DNA sequences, making it difficult to reconstruct the genome using normal sequencing techniques that require the chromosomes to be fragmented. With the difficulty in sequencing the genome, and the complexity attributed to the redundancy and specialization of most genes, it is a relatively difficult process to study the genetics of the wheat genome. Even though the process is complex, a lot of advances have been made in trying to refine the genome complexity and identify the location and function of wheat genes. The first big genome analysis of wheat was carried out in the hexaploid wheat variety Chinese Spring by the Earlham Institute (Clavijo et al. 2017), later being replaced by the most recent genome assembly by the International Wheat Genome Sequencing Consortium (IWGSC) (IWGSC 2018). The latest instalment, as per the submission of this work, is the second version of their reference sequence, comprising an estimated coverage of 94% of the genome with a total of 107,891 high-confidence protein-coding genes, divided in different tissues and developmental stages in order to create different co-expression networks (Zhu et al. 2021).

1.2 Root pathogens of wheat

Understanding the wheat genome is a pre-requisite to revealing how wheat responds to its surroundings. With the human population of the planet continuing to grow, the demand for food, especially wheat is continuously rising. Unfortunately, along with the increase in wheat production a rise in adversities has also been observed, namely the numerous abiotic and biotic stresses that wheat is subjected too. A lot of work has been undertaken to develop tolerance in wheat to osmotic and salt stress, and resistance to numerous diseases and herbivores. Among the major diseases in wheat, one of the potentially most devastating is *Fusarium* Head Blight (FHB), most commonly caused by *Fusarium graminearum* (*Fg*) and *Fusarium culmorum* (*Fc*). Along with FHB a number of different diseases contribute to the huge yield loss reported each year for wheat. These include the different rust diseases (yellow, brown and stem rust), powdery mildew and more recently wheat blast (Figueroa, Hammond-Kosack, and Solomon 2018). The association made between the impact of these diseases of foliar and floral tissues and the yield loss comes mainly from the capability of farmers and breeders alike to be able to visualize, differentiate and quantify the different diseases in the field. This is mainly due to the development of the disease in the head and leaves of the wheat, where the effects of the fungi are easily observed. However, it is important to note that some of the most destructive diseases of wheat and other crops are invisible to the growers until it is too late. These diseases develop below ground where they affect the root system of the plant and can spread through the field and cause severe developmental impairments to the growth of wheat and grain formation.

There are many types of root diseases, with several coexisting in the same field. The most common ones of wheat and barley comprise of Pythium root rot (PRR), Rhizoctonia root rot (RRR), *Fusarium* root rot (FRR) and take-all (Cook 2007). The thesis will mainly focus on the take-all and FRR diseases in cereals, with the characterization of each disease being carried out in more detail further in the introduction and the following chapters. Pythium root rot has a variety of hosts, and it is generally associated with soils with poor drainage allowing

the accumulation of considerable amounts of water which allows the oomycete to proliferate in and move through. This disease is mainly caused by *Pythium ultimum* and *Pythium irregulare*, although most of the Pythium family is capable of infecting the root system to some extent (Martin and Loper 1999). If allowed to thrive in the field the oomycete is known to form oospores, a thick-walled class of sexual spores that are able to survive extreme conditions even in the absence of previous crops (Martin and Loper 1999). *Pythium* is also capable of producing glycoproteins that enable zoospores, a class of asexual spores, to adhere to the root tissue mucilage, where they are then able to germinate and penetrate the cell wall leading to the full infection of the tissue within minutes to hours of infection (Martin and Loper 1999). Rhizoctonia root rot works in a similar way to Pythium, where the prominent species *Rhizoctonia solani* is capable of infecting roots of both dicot and monocot species. Like Pythium, it can remain in the debris of the previous crop, but also survive deep in the ground as thick-walled hyphae or form condensed hyphal structures called sclerotia (Okubara, Dickman, and Blechl 2014). Although described as a necrotrophic fungus, *Rhizoctonia solani* has also been showed to possess a short biotrophic phase, mainly associated with external fungal growth and the creation of concentrated hyphal cushions, a known important structure during the necrotrophic phase that is able to penetrate the epidermal cells of the root and then completely obstruct the uptake of water, normally leading to the death of the plant (Dodman and Flentje 1970; Kouzai et al. 2018). This early biotrophic phase is highly sensitive to plant hormone salicylic acid (SA), a known hormone involved in plant resistance to biotrophic fungus, capable of reducing the number of hyphal cushions produced by the fungus, leading to plant resistance to RRR in the early stages of infection (Kouzai et al. 2018).

1.2.1 Fusarium diseases of wheat

As described previously, *Fusarium* diseases are one of the most prominent diseases found in wheat, being capable of infection different tissues, from root, to stem, leaves and heads of the plant. Although the *Fusarium* genus contains a complex and diverse group of fungi, for simplicity, the term *Fusarium* will be used to exclusively refer to *Fg* and *Fc* in the

thesis, unless otherwise stated. The perfect conditions for the proliferation of the disease occur mainly in warm and humid environments, although the fungus is known to adapt easily to cooler and more arid regions, selecting different strategies and tissues to colonize, showing the dangerous adaptability of *Fusarium* species to different conditions (Parry, Jenkinson, and Mcleod 1995). In humid environments the fungus heavily relies on the local rainfall for the spread of its macroconidia (asexual spores) in order to infect the ears of wheat and other crops (Fig. 1-1) (Parry, Jenkinson, and Mcleod 1995). *Fg* is also capable of producing sexual spores, called ascospores, which are mainly associated with infection through wind dispersion (Fig. 1-1) (Markell and Francl 2003). Another ability associated with these *Fusarium* species is their capacity to live saprotrophically in the debris of previous crops (Fig. 1-1), being capable of surviving for several years if left unattended, leading to the re-emergence of the disease in following years (Scherm et al. 2013).

Unlike biotrophs that mainly use living cells as their source of nutrition, or necrotrophs which main supply of nutrients originate from the death of host cells, *Fusarium* infection is more closely related to hemi-biotrophs, which normally contain a short biotrophic phase before switching to a more aggressive necrotrophic lifestyle (Brown et al. 2010; Ding et al. 2011). The infection process of FHB starts around mid-anthesis, when wheat is most susceptible, and the fungus can penetrate the spikelet through stomata, the floret mouth as well as the crevices formed between the palea and lemma. The fungal hyphae can then spread through the apoplast of the cells constituting a temporary biotrophic phase of colonization of the tissue (Beccari, Covarelli, and Nicholson 2011). This phase is mainly characterized with the creation of infection cushions and intercellular growth of the fungus between the cells of wheat without causing any symptoms of disease (Brown et al. 2010; Brown et al. 2011). During this phase *Fusarium* is believed to be mainly feeding from the nutrients of the extracellular exudates in the apoplast of the host system (Brown et al. 2010). After a short period of external and intercellular growth, the fungus then switches to a necrotrophic lifestyle, normally associated with a high production of cell wall-degrading enzymes and trichothecene mycotoxins,

accompanied with hyphal intracellular growth (Kang and Buchenauer 2000; Brown et al. 2010). This leads to the partial or complete bleaching of the ear, followed by the production of shrivelled and discoloured grains (Parry, Jenkinson, and Mcleod 1995). These grains can be easily dispersed during harvest leading to another route for the fungus to propagate in the field, and these grains are normally excluded from the final harvest count, leading to a reduction of the yield. These grains can contain high amounts of mycotoxins, that are harmful to both humans and animal stock, leading to further restrictions on their use based on the level of the toxins in the grain. An estimated total of 7.67-billion-dollar economic loss due to FHB occurred in the United States of America during the period from 1993 to 2001 (McMullen et al. 2012), while in Australia a total loss of 80 million dollars per year is credited to be related to poor grain quality from FHB (Murray and Brennan 2009).

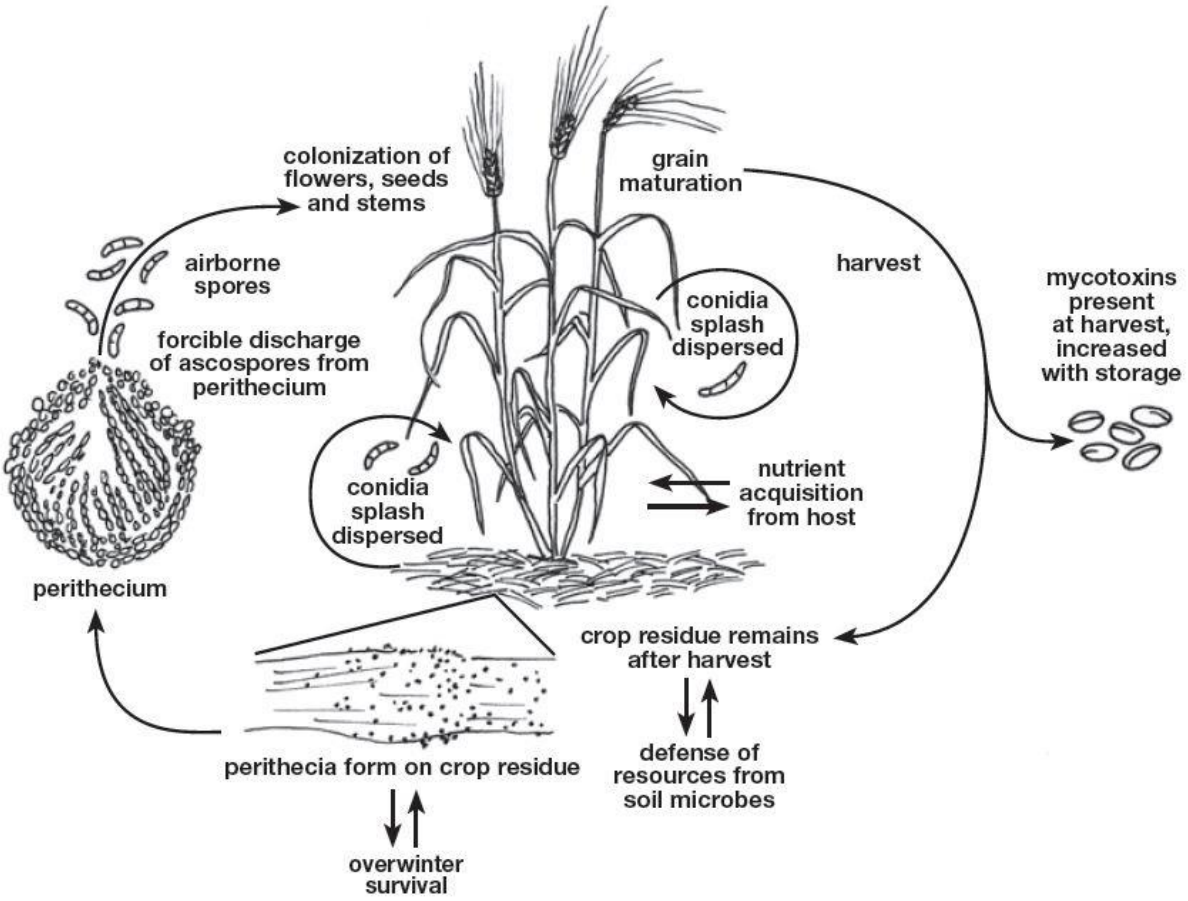

Figure 1-1 The life cycle of Fusarium graminearum and Fusarium culmorum in wheat (taken from (Trail 2009)).

As described above many *Fusarium* species can infect wheat, with the most studied disease being FHB. However, many of the same *Fusarium* species are also capable of infecting roots leading to FRR and *Fusarium* crown rot (FCR). One of the main sources of inoculum is from debris of previous crops, as well as from the use of infected unhealthy seeds (Scherm et al. 2013). Once the conidia of *Fusarium* germinate, the fungus can proliferate on the surface of the roots before penetrating and colonising in a biotrophic manner before becoming necrotrophic, reminiscent of FHB. If this transition happens early in the plant's life, it can cause the total browning and death of the root system, leading to the complete blight of the seedling (Scherm et al. 2013). If it happens at later stages, the disease normally spreads through most of the root system, being able to infect the crown of the plant before colonising into the first two internodes of the main stem which becomes necrotic and causing a pink discoloration due to the production of conidia (Scherm et al. 2013). FRR can occur in very different environments because of the different strategies employed by the pathogen. In a very warm and humid environment *Fusarium* is capable of reproducing and proliferating rapidly leading to a more virulent attack on the plant (Chekali et al. 2011). In a dry environment, the fungus cannot proliferate effectively but it is able to take advantage of the drought stress of the host allowing it to easily infect the crop (Liu and Liu 2016). It has also been shown that a combination of the two environments may lead to a worse outcome to the plant, especially when the initial stages of infection are coincident with a wet environment, helping the fungus proliferate, but then changes to become a dry environment in later stages where the fungus takes advantage of the stress to infect the plant more efficiently (Smiley et al. 2005).

1.2.2 Take-all disease

While *Pythium* and *Rhizoctonia* species are known to have a wide range of hosts, and *Fusarium* species are capable of infection a variety of tissues in cereal plants, take-all is more specialized, being mainly associated with the roots of grain crops, with specific impact in wheat cultivation. Take-all, mainly caused by *Gaeumannomyces graminis* var. *tritici* (*Ggt*), generally has only a low impact in the first year of infection, using the debris of that year to create a build-up of inoculum for the following year. If left unattended take-all can cause severe damage to the entire field on the second year of infection, leading to shrivelled wheat plants, with poor grain quality even if the plant manages to survive to maturity (Gutteridge, Bateman, and Todd 2003). Even though take-all is one of the most studied root diseases, finding genetic resistance in wheat has been incredibly difficult. Most of the varieties of both winter and spring wheat demonstrate high susceptibility when it comes to their response to take-all fungal infection (McMillan et al. 2018). The fungus can grow undetected in the rhizosphere of plants in the field, normally characterized by the growth of dark pigmented runner hyphae across the surface of the root (Fig. 1-2) (Skou 1981). It then forms hyaline hyphae that are capable of penetrating the root to the cortex where the fungus then feeds on the plant nutrients. The fungus then produces perithecia, with asci and ascospores (Fig. 1-2), normally formed through self-fertilization, although outcrossing is also possible but less regular in nature (Pilgeram and Henson 1992). Asexual spores can also be produced under *in vitro* conditions, but their role in nature is not known (Deacon 1973; Palma-Guerrero et al. 2021).

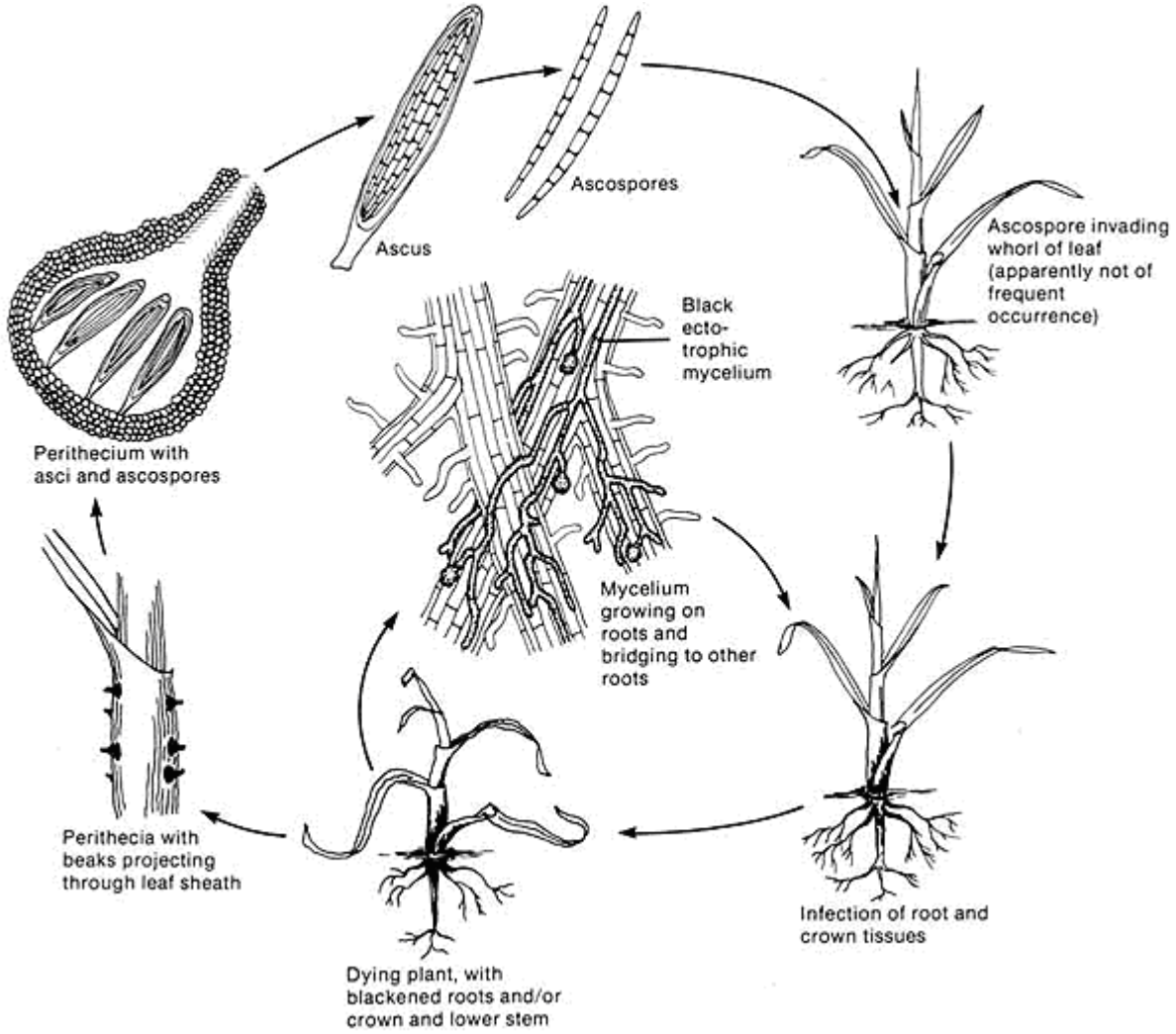

Figure 1-2 Life cycle of Gaeumannomyces graminis var. tritici in the roots of wheat (adapted from (Skou 1981)).

The roots of the plants will then become increasingly necrotic due to the infection process and this will eventually lead to the bleaching of heads and even death of the entire plant (Cook 2003). It is normally at these later stages of infection that the disease is diagnosed in the field, making it too late for any intervention to be carried out, causing a high loss in crop yield. If not properly disposed of, the fungus can survive saprophytically in the field, inside the dead roots of the previous crop, leading to the repeat of the cycle in the following season (Cook 2003).

1.3 Role of plant hormones in plant defence

In the natural environment several species developed the ability to feed out of other species in order to survive, as previously described in the case of the root pathogens of wheat. However, wheat and other hosts have also developed new strategies to protect themselves from such pathogens by evolving new mechanisms to either prevent infection or minimise the spread of the pathogen. The most characterized plant mechanism against biotic stress is the plant's pathogen-associated molecular pattern (PAMP)-triggered immunity or its ability to produce an effector-triggered immunity (Spoel and Dong 2012). PAMP-triggered immunity relies on plant receptors capable of recognising pathogen-derived molecules that serve as elicitors that cause a cascade response in the plant in order to minimise the pathogen spread and infection, causing an overall non-specific basal resistance of the plant to the pathogen (Spoel and Dong 2012). Effector-triggered immunity is a more specialised response to the pathogen, where avirulence factors (generally pathogen-derived effectors) are recognised by the plant resistance proteins, which cause a more pronounced resistance response to the pathogen, normally associated with programmed cell death in the area of infection leading to a decline in the fungus spread and infection (Spoel and Dong 2012). Although stronger than the PAMP-triggered immunity, due to its specificity, a change in or loss of the pathogen effector could lead to the pathogen being no longer recognised by the plant's resistance proteins (Spoel and Dong 2012). Both resistance mechanisms, independent of their method of pathogen detection, heavily rely on the plants phytohormone response to quickly deploy their defence response, where SA and jasmonic acid (JA) play a significant role (Lim et al. 2017). While SA is part of the small phenolic family produced by the shikimate pathway, JA is part of a large and diverse family of oxygenated fatty acids called oxylipins, which contains several members that play a role in abiotic and biotic stress responses (Lim et al. 2017). One of the first steps of JA synthesis is the oxygenation of either the linoleic acid or linolenic acid in carbon 13 by a 13-lipoxigenase (13-LOX) (Fig. 1-3) (Howe and Schilmiller 2002). Another type of oxygenation can occur in carbon 9 by a 9-lipoxigenase (9-LOX) (Fig. 1-3), leading to a

different pathway that features another set of compounds involved in plant defence mechanisms against different stresses in a similar role to JA (Howe and Schilmiller 2002). The hormone JA can be further transformed into its bioactive form jasmonyl-isoleucine (JA-Ile), through the conjugation of JA with isoleucine by Jasmonate Resistant 1 (JAR1) (Fig. 1-3), which then interacts with JASMONATE ZIM DOMAIN proteins to mediate gene expression in the cell (Wasternack and Hause 2013). One of the most common elicitations where JA is the prominent signalling hormone is in response to the mechanical wounding and feeding by herbivores on the plants leaves and stem tissues (Wasternack and Hause 2013). When it comes to pathogen response signalling in the plant, SA is mostly associated with biotrophic pathogens while JA is more associated with necrotrophic pathogens, although there is evidence that JA's counterparts in the 9-LOX pathway also have a function in biotrophic pathogen response (Wasternack and Hause 2013; Vicente et al. 2012). One such example is the potential role of methyl jasmonate production in the JA pathway to act as a long distance signal to other plants when a tissue is damaged due to herbivory, causing the other plants to prepare for a possible herbivore attack (Heil and Ton 2008). Other roles of JA originating from herbivore wounding is the induction of the production of several toxic and unpalatable compounds by the plant, as well as the down-stream production of volatiles that impair the reproduction of the herbivore, or cause the luring of the herbivore's natural predators (Wasternack and Hause 2013).

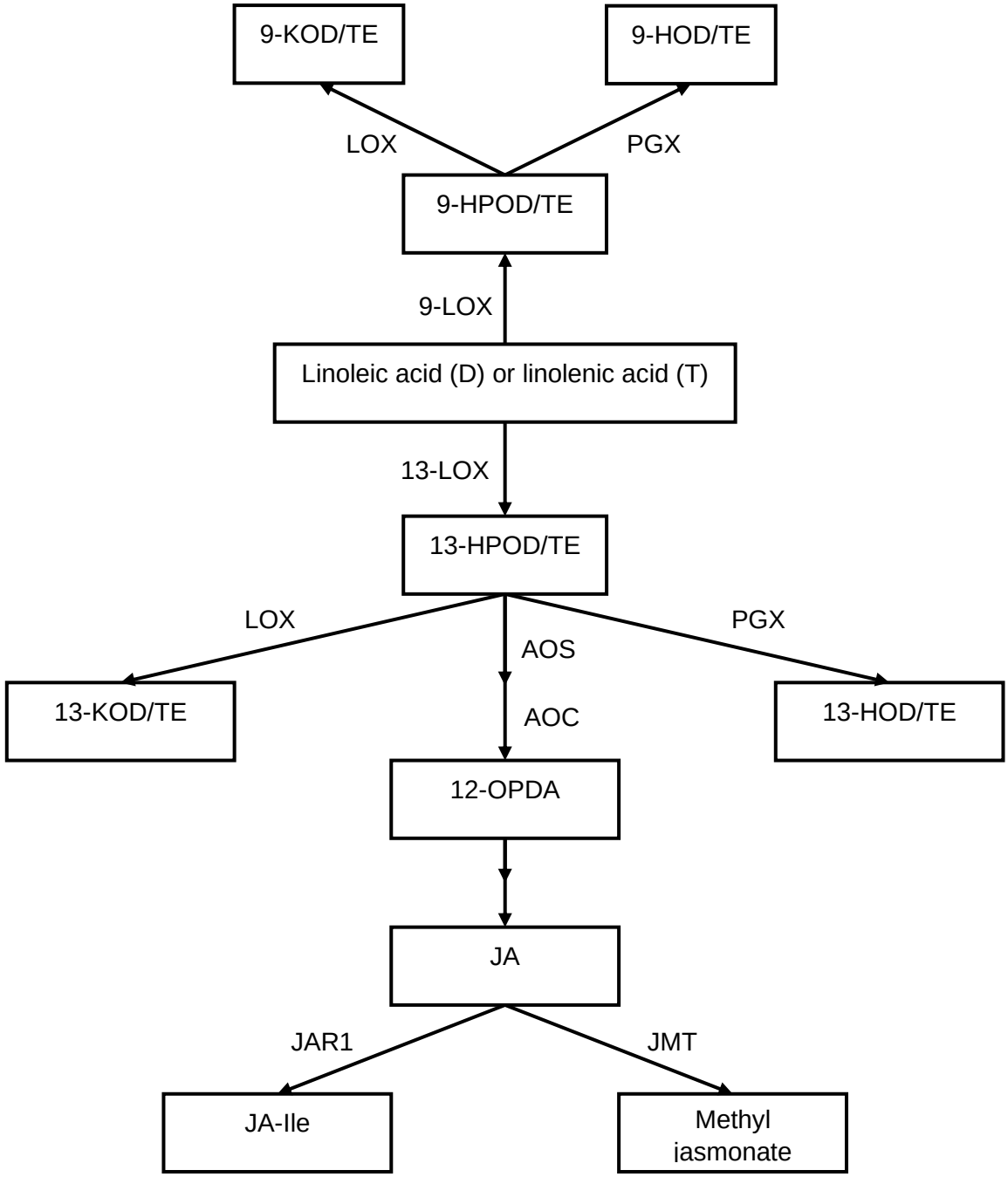

Figure 1-3 Simplified schematic representation of plant lipoxygenase pathway, showing the main oxylipins produced through the 9-lipoxygenase (9-LOX) and 13-lipoxygenase (13-LOX) pathways. The 9-LOX and 13-LOX enzymes modify either linoleic acid or linolenic acid to produce hydroperoxyoctadecadienoic acid (HPODE) or hydroperoxyoctadecatrienoic acid (HPOTE), respectively. These are subsequently modified to form hydroxyoctadeca-(dienoic/trienoic) acid (HOD/TE) oxylipins through a peroxygenase (PGX) or ketooctadeca-(dienoic/trienoic) acid (KOD/TE) oxylipins through a lipoxygenase (LOX). 13-HPOTE can be further transformed by allene oxide synthase (AOS) and allene oxide cyclase (AOC) to 12-oxo phytodienoic acid (12-OPDA), leading to the production of jasmonic acid (JA), which can be further conjugated with isoleucine (Ile) by Jasmonate Resistant 1 (JAR1) to produce JA-Ile, or transformed by jasmonic acid carboxyl methyltransferase (JMT) to produce methyl jasmonate.

When it comes to the role of JA in pathogen response the story gets more complicated. Mutations in the *CORONATINE INSENSITIVE 1* (*COI1*) gene, an important gene that interacts with JA-Ile, causes an increase in susceptibility to fungi *Plectosphaerella cucumerina, Alternaria brassicicol*a and *Botrytis cinerea* in *Arabidopsis thaliana* (Thomma et al. 1998). On the other hand, some strains of the fungus *Fusarium oxysporum* are capable of producing JA and JA-Ile and use the plant's jasmonate-COI1 interaction to exploit the plant's defence response and hijack the JA pathway to benefit its infection (Cole et al. 2014). This susceptibility is independent from SA and can easily be overcome by mutating *coi1* in Arabidopsis (Cole et al. 2014), thus demonstrating that some fungi can exploit the plants JA pathway to benefit their growth, rather than being impaired by this defence mechanism. Another example of JA hijack is the ability of *Pseudomonas syringae* to mimic JA-Ile in the cells of tomato through the synthesis of the JA-Ile-mimicking compound coronatine, which leads to an inhibition of the SA pathway, which the bacteria exploits to infect the plant (Yan and Xie 2015). Much like with *Fusarium oxysporum,* Arabidopsis mutants in *coi1* can easily derepress the SA pathway and confer resistance to *Pseudomonas syringae* (Yan and Xie 2015). Apart from the 13-LOX JA pathway, the 9-LOX pathway is also another important pathway in the plant response to pathogens, increasing the level of complexity of the oxylipin production by the plant in response to external threats. The 9-LOX proteins in both *Arabidopsis* and maize tend to have a variety of sub-cellular localizations, being generally localized in the cytoplasm or the tonoplast of the cell, unlike the 13-LOX proteins that have all been reported to accumulate in the plastids of the cell (Tolley et al. 2018). In *Arabidopsis thaliana*, following exogenous application of 9-LOX pathway metabolites (Fig. 1-3), 9-hydroxyoctadecatrienoic acid (9-HOTE) and 9-ketooctadecatrienoic acid (9-KOTE), the number of lateral roots decreased, and an increase in root waving was observed, partially due to the uneven deposition of callose throughout the root system (Vellosillo et al. 2007). Disrupting the expression of the *Arabidopsis* 9-LOX genes (*AtLOX1* and *AtLOX5*), resulted in the number of lateral roots increasing as well as an increased susceptibility to virulent strains of *Pseudomonas syringae* and the obligate biotrophic fungus *Golovinomyces cichoracearum* (Vellosillo et al. 2007; Marcos et al. 2015).

It is suggested that the dual effect on cell wall architecture and defence is due to an interaction between the 9-LOX pathway and the brassinosteroid signalling pathway where both modulate the root cell architecture, mainly by controlling the callose deposition and hindering infection and colonisation by pathogens (Marcos et al. 2015). The Arabidopsis *Atlox1* mutant was also shown to increase susceptibility to *Hyaloperonospora arabidopsidis*, and *Alternaria brassicicola*, while overexpression of its orthologue in pepper (*Capsicum annuum*), *CaLOX1*, increased resistance to all beforementioned pathogens (Hwang and Hwang 2010). The silencing of *CaLOX1* was also demonstrated to cause increased susceptibility to *Xanthomonas campestris* pv *vesicatoria* and *Colletotrichum coccodes*, with a reduction in expression of several defence genes as well as lower production of reactive oxygen species (ROS), SA accumulation and reduced lipid peroxidation (Hwang and Hwang 2010). In tobacco, the 9-LOX pathway has been shown to be involved in the regulation of programmed cell death by manipulating the production of ROS in the mitochondria of the cell, increasing resistance to bacterial pathogen *Ralstonia solanacearum* (Cacas et al. 2005; Gao et al. 2007). Disrupting the expression of the tobacco 9-LOX gene *NtLOX1* decreased the hypersensitive response-mediated resistance to the soilborne oomycete pathogen *Phytophthora parasitica*, providing evidence of a role of these pathways in resistance towards root pathogens (Rance, Fournier, and Esquerre-Tugaye 1998). On the other hand, by being involved in the production of ROS, this pathway can also benefit fungi that manipulate the plant ROS system to enhance infection. In maize it has been shown that 9-LOX *ZmLOX3* is involved in stimulating production of mycotoxins by *Fusarium verticillioides*, where the fungus appears to manipulate the plant to increase the expression of the 9-LOX gene in order to create a ROS response that results in an increase of the production of the mycotoxin fumonisin (Gao et al. 2007). Disrupting the expression of host 9-LOX *ZmLOX3*, decreased the ROS activation in the plant cells which led to a decreased production of fumonisin, lower conidial production by *Fusarium verticillioides* as well as decreased infection by two other fungi, *Colletotrichum graminicola* and *Cochliobolus heterostrophus* (Gao et al. 2007). It has also been shown in maize that following disruption of *ZmLOX3*, the roots exhibit an increased production of jasmonic and salicylic acid as well as

ethylene, which seemed to attract more root-knot nematodes, like *Meloidogyne incognita* (Gao et al. 2008). The maize *Zmlox3* mutants also display delayed seed germination and overall development of the maize plant, where the roots and shoots of seedlings are shorter than the wild type, along with having a shorter life cycle with most mutant plants senescing 10 days earlier than their non-mutated counterparts, although no effect was observed on kernel number and size (Gao et al. 2007). Even though the disruption of *ZmLOX3* resulted in higher resistance to *Fusarium verticillioides* and increased production of JA, the maize 9-LOX gene *ZmLOX12* displayed the exact opposite, with its mutated variant leading to decreased resistance to *Fusarium verticillioides* with increased levels of fumonisin and lower amounts of jasmonates like JA-Ile and 12-oxo phytodienoic acid (12-OPDA) (Christensen et al. 2014). This demonstrates that the 9-LOX pathway is involved in the production of different oxylipins with different effects in resistance and plant response depending on the external stimuli involved. Another pair of maize 9-LOX paralogs, *ZmLOX4* and *ZmLOX5*, display different roles in plants although having 94% amino-acid sequence similarity. *ZmLOX4* is expressed in the roots and in the shoot apical meristem, similar to the root-specific 9-LOX *ZmLOX3*, while *ZmLOX5* is only expressed in the aerial tissues of the plant (Park et al. 2010). This spatial difference in expression was also observed in the expression profile of the two genes to insect and pathogen attack, with *ZmLOX4* being only induced in root related wounding and infection, and *ZmLOX5* in leaves and stems (Park et al. 2010).

In the characterization of the 13-LOX and 9-LOX pathways, one of the most interesting findings is the 9-LOX tissue specific response, when compared to the more dispersed response by 13-LOX/JA. The complex disparity between root and shoot defence responses observed in the 9-LOX response is not entirely unusual, as the rising number in studies on tissue-specific gene response to certain pathogens corroborate the differences in hormone deployment towards aerial and subterranean infections. Regarding the root diseases explored in this thesis, limited work has been performed in the characterisation of the host specific hormone response in the roots during FRR and take-all infection, and if this response is

different from the general plant response to necrotrophs in the leaves and heads of the plant. A description of FHB and FRR development in plants primed with different plant hormones has already demonstrated to promote differences in plant resistance/susceptibility to *Fusarium*, that is dependent on the initial tissue the infection originates (Haidoulis and Nicholson 2020). In the comparison between the necrosis progression of the disease between the two tissues, similar responses were observed for the plants primed with exogenous auxin and cytokinin, where auxin promoted disease resistance and cytokinin lead to more susceptibility in both roots and heads (Haidoulis and Nicholson 2020). The hormones that had contrasting effects to both tissue infections was JA and ethylene, that contributed to the plant resistance in the roots, while increasing susceptibility to *Fusarium* in the head (Haidoulis and Nicholson 2020). SA had a moderate role in disease susceptibility in the roots, but no effect on the heads (Haidoulis and Nicholson 2020). The disparity between these three hormones between FHB and FRR is proposed to be due to the different life cycle phases the fungus can adopt during the colonisation of the tissue, where *Fusarium* might adopt a necrotrophic lifestyle quicker in the roots than in the head. This in turn leads to an increase in plant resistance linked with the increase in the production of JA and ethylene; and an increase in susceptibility with the increase in exogenous SA (Haidoulis and Nicholson 2020). It is also proposed that the fungus stays in biotrophic phase longer in the head when compared to the roots, explaining the increase in susceptibility in the initial stages of infection upon exposure to exogenous JA and ethylene (Haidoulis and Nicholson 2020). The effect of JA and methyl jasmonate in the head and leaves as also be reported to produce different results depending in the stage of infection it is applied, leading to susceptibility when applied pre-infection, correlating with a more biotrophic phase of the fungus, while increasing resistance in post-infection during the necrotrophic phase (Makandar et al. 2010; Ameye et al. 2015), reinforcing the connection between the two different infection phases of the fungus with the hormone role in plant resistance/susceptibility to *Fusarium*.

In regard to take-all, although the plant hormone response to take-all is still poorly understood, different transcriptome analysis of the plant response to the disease have already provided important evidence in the understanding of the role of hormones upon *Ggt* infection. The study of tissue-specific responses in the plant has greatly benefited from next generation sequencing, especially its use in RNA sequencing (RNA-seq) technologies. This technology has been a great asset in the full characterization of the transcriptome of different eukaryotic organisms, taking into account not only the tissue, but the different developmental stages as well as certain conditions the organism has been exposed too, from chemical exposure to pathogen infection (Stark, Grzelak, and Hadfield 2019). Generally, in terms of plant-microbe interaction, plant RNA-seq and subsequent transcript analyses are used to draw a differential gene expression profile between the control treatment and the treatment with the corresponding pathogen of interest, where the levels of transcripts and their isoforms are compared between the two conditions (Wang, Gerstein, and Snyder 2009; Stark, Grzelak, and Hadfield 2019). Such approach has been used by Zhang and colleagues in the characterization of the wheat root response to *Ggt* infection (Zhang et al. 2020). The global analyses of the plant response demonstrated a higher down-regulation of plant genes in comparison to up-regulated genes upon infection, with the majority being part of pathways associated with resistance against pathogens (Zhang et al. 2020). Differentially expressed genes involved in cell reorganisation and regulation, along with signal transduction and pathogenesis-related proteins, were highlighted among the most highly differentially expressed, with some showing a potential role in wheat root resistance against take-all (Zhang et al. 2020). The main hormone pathways exhibiting the most differential expression upon infection were involved in JA and ethylene pathways, known hormones involved in the response to necrotrophs like take-all. Unusually, a number of differentially expressed genes was also observed for SA, a hormone more closely connected to biotrophs (Zhang et al. 2020).

This activation of proteins involved in the two antagonistic hormone pathways between SA and JA was further explored in another independent RNA-seq analyses by Kang and

colleagues (Kang et al. 2019). In this study a focus was made in the differential gene response of the wheat root to the individual root colonization by *Ggt*, but also the effect on take-all development in wheat roots primed with beneficial bacteria *Bacillus velezensis* (Kang et al. 2019). Upon infection with only *Ggt*, an increase in SA accumulation is observed accompanied with an increase in *Pathogenesis-related protein 1* (*PR1)* genes. The increase in SA accumulation was higher than JA accumulation, with the JA-responsive gene *Plant defensin 1.2* (*PDF1.2*) being inhibited upon infection (Kang et al. 2019). This discrepancy was further accentuated in the wheat roots primed with *Bacillus velezensis*, leading to a higher accumulation of SA when compared to JA (Kang et al. 2019). As previously described, JA is the most common hormone produced during the plant defence against necrotrophs, suggesting a unique mechanism in the root defence against *Ggt* where the SA pathway activation is preferred over JA.

Overall, the previous studies highlight that the general plant response to a necrotrophic infection seem to be different between roots and more aerial tissues of the plant like leaves and heads. This reinforces the importance of the study of root specific diseases, as overall extrapolation from plant-microbe interactions above ground can create the wrong assumption to the real mechanism underlying plant defence to root pathogens. It is thus important to provide more insight into the specific mode of action employed by the plant to defend itself from underground pathogens, along with its ability to continue to gather nutrients for the normal developmental of the plant while interacting with beneficial microorganisms.

1.4 Brachypodium distachyon as a model crop species

Most of the root diseases described thrive where the debris is retained from the previous crop, but disease severity is also affected by the plant density in the field, the amount of nitrogen fertilization, as well as environmental factors brought about by climate change (Scherm et al. 2013). On top of that, early diagnosis of the disease is impossible without completely removing the plant from the soil, making in-field phenotyping extremely difficult

when compared to leaf and head diseases. Trying to study the disease progression and resistance *in vitro* makes it very difficult to make a proper live assessment without causing permanent damage to the system, especially in wheat where the root system is considered too complex. This is mainly due to the fast growth of the primary roots and its ability to quickly branch into multiple secondary and lateral roots. To try and bypass this problem, many scientists have resorted to the plant model *Arabidopsis thaliana* since it has a diploid genome, and real time phenotyping of its roots is a well-established practice. However, difficulties arise due to the significant differences between the phylogeny of the two species, with many genes not being represented or having a different function in the other genome. In the last decade, another potential model has been put forward that has a closer relationship to wheat. *Brachypodium distachyon* (Bd) is a diploid monocot grass, with a genome of 272 Mbp arranged in 5 chromosomes, making it one of the smallest in the grass family (IBI 2010). It has a relatively short life cycle from 8 to 10 weeks, capable of growing in undemanding growth conditions. Normally reaching a height of around 30 centimetres, *Bd* is capable of being kept in a growth chamber in considerable numbers, economizing and reducing the space that the same amount of wheat would take on a small plot of land (Draper et al. 2001). The most studied line of *Bd* is Bd21, a line that has been recently sequenced to an 8-fold coverage with over 25,000 protein-coding sequences predicted (IBI 2010). Due to its closer phylogenetic relationship with wheat than *Arabidopsis thaliana*, the genomes of the species have a stronger syntenic relationship where more than 77% of the *Bd* genes have a high EST (expressed sequence tag) match with the genes of hexaploid wheat (Huo et al. 2009). *Bd* also has available an abundant library of mutagenized lines, including an EMS as well as a T-DNA insertion mutant collection that is continuously being expanded due to the efforts of the group lead by John Vogel in the Joint Genome Institute, USA, working to increase the range of genes with a disruptive mutation in *Bd* (Vain et al. 2008; Bragg et al. 2012; Collier et al. 2016). Apart from creating a resource library of T-DNA mutants for *Bd*, the Vogel group is also responsible for one of the biggest projects behind the full characterization of *Bd*, with the full sequencing of more than fifty different lines from multiple locations (Gordon et al. 2017). From

preliminary studies on the different genomes of several accessions of *Bd*, a set of 54 accessions were selected from different locations, but with most originating from Turkey and Spain, with the addition of the Iranian control accession Bd21 and its close relative Bd3-1 (Gordon et al. 2017). This set of accessions provided the primary source for the analyses of *Bd* pan-genome, referred to in this thesis as Brachypan, and were fully sequenced using Illumina and assembled using Bd21 as a genome reference (Gordon et al. 2017). Each accession has a full set of predicted gene coding sequences which were further divided into two broad categories based on their conservation in the whole Brachypan panel: the 'core genes'' refer to genes found in at least 53 out of the 56 accessions, and the 'shell genes' which are found in 3 to 52 accessions (Gordon et al. 2017). A small set of genes, considered to be possible anomalies make up a third group called the 'cloud gene cluster', which is characterized as being unique to just 1 or 2 accessions, but these are generally omitted in the overall analyses. Out of a set number of predicted genes from a high-confidence pan-genome data set (containing 53 out of the 56 lines), around 55 to 60% are considered core genes, with the remaining being part of a combined list of shell genes that have a reference annotation in all versions of the assembly of Bd21, as well as novel genes not found in the Bd21 accession (Gordon et al. 2017). When looking at each individual accession, rather than the overall panel, an average of 73% of its genes are considered core, against the 27% that are considered shell or cloud, demonstrating how closely related each line is to the other members of the Brachypan panel. The shell genes that are present, however, together with non-coding sequences, can still provide around 3,933,264 single-nucleotide polymorphism (SNPs) used in a construction of a phylogenetic tree that groups the accessions into three main clusters. Two of the clusters coincide with the accession original location, where all 17 accessions from cluster 1 are exclusive to the north-eastern region of Spain, and the 27 lines from cluster 2 are exclusive to the middle east, mainly mainland Turkey (Fig. 1-4). The remaining 9 lines did not have any specific geographical location; however, they all share the same late flowering trait (Gordon et al. 2017).

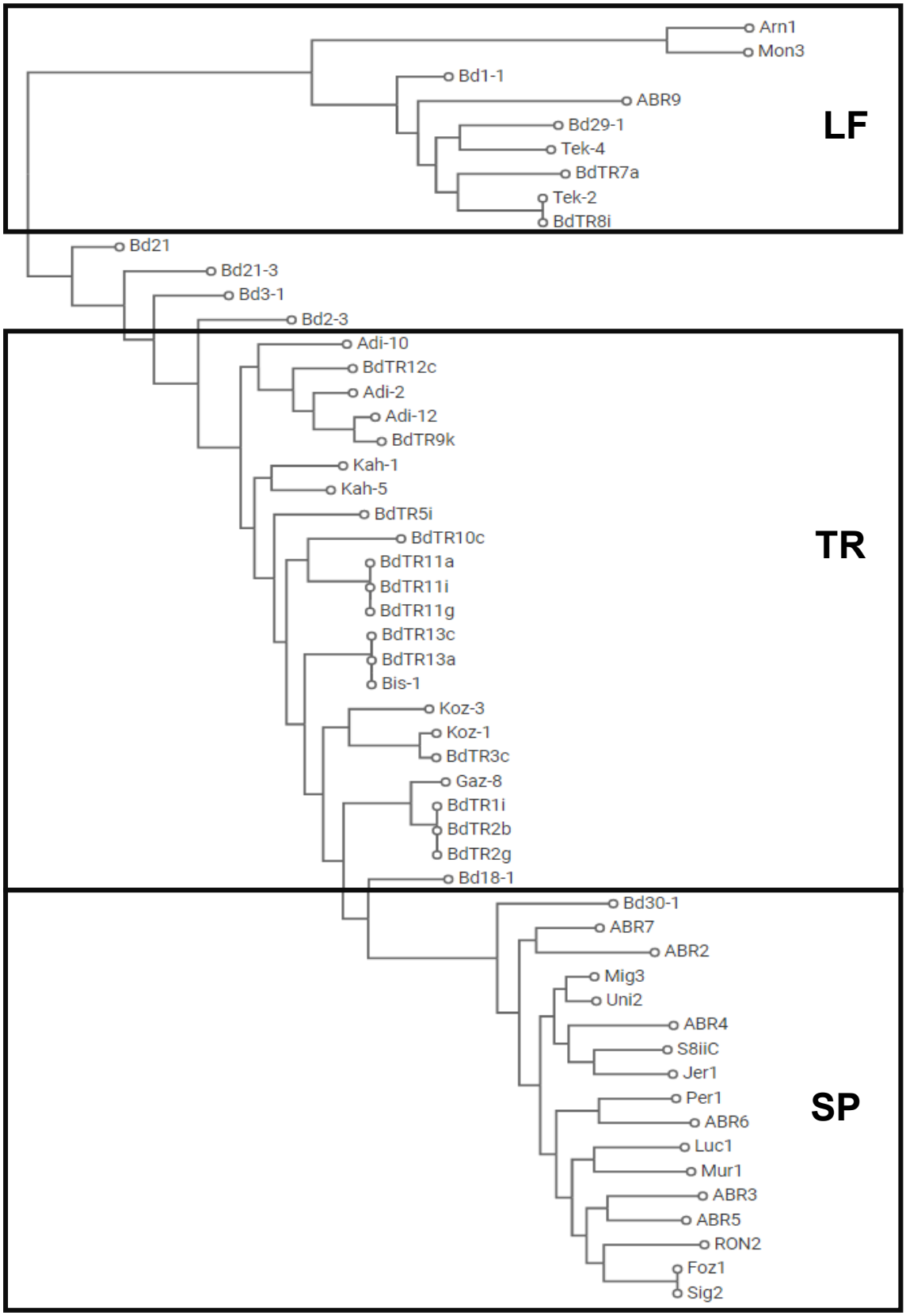

Figure 1-4 Brachypan phylogenetic tree constructed from 54 different Brachypodium accession. The tree is divided in three main clusters comprising late-flowering (LT), Turkey (TR) and Spanish (SP) accessions (adapted from (Gordon et al. 2017) and https://brachypan.jgi.doe.gov/).

In addition to this genomic data, several different populations have been created through crossing selected accessions in order to study the genetic basis of traits in detail and to isolate the genes and alleles responsible for differences between accessions (Table 1-1). The most studied population to date is that produced by crossing the first sequenced accessions, Bd21 and Bd3-1. The availability of these populations is crucial for the undertaking of genetic analyses due to the difficulty of crossing *Bd*. Difficulties are mainly associated with the small size of the flowers and the closed floret structure which makes it difficult to access the sexual organs in order to undertake emasculations without damaging the floral tissues. Another important aspect related to the use of these populations to extrapolate findings into wheat, is due to the high level of synteny and similarity between the genomes of wheat and *Bd* (Huo et al. 2009). A significant number of the markers used in the construction of the genetic and physical maps of *Bd* can be directly correlated to the wheat genome. One of the earliest examples of the use of the homology and synteny of the markers, was the fine mapping of the *Ph1* locus, a known stabilizer of meiosis in wheat, the absence of which facilitates the crossover between the three homeologous genomes in wheat and also to its close relatives (Griffiths et al. 2006). The fine mapping of the wheat *Ph1* region has been challenging (Borrill, Adamski, and Uauy 2015; IWGSC 2018), however making use of the rice and *Bd* genetic maps and markers, the region was refined to a 2.5 Mbp region within the original 70 Mbp region delineated in the chromosome 5B of wheat (Griffiths et al. 2006). This led to the meiosis gene *cdc2* being put forward has a good candidate for the gene responsible for the effects conferred by the *Ph1* locus (Griffiths et al. 2006).

Table 1-1 Populations generated from different Brachypodium distachyon accessions.

Population	Developed by
Bd21 x BdTR13k	Michael Ayliffe – CSIRO (Ayliffe et al. 2013)
Tek-4 x BdTR10h	Michael Ayliffe – CSIRO (Ayliffe et al. 2013)
Bd21 x ABR6	John Doonan - Aberystwyth University (Bettgenhaeuser et al. 2017)
Luc1 x Jer1	Jan Bettgenhaeuser – TSL (Bettgenhaeuser et al. 2018)
Luc1 x Foz1	Jan Bettgenhaeuser – TSL (Bettgenhaeuser et al. 2018)
Bd21 x Bd3-1	David Garvin - USDA-ARS (Garvin et al. 2008)
Bd2-3 x Bd21	David Garvin - USDA-ARS (Garvin et al. 2008)
Bd3-1 x Bd1-1	David Garvin - USDA-ARS (Garvin et al. 2008)
Bd3-1 x Bd2-3	David Garvin - USDA-ARS (Garvin et al. 2008)
Bd21 x Bd1-1	David Garvin - USDA-ARS (Garvin et al. 2008)
Bd30-1 x Bd21	David Garvin - USDA-ARS (Garvin et al. 2008)
Koz-3 x Bd1-1	Daniel Woods - U. Wisconsin, Madison (Woods et al. 2019)
Ron-2 x Bd1-1	Daniel Woods - U. Wisconsin, Madison (Woods et al. 2019)
Koz-3 x Bd29-1	Daniel Woods - U. Wisconsin, Madison (Woods et al. 2019)
BdTR12c x Bd1-1	Daniel Woods - U. Wisconsin, Madison (Woods et al. 2019)
Bd21 x Bd29-1	Daniel Woods - U. Wisconsin, Madison

Bd has proved to be a useful tool, not only in its own right, but also as a means to tackle deciphering the complex genome of wheat. Recently it has been used to investigate responses to different wheat abiotic and biotic stresses, with a particular interest made in different wheat diseases. One of the most relevant examples is the mimicking of the symptoms of FHB of wheat in *Bd*, where upon infection, small brown spots appear on the lemma, spreading quickly to adjacent florets, eventually leading to the bleaching of spikelet above the point of infection, with colonisation spreading to the rachis and the peduncle, similar to the symptoms in wheat (Peraldi et al. 2011). Another important observation was that the levels of DON mycotoxin production by the fungus during infection in *Bd* was similar to those of wheat, which makes it a much more appropriate model than *Arabidopsis thaliana* in which only very low levels of DON accumulate (Peraldi et al. 2011).

Since the discovery of *Bd* being a good model for the study of *Fusarium*, many other cereal pathogens have been shown to infect *Bd* and cause similar symptoms to those observed on wheat or barley. The next one to have favourable results in *Bd* was rice blast, a rice, wheat and barley disease, caused by the fungus *Magnaporthe oryzae*. Upon inoculation into the leaves of *Bd*, the fungus was able to produce melanized appressoria capable of penetrating into the host and forming hyphal branches in the epidermal cells, before spreading

and infecting the sheaths and stems of *Bd*, mimicking perfectly the symptoms in both rice and barley (Routledge et al. 2004; Wang, Wang, Li, et al. 2012). The only difference was observed in the detached leaf assessment, where the symptoms of the disease was more easily observed in *Bd* than rice, which was credited to the ability of *Bd* to keep its leaves green for longer after being detached (Wang, Wang, Li, et al. 2012). Another important observation was that by using 21 different accessions of *Bd* a range of symptoms was observed ranging from susceptible accessions displaying rapid spread of *Magnaporthe* lesions, to highly resistant accessions with highly localized necrotic flecks, highly reminiscent of the susceptible and resistant phenotypes found in different rice varieties (Routledge et al. 2004). Different mutants of *Magnaporthe* which cause a disruption in the efficient formation of the fungus appressorium (*Δcpka*, *Δmac1*, *Δmpg1* and *Δpmk1*) lead to a resistance response in rice. Resistant phenotypes were also observed for these mutants in *Bd*, further exemplifying the similarities in the host-pathogen interaction in both species (Wang, Wang, Li, et al. 2012).

The next diseases to be shown to be phenocopied in *Bd* were eyespot and Ramularia leaf spot, diseases of wheat and barley respectively. Upon infecting the stem base with different *Oculimacula* spp., the fungi responsible for eyespot disease, the typical brown eye-shaped lesions were observed in *Bd*, along with the infection and colonisation of consecutive leaf sheaths (Peraldi et al. 2011). In a different study, *Bd* was able to help understand the genetic relationship between two sources of resistance to eyespot promoted by the genes *Pch1* and *Pch2*. These genes originate from two different sources and are localized on the distal part of the long arm of homoeologous chromosomes 7D and 7A, respectively, and it had been postulated that the two genes were homoeloci (Pasquariello et al. 2017). However, through exploitation of synteny and use of the *Bd* genetic map, further genetic markers were identified and studied. These markers permitted the relative position of the two genes to be related to one another and to allow the authors to conclude that the location of the *Pch1* gene did not correlate with *Pch2*, demonstrating that the two genes were not homoeloci (Pasquariello et al. 2017). This demonstrates that *Bd* is not only useful in the study of the

phenotypic response to the pathogen, but also for understanding and improving genetic studies that had reached a stalemate in the original wheat host. Similarities between barley and *Bd* was also observed upon infection with *Ramularia collocygni*¸ the causal fungus of Ramularia leaf spot, where the typical necrotic lesions where observed, in addition to the production of the characteristic swan neck shaped conidiophores, demonstrating the ability of *Ramularia* to complete its life cycle in *Bd* as it does in barley. Differences in response to the fungus by the two most well studied accessions of *Bd*, Bd21 and Bd3-1 were observed, where the latter, under specific conditions, displayed a higher level of necrotic lesions than Bd21 (Peraldi et al. 2014). This provides one of the first examples where a population study could be undertaken in *Bd* for the understanding of resistance against a cereal disease.

Even though *Bd* was shown to be a good model for the study of hemi-biotrophic and necrotrophic fungi, it generally displayed resistance to wheat diseases caused by biotrophic pathogens, which include all of the rust diseases as well as powdery mildew (Draper et al. 2001; Ayliffe et al. 2013). Wheat stem rust (*Puccinia graminis* f. sp. *tritici*), wheat stripe rust (*Puccinia striiformis* f. sp. *tritici*) and wheat leaf rust (*Puccinia triticina*) were generally unable to infect *Bd* which displayed an intermediary non-host resistance to these pathogens. Most of the fungi were unable to fully colonize the *Bd* tissue and complete their life cycles, however *Puccinia brachypodii* as well as some isolates of wheat stripe rust and barley stripe rust (*Puccinia striiformis* f. sp. *hordei*) displayed different arrays of infection across the Brachypan panel, demonstrating the complicated interaction between different fungal isolates and different non-host accessions (Draper et al. 2001; Barbieri et al. 2012). Two populations generated between the rust-resistant *Bd* accessions Jer1 and Foz1 and the susceptible accession Luc1, identified two sources of resistance to stripe rust closely linked with putative NB-LRR (nucleotide binding - leucine-rich repeat) gene clusters in chromosome 2 (Yrr3), and chromosome 4 (Yrr1). While both regions are linked with resistance to wheat stripe rust, only Yrr3 was additionally associated with resistance to barley stripe rust (Bettgenhaeuser et al. 2018). This highlights how *Bd* can prove a powerful tool for defining chromosomal regions

conferring potent disease resistance in a short amount of time, even when the *Bd* accessions are closely genetically related (Gordon et al. 2017). Another fungus that exhibits a strong resistant response from *Bd* is powdery mildew, *Blumeria graminis*, where the specialized isolates for wheat, oats and barley all failed to efficiently infect *Bd* (Draper et al. 2001). The fungal pathogen *Zymoseptoria tritici*, the causal fungus of *Septoria tritici* blotch, is also unable to complete its life cycle in *Bd* (O'Driscoll, Doohan, and Mullins 2015). The first study determined that Septoria infection with isolate IPO323 in *Bd* is similar to an incompatible interaction with wheat, demonstrating pale water-soaked lesions and necrotic lesions with no significant sporulation and stomatal penetration (O'Driscoll, Doohan, and Mullins 2015). Different resistance patterns were obtained when using different accessions of *Bd*, where Bd1-1 displayed no lesions and Bd21-1, Bd29-1 and Bd30-1 developed large necrotic lesions surrounded by regions of senescence, demonstrating the diversity within the Brachypan panel response (O'Driscoll, Doohan, and Mullins 2015). By using a different Septoria isolate 560.11, further diversity was observed where the isolate was able to penetrate the stomata and grow intracellularly, but it failed to form any mature pycnidial structures and complete its life cycle (Reilly et al. 2020). The higher virulence of this isolate in *Bd* correlates with the higher susceptibility observed in wheat potentially indicating similar susceptibility factors between the two species of host (Reilly et al. 2020).

As described so far, the study of diseases that heavily affect wheat can benefit from similar studies performed in *Bd*. Most of the wheat disease symptoms are able to be replicated in several tissues of *Bd*. Even though some fungi are unable to complete their cycle they can still produce a similar genetic response from *Bd* accessions as appears in wheat, demonstrating that it can still play a role as a good plant model for the study of genetic response to pathogens. Coupling that with the compact and simplified genome of *Bd*, understanding of the basic genetics and mechanisms behind each response can be obtained in a relatively short amount of time, when compared to the much longer and more complex process associated with disease characterization in wheat.

1.5 Project overall objectives

The main purpose of the current project is to make use of the model plant *Brachypodium distachyon* to understand the plant response upon being infected with *Fusarium* root rot and take-all. Previous work has already shown that *Bd* exhibits the same symptoms as wheat when infected with *Fusarium* and *Geaumannomyces* runner hyphae in the roots (Peraldi et al. 2011; Sandoya and Buanafina 2014). Work done on *Rhizoctonia* root rot established a protocol that was able to mimic the root disease of wheat in *Bd*, going as far as uncovering potential sources of resistance using a small set of accessions from the Brachypan panel (Schneebeli, Mathesius, and Watt 2015; Schneebeli et al. 2016). However no proper methodology has been developed to use Bd's full potential in analysing the development of these two diseases *in vitro* and in real time, as they mainly relied on use of a destructive single time point assessment approach. This project will make use of a new protocol for efficient infection of *Bd* by these two pathogens, undertaking continual non-destructive assessment of the progression of the diseases, as well as to document novel response mechanisms of *Bd*. A focus will be made on the investigation of the genetic basis underlying resistance and susceptibility phenotypes of *Bd* to either of the diseases, with a view to identifying resistance genes to both diseases. An optimized approach will be used to study the different accessions within the *Bd* Brachypan panel, using Bd21 as the control line. Upon identifying a significant differential in resistance between different accessions, the available populations already established for *Bd* will be used to study the genetic basis of resistance / susceptibility. The regions of interest will then be compared to their corresponding syntenous regions in wheat in an attempt to identify potential candidate genes responsible for resistance in both hosts.

In the last two decades an increasing number of genes involved in disease resistance to necrotropic and hemi-biotrophic pathogens such as *F. graminearum* and *G. graminis* var. *tritici* have been identified in cereal species. Host responses to these pathogens generally involves activation or interaction with the jasmonic acid pathways often acting in concert with

ethylene (Robert-Seilaniantz et al. 2007; Chen et al. 2009). Jasmonic acid is synthesised by the lipoxygenase pathway where it is a product of the 13-LOX branch. In the current project, however, the 9-LOX branch of the network, which is documented as having a role in root development and disease response, is selected for further study. Using homology, the 9-LOX genes will be identified, and the T-DNA mutant lines will be analysed for their potential role in resistance to root diseases.

The third approach and last section of the thesis will be the study of the response of *Bd* to the most important virulence factor of *Fusarium* species infecting wheat, the mycotoxin deoxynivalenol (DON). A series of RNA-seq analyses will be performed using the control line Bd21 to study the response to DON. Broad analyses will be made to identify the most significantly affected pathways in *Bd*. In addition, the response of both *Bd* and wheat to DON will be compared to identify common DON responsive genes. Selected genes will be examined for their potential role in resistance to *Fusarium* diseases through the use of wheat TILLING resources, consisting of over 2500 ethyl methanesulfonate (EMS) mutagenized lines developed in either durum wheat cultivar Kronos or in the bread wheat cultivar Cadenza (http://www.wheat-tilling.com/).

Chapter 2. Variation in Take-all resistance among *Brachypodium distachyon* accessions

2.1 Introduction

Soil borne diseases of crops are one of the most difficult diseases to study, especially from the perspective of assessing resistance. One of the most important root diseases is take-all, caused by the fungus *Gaeumannomyces graminis* var. *tritici* (*Ggt*) (Hornby et al. 1998). The search for natural resistance to take-all in crops like wheat and barley has largely been unsuccessful. Numerous studies have been conducted using a wide range of varieties of wheat and barley on their response to take-all, and even though barley was slightly more resistant than wheat, all the varieties displayed high levels of susceptibility to the disease, deeming them unviable to withstand the disease successfully (Cook 2003; McMillan, Hammond-Kosack, and Gutteridge 2011). One of the most affected groups was bread wheat, exhibiting earlier symptoms and death. In the field, if bread wheat is a monoculture affected by take-all disease, the disease can significantly reduce the viability and yield of the crop for up to three years. However, it has been documented that if cultivation of wheat is continuous, it leads to a reduction of take-all in the field, known as take-all decline (TAD) (Hornby et al. 1998). This event is characterized by the adaption of the rhizosphere over the years to the monoculture, leading to the competition between the take-all fungus with other soil borne microorganisms that are less harmful to the plant. One of the best-known examples of such competition, is the antagonistic properties of *Pseudomonas fluorescens*, a soil born bacterium capable of producing 2,4-diacetylphloroglucinol (DAPG) that has been shown to act as an effective antibiotic against the take-all fungus (Weller et al. 2007). Both the abundance of take-all and *Pseudomonas* has also been demonstrated to be manipulated by host factors. In the first year of sowing, some varieties of wheat can lead to a decreased level of growth of *G. graminis* var. *tritici*, coupled with an increase of the population of *Pseudomonas*. This host dependent alteration in the rhizosphere microbiome is reflected in an increase in yield and

reduced symptoms of take-all in the second year of sowing, either using the same variety or a different one. This phenomenon, denominated take-all inoculum build-up (TAB), has been proven recently to be a viable mechanism for constraining take-all infection in the field (McMillan, Gutteridge, and Hammond-Kosack 2014; McMillan et al. 2018). The standard example for this experiment is the use of the low TAB cultivar Cadenza against the high TAB cultivar Hereward. If, during the first year, the area was cultivated with Cadenza, in the subsequent second and third years the total number of infected roots with take-all was considerably lower than on the roots of plants grown in the area where Hereward was the cultivar in the previous season (McMillan et al. 2018). This was also reflected in the grain yield obtained at the end of the experiment, where the cultivars grown in the low TAB soil had an average of 30% more yield than the cultivars grown in the high TAB soil (McMillan et al. 2018). Since the amount of take-all build up in the first year greatly influences the impact of the fungus in the following years, the manipulation of the cultivars in the first year is essential to take advantage of the take-all build up and the ensuing take-all decline. This previous work shows a correlation to this important take-all trait, where using cultivars that lead to a low / high build up in the first year, leads to its corresponding impact on the second and third years. Unfortunately, cultivars with low first year TAB do not seem to promote the same effect when used in the second and third year, demonstrating how important the first year of take-all build up is for the take-all disease progression in the field in subsequent seasons (McMillan et al. 2018).

Even though most cereals and grasses are susceptible to take-all, oats exhibit complete resistance to the disease due to its ability to synthesise avenacin, a saponin known to protect oats against several soil-borne diseases including take-all (Osbourn et al. 1994). Trying to transfer this to other crops is difficult however, mainly due to the large number of biosynthetic steps necessary to produce this compound *in planta*.(Haralampidis et al. 2001; Qi et al. 2004; Qi et al. 2006; Geisler et al. 2013; Mugford et al. 2013). Avenacin biosynthesis is controlled by a gene cluster unique to the oat family, but even though most of the genes

involved are localized relatively near to each other in the oat genome, the pathway is highly complex (Leveau et al. 2019). So far two distinct pathways have been identified that are important in the synthesis of avenacin. The isoprenoid pathway is involved in the creation of the triterpene scaffold, while the shikimate pathway is the origin of the N-methyl anthranilate acyl group (Leveau et al. 2019). A lot of work has been done to identify all the different enzymes involved in these two pathways, however much more research is required before starting the process of transferring it to other plant species. Even if the entire pathway is identified and characterized, this is not an ideal solution in the long run, due to the existence of a variety of take-all known as *Gaeumannomyces graminis* var. *avenae*, a relative of var. *tritici*, that has the ability to produce the enzyme avenacinase which is capable of detoxifying avenacin and resume the normal take-all like symptoms in the root system of the plant (Osbourn et al. 1994).

Numerous attempts have been made to try and identify resistance to take-all. To date, no genetic resistance in wheat has been characterized, and the only strategy to tackle the disease is the continuous growth of wheat in the field leading to TAD. This strategy is not a cost-effective measure due to the severe yield losses that can occur during the process, making the need to find a more efficient way to prevent the disease important. In the first part of this chapter a novel approach will be made in trying to identify resistance to take-all within a diverse collection of accessions (the Brachypan panel) of the grass model species *Brachypodium distachyon* (*Bd*) and its existing mutant library. The second part will be mainly focused on the characterisation of the plant hormone response to the take-all. As described in the previous chapter, the role of plant hormones in the response to take-all is still poorly understood. In order to further investigate the plant hormone response to the disease, another approach using the *Bd* T-DNA mutant collection will also be used to study the potential role of 9-LOX oxylipins, a novel class of hormones with an important role in the roots and in disease resistance. A potential correlation between the 9-LOX and the JA/SA hormone response to take-all, described in the last chapter, will also made.

2.2 Materials and Methods

2.2.1 Brachypodium lines and seedling preparation:

The 58 *Bd* Brachypan accessions lines: Adi-15, Adi-4, Gaz-8,Kah-1, Kah-5, Kah-6, Koz-5, Mig3, Mon3, Tek-2, ABR2, ABR4, ABR6_r, ABR7, Adi-10, Adi-12, Adi-2, Adi-9, Bd1-1, Bd18-1, Bd21-3, Bd21Control, Bd2-3, Bd3-1_r, BdTR10C, BdTR10d, BdTR10h, BdTR11A, BdTR11e, BdTR11G, BdTR11I, BdTR12b, BdTR12c, BdTR13a, BdTR13b, BdTR13C, BdTR13k, BdTR13n, BdTR1i, BdTR2B, BdTR2G, BdTR3m, BdTR5I, BdTR9K, BdTR9m, Bis-1, Foz1, Gaz-1, Gaz-2, Jer1, Koz-1, Koz-3, Luc1, Per1, Sig2, Sin2, Tek-4 and Uni2 were part of the Sainsbury Laboratory Collection kindly donated by Mathew Moscou.

Mutant Bd21 lines BdAA615, BdEE8495 and BdBB7035 were obtained from the BrachyTAG collection (John Innes Centre) as a kind gift from Philippe Vain (Thole et al. 2012). Homozygosity of the respective mutation of interest was previously verified by the group.

Selected seeds of *Bd* were soaked in water for 5-10 minutes. With the use of fine tweezers, the husk (lemma) of the seeds was peeled off. The seeds were then placed in a circle onto two water-soaked filter paper disks in a 9 cm circular Petri dish. The Petri dishes containing the seeds were covered with aluminium foil and placed in a 4 ºC chamber for two days. After two days the seeds were transferred to a 22 ºC chamber for 24 h in the dark. Germinated seeds where then transferred to a filter paper surface in a 10 cm plastic box containing 50 ml of 0.8 % DIFCO Bacto agar media and placed on a 30 º angle in a 22 ºC growth chamber in a 16 h/8 h light/dark cycle.

2.2.2 Gaeumannomyces cultivation and maintenance:

Ggt isolate T5-2 was cultivated using a piece of agar of an existing culture immersed in a mineral oil solution. Mycelium plugs from *Ggt* isolates 18e and 1d where kindly donated by Vanessa E. McMillan from Kim Hammond-Kosack's group in Rothamsted Research. The fungal isolates were then transferred into a Petri dish containing Potato Dextrose Agar media

(PDA; 3.9% PDA DIFCO). The fungus was incubated for 4-6 days in a 22 ºC growth chamber with a 16 h/8 h light/dark cycle.

2.2.3 Inoculation procedure:

Two accessions were placed side by side in a petri box using random distribution. Seedlings of *Bd* (3 to 4-day old) were inoculated with *Ggt* mycelium plug either in the middle section or the tip of the primary root, in case of the oxylipin mutant analyses, or just the middle section in case of the BrachyPan accessions, and left to grow for two weeks.

After inoculation, the seedlings were placed at a 30º angle in a 22 ºC growth chamber in a 16 h/8 h light/dark cycle. The roots were photographed every two days until a maximum of 15 days post inoculation (dpi). The length of root tissue exhibiting necrotic lesions (brown/black discoloration) were then measured using the image processing program ImageJ.

2.2.4 Metabolomic analysis:

A total of up to 5 replicates with 10 *Bd* seedlings per replicate for both control and infected treatments were grown for a maximum of 10 days, with the seedlings from the infected treatment being infected with *Ggt* at 6 days. Each replicate was then collected, with the root being severed from the leaf at crown level, followed by deep freezing in liquid nitrogen. The tissue was then ground using a mortar and pestle, under liquid nitrogen until a fine powder was obtained. The powder was collected in a previously weighed standard 1.5 mL Eppendorf collection tube, and its weight measured again. The samples were then mixed with 2 mL of 2:1 (v/v) chloroform/methanol mixture, and then sonicated for 15 minutes in a water bath. They were then centrifuged for 10 minutes at 805 x g, and the supernatant was collected into a fresh tube. The samples were then sonicated and centrifuged two more times, having the supernatant collected in each time. The supernatant was then air dried between 1 to 2 days.

To extract the oxylipins of interest from the supernatant, a SepPak tC18 SPE column kit was used. The columns were first pre-conditioned with 5 ml of methanol. Afterwards, the dry supernatant was resuspended in 1.5 mL of 1:4 (v/v) methanol/water solution and acidified

with 80 µL pure acetic acid. The solution was loaded into the pre-conditioned SepPak column. After all the solution passed through the column, the column was washed two times with 5 ml of water, and then one time with 5 ml of n-hexane. The column is then dried and eluted with 5 mL of methyl formate. The samples were collected in a glass vial containing 6 µL of 30 % glycerol in methanol, and then left overnight to air dry. On the day of observation, the samples were reconstituted in 50 µL of methanol containing 40 nM of the internal standard solution (IS2) and analysed in Liquid Chromatography – Mass Spectrometry (LC-MS). The LC-MS analyses was performed by Paul Brett from the Metabolomics platform at John Innes Centre, using pure 9-HODE and 13-HODE as control for the analyses of two types of oxylipin. The area under the corresponding LC-MS peak was calculated and standardized using the previously weighed frozen tissue powder for each sample.

2.2.5 Data analysis:

For the final disease score, the area under the disease progression curve (AUDPC) was calculated using the necrotic lesion measurements for each day. For the BrachyPan analyses, Bd21 AUDPC was considered 100 % infection, with all the remaining accessions having a calculated disease percentage relative to Bd21. The cumulative raw AUDPC was used in the analyses of the differences between Foz1 and Luc1 with the different *Ggt* isolates.

All the data scores were analysed using a linear mixed model (REML), each accession, date and experiment was characterized as fixed effects, while the plates were considered random effects. The residual effect was also checked for its normality and equal variance between the accessions where no further transformation was necessary. The final model was used for the calculation of the predicted means used in the final visual comparison between the lines. An analysis of variance (ANOVA) pairwise comparison using Tukey statistical analyses was performed to calculate the p-value between the different accessions and mutants for the study of the magnitude of differences between their scores. Both analyses were carried out using Genstat 19th edition and RStudio with R version 3.5.0.

2.3 Results

2.3.1 Analyses of take-all development in the Brachypan panel

For the phenotypic characterization of the take-all disease the whole set available from Brachypan was used. The first experiment consisted of the analyses of the two most well studied Brachypodium accessions, Bd21 and Bd3-1, for which an already well developed and studied population is available (Garvin et al. 2008). The experiment consisted of six plates with four seedlings for each accession, amounting for a total of 24 seedlings. When the AUDPC was compared between the two accessions, using a standard t-test, no significant difference was observed (p-value 0.94) (Fig 2.1).

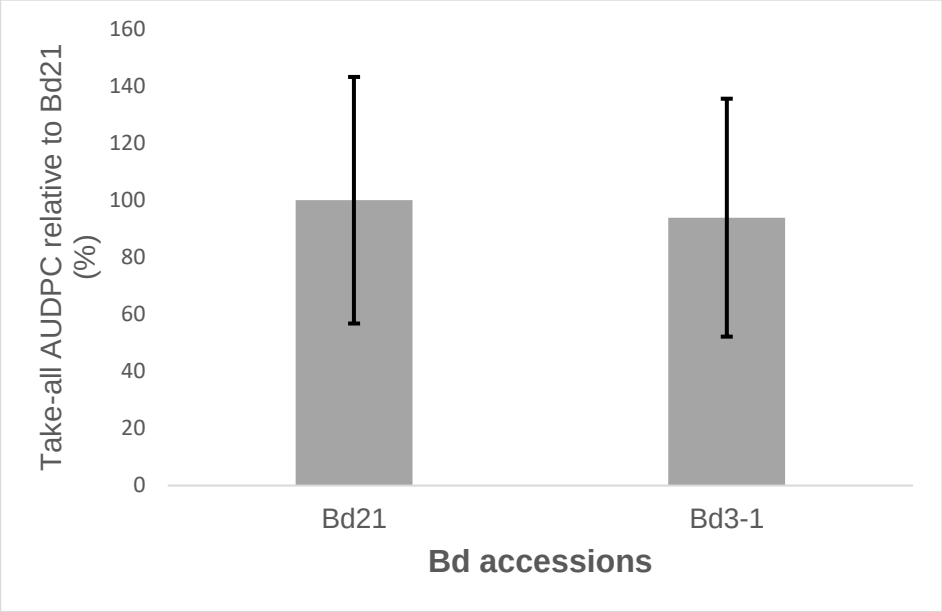

Figure 2-1 Take-all disease progression in the roots of Bd accessions Bd21 and Bd3-1. The disease progression was calculated relative to the control accession Bd21. Error bars represent standard deviation.

The next experiment was made using 32 additional lines from the Brachypan panel including all the available parents of existing populations currently available in the lab. A wide differential was observed through the panel, demonstrating a promising use of Brachypodium in unveiling resistance to take-all disease (Fig 2.2). In this experiment each plate contained two accessions with three seedlings of each. Every accession was randomly distributed in a maximum of four plates each, amounting for every single accession having a total of 12

seedlings overall. An overall ANOVA analysis was performed on the predicted means of each line. The most promising differential was observed between the parents of a population, Luc1 and Jer1, with a p-value < 0.0001. The development of a mapping population could be used to determine the genetic basis of variability in response to take-all. Crossing Brachypodium is a very difficult technique that fails most of the time, making all the available populations very precious. The cross between Luc1 and Jer1 was successfully made by the Moscou group in the Sainsbury laboratory in order to study resistance to yellow rust (Bettgenhaeuser et al. 2018). They generously donated their F2 population from which I developed an F5 generation to be used for screening against take-all.

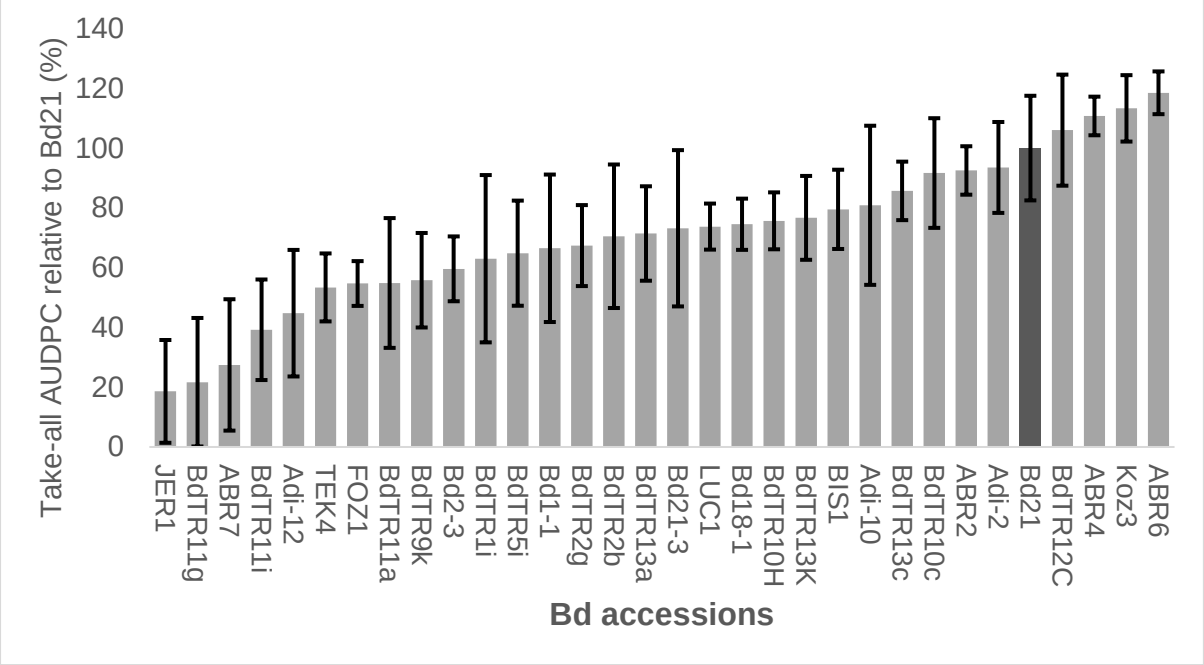

Figure 2-2 Disease score of take-all AUDPC progression relative to Bd21 (bold grey) for 32 accessions of the Brachypan panel including the parents of known Bd populations (Bd21, BdTR13k, Tek-4, BdTR10h, ABR6, Luc1, Jer1, Foz1, Bd2-3, Bd1-1, Koz-3, BdTR12c). Error bars represent standard deviation.

The lines Luc1 and Jer1 were also tested two more times to see if the results were reproducible. Each plate had 3 seedlings of each accession, where in the first experiment a total of 12 seedlings were used for each accession, while the second experiment had a total of 15 seedlings. Jer1 consistently had a delayed initiation of symptoms that lead to a reduced length of necrotic root by the end of the experiment (Fig 2-3). Jer1 did, however display the most variability both within and between experiments, with the second experiment (Jer1-2) displaying a higher rate of infection when compared to the first experiment (Jer1-1) (Fig 2-3). Luc1 on the other hand exhibited low variability within and between experiments apart from the last timepoint in the second experiment where disease progress stalled for an unknown reason. By performing a simple t-test analysis comparing each day within their own experiment, the first 7 days in both experiments remain statistically different with a p-value less than 0.0001. The stalling of disease progress in Luc1 after 7 days led to a loss of significance on the second experiment for 10 dpi (p-value=0.0137). The two experiments however still provide strong evidence of a reproducible difference in resistance to colonisation between Jer1 and Luc1. This suggests that the population available from the Moscou group might be used to investigate the genetic basis for the difference in resistance to the pathogen.

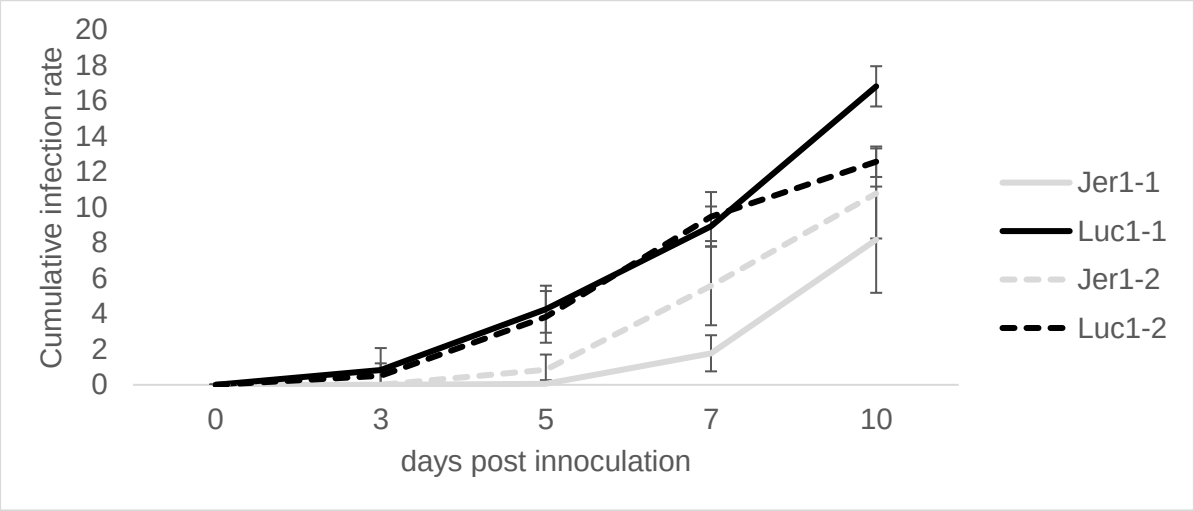

Figure 2-3 Cumulative infection rate from two independent experiments using the Bd accessions Jer1 and Luc1. First experiment displays higher differential between Jer1-1 and Luc1-1 when compared to second experiment with a loss of significance between Jer1-2 and Luc1-2 on the last day. Error bars represent standard deviation.

While generating the F5 population, additional lines from the Brachypan panel were obtained and bulked up. They were studied for their response to take-all to establish whether the same range of differential resistance to *Ggt* is present among other accessions. The experimental design for the new set of lines had the same layout has the previous experiment. After observing the new lines, a notable differential in resistance was again observed among the different lines (Fig 2-4). Within this set were one of the most resistant as well as one of the most susceptible lines observed so far, with Koz5 being almost completely resistant to the disease with a predicted score of around 0, and the line BdTr12b showing almost twice the level of susceptibility of Bd21 with a predicted score of 198. These results display one of the most promising findings of take-all resistance in grasses to date by using a close relative of wheat apart from oats. Unfortunately, there is no population between those two accessions, or between either of these accessions and any other in the panel, making it difficult to exploit due to the amount of time and work necessary to make it a viable option to pursue further.

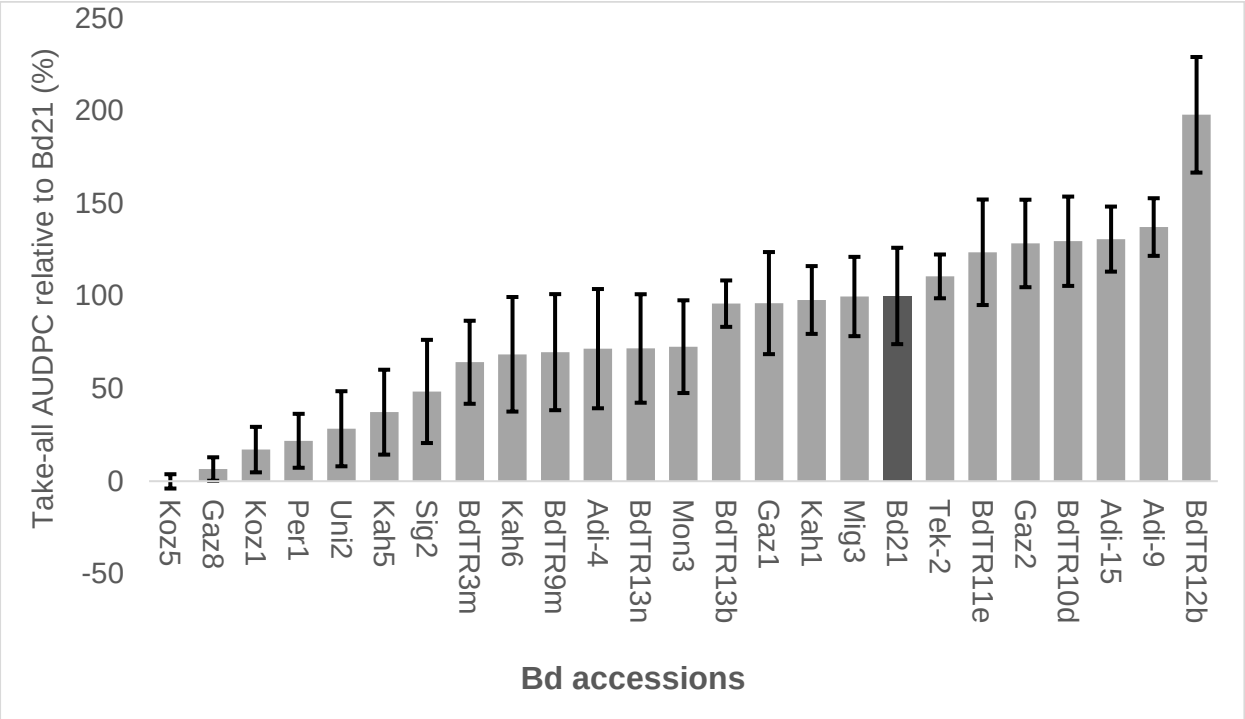

Figure 2-4 Third set of Brachypan accession disease score relative to Bd21 (dark grey) with Koz5 displaying the highest resistance and BdTR12b the highest susceptibility of Bd. Error bars represents standard deviation.

A selection of accessions from the initial Brachypan screening were also re-tested to determine whether the gradient of resistance was also consistent between experiments for a larger set of genotypes. A total of two experiments were combined, where the layout was the same as the second and third experiment discussed earlier. The gradient was successfully replicated where Sig2, Koz5, Gaz8, Koz1 and Kah5 continue to appear to be highly resistant, while ABR4 and Koz3 continue to be highly susceptible (Fig 2-5). A greater variability was observed with the lines that displayed more resistance to the pathogen, with the most variable line being accession Per1 in which seedlings varied from being highly susceptible to highly resistant when compared to the control Bd21, although its predicted mean is still considerably lower as observed in the previous experiment (Fig 2-5). A similar accession to Bd21, Bd21-3 had a predicted mean of 75 in the previous experiment, increasing to 143 in the second trial. Most of the lines exhibiting intermediary phenotypes to the disease remained within the spectrum. The most drastic changes were observed with accession Adi-12 that lost its resistance phenotype from the previous experiment from 45 to 129, and accession ABR2 which doubled its score from 95 to 212 (Fig 2-5).

A complete assessment of the potential differences between root architecture before and after infection was also carried out. The majority of accessions had a similar root growth rate before infection, with only some replicates demonstrating a delayed root germination. This delay was not correlated with any Brachypan region or *Bd* accession but was instead observed randomly within the Brachypan set. The root architecture and growth differed after infection, with the accessions with a better resistance being able to grow in a faster rate and produce more lateral roots. The opposite was observed in the more susceptible accessions, which displayed a reduced number of lateral roots and a slower primary root growth, associated with the more advanced necrotic lesion spread in the root.

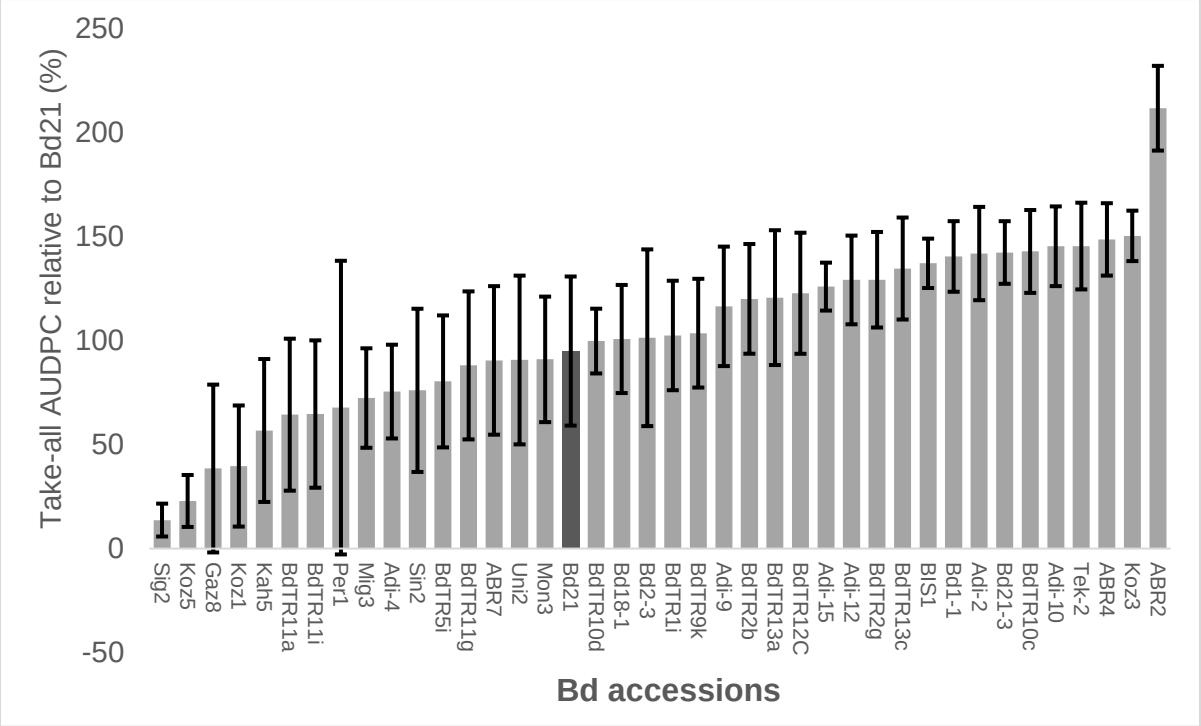

Figure 2-5 Second experiment using a selection of Bd accessions from previous experiments. All scores were made relative to Bd21 (dark grey), with the most resistant and susceptible accession maintaining their phenotypes. Error bars represent standard deviation.

All the different experiments were combined into a summary plot in order to visualize the full spectrum of resistance across the Brachypan panel (Fig. 2-6). When comparing the different accessions, there was no evidence that resistance was associated with the geographical origin, with the Turkish accessions and the Spanish accessions displaying a similar range of infection severity. Most of the Turkish susceptible accessions fall between accessions Bd21 and Bd21-3 as observed before, while accessions Koz5, Gaz8, Koz1, Kah5 and Sig2 remain the most resistant; and accessions Koz3, ABR6, ABR2 and BdTR12b the most susceptible. While the combining of the data led to a higher variation within each accession it did not change the differential between the parents Jer1 and Luc1.

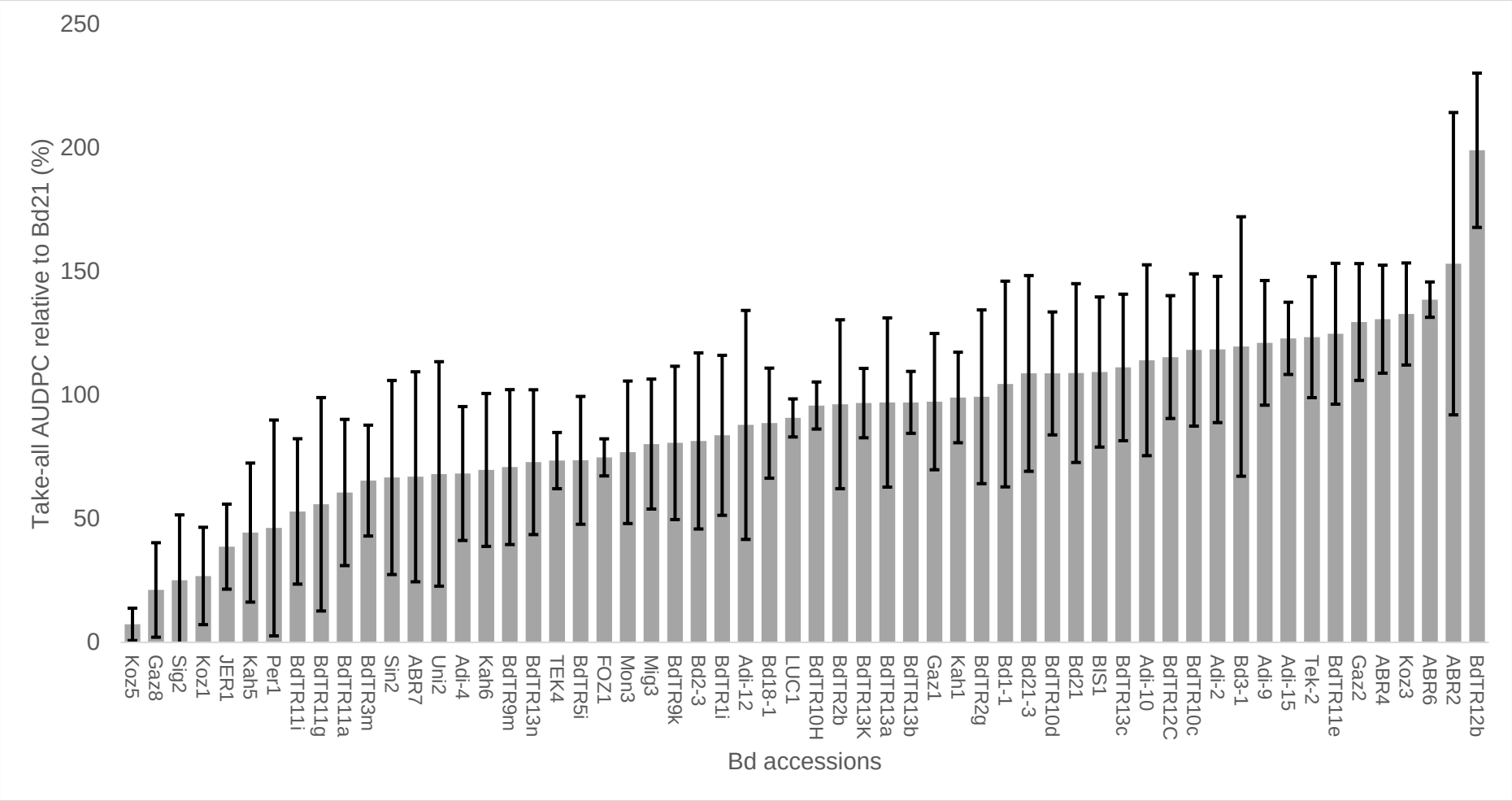

Figure 2-6 Brachypodium accession from the Brachypan panel were infected with Ggt. Their AUDPC were calculated and relativized to that of Bd21. Luc1 and Jer1 were the most differentiated parents observed in this analysis. Error bars represent standard deviation

In order to analyse the full story of all the combined data for the accessions that are parents to mapping populations an ANOVA analysis was performed for all relevant accessions (Table 2-1). There was no significant difference in susceptibility between parents in most sets (p-value greater than 0.05, with Luc1 and Jer1 displaying the greatest differential with a p-value of 0.0024. The next largest differential was between accessions Bd3-1 and Bd2-3 with a p-value of 0.0304. As previously stated, the F2 population between Luc1 and Jer1 was kindly donated by the Moscou group and subsequently harvested and re-sown until obtaining a stable F5 population by single seed decent.

Table 2-1 Bd accession parents to available mapping populations, with its respective pairwise p-value from the model ANOVA analyses and its corresponding predicted means.

Parent 1	Parent 2	p-value	Score 1	Score 2
Bd21	BdTR13k	0.9999	108.91	96.76
Tek-4	BdTR10h	0.9999	73.5	95.78
Bd21	ABR6	0.5537	108.91	138.61
Luc1	Jer1	0.0024	90.76	38.7
Luc1	Foz1	0.9999	90.76	74.81
Bd21	Bd3-1	0.9999	108.91	119.65
Bd2-3	Bd21	0.1004	81.45	108.91
Bd3-1	Bd1-1	0.9999	119.65	104.89
Bd3-1	Bd2-3	0.0304	119.65	81.45
Bd21	Bd1-1	0.9999	108.91	104.47
Koz-3	Bd1-1	0.5243	132.8	104.47

After obtaining the seeds of the F5 population between Luc1 and Jer1 the parents of the population were once again tested using two different isolates of take-all, Ggt-1d and Ggt-18e. The change in isolate was made due to the variable infection observed using isolate *Ggt* T5-2 which could pose a problem in a population analysis. The first test was performed using a 5-day post inoculation trial to verify whether the isolates where able to be grown and infect under the same conditions. A total of four plates per isolate were set up with 3 seedlings of each accession in each plate, amounting to a total of 12 seedlings of each accession for each isolate. After 5 dpi both isolates were able to infect the roots, with isolate Ggt-1d being slightly more aggressive than isolate Ggt-18e (Fig 2-7a). However, significant difference in resistance to the two isolates was observed between the two accessions, where Ggt-18e displayed a

statistical t-test p-value of 0.0175 and Ggt-1e a p-value of 0.313 at 5 dpi. In the second trial, the fungus was left to colonise for a total of 12 days, in order to determine whether any differential between the accession's resistance would be observed in later stages. The layout was similar to that in the first trial, with the addition of one more plate per isolate, increasing the number of seedlings per accession per isolate to 15. Take-all isolate Ggt-1d continued to be more aggressive than isolate Ggt-18e, but both isolates displayed very similar growth in both accessions. No significant resistance differential was observed between the accessions with isolate T5-2; having a p-value>0.3 between 5dpi and 12dpi for both isolate pairwise comparisons (Fig 2-7b). With the variability in infection observed under isolate T5-2 coupled with the loss of the resistance differential between accessions Luc1 and Jer1 with isolates Ggt-1d and Ggt-18e, it was deemed impractical to proceed to the phenotyping and QTL analyses of the F5 population.

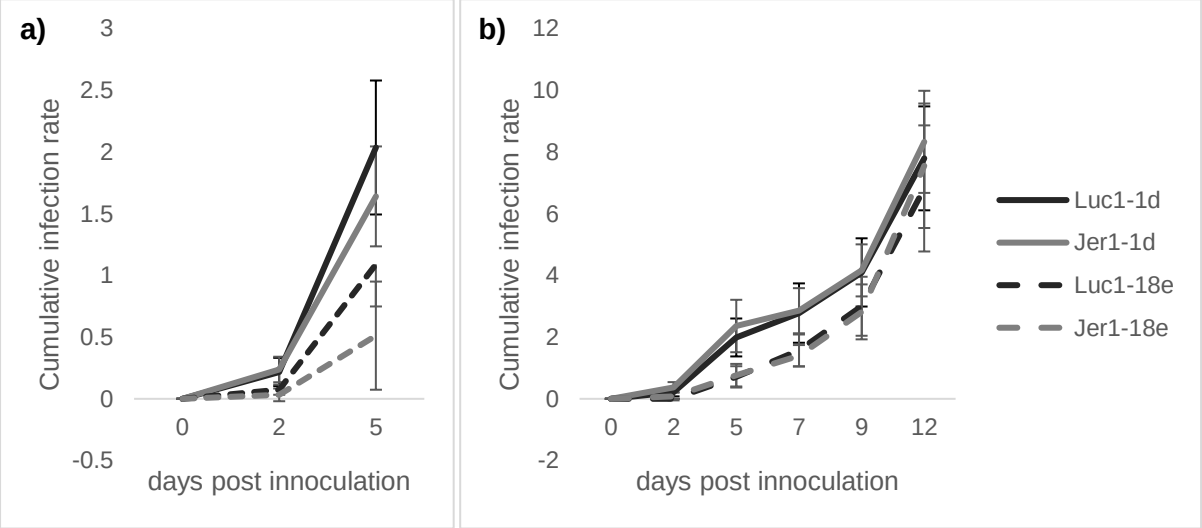

Figure 2-7 Bd accessions Luc1 and Jer1 cumulative infection rate from take-all isolates Ggt-1d and Ggt-18e. a) first experiment accessing the infection success of the isolates during the first 5 dpi; b) second experiment following the same methodology but for a total of 12 dpi.

2.3.2 Analysis of the potential role of putative Bd 9-lipoxygenases response to take-all

In addition to investigating variation in natural resistance among accessions of *Bd*, other strategies can be used to gain insight into mechanisms involved in resistance to take-all. In the previous chapter, the role of oxylipins was highlighted as one of the major contributors for disease resistance against necrotophs. Overall, the evidence suggests that the 9-LOX oxylipin pathway may be important not only in the development of the roots, but also in affecting the way the plant responds to root pathogens. In order to study the 9-LOX pathway in *Bd* and its potential role in take-all infection, the 9-LOX proteins in Arabidopsis (*AtLOX5*) and maize (*ZmLOX3*, *ZmLOX4* and *ZmLOX5*) where used to identify orthologues in *Bd* using EnsemblPlants (https://plants.ensembl.org/index.html, Table 2-2). Since *AtLOX1* and *ZmLOX12* display more specificity to the dicot and monocot groups respectively, they were not considered in the present investigation, that focussed on the 9-LOX pathway genes that have similar roles in both dicot and monocot plants.

Table 2-2 Brachpodium distachyon orthologues of the 9-LOX genes AtLOX5 in Arabidopsis and ZmLOX3, ZmLOX4 and ZmLOX5 in maize with their corresponding EnsemblPlants Target %id similarity (https://plants.ensembl.org/index.html).

Arabidopsis thaliana		
***AtLOX5* (AT3G22400)**		
Species	*Orthologue*	*Target %id*
Brachypodium distachyon	*Bradi1g09260*	54.75 %
Brachypodium distachyon	*Bradi1g09270*	54.58 %
Brachypodium distachyon	*Bradi1g11670*	53.91 %
Brachypodium distachyon	*Bradi1g11680*	55.93 %
***Zea mays* (maize)**		
***ZmLOX3* (Zm00001d033623)**		
Species	*Orthologue*	*Target %id*
Brachypodium distachyon	*Bradi1g11680*	83.37 %
***ZmLOX4* (Zm00001d033624)**		
Species	*Orthologue*	*Target %id*
Brachypodium distachyon	*Bradi1g11670*	73.68 %
ZmLOX5 (Zm00001d013493)		
Species	*Orthologue*	*Target %id*
Brachypodium distachyon	*Bradi1g11670*	73.26 %

The two genes that appeared to be the most likely candidates as 9-LOX genes in Brachypodium were *Bradi1g11670* and *Bradi1g11680,* which are orthologues of both *AtLOX5* and all of the 9-LOX genes selected from maize (Table 2-2). For simplification reasons in the rest of the thesis the genes *Bradi1g11680* will be named *BdLOX1a* and *Bradi1g11670*, *BdLOX1b*. In the analyses of the overall gene expression profile of both genes using the Brachypodium eFP browser (http://bar.utoronto.ca/efp_brachypodium/cgi-bin/efpWeb.cgi), *BdLOX1a* displays the highest absolute expression in roots and young shoots and leaves, while *BdLOX1b* is limited to root tissue and root nodes, reinforcing the previous findings of the 9-LOX genes being mainly involved in the plant root system.

In order to study the possible effects of these genes in take-all resistance, the available Brachy-Tag mutant collection was used. The Brachy-Tag collection is an *Agrobacterium*-mediated transformation of Bd21, developed in the John Innes Centre by Dr Philippe Vain and Dr Vera Thole, containing more than 5000 T-DNA mutant lines (Vain et al. 2008). The transformation was performed using embryogenic calli of Bd21 with a T-DNA vector containing a green fluorescent protein and a hygromycin resistance gene used for identification of successfully transformed calli and also for mutant plant selection (Thole et al. 2012). Using the available T-DNA mutant library three mutants containing T-DNA insertions within the coding region were selected for further analyses (Fig 2-8), one line for *BdLOX1a* (*lox1a* – BdAA615) and two lines for *LOX1b* (*lox1b-1* – BdBB7035 and *lox1b-2* – BdEE8495). The three mutant lines were previously grown and selected to obtain plants homozygous for the mutation in the respective genes.

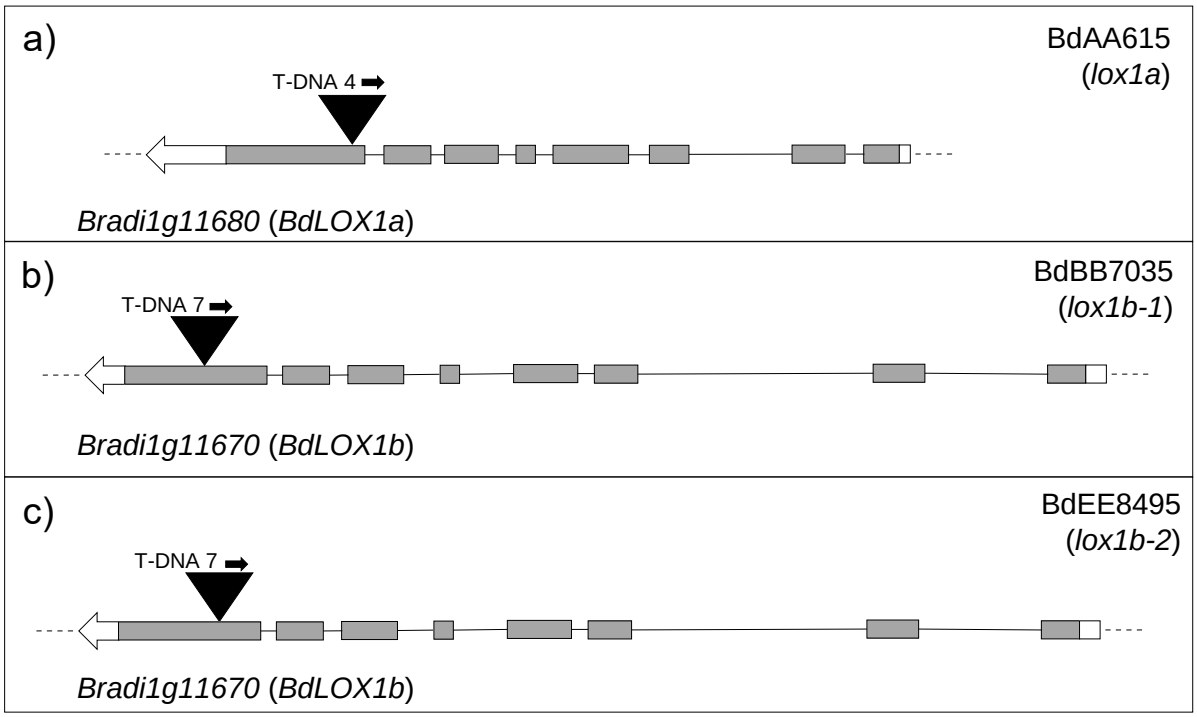

Figure 2-8 Bd genes Bradi1g11680 (BdLOX1a) and Bradi1g11670 (BdLOX1b) sequences illustrating their corresponding T-DNA insertion in the BrachyTag mutant lines BdAA615, BdBB7035 and BdEE8495. a) representation of the T-DNA insertion of mutant Bdlox1a in the eight exons of the gene sequence of BdLOX1a in the mutant line BdAA615.b) and c) representation of the T-DNA insertion of mutants Bdlox1b-1 and Bdlox1b-2 in the eight exon of the gene sequence of BdLOX1b in the respective mutant lines BdBB7035 and BdEE8495.

Seedlings of all the lines were grown and inoculated with mycelium plugs of take-all isolate *Ggt* T5-2 as done previously in section 2.3.1, but unlike previous experiments where the plugs were placed only on the middle section of the roots, they were also placed in the tip of the root, to increase the assessment of fungus infection in the roots of each mutant line. Four independent experiments were performed where the necrotic lesions were measured in the same way as previously. In the first experiment six plates with four seedlings of each mutant and its corresponding control (WT for the target gene but selected from the progeny of the original heterozygous plant) were placed side by side. Seedlings in three plates were inoculated at the tip, and the other three in the middle section of the root. This resulted in 12 seedlings per line per infection section. A pairwise ANOVA was performed but no significant difference was observed in the AUDPC of take-all between WT and mutant seedlings, with all mutant-control comparisons demonstrating a p-value >0.99, with the exeption from mutant *lox1a* in middle section infection which displayed a p-value of 0.5 (Fig 2-9a). The second

experiment was an exact replica of the first, using the same infection points, mutant lines and number of seedlings. No significant differences were obtained between the mutant lines and their corresponding control, although the overall p-value of each pairwise comparison was lower than the first experiment, with the lowest p-value originating from *lox1a* in middle section infection with a p-value around 0.12 (Fig 2-9b). The third experiment followed the same layout as the previous experiments, and again no significance was observed within each mutant line pairwise comparison with all p-values being higher than 0.99 part from mutant *lox1b-1* with the infection of the tip of the root, with a p-value around 0.25 (Fig 2-9c). The small differential observed in mutant line *lox1a* with infection in the middle section observed in the previous two experiments was lost in the third experiment with the p-value increasing to 0.99. In a fourth experiment, the lines were limited to mutant *lox1a* with both middle and tip infection, as well as mutant *lox1b-1* with only the tip infection (Fig 2-9d). No significant difference was observed with *lox1a* middle infection, having a p-value around 0.99. The difference in AUDPC between WT and *lox1a* mutant for tip infection displayed a p-value of 0.06, with the mutant lines displaying more resistance than the corresponding control line. The same is observed with mutant *lox1b-1* displaying a p-value of around 0.04. Even though it is hard to derive strong conclusions because of the lack of significant p-values in the first experiments, there was, overall, evidence for a potential, but minor, role of lipoxygenases, especially in the pathway related to the *lox1a* and *lox1b-1* mutant line, in response to take-all.

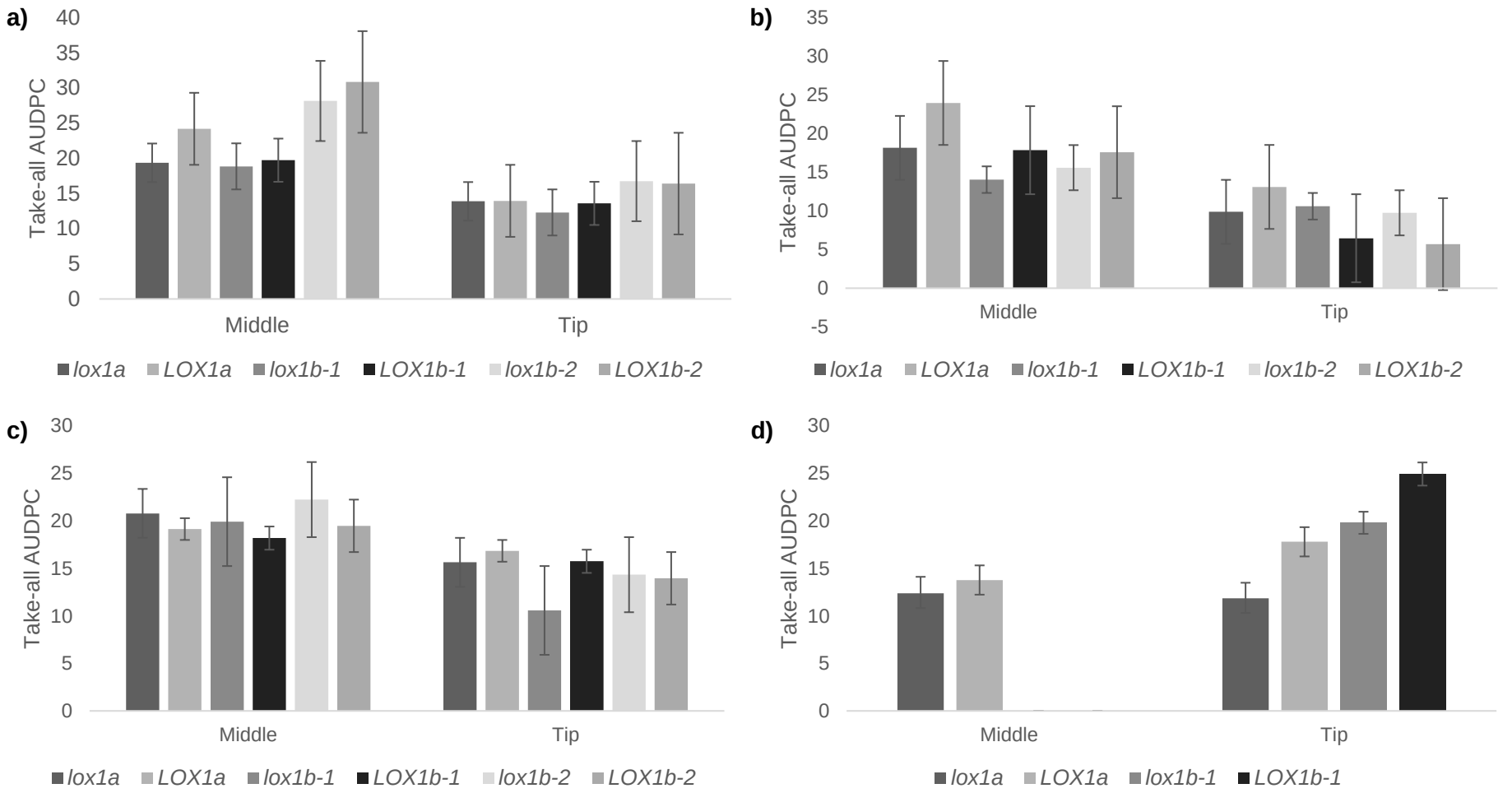

Figure 2-9 Take-all AUDPC of mutant lines lox1a, lox1b-1 and lox1b-2 and their corresponding control (LOX1a, LOX1b-1 and LOX1b-2, respectively), infected either on the middle section or on the tip of the root. a) first set, b) second set and c) third set corresponding to the study of 12 seedling of each line in their respective infection section. d) fourth set limited to middle section infection of lox1a/LOX1a and the tip infection of lines lox1a/LOX1a and lox1b-1/LOX1b-1.

Despite the inability of obtaining significant differences in the T-DNA mutant lines, a metabolomic analysis for the quantification of the 13-LOX and 9-LOX oxylipins was carried out on the line *lox1a* in order to establish which oxylipins were disrupted by the mutation in this gene. A total of 8 replicates per treatment where used, consisting of 8 seedlings each. The treatments consisted of the mutant line and its corresponding control grown for 10 days under normal conditions or infected with *Ggt* T5-2 for 4 days, to determine whether infection by the pathogen is able to induce the production of any of the compounds. To restrict the analyses to individual tissues the 8 *Bd* plants of each replicate were separated into leaf and root tissue for independent analysis. Using a LC-MS approach, the compound 9-HODE (hydroxyoctadecadienoic acid, a metabolic compound from the 9-LOX pathway) and 13-HODE (from the 13-LOX pathway) amounts were quantified. The purified version of each compound was used as control for the establishment of peaks under the LC-MS for the accurate quantification of the compounds under the experiment set up.

Measurement of the amounts of oxylipins in some replicates was unsuccessful. The most probable cause for the problems obtained in this analysis is that the amount of tissue in the samples was too low to permit quantification by LC-MS. In the root tissue quantification, the *lox1a* uninfected samples were reduced to 4 replicates for 13-HODE measurement and 5 for 9-HODE. Both *lox1a* infected and control samples were reduced to 3 replicates for 13-HODE and 9-HODE. The control *LOX1a* (WT) infected samples was reduced to 5 replicates for 13-HODE and 9-HODE, with the control uninfected samples to just 6 replicates. In the shoots, the *lox1a* infected samples were reduced to 4 replicates, and to 5 in the non-infected samples, both for 13-HODE and 9-HODE. The control infected were just reduced to 6 samples, while the non-infected contained all 8 replicates, for both 13-HODE and 9-HODE.

The remaining replicates were quantified but variation within replicate samples was high, particularly for 9-HODE in the shoot tissues (Fig 2-10). The most probable explanation is that the oxylipin concentrations in the samples might have been too close to the threshold of detection leading to the inconsistency seen between replicates due to the inability of the machine to give a precise quantification value so close to its limit capabilities.

The results do show that take-all seems to be able to induce the 13-LOX and 9-LOX pathway in the roots upon infection in both the mutant and wild type plants. However, this difference was not significant overall, although the lowest p-value was obtained with pairwise comparison between control and infected roots in the mutant *lox1a* in the 13-HODE quantification with a value of 0.014. The difference in the control and infected wild type pairwise comparison was not significant with a p-value of 0.075. Although the tendency for the infected roots to have a higher amount of 9-HODE oxylipins than the non-infected was observed none of the differences were statistically significant (Fig 2-10). When looking at the production of oxylipins in the shoots, the levels of 13-HODE were similar to the roots, however, there appeared to be a higher quantity of 9-HODE being produced (Fig 2-10). It is hard to conclude if the amounts are reliable, due to the fact that the LC-MS malfunctioned during the reading of the oxylipins of the shoot and samples had to be re-run, not only leading to the loss of replicates but also potentially creating misleading quantification values. No significant differences were observed between infected and non-infected shoot tissues, where the lowest p-value of 0.66 was observed between control 9-HODE infected/non-infected pairwise comparison. There is no evidence that mutant *lox1a* is capable of disrupting the production of either 13-HODE or 9-HODE, possibly due to the compensated effect caused by the activity of the paralogous gene *LOX1b*. It would be interesting to determine whether the double mutant of *lox1a* and *lox1b* is sufficient to completely impair the production of either 9-LOX or 13-LOX metabolites like 9-HODE and 13-HODE, and therefore obtain additional information on the potential role of oxylipins in the resistance of *Bd* to *Ggt*.

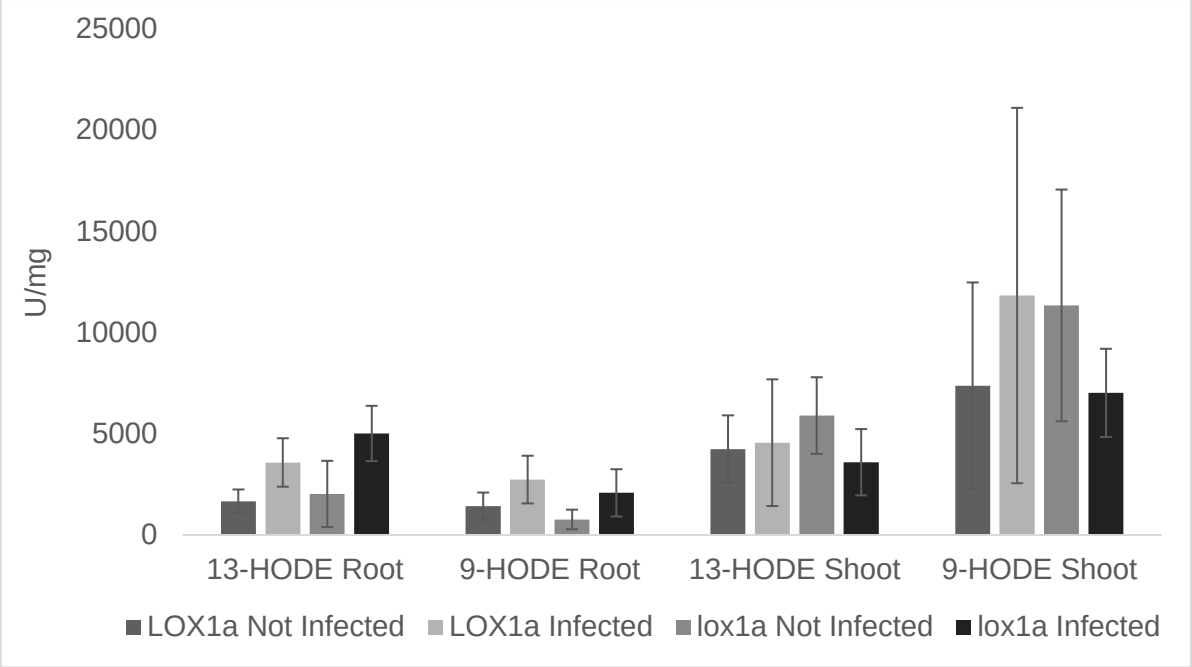

Figure 2-10 Quantification of the oxylipins 13-HODE and 9-HODE (area under the LC-MS peak measurement "U" per mg of tissue used) on the root or shoot tissue of the mutant lox1a and its control LOX1a, either under normal conditions or 4dpi by take-all Ggt T5-2.

2.4 Discussion

2.4.1 Take-all infection of different Bd accessions

Brachypodium distachyon has proved to be a powerful model for the study of several crop diseases. Such examples include the characterization of rice blast, that not only was able to demonstrate that the symptoms caused by the fungus *Magnaporthe oryzae* were similar between rice, barley and *Bd*, a resistance differential was observed when analysing a total of 21 different accession from the Brachypan panel (Routledge et al. 2004). Another similar approach using the Brachypan panel was undertaken in the characterization of wheat and barley stripe rust going further into characterizing three lines that displayed different susceptibilities to stripe rust (Bettgenhaeuser et al. 2018). By analysing the populations between the crossing of these lines, Luc1xJer1 and Luc1xFoz1, two QTL regions containing NB-LRR were found to be potential targets in conferring resistance to stripe rust (Bettgenhaeuser et al. 2018). These results provide encouragement that *Bd* has potential for the development of a pathosytem to study take-all resistance that can then be translated to

wheat and therefore give insight into novel mechanisms to control take-all infection in the field. After establishing that *Ggt* is capable of infecting the roots of *Bd*, the Brachypan panel was studied for resistance to take-all progression in the roots. A total of five independent experiments were conducted having in mind not only characterising the greatest number of accessions from Brachypan but also in re-testing their infection profile for take-all to create robust data set. The summary of the five experiments was compiled into one single dataset (Fig 2-6), demonstrating a wide range of susceptibility within the panel, from accessions that display high tolerance to disease progression to accessions that are characterized with severe necrotic lesions and premature death. A broad disease resistance to take-all is hard to obtain, especially in hexaploid wheat, with most hosts displaying a similar susceptibility to *Ggt*, with little differences in resistance among different cultivars and accessions (Palma-Guerrero et al. 2021). Most of the documented sources of resistance are observed in distant relatives of wheat, like rye and oats (Wilkes, Marshall, and Copeland 1999; Papadopoulou et al. 1999). It is predicted that the main source of resistance found in rye is derived from the production of hydroxamic acids, mainly 2,4-dihydroxy-1,4-benzoxazin-3-one (DIBOA), which was found to inhibit the growth of the fungus as low as 0.5 mM in culture media (Wilkes, Marshall, and Copeland 1999). Wheat on the other hand is only documented to mainly produced 2,4-Dihydroxy-7-methoxy-1,4-benzoxazin-3-one (DIMBOA), another hydroxamic acid, which requires higher amounts of the compound to compromise *Ggt* normal growth (Wilkes, Marshall, and Copeland 1999). In oats the main fungicide is better characterized, being part of the saponin group of molecules, the avenacins. The unusual fluorescent avenacin A-1 is important for the oat resistance to root diseases, especially to infection by *Ggt* (Papadopoulou et al. 1999). This is correlated with a sugar group present in avenacin A-1, conferring its ability to work as a fungicide, an ability which is lost once the avencin is cleaved by an enzyme, avenacinase (Papadopoulou et al. 1999). This enzyme is present in a relative of *Ggt*, *Gaeumannomyces graminis* var*. avenae*, which is capable of infecting oats (Bowyer et al. 1995). There are no studies to my knowledge that confirm the existence of avenacin A-1 or DIBOA in *Bd*, but it is unlikely that these are the source of resistance observed in the panel,

as there is no evidence that these compounds work in a dose-dependent manner, which would be the most likely scenario to explain the differential between the lines if the cause of resistance was attributed to the production of a single antifungal agent.

Although, the different levels of resistance observed in the panel might not be associated with the production of a single compound, it is possible that it derives from a crosstalk between different responses in the plant. This scenario has been observed in the screening of several lines of diploid *Triticum monococcum*, a wheat relative closed linked to the ancestor of the group A chromosomes, which displayed a similar differential response to *Ggt* (McMillan, Gutteridge, and Hammond-Kosack 2014). By analysing 34 different lines of *T. monococcum* grown over a period of five years in field conditions, a total of five lines displayed moderate resistance to take-all infection, while two lines, MDR031 and MDR046, displayed consistent high resistance over all the different trials (McMillan, Gutteridge, and Hammond-Kosack 2014). By performing diversity array technology genotyping between the whole genome of *T. monococcum*, no specific relationship was established to a potential source of resistance to take-all, suggesting a more complex response of these lines to the fungus infection (McMillan, Gutteridge, and Hammond-Kosack 2014). This scenario could be translated to the *Brachypodium* panel, where a similar diverse and complex response by *Bd* was observed. McMillan and colleagues theorise that the resistance could be linked to the geographical location of where the lines of *T. monococum* originated from, with both lines MDR031 and MDR046 originating from southeast Europe/Turkey region (McMillan, Gutteridge, and Hammond-Kosack 2014). Such correlation is not observed in the present study, with lines originating from Turkey and Spain, along with the *Bd* lines associated with late flowering, displaying similar differentials in response to take-all, with no specific group being significantly more resistant than the other.

In order to identify other sources of resistance that can be translated or transferred into hexaploid wheat, other distant relatives of wheat have also been assessed for their ability to respond to take-all. One such resistance has been identified in *Haynaldia villosa*, a species

already used as a subject of gene transfer in order to improve wheat's ability to withstand certain diseases (Chen et al. 1995; Yildirim et al. 2000; Li et al. 2002), or to increase its quality (De Pace et al. 2001). An amphiloid hybrid between *Haynaldia villosa* and *Triticum durum*, TH3, is also highly resistant to take-all (Ren et al. 2003). A crossing between TH3 and wheat was performed, and the F1 population analysed, showing a promising resistance originating from chromosome 3 of *Haynaldia villosa* (Huang et al. 2007). A similar approach was performed using the take-all resistant wild wheat relative *Psathyrostachys huashania* Keng hybrid with wheat, where a chromosome 2Ns substitution from *Psathyrostachys huashania* with chromosome 2D from wheat, exhibited enhanced disease resistance to take-all (Bai et al. 2020). Both studies display a potential strategy for conferring resistance in wheat against take-all, but rely heavily on the stability of the resistant chromosome region insertion from wild relatives. In this study, *Bd*, a closer relative of wheat, shows a promising contribution to understanding take-all resistance. By understanding the genetic and mechanistic basis of resistance to the fungal spread in the roots observed in the Brachypan panel it could provide a better understanding of promising pathways for take-all resistance that could be directly translated into wheat without the need for chromosome transfer.

Although direct wheat resistance to take-all has not been established, mainly due to the high susceptibility of most hexaploid wheat cultivars, different mechanisms to control take-all build up in the soil have been observed. McMillan and colleagues have proved that by using several cultivars of wheat in field conditions, several differences have been observed during the TAB in the first year (McMillan, Hammond-Kosack, and Gutteridge 2011; McMillan et al. 2018). This correlation between certain cultivars and low TAB in the first year led to low take-all development in the following years, reflected in a higher yield when compared to wheat cultivars grown in higher TAB soil (McMillan et al. 2018). Even though an association between certain cultivars in promoting low TAB in the soil was established, it is believed that other environmental and rhizosphere biomes also influence the TAB, making the study of the genetics behind the correlation between wheat cultivars and TAB hard to establish (McMillan

et al. 2018). It would be interesting to establish whether the accessions from the Brachypan panel that show a high tolerance to the disease, can also contribute to low TAB in the soil, thus making the association between plant genetics and TAB easier to establish by using the Brachypan panel sequenced genomes.

By studying the differential in disease resistance in the Brachypan panel, when looking at their p-values, the best differential between parents was observed between the accessions Luc1 and Jer1, where Luc1 was the most susceptible parent and Jer1 the most resistant. This is reminiscent of Bettgenhaeuser et al, 2018, where Luc1 and Jer1 showed significant differences in their response to wheat stripe rust, with Luc1 displaying a large area of leaf infection and leaf browning at 14 days post infection with *Puccinia striiformis* f. sp. *tritici*, and Jer1 displaying no leaf browning and scattered localized points of fungus infection that failed to efficiently spread within the leaf tissue (Bettgenhaeuser et al. 2018). Foz1, another *Bd* assession, was also crossed with Luc1, as it shows the same phenotype as Jer1 in the stripe rust leaf infection (Bettgenhaeuser et al. 2018). Both crosses were performed and taken to F2 generation where a genetic map was created using 179 genotyped lines for the Foz1xLuc1 crossing and 188 lines for the Jer1xLuc1 crossing. In order to try to localise the genetic regions involved in the resistance phenotype to stripe rust, quantitative trait loci (QTL) analyses were performed. The QTL analyses of the crossing of Foz1xLuc1 demonstrated that Foz1 resistance is mainly conferred by two major effects within its genome, the biggest effect coming from chromosome 4, named loci *Yrr1*, with the second highest effect coming from chromosome 2, named loci *Yrr3*. The analyses of the crossing between Jer1xLuc1 identified one major resistance region in Jer1 co-localising with *Yrr3* (Bettgenhaeuser et al. 2018). It is conceivable that the resistance of Jer1 against stripe rust, could be involved in resistance against take-all. However, it is probably not the main source of take-all resistance in this accession. The resistance of Foz1 to stripe rust, derives from locus Yrr1 and from locus *Yrr3*, which it shares with Jer1. Foz1 does not, however, display a similar level of resistance to take-

all as Jer1, making it unlikely that the NB-LRR cluster in locus *Yrr3* is the main cause of the resistance of this accession to take-all.

The differential observed between Jer1 and Luc1 also appeared to be restricted to isolate *Ggt* T5-2, where three out four experiments showed a significant difference with a p-value lower than 0.0001 between Jer1 and Luc1. On the experiment where some significance was lost, the differential between the two lines was still maintained over most of the period of infection, only losing its differential at 10 dpi (Fig 2-4), where the p-value rose to 0.007, but still remained statistically significant. The differential between the two accessions was lost when using different isolates of *G. gramminis*, *Ggt* 18e and *Ggt* 1d, with Jer1 losing its resistance phenotype and having a similar level of susceptibility to that of the susceptible parent Luc1 (Fig 2-7), with the lowest p-value being around 0.3 between the two independent experiments. As there have been no reports to date of race -specific resistance within *Ggt* it is more likely that the difference in response to the different isolates relates to differences in their aggressiveness. Isolate *Ggt* T5-2 may be considered to be moderately aggressive and use of this isolate revealed small but significant differences in the resistance of accessions Jer1 and Luc1. This differential in resistance was lost when using isolates *Ggt* 18e and *Ggt* 1d and it is probable that this was because of the greater aggressiveness of these isolates than isolate T5-2. Isolate T5-2 was itself variable in its virulence, as is evident in Fig 2-3 where the second experiment Jer1 was more susceptible than in the first experiment, possibly due to a higher aggressiveness of the isolate or more disease-conducive conditions. This is also observed in the variation within each accession, where in the overall analysis (Fig 2-6) the average standard deviation within each accession stood at around 28 %. This indicates the importance of the use of different isolates in order to tackle variable disease phenotypes. Differences in plant resistance to different isolates of *Ggt* has been poorly documented, with the majority of wheat varieties having similar susceptibility to the disease (McMillan, Gutteridge, and Hammond-Kosack 2014). The occurrence of isolates with different levels of virulence towards wheat infection has however been documented, with most isolates

displaying moderate to severe disease root infection (Kwak et al. 2009). Although differences in virulence were observed, the focus of the study by Kwok and colleagues was more focused in the rhizosphere interaction between *Ggt* and *Pseudomonas fluorescens* (Kwak et al. 2009), leading to a very general and not robust study between the interaction of wheat roots and different *Ggt* isolates. In this study the differences in aggressiveness of the *Ggt* isolates were crucial in the understanding of consistent disease resistance from the different *Bd* accessions. The resistance phenotype from Jer1 to isolate T5-2 collapsed upon infection with isolates that displayed a higher level of aggressiveness in infection. Due to this resistance collapse and the variation in disease symptoms, a QTL analyses in order to identify resistance loci from the F5 population of Jer1xLuc1, with only around 192 lines, would be highly challenging, making the population analysis impractical to perform.

Race-specific resistance is often observed against biotrophic and hemi-biotrophic pathogens (Jones and Dangl 2006). An example comes from the beforementioned study by Bettgenhaeuser et al, 2018, where locus *Yrr1* was not consistently associated to resistance to all isolates of wheat stripe rust and did not seem to be involved in conferring resistance to barley stripe rust B01/2 (Bettgenhaeuser et al. 2018). Locus *Yrr3* on the other hand was associated with resistance to all the isolates used in the study. Another study observed different responses of *Bd* accessions to the fungus *Magnaporthe oryzae*, the causal fungus of rice blast, where isolate IE1K was the most aggressive, being able to efficiently infect most of the accessions of *Bd* after just two dpi (Sandoya and Buanafina 2014). Isolates IA45 and 18-1, however, displayed a big diversity between their infection profile in the accessions of *Bd*, with only slight signs of infection observed at 5 to 6 dpi, followed by no disease progression after 8 dpi (Sandoya and Buanafina 2014). In the same study, *Sclerotinia homoeocarpa*, the causal soil-borne fungus of dollar-spot disease, also had an aggressive isolate, S005044B, which produced highly susceptible phenotypes in the accessions of *Bd*, while isolate 241 ShMp-2 only generated intermediate levels of susceptibility (Sandoya and Buanafina 2014).

Despite the difficulty of analysing the Jer1xLuc1 population the Brachypan has displayed potential as a tool to study resistance to take-all with data on its progression in the root system, something that is not achievable using wheat. Due to the constrains involving the difficulty in crossing different *Bd* accessions and the short amount of time during the thesis to produce a reliable population, no further action was taken in the characterization of other resistant accessions identified in this chapter. However, the large differential in resistance to take-all among the accessions could be exploited in future studies by producing new populations using accessions that display differences in response like a combination from resistant accessions Koz5, Gaz8, Koz1, Kah5 and Sig2; and the susceptible Koz3, ABR6, ABR2 and BdTR12b.

2.4.2 Take-all infection of Bd putative 9-LOX mutants

The study of different accessions of *Bd* provides encouragement of its use to study the response to take-all, establishing a system where infection rates can be measured in real time and compared, creating a powerful tool for take-all research. Due to their involvement in disease response, the 9-LOX jasmonates became of particular interest, particularly as they have also been shown to have a role in root development (Vellosillo et al. 2007). In order to establish their role in the roots and defence against pathogens, a selected set of mutants from the BrachyTag library was investigated to examine their potential role in resistance to take-all. Using the 9-LOX genes identified in Arabidopsis (*AtLOX5*) and maize (*ZmLOX3*/*4*/*5*), two genes were identified as being potential 9-LOX genes in *Bd*, *Bradi1g11670* (*BdLOX1b*) and *Bradi1g11680* (*BdLOX1a*). Using BrachyTag mutant collection, three mutants suffering T-DNA insertions within their coding sequence were selected, one for *BdLox1a* (BdAA615 – *lox1a*) and two for *BdLOX1b* (BdBB7035 – *lox1b-1* and BdEE8495 – *lox1b-2*). Four experiments were conducted to evaluate whether the mutants displayed any differential response upon *Ggt* infection (Fig 2-9). In all four experiments no significant differential was observed between the AUDPC of the mutant and its corresponding wild-type sister line. Disease levels in the *lox1a* mutant tended to be less than those of the WT sister line although this difference was not

significant except in in the third experiment (p-value of 0.06) in the infection of the root tip (Fig 2-9d). The mutant *lox1b-1* also demonstrated a potential role as a susceptibility factor, where the p-value in the fourth experiment was 0.04 (Fig 2-9d). Although not significant overall, there was a slight decrease in take-all symptoms in these two mutants, which might suggest that the two genes are redundant with each other and able to complement the effect of the other when one is disrupted. So even though a promising effect is visualized, a significant effect is not observed due to the expression of the other gene. This is further validated when looking at the LC-MS quantification of 13-LOX and 9-LOX oxylipins, 13-HODE and 9-HODE respectively. No significant differences were observed in the production of either of the two compounds when comparing their quantities in the mutant *lox1a* against its respective control in the roots and shoots of *Bd* (Fig 2-10). When comparing to infected roots and shoots, there is a slight increase of both 9-HODE and 13-HODE production, however this increase is similar between the control and the mutant, where the higher production of the two oxylipins does not seem to have been disrupted by the lack of a functional BdLOX1a (Fig 2-10). This is also observed in maize, where the production of 9-LOX derived oxylipins is abolished in the mutant lines containing a disruption in Zm*LOX3*, Zm*LOX4* and Zm*LOX5*, but mutant lines Zm*lox3*, Zm*lox4* and Zm*lox5*, and double mutants Zm*lox3/5* and ZM*lox4/5* show no significant change to the production of 9-LOX oxylipins in the plant (Christensen et al. 2014; Christensen et al. 2015). Although technically challenging, the production of double mutants using *Bd* is required to establish whether this is the case for BdLOX1a and BdLOX1b.

It is possible that inoculation was carried out at the wrong stage to identify an effect of disruption of the LOX1 genes. Since the 9-LOX mutant has been observed to produce more lateral roots (Vellosillo et al. 2007), it could be that in an older seedling where potentially more lateral roots have been formed, the infection would be reduced due to the fact the plant had a more elaborate root system that it could use to compensate for the infection of individual roots. This is also hard to visualize, due to the fact that the current methodology is constricted by the size of the plastic box used for these experiments, where letting the seedling grow for longer would cause stress due to its inability to expand beyond its boundaries.

However, it is promising to observe a potential role of the 9-LOX pathway in the response against take-all, an interaction that has not been reported until now, and hopefully when using more advanced technologies and the ever-growing libraries available to study crops, a proper assessment can be made in understanding the mechanisms of take-all resistance using the 9-LOX derived oxylipins.

Overall, the work reported in this chapter shows how *Bd* can be used to do a rapid and real-time assessment of resistance to take-all, something that was not achieved in crops before. It was also possible to obtain a panel of *Bd* accessions showing a wide range of responses to take-all, from resistant to highly susceptible lines. Most cereal crops, especially wheat, are predominantly susceptible to take-all, making it difficult to study any population with great success (McMillan, Gutteridge, and Hammond-Kosack 2014). Although the available populations in *Bd* do not illustrate the best differential in the panel, it is promising to see such a response from a close relative of wheat, paving the path forward to use this material to understand take-all infection and create model-to-crop translation models capable of battling such disease.

Chapter 3. Variation in *Fusarium* root rot resistance among *Brachypodium distachyon* accessions

3.1 Introduction

Fusarium diseases are one of the most destructive crop diseases worldwide, being capable of infecting a diverse number of crop plants, where wheat is one of the most affected. The most common *Fusarium* disease in wheat is *Fusarium* Head Blight (FHB). FHB is characterized by the penetration of the fungus into the spikelet of the plant during mid-anthesis, leading to the bleaching of the spikelet and the production of shrivelled poor-quality grains (Guenther and Trail 2005). The bleaching of the spikelet is mainly caused by a mycotoxin produced by the fungus, called deoxynivalenol (DON) which can be toxic to humans, which has led to legislation on the amount of the toxin that can be present in the grain (Desjardins and Hohn 1997; Fung and Clark 2004; US FDA 2010). These combined events lead to a considerable reduction of yield and a huge loss of income for the wheat industry. *Fusarium* species, *Fg* and *Fc,* are capable of not only infecting the florets of wheat, but also penetrate the root tissue, normally through tissue disrupted on the emergence of the primary root, but also through root hairs and during the formation of secondary and auxiliary roots, leading to what is known as *Fusarium* root rot (FRR) (Beccari, Covarelli, and Nicholson 2011). This route of infection is not so well known and characterized as the more famous FHB and presents added difficulties for conducting an early detection of the disease in the field. It also proves to be a challenge to recreate the disease in a robust system *in vitro* where the study of the infection of wheat roots by *Fusarium* is difficult and generally involves a destructive analysis of the root system thereby preventing continued real-time investigation of infection and colonisation. Another difficulty in limiting the effects of FRR in the field is the fact that *Fusarium* has a biotrophic phase where it grows and colonizes the roots of the crop without showing any symptoms (Kang and Buchenauer 2000). When it transitions to its necrotrophic phase, it is characterized by an increased production of trichothecenes, like DON, and cell

wall-degrading enzymes leading to necrotic lesions and the eventual death of the root system and the entire plant (Kang and Buchenauer 2000).

Due to the difficulties arising from studying root rot there is a large imbalance of studies between FHB and FRR, leaving the search for a source of resistance to FRR an obscure topic in the *Fusarium* story. The most relevant discoveries for unravelling the mechanisms of FRR response in the plant was by using the closest still visible tissue to the root system, the crown of the plant, located between the beginning of the root system and the main stem of the plant. One of the most relevant experiments on *Fusarium* crown rot (FCR) from the perspective of the present study was the analyses of the transcriptional similarities between the *Bd* and wheat responses to the fungus (Powell et al. 2017). A large number of pathogenesis related (PR) genes were similarly up-regulated in both species, where PR1, PR2 and PR3-like genes were significantly increased at 7 dpi (Powell et al. 2017). Other pathogen related responses were also observed, like the increase of pathogen sensing and signalling like molecules, such as leucine rich repeat receptor-like kinases: WRKY, MYB, NAC transcription factors: ABC transporters: as well as an increase in expression of genes involved in metabolism of reactive oxygen species (Powell et al. 2017). All these are well known *Fusarium* response genes in wheat, indicating that there is strong synteny between the two species in response to *Fusarium*. This was further proved by the similar induction of several genes belonging to phenylalanine and tryptophan biosynthesis, known indicators of a *Fusarium* response in wheat. The only significant different between *Bd* and wheat in their response to FCR was the absence of benzoxazalinones, like BOA and MBOA in *Bd*, which are highly expressed in wheat. This lack of induction was visualized in several accessions of *Bd*, suggesting that the absence of synthesis of these compounds is conserved in the *Bd* panel. Barley has also been previously reported not to be able to produce benzoxazalinones but rather produce the phytoalexin gramine, however, even though *Bd* is more closely related to barley than wheat, it does not synthesise gramine either, suggesting it might have a different pathway for the production of phytoalexins (Powell et al. 2017). These findings could demonstrate that *Bd*

might possess novel pathways not found in wheat and barley involved in its response to *Fusarium*, potentially leading to new sources of resistance not yet discovered.

It is widely accepted that the most cost-effective means of controlling *Fusarium* diseases of cereals is through the deployment of resistant varieties. Several studies have been conducted in dissecting wheat resistance to FCR using quantitative trait locus (QTL) analysis to identify chromosome regions responsible for partial resistance to the disease. A total of 25 independent studies have been conducted finding potential sources of disease resistance in more than 40 different QTL regions. These are described in more detail in the next chapter but the main conclusion from the majority of the publications is that FCR resistance relies on a combination of multiple genes, with no evidence for major gene resistance, demonstrating how complex the relationship between *Fusarium* and wheat can be when it comes to the host resistance to the fungus.

Other alternative methods have been proposed, like the use of biological control agents to minimize the growth of *Fusarium* in the soil. One example is the use of different *Streptomyces* isolates, where inhibitory strains of the Gram-positive bacteria are able to considerably reduce the amount of *Fusarium culmorum* growth in the root system, when grown with the plant before inoculation (Winter et al. 2019). Interestingly, when grown on the presence of non-inhibitory strains of the bacteria, *Fusarium culmorum* grew to higher amounts than the control, along with higher amounts of *Streptomyces* in the rhizosphere (Winter et al. 2019). Interestingly, *Fusarium* as also been shown to be able to tackle the inhibitory properties of *Streptomyces,* where *in vitro* most of the *Fc* isolates where able to counter the inhibitory strains of the bacteria (Winter et al. 2019). This dynamic interaction between the fungus and the bacteria in the field demonstrated to be crucial, where the initial biomass in the soil of each microorganism might prove to be the decisive factor in controlling FRR and FCR in wheat.

Most studies on *Fusarium* infection have been conducted in the head or the crown of the plant, with only a very limited amount of work on FRR development. This is mainly due to the difficulty in characterizing the disease progression without resorting to a destructive

approach. In this chapter the methodology employed in the characterization of take-all in the roots of *Bd* will be adapted in the analyses of FRR to establish one of the first real time studies in FRR development in the roots. In addition, a series of tests will be conducted to identify possible sources of resistance to FRR in the Brachypan panel.

3.2 Materials and Methods

3.2.1 Brachypodium lines, seedling preparation and inoculation:

The Brachypan panel accessions and seedling preparation were the same as the previous chapter. The exception was made for the reassessment of the experiments comprising Fig. 3-5 and Fig. 3-6 where the roots were all infected in the primary root tip with *Fg* slurry instead of a mycelium plug. The slurry was obtained by blending Petri dish culture colonies using a conventional food processor and applied to the root tip using single droplets from a 15 mL conventional syringe. The slurry was then removed after 2 days, so that *Fg* had its the main source of nutrients and fungus inoculum originating from the root system.

For the analyses of the overall death the seedlings remained in their original trays and the senescence of the plant was scored and photographed every two days between 14 days to 21 days after inoculation. Each line was scored with a number from 0 to 3 in relation to its senescence due to the disease (Table 3-1).

Table 3-1 Score system for the assessment of overall death of the seedling by Fusarium graminearum infection.

Score number	Score description
0	Green leaves with no visual hyphal growth.
1	Some hyphal growth can be seen. Necrosis of the tip of the leaves and the petiole.
2	Leaves are shrivelled with some patches of green tissue. Hyphal growth present in the majority of the tissue.
3	Leaves completely necrotic with high density of fungal growth.

3.2.2 Fusarium cultivation and maintenance:

Fg DON producing isolate K2-5 was cultivated using mycelium plugs from a cryopreserved existing stock. The mycelium plug was transferred into a Petri dish containing either V8 media (1.8 % Bacto Agar DIFCO, 20 % commercial V8 solution) or PDA media (3.9 % PDA DIFCO). The fungus was then placed for 2-3 days in a 22 ºC growth chamber with a 16 h/8 h light/dark cycle. The inoculation procedure was the same as used previously in Chapter 2.

3.2.3 Data analysis:

The data analyses and statistics were performed like the previous chapter. No transformation of the scores was needed for any dataset.

3.3 Results

3.3.1 Initial analyses of Fusarium root rot development in the Brachypan panel under infection of the middle section of the root

The previous studies demonstrate that FRR and FCR study in wheat is difficult even though positive results were obtained in most studies. For this reason, there is a need to use a simpler model to try to minimize the variation caused by large polyploid genome species like wheat in which effects of one homoeologue may be masked by those of others. Previous work has demonstrated that *Bd* shows a similar phenotypical and gene expression response to *Fusarium* infection to that of wheat and barley. Coupling with the successful root assay system developed in the previous chapter to study take-all disease progression in the roots, the same strategy was employed for the study of differential resistance responses against *Fusarium* using the Brachypan panel. The first two lines used were Bd21 and Bd3-1, as the parents of the most developed population available for *Bd* (Garvin et al. 2008). Just like take-all in the previous chapter no significant differences were observed in resistance of these two accessions (Fig 3.1), with a p-value around 0.7.

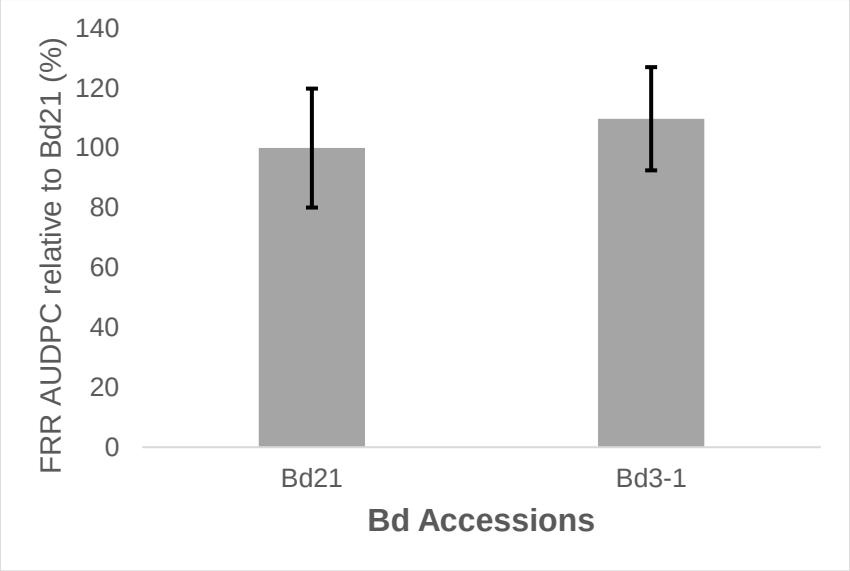

Figure 3-1 FRR disease progression in the roots of Bd accessions Bd21 and Bd3-1. The disease progression was calculated relative to the control accession Bd21. Error bars represent standard deviation.

The next step was to test the first set of 32 Brachypan accessions that include the parents of current *Bd* populations like the previous chapter. A smaller differential between the different accessions was observed when compared to the differential observed for take-all, with the majority of the accessions falling between 80 to 120% when compared to Bd21 infection rate (Fig 3-2). *Fg* generally displayed faster formation of necrotic lesions in the roots than *Ggt* in all accessions, demonstrating necrotic lesions after 24 hours, when compared to *Ggt* that only started producing necrotic lesions around 2-3 dpi. Another phenotype that was commonly observed in the majority of the accessions under FRR, and not observed under take-all, was the disruption of the primary root growth upon contact with *Fg*, leading in some cases to an increase in the formation of lateral and secondary roots. The growth of the lateral and secondary roots were also disrupted if they came into contact with *Fg* hyphae.

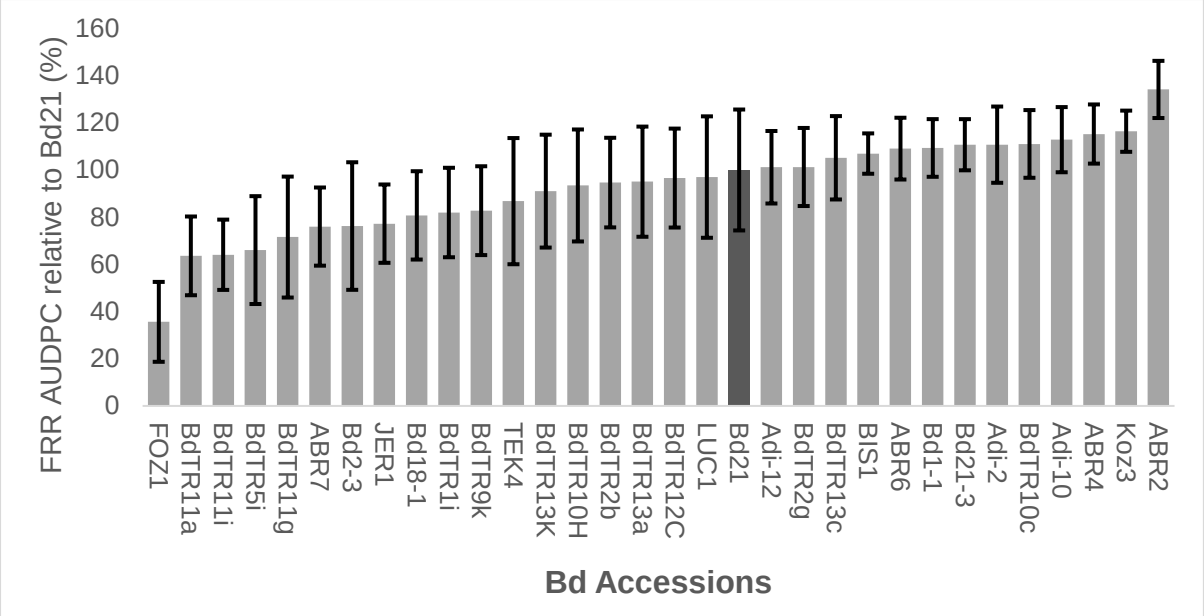

Figure 3-2 Disease score of FRR AUDPC progression relative to Bd21 (bold grey) for 32 accessions of the Brachypan panel including the parents of known Bd populations (Bd21, BdTR13k, Tek-4, BdTR10h, ABR6, Luc1, Jer1, Foz1, Bd2-3, Bd1-1, Koz-3, BdTR12c). Error bars represent standard deviation.

When seeking potential parents from which a population can be used to study genetic responses to FRR, the major differential observed was between Luc1 and Foz1, with a p-value lower than 0.0001. Luc1 was also one of the parents used in the analysis of take-all resistance in the Luc1 x Jer1 population discussed in the previous chapter. The Luc1 and Jer1 differential in *Fg* infection is however lower than that under take-all with a p-value of 0.0120. The only other parental duo that displays a low p-value is that between Bd21 and Bd2-3, with a p-value around 0.0017. No other parents of mapping populations exhibited significant differences in FRR resistance, and all other comparisons displayed a p-value higher than 0.7, highlighting the population of Luc1 x Foz1 to be the best candidate for a population analysis against FRR.

The remaining Brachypan panel accessions demonstrated a greater range of susceptibility to FRR than the first set, with lines Koz5, Per1, Gaz8, Koz1, Sig2 and Kah5 showing the greatest resistance to the development of FRR (Fig 3-3). Gaz2 also displayed more susceptibility than the most susceptible line from the first set, ABR2 (Fig 3-2), showing on average up to 74 % more severe symptoms than Bd21 (Fig 3-3), followed by ABR2 and Gaz1 with 34 % (Fig 3-2) and 32 % (Fig 3-3) respectively.

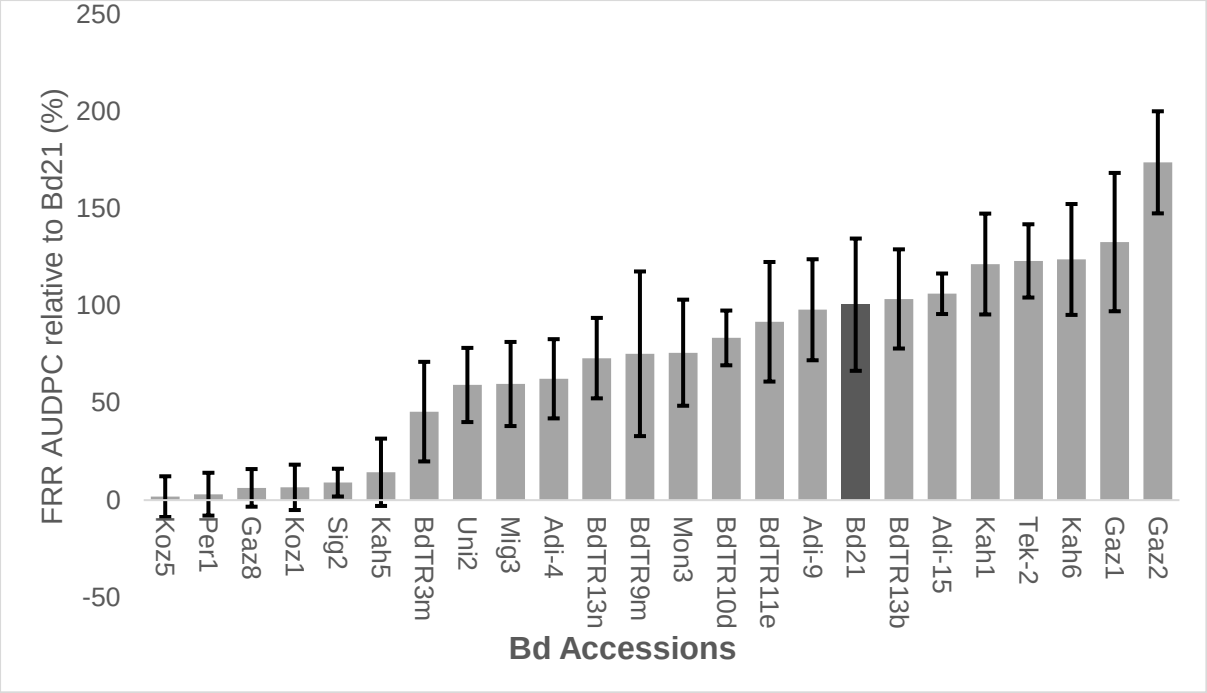

Figure 3-3 FRR AUDPC on the third set of Brachypan containing the remaining Bd accessions. Each accession was relativised to Bd21 (dark grey). Error bars represent standard deviation.

In order to assess whether the phenotypes are consistent between experiments, part of the Brachypan panel was infected in two additional independent experiments similar to chapter 2. The focus was mainly directed to the lines that showed the most resistant and susceptible phenotypes. All datasets were combined, and a general histogram was created containing the first three original datasets along with the two additional experimental repeats (Fig 3-4). Lines Koz1, Kah5, Ko5 and Sig2 remain significantly more resistant than Bd21, although with a higher relative AUDPC than the previous experiment, having similar susceptibility to that of Foz1 that maintained its relative AUDPC from the first experiment. The accessions Gaz1 and Gaz2 remained among the most susceptible lines, followed by Tek-2 and BdTr12b that displayed an increase in their relative AUDPC by 24% and 114%, relatively.

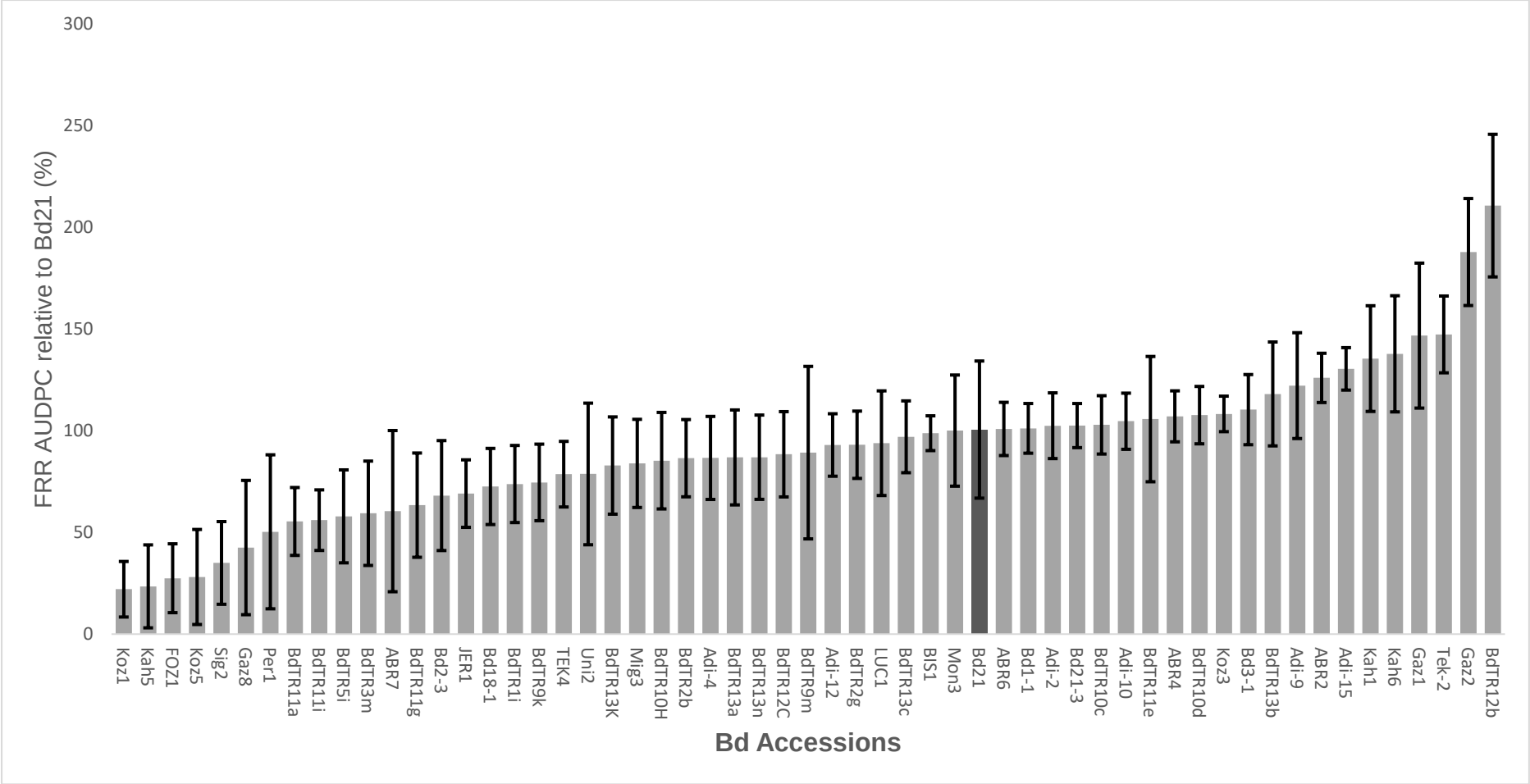

Figure 3-4 FRR AUDPC of the Brachypan accessions from the conjugation of the previous three experiments with two repeats performed on selected accessions. Their overall AUDPC were calculated and relativized to that of predicted overall score of Bd21 (dark grey). Luc1 and Foz1 were the most differentiated parents observed in this analysis. Error bars represent standard deviation.

By analysing the pairwise comparison of the parent lines of existing *Bd* populations, Foz1 and Luc1 continued to display a good differential between each other, with a p-value of $2.4206e^{-11}$, indicating the potential of this population to study FRR resistance. The next parents that showed an interesting differential was between lines Bd3-1 and Bd2-3, with a p-value of 0.0007 (Table 3-2), however the relative AUDPC of the most resistant line Bd2-3 is still relatively high which might cause difficulties when performing a population analysis. The remaining parent differentials had p-values higher than 0.38 (Table 3-2), including the differential between Luc1 and Jer1, that in the previous chapter had significantly different levels of resistance against take-all disease.

Table 3-2 Bd accessions parents of developed populations with their respective p-value and predicted means for FRR necrotic lesions progression on the roots. The analysis was performed using an ANOVA pairwise comparison.

Parent 1	Parent 2	p-value	Score Parent 1	Score Parent 2
Bd21	BdTR13k	0.9999	100.6	82.91
Tek-4	BdTR10h	0.9999	78.66	85.3
Bd21	ABR6	0.7337	100.6	100.91
Luc1	Jer1	0.5676	93.9	69.11
Luc1	Foz1	<0.0001	93.9	27.49
Bd21	Bd3-1	0.4831	100.6	110.4
Bd2-3	Bd21	0.3787	68.14	100.6
Bd3-1	Bd1-1	0.9999	110.4	101.19
Bd3-1	Bd2-3	0.0007	110.4	68.14
Bd21	Bd1-1	0.9999	100.6	101.19
Koz-3	Bd1-1	0.9999	108.3	101.19

3.3.2 Re-analyses of the Fusarium root rot progression in Brachypan panel under primary root tip infection

The F2 population of the crossing between Luc1 x Foz1 was kindly donated by the Moscou group at The Sainsbury Laboratory, in a similar strategy to the previous chapter, and was taken to the F5 population. Since infection in the middle section of the root could be variable, and *Fg* has the ability to disrupt the primary root growth, it was proposed to check the infection pattern of the parents Luc1 and Foz1 by direct infection of the root tip. This was made with the intention to observe if by disrupting the growth of the primary root, a more consistent increase in necrotic lesions per day could be observed, thus contributing to a

clearer assessment of the population. Since there is the possibility of variability in *Fg* fitness and virulence from different Petri-dish cultures, potentially contributing to variability within the experiment, a blended mycelium slurry from all growth plates was used to homogenise the *Fg* mycelium within the experiment. When using the combined strategies of root tip infection with mycelium slurry, in the first analyses there was no differences between Luc1 and Foz1, both having very similar growth rate of infection (Fig 3-5), where the lowest p-value was around 0.82 at 5 dpi. In the second analyses, Foz1 did demonstrate lower infection than Luc1 at 7 and 10 dpi (Fig 3-5), with a p-value <0.0001. It is noticeable however that the virulence of the fungus is considerably reduced when compared to the growth rate of the first experiment with a reduction in the final necrotic AUDPC of the susceptible accession Luc1 by two thirds, from 15 to just 5, and Foz1 from 15 to 3 (Fig 3-5).

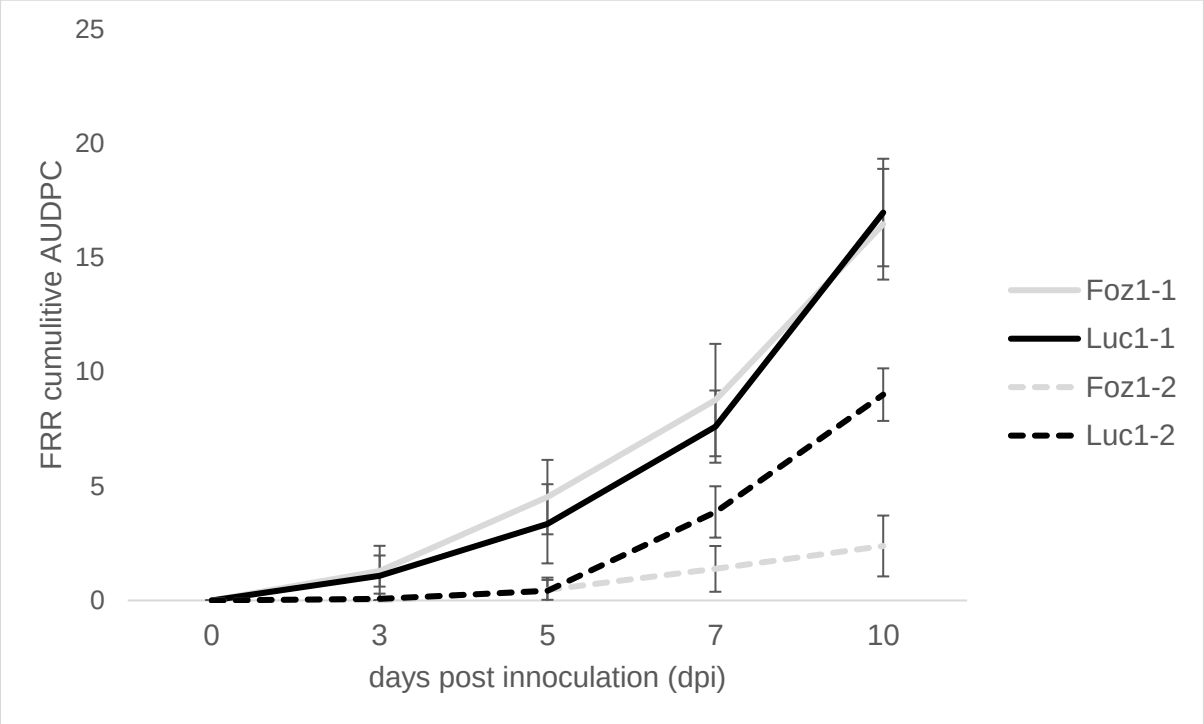

Figure 3-5 Cumulative AUDPC of FRR from two independent experiments using the Bd accessions Foz1 and Luc1. First experiment displays higher infection between Foz1-1 and Luc1-1 when compared to second experiment. The second experiment displays an increase in its differential between Foz1-2 and Luc1-2 on the last two experiment days. Error bars represent standard deviation.

Since the reanalyses of the parents Foz1 and Luc1 under new methodology led to a loss of differential, especially in a higher disease pressure, it was decided to reanalyse the entire Brachypan panel with a fresh stock of *Fg* using the root tip infection with a homogenized mycelium slurry. The fresh stock of *Fg* came from the collection of frozen isolates in the laboratory, making it a reliable source of a virulent strain of the fungus, making it possible to analyse the response of the panel to the same level of virulence throughout the experiment. The scoring of the disease proved to be more consistent, with the lines varying between 54 to 120 of relative AUDPC. Lines Koz1 and Sig2, still displayed more resistance than Bd21, however their relative AUDPC increased from 22.08 and 35.01, to 56 and 70 respectively (Fig 3-6). Accessions Koz5 and Kah5 also showed an increase in their relative AUDPC, losing the resistance observed in the previous experiment, being more closely comparable to Bd21, with a new score of 86.28 and 105.47, respectively (Fig 3-6). Lines Gaz1 and Gaz2, although not demonstrating a high relative AUDPC like in previous experiments, remained susceptible to the fungus (Fig 3-6), with scores of 95.2 and 97.28, respectively. Accession Tek-2 went from being one of the most susceptible lines to the most resistance line of this set (Fig 3-6), decreasing from a relative AUDPC of 147.38 to 53.89. Due to having the same level of virulence through the entire set, this led to most of the lines having very similar infection patterns. Unfortunately, the Foz1 and Luc1 differential was lost, where the two lines have identical infection patterns, with a p-value of 0.43, making the use of the Foz1 x Luc1 population not worth pursuing. The only other parent differential lower than Foz1 x Luc1, is between lines Bd1-1 and Bd3-1, with a p-value of 0.0016. However, like the differential observed in the previous experiment between Bd2-3 and Bd3-1 (Table 3-2), the limited differential in susceptibility observed between these accessions suggests that identifying genetically based differences would be difficult during the population analysis.

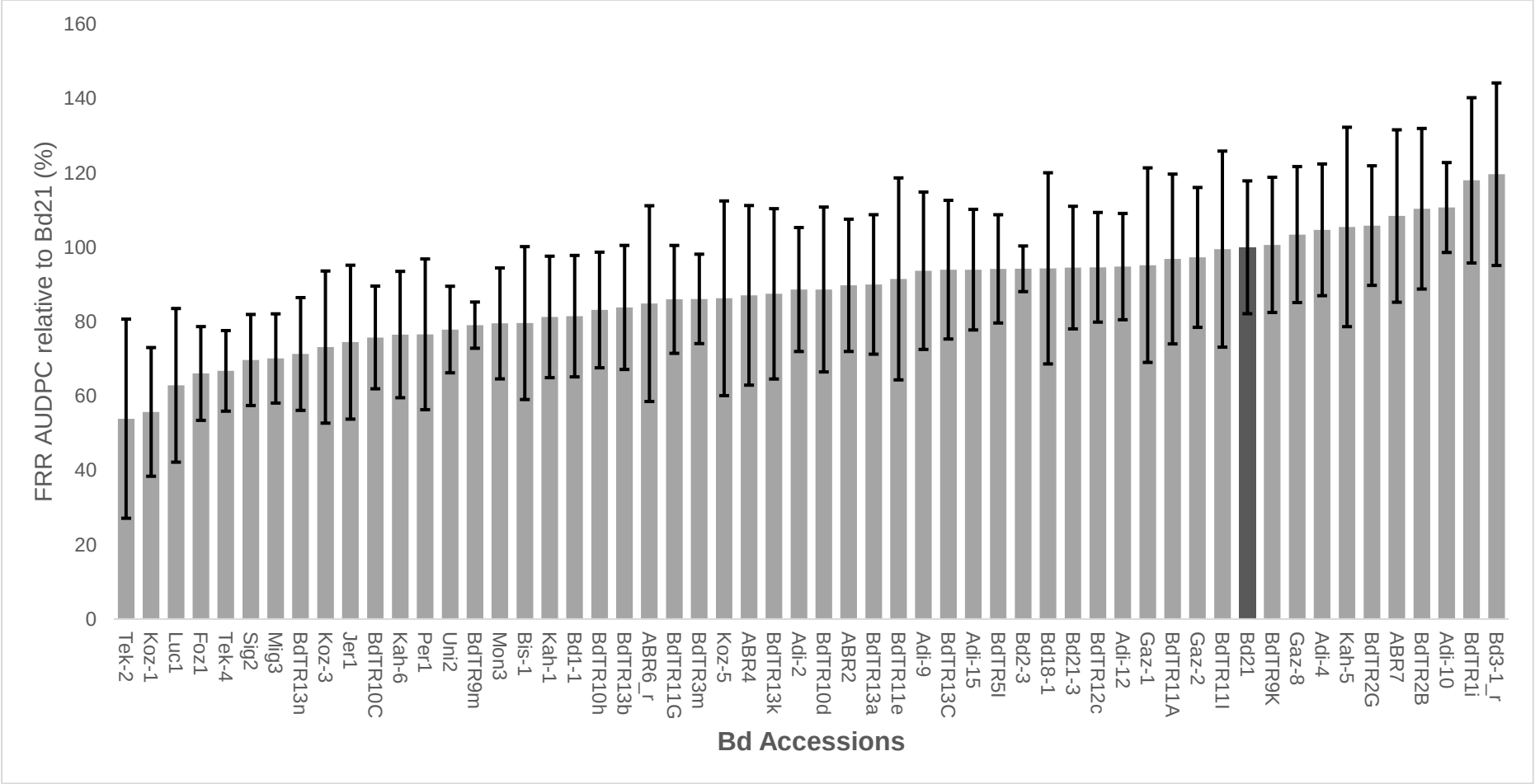

Figure 3-6 Re-analyses of FRR AUDPC for the entire available Brachypan accessions with new mycelium plugs of Fg. Every accession was relativised to Bd21 (dark grey). An overall increase in susceptibility was observed throughout the panel. Error bars represent standard deviation.

3.3.3 Analysis of Fusarium-mediated overall death of the seedling in the Brachypan panel

A second phenotype was visualized in the lines suffering from FRR, where the overall death of the seedling at around 20 dpi contrasted markedly between the different accessions. A scoring system was established in order to differentiate the different levels of disease severity of the plant, from completely green to complete death (Fig 3-7). The necrosis of the plant is characterized by the root system suffering from severe necrotic lesions and the growth of *Fusarium* hyphae on the surface on the leaves of the seedling. The first class (0) consists of leaves that remain completely green and present no visual hyphal growth in the surface of the leaves (Fig 3-7 0). The leaves over time became necrotic, starting with the tips and the petiole of the leaf. When this was observed, it is considered the second class (1) of necrosis of the seedling (Fig 3-7 1). The next class (2) consists of the necrotic lesions expanding to the borders of the leaf and starting to move inward towards the primary vein. The hyphal growth is easily observed in the petiole and in parts of the leaf (Fig 3-7 2). The final class (3) is the complete death of the leaf, with the necrotic tissue comprising more than 90% of the surface of the leaf containing a large amount of hyphal growth in the entire leaf tissue (Fig 3-7 3).

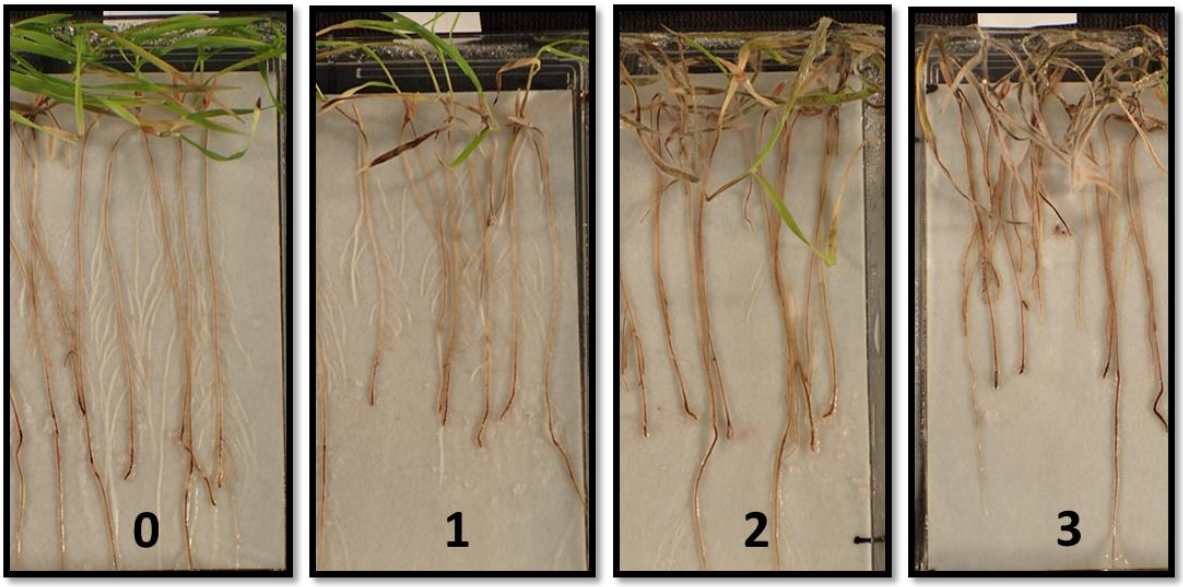

Figure 3-7 Score system of the overall death of the Bd seedling by Fusarium. 0 – Consisting of seedling with minimal signs of Fusarium hyphal growth and overall green leaves. 1 – Some signs of hyphal growth, mainly on the roots, with leaves displaying necrotic tips. 2 – Visible hyphal growth in the roots and crown of the seedling, large necrotic lesions on the leaves. 3 – Fusarium hyphal growth in all the tissues of the seedling, with the complete death of the seedling.

By using this new scoring system, the same plants as used in the previous root rot analysis were reanalysed for the overall death of the seedling phenotype. Although the overall death of the seedling is mainly quantified due to the necrosis in the cotyledons and first leaves, and not the development of necrosis in the roots, the phenotypes will still be characterised in the thesis as mainly related to FRR due to the origin of infection being in the primary root. However, since the overall infection involves the whole plant and not just the root infection, correlations can still be drawn to FCR, and to some extend FHB, as the nature of infection is not strictly related to the root and can still draw parallels to those two diseases.

The Brachypan panel displayed a very large differential between the lines, with some members of the panel showing very high levels of resistance while the majority were highly susceptible (Fig 3-8). Even though the variability within each line is generally high, overall, the lines also demonstrate a good differentiation between each other, bypassing the problem observed in the necrotic lesion phenotype, where the differential was too low to undertake population analysis. The overall death of the seedling to the fungus differs significantly from the necrotic quantification from the previous experiments but several lines were consistently resistant or susceptible for both assessment types. For example, Bd21 and Bd3-1 remained susceptible with a predicted score of 2.58 and 2.67, respectively (Fig 3-8), while lines Sig2 and Per1, remained among the most resistant of the panel, with a predicted score of 0.1 and 0.18, respectively (Fig 3-8). The accessions Foz1, Luc1 and Jer1, that demonstrated different responses to take-all and FRR in previous experiments, were all relatively resistant according to the new assessment of ‘overall death’, displaying a predicted score between 0.43 and 1.28 (Fig 3-8). On the other hand, accessions ABR6 and ABR7, as well as BdTR2b, that displayed high levels of necrotic lesions in the root, displayed the strongest resistance to FRR ‘overall death’, with leaves of all seedlings remaining green (Fig 3-8).

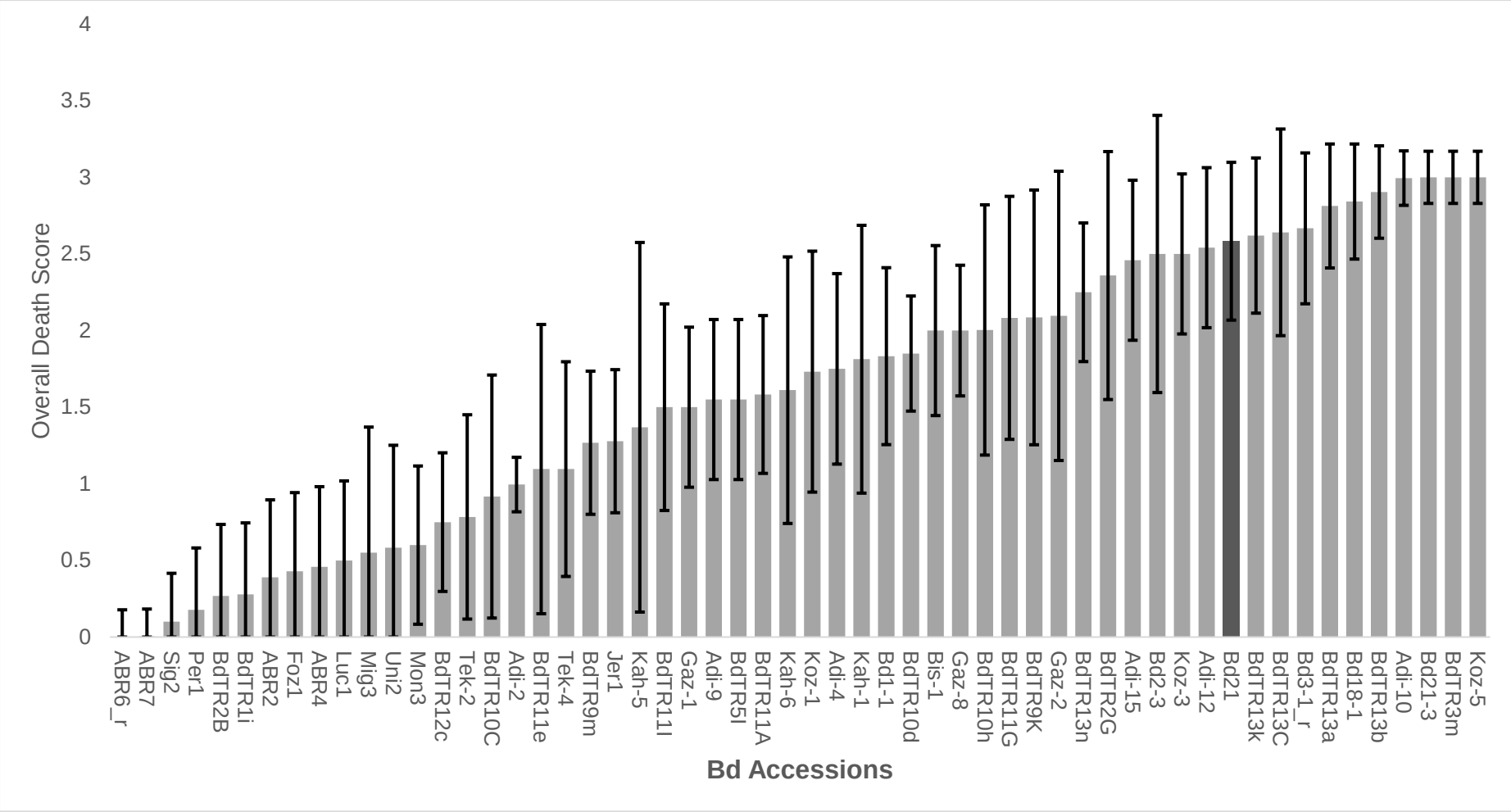

Figure 3-8 Predicted mean of the score for overall death of the seedling from the Bd accessions from the previous experiment after 20 dpi with Fg. Control accession Bd21 (dark grey) and ABR6 are the parents with the best differential. Error bars represent standard deviation.

To verify the best population for the analyses of the overall death of the seedling due to FRR, a pairwise ANOVA comparison was executed for all respective accessions (Table 3-3). By correlating the population table to the data obtained in the overall death, ABR6 and Bd21 displayed the greatest contrast in their phenotype, with a p-value of $4.753e^{-10}$. All the ABR6 plants remained green with low levels of hyphal growth (stage 1) while Bd21 has more than 80 % of its seedling displaying total death (stage 4), with the remaining 20 % in stage 3. Other researchers in the Nicholson group had already observed that the population of ABR6 and Bd21 as a good population for the study of *Fusarium* head blight in *Bd*, making the study on FRR reinforced by the potential of ABR6 to be a good source of resistance against *Fusarium* diseases.

Table 3-3 Bd accessions parents of developed populations with their respective p-value and predicted means for the overall death phenotype. The analysis was performed using an ANOVA pairwise comparison.

Parent 1	Parent 2	p-value	Score Parent 1	Score Parent 2
Bd21	BdTR13k	0.9999	2.58	2.62
Tek-4	BdTR10h	0.1401	1.09	2
Bd21	ABR6	< 0.0001	2.58	0
Luc1	Jer1	0.4752	0.5	1.27
Luc1	Foz1	0.9999	0.5	0.43
Bd21	Bd3-1	0.9999	2.58	2.67
Bd2-3	Bd21	0.9999	2.5	2.58
Bd3-1	Bd1-1	0.8583	2.67	1.83
Bd3-1	Bd2-3	0.9999	2.67	2.5
Bd21	Bd1-1	0.5949	2.58	1.83
Koz-3	Bd1-1	0.8583	2.5	1.83

3.4 Discussion

In this chapter the study of *Fusarium* infection on the root can be divided into two different methodologies and three different disease quantification strategies. The discussion will thus be divided into two main parts correlating to the two main methodologies used. The first methodology comprises the quantification of necrotic lesion progression in the primary root growth originating from a *Fusarium* mycelium plug inoculum in middle section of the root. Since this was the same methodology used in the previous chapter in the characterization of *Bd* resistance towards take-all, a comparison of the Brachypan response to both diseases can also be performed. The second methodology comprises an initial infection of the primary root tip with a Fusarium slurry, accompanied by the disruption of the primary root growth. This can then be separated into two different disease quantifications, where the first analyses consist of the necrotic lesion progression in the roots in the early stages of FRR, and the second analyses on the overall death of the seedling during late stages of infection.

3.4.1 FRR development from the infection of the middle section of the primary root

In the global analyses of the response of accessions in the Brachypan panel to FRR and take-all in the middle section of the root (Fig 2-6 and Fig 3-4), two groups were identified, one relating to the accessions that respond similarly to both diseases (group I), and secondly, the accessions with contrasting levels of resistance between the two diseases (group II).

The first accession that serves as a robust example of common susceptibility in group I is accession Bd3-1, which had an AUDCP to take-all and FRR, similar to the 'control' susceptible accession Bd21, (Fig 2-6 and Fig 3-4). FRR symptoms developed more rapidly in the first 5 dpi than those of take-all while at later stages (5 to 12 dpi) the relative rate of colonisation for the two diseases were similar. This suggests that *Fg* more rapidly infects and colonise root tissues than *Ggt* but this requires confirmation through examination of biomass accumulation of the two pathogens. This does, however, represent one of the first studies to

examine progress of these two diseases, without the interference of variable environmental and biological factors in the rhizosphere.

Comparable, to Bd3-1, the majority of accessions in group I display a similar high level of susceptibility to both diseases, highlighting the broad range by these two fungi in infecting root systems. Some accessions within group I, however, were relatively resistant to both FRR and take-all. These included accessions Koz5, Per1, Gaz8, Koz1, Kah5 and Sig2 (Fig 2-6 and Fig 3-4). These are potentially the most interesting within group I, as they may have common resistance mechanisms operating against the two diseases. Resistance against root pathogens is poorly understood, not only due to the difficulty in methodology but also to the preference in studying aerial tissues where disease progression is more easily assessed. In the analyses of potential sources of resistance to another *Fusarium* pathogen, *Fusarium oxysporum,* in the roots of *Arabidopsis thaliana*, the triple mutant in the U-box type E3 ubiquitin ligases group cluster *pub22/23/24*, which play a role in the negative regulation of microbe-associated molecular pattern (MAMP)-triggered immune responses, displayed an increase in resistance to infection by *F. oxysporum*. Disruption in the triple E3 ubiquitin ligases also promoted resistance to *Pseudomonas syringae*, *Hyaloperonospora arabidopsidis* and *Piriformospora indica*, indicating a role in broad disease resistance conferred by the suppression of MAMP negative regulators (Chen et al. 2014). It would be interesting to determine whether a similar broad mechanism of resistance lies behind the common resistance to FRR and take-all observed with the aforementioned accessions identified in this study.

The resistance between the different group I accessions does not appear to originate from a shared phylogenetic relationship (Fig 1-3). Interestingly, resistant accession Kah5 and susceptible accession Kah1 although being close phylogenetically (Fig 1-3) (Gordon et al. 2017), displayed very different disease progression scores to both diseases. The same profile is observed between susceptible accessions Gaz1 and Gaz2 and resistant accession Gaz8, although Gaz8 sits phylogenetically between Gaz1 and Gaz2 in the combined phylogenetic

trees independently produced by the Vogel group at the Joint Genome Institute (Gordon et al. 2017; Gordon et al. 2020). These two examples, coupled with the remaining resistant accessions Per1, Koz1, and Sig2, also not demonstrating a close phylogenetical relationship (Fig 1-3), indicates that disease resistance to infection at the mid-point of the root within group I to both diseases has evolved separately in these accessions. These could be coupled with a gene-for-gene resistance model, where these specific accessions developed targeted defence mechanisms to resist certain pathogens.

In the analyses of group II, the best examples comprise the resistant parents to middle section disease spread, Jer1 and Foz1 for take-all and FRR, respectively. Foz1 displayed the highest level of resistance against FRR with a relative percentage of 36% (Fig 3-4), compared to take-all of 55% (Fig 2-6). Jer1 on the other hand has a relative percentage of 77% to FRR (Fig 3-4) and 19% to take-all (Fig 2-6). Contrasting to the resistance accessions of Group I, the differences in susceptibility to the two diseases in these *Bd* accessions indicates that resistance to take-all and FRR function through different mechanisms.

Overall, this methodology of root assessment in *Bd* in the characterization of both diseases demonstrates the advantages of using *Bd* as a model. Determining FRR resistance in wheat has not been extensively reported, and limited variation in resistance between different lines has been found. Resistance to infection in the spikelet has been shown to be genetically different to that of *Fusarium* infection in the base of the plant, such as crown rot and root rot, making sources of resistance between the two types of tissues not interchangeable (Liu and Ogbonnaya 2015; Su et al. 2021; Haidoulis and Nicholson 2020). In an attempt to translate resistance to FRR, a number of studies have been conducted in the characterization of FCR, which present similar mechanism as observed in FRR, as it is sometimes the direct consequence of FRR development (Minati 2020; Covarelli et al. 2012). Reports on direct phenotyping of FRR progression and resistance is particularly scarce, especially in cereals. FRR in pea caused by *Fusarium solani fsp. pisi,* is one the few studies where differential resistance in the root has been observed, with a corresponding QTL, *Fsp-*

Ps 2.1 explaining up to 53.4 % of the variance, although no specific candidate gene has been identified as the cause of resistance (Coyne et al. 2019). Variability among wheat cultivars was also noted when infected with different species of *Fusarium*, with cultivar Rasheed being the most resistant to infection by *Fusarium* in roots, and cultivars Res. 22 and AG3 the most susceptible (Minati 2020). It is worth noting that the work by Minati was performed using invasive root phenotyping at a single time point in a variable environment. In a similar strategy, the decline of root growth after infection with *Fc* was also studied in barley, with cultivar Mart1 displaying the lowest decline from the panel at 7 dpi. This cultivar has shown to be resistant to other pathogens such as *Pyrenophora graminea*, *Puccinia spp* and *Bipolaris spp*, possibly suggesting a common broad disease resistance response by Mart1 to these different pathogens (Tufan et al. 2017).

3.4.2 FRR and overall seedling death characterisation under primary root tip infection

Analyses of FRR resistance can also depend on the methodology used in the visualization of *Fusarium* infection in the roots. As observed in this study, changes in infection site in the root may have a large impact on the level of resistance observed in an accession. When roots were infected at the tip the differential observed between the different accessions collapsed, with all the previously reported resistannt acessions displaying between a moderate resistance to complete susceptability (Fig 3-6). One of the main phenotypes observed occasionally in the mid-root infections, and present in all the accessions infected in the tip of root was the clear disruption of the primary root growth by *Fg*, which was not observed with *Ggt* infection. This phenotype may be associated with the *Fg* mycotoxyn deoxynivalenol (DON), a chemical capable of disrupting protein synthesis and cell wall synthesis, along with other negative effects, that could lead to the inability of the meristem to produce new cells and expand (Miller and Ewen 1997; Shifrin and Anderson 1999). The effect of DON was studied in the root meristem of several crops (wheat – *Triticum aestivum*, rye - *Secale cereale* and broad beans - *Vicia faba*), where it was shown to severely affect the spindle fibre formation, leading to the inability of the chromosomes to be pulled to the cell poles, producing an excess

condensation of prophase chromosomes, in case of wheat and rye, and meta- to anaphase chromosomes in case of broad beans (Packa 1997; Packa and Sliwinska 2005). This arrest led to an increase of the G2/G1 ratio in the cells, with DON specifically contributing to the arrest during the G2 phase, preventing the cells from progressing to the mitosis phase (Packa and Sliwinska 2005). This toxicity effect of DON in the dividing cells of the root meristem could be the main cause of the inability of the *Bd* primary root, along with any root that came into contact with the fungus, to continue to grow in these experiments.

Another phenotype associated with the second methodology of FRR infection, was the overall death of seedling, which revealed a high differential in resistance within the Brachypan panel. During the establishing of a scoring system for the progression of overall death of seedling, *Fg* displayed the ability to grow superficially through the initial point of infection in the roots, colonising the root tissue without causing visual necrotic lesions to plant, being able to establish around the petiole, cotyledons and first leaves, eventually causing dispersed points of infection in all different tissues. This has been observed in the root infection profile in wheat, where stem-base colonisation by *Fg* originated from symptomless growth of the fungus from the root to the stem (Wang et al. 2015). The differences between the level of fungal growth to the stem also correlated with the level of resistance of the cultivar, where resistant Florence-Aurore displayed low levels of stem-base colonisation, when compared to more susceptible varieties (Wang et al. 2015). This was observed between the visual fungal growth of the ABR6-like and Bd21-like lines, where ABR6-like plants show limited symptomless growth of the fungus in the surface of the root, compared to the more susceptible Bd21-like lines. Wang and colleagues hypothesise however that the spread of the fungus happens internally from the point of infection in the roots, advancing between the epidermis and parenchyma cells (Wang et al. 2015). In this study however, external growth of the fungus was also visualised, demonstrating the capacity of the fungus to spread biotrophically through the seedling before switching to its necrotrophic phase and causing several points of infection. Resistance in Florence-Aurore was also correlated with disturbed migration of *Fg* infection

from the root epidermis into the cortex (Wang et al. 2015), which later correlates with resistance due to quantitative limitation of the pathogen growth in the initial stages of infection (Vergne et al. 2010). It would be interesting to analyse the root infection profile in the roots of ABR6, to try an examine if the same mechanical disruption of fungal growth is also observed.

In summary, this chapter demonstrates how *Bd* could prove to be a potent tool to study root diseases. FRR is normally considered a disease that proves challenging to record and score since the scoring of the disease normally leads to the complete destruction of the root system. The present work made it possible to score the disease without the disruption of the root system, and to record the disease progress in real-time. Due to the ability to document(photograph) the disease on a day-to-day basis and create a permanent record, it is possible to go back to the data at any time, to analyse other phenotypes, like overall death of the seedling and lateral root formation. Overall *Bd* proved to be a powerful tool to take the analyses of *Fusarium* root rot to a stage not yet made in wheat. In the next chapter the population of ABR6 and Bd21 will be analysed for the overall death of the seedling phenotype. It will make use of the available F8 population, along with genetic map and genetic markers already generated for the population in order to undertake a quantitative trait locus (QLT) analysis to genetically characterise the resistance visualised in ABR6.

Chapter 4. QTL Analyses of the *Bd* population ABR6xBd21

4.1 Introduction

The study of populations for understanding the genetic basis of resistance to a disease within a specific cultivar has been a common practice in tackling the complexity of the wheat genome to minimize the region of resistance to a small section of its chromosomes. It relies on the design of markers which can differentiate between the genome of the resistant and susceptible varieties due to a single-nucleotide polymorphism (SNP) between the two parents. By using a set of markers spread across the wheat genome, a karyotype can be created for each line of the population where each section of its DNA is identified as either being from the resistant or the susceptible parent, or in some occasions has having a mix of the two (heterozygous). The most common SNP-based marker system used in generating wheat maps is Kompetitive allele specific PCR (KASP), The genetic map generated on the basis of recombination within the population is used for undertaking quantitative trait loci (QTL) analysis of the entire population response to a certain trait, as in this case being a disease score. The most studied QTL of wheat against FHB, is called *Fhb1*, located in chromosome 3BS, originating from the resistant Chinese spring cultivar Sumai 3 (Niwa et al. 2014). The first suggestion for the possible function of *Fhb1*, was the expression of a glucosyltransferase capable of detoxifying the virulence factor DON, thus impairing the infection by *Fusarium* (Lemmens et al. 2005). More recently several studies have been made, dismissing the existence of a glucosyltransferase, and highlighting new candidates that brought forward other hypotheses. sometimes contradictory to each other. The first study was able to restrict the *Fhb1* locus to just 28 genes, suggesting a Gly-Asp-Ser-Leu (GDSL) lipase gene as a potential candidate due to its high expression upon *Fusarium* infection (Schweiger, Steiner, et al. 2013). The next one was able to demonstrate the role of another gene in the locus, a pore-forming toxin-like gene, that seemed to correlate with the resistance of FHB (Rawat et al. 2016), however it was quickly questioned, since the gene phenotype was not able to be replicated,

and was identified as being expressed in susceptible varieties (Jia et al. 2018). The latest hypothesis comes from the combined finding of two independent studies, both dealing with a histidine-rich calcium-binding protein (TaHRC) within the locus. The first hypothesis suggests that a deletion found on the gene, leads to a loss of function, enhancing resistance (Su et al. 2019). The other hypothesis suggests that the deletion shifts the start codon upstream leading to a gain of function mutation through production of a larger protein (Li et al. 2019). The third hypothesis combines the two, where it suggests that the mutation, regardless of how it impacts the function of TaHRC, results in it being incapable of forming a functional heteromultimer complex with its corresponding homoeologues in chromosomes 3A and 3D, making the complex unexploitable to *Fusarium* during infection, thus leading to resistance (Lagudah and Krattinger 2019). The *Fhb1* QTL will remain to be a mystery until further experiments can be carried out to deconstruct the QTL further, as well as efficiently analysing the possibility of multiple genes within the locus being responsible for conferring the resistance to FHB in the plant.

Fhb1 is part of countless QTLs identified in wheat and other crops for *Fusarium* resistance, with the great majority being associated with FHB, amounting to an outstanding 500 QTL with around 104 being described as major QTLs (Buerstmayr, Steiner, and Buerstmayr 2020). These can be further separated into QTLs identified in studies involving resistance to the spread of the disease upon specific tissue inoculation, and QTLs involving overall field inoculation. Both studies indicate that *Fusarium* resistance is normally attributed to more than one QTL, where resistance to point inoculation is controlled on average by 3 QTLs, with a maximum of 8 QTLs at a time, while field resistance map on average to 6 different QTLs with up to 17 QTLs at the same time (Buerstmayr, Steiner, and Buerstmayr 2020). The diverse set of responses in field studies is normally attributed not only to the intrinsic response of the host to *Fusarium*, but also to the impact of the plant morphology and the environmental conditions on the virulence and infection of the fungus (Buerstmayr, Steiner, and Buerstmayr 2020). One such example is the influence of Reduced height (Rht) *Rht-D1b* or *Rht-B1b* genes,

which are associated with a semi-dwarf phenotype in wheat but are also correlated with more susceptibility to *Fusarium* infection (Srinivasachary et al. 2008; Srinivasachary et al. 2009). In fact 40% of the QTL detected to have an effect on plant height overlap with QTL associated with FHB resistance (Buerstmayr, Steiner, and Buerstmayr 2020). Other traits like anther extrusion and heading date / flowering time are also associated with *Fusarium* resistance. One of the most recent findings summarize the effect of anther extrusion, where removing all anthers before inoculation significantly reduced the efficiency of the fungus to infect and develop in the early stages of infection but did not prevent fungal growth within the spike. Even though not preventing infection by the fungus, it did significantly disrupt the establishment of the fungus (Steiner et al. 2019). The same was observed for the vernalization response (*Vrn*) and photoperiod response (*Ppd*) genes¸ that are behind the determination of flower and heading time of wheat, that frequently mapped to numerous *Fusarium* resistance QTL (Buerstmayr, Steiner, and Buerstmayr 2020). There have, however, been numerous difficulties in establishing a correlation between particular traits and *Fusarium* disease severity (Buerstmayr, Steiner, and Buerstmayr 2020). This demonstrates how important it is to understand *Fusarium* resistance and how it does not rely on a single mechanism adopted by the plant against the pathogen, but reflects a combination of different genetic, morphological, and environmental effects.

In this chapter the differential obtained between ABR6 and Bd21 in the *Fusarium* mediated overall death of the seedling will be analysed in order to characterise the genetic basis of the resistance. For this a QTL analyses will be performed using the available F8 population of ABR6 x Bd21, establishing one of the first QTL analyses for resistance against FRR.

4.2 Materials and Methods

4.2.1 Brachypodium lines, seedling preparation and inoculation:

The 100 F8 lines from the crossing between ABR6 x Bd21 was kindly donated by the Sainsbury Laboratory Collection in collaboration with Mathew Moscou's group. The F8 seeds were grown and the F9 seeds were harvested prior to this work.

The population analysis followed the seedling preparation, the inoculation procedure and the overall death scoring described in chapter 2 and 3. The lateral root number was counted by eye with ImageJ using the photographs taken during the overall death scoring system used in chapter 2.

4.2.2 Fusarium cultivation and maintenance:

The *Fusarium* cultivation and maintenance followed that of the previous chapter. A fresh culture of *Fg* was used each time as recommended for optimal disease scoring as discussed in chapter 2.

4.2.3 QTL analysis:

For the QTL analyses the predicted means using the two most differential days (11 and 14 dpi) was performed as in the previous chapter for both overall death and lateral roots. Preliminary data analyses was performed using Genstat 19, and no transformation of the scores was needed for any dataset. The F8 genetic and physical map provided by the Moscou group containing a total of 169 different KASP markers (Bettgenhaeuser et al. 2017), was used in the analyses with Genstat 19. The overall death score and lateral root number were analysed using a single trait linkage analysis with the Kosambi mapping function and LOD threshold of 3.0. The composite interval mapping (CIM), using the detected candidate QTL from the simple interval mapping (SIM) as cofactors, was used to produce the final QTL location. The final QTL model was then fitted to produce the final QTL map and peaks with their respective variance.

4.2.4 KASP analysis:

For the DNA extraction seedlings of 96 out of the original 100 lines from the population were grown for 7 days in a Petri dish. Two seedlings of each line were selected and placed in two corresponding 1.2 mL 96 well plates. The plates were then freeze dried overnight. The plates were then taken to a Spex GenoGrinder 2010 and the samples were ground to a fine powder using tungsten beads for 3 to 4 rounds at 20 Hz for 2 min. The DNA extraction buffer was made with 100 mL Tris-HCl [1.0 M, pH 7.5], 100 mL EDTA [0.5 M, pH 8.0], 125 mL SDS [10 % w/v] and 675 mL dH_2O in a full volume of 1L. 500 µL of extraction buffer were added to each well, sealed and shaken to mix all the powder. The two plates were placed in a preheated water bath at 65 ºC for 60 min and shaken every 15 min. The plates were placed in a 4 ºC fridge for approximately 15 min, before adding 250 µL 6.0 M ammonium acetate, mixed and placed back in the fridge for a further 20 min. The samples were centrifuged at 2916 x g for 15 min. Around 600 µL of the supernatant was then transferred to two new 96 well deep-well plates containing 360 µL chilled propan-2-ol. The new plates were centrifuged at 2916 x g for 15 min, the supernatant was discarded, and 500 µL 70 % v/v ethanol was added. A further centrifuge at 2916 x g for 15 min was made, the supernatant was discarded, and the plates were left to dry on the work bench for 30 min. The samples were then resuspended in 100 µL of dH_2O, vortexed, and stored in the fridge at 4 ºC until the KASP analyses.

For the primer design to generate additional KASP markers the sequences for ABR6 and Bd21 were obtained using the genome portal from the Joint Genome Institute (https://genome.jgi.doe.gov/). The sequences were then aligned using Clustal Omega (https://www.ebi.ac.uk/Tools/msa/clustalo/) to search for mutations that could differentiate the genomes of ABR6 and Bd21. The primers were designed by hand and tested for their alignment and properties using the Primer Blast from NCBI (https://www.ncbi.nlm.nih.gov/tools/primer-blast/). Each genotype was then tagged with a VIC or FAM tail at the 5' end of each forward selective primer to differentiate between ABR6 and Bd21 sequences respectively. A full list of the primers is available from Table 4-1.

A total of 2 µL (10 mg/mL) of the DNA sample was transferred to a KASP-compatible 384 PCR plate containing 2 µL of KASP mix with 0.07 µL primer mix (12 µL of each allele forward primer and 30 µL of the common reverse primer, diluted in an additional 46 µL of dH_2O). The samples were placed in a MasterCycler (LGC Genomics) and according to the properties of each primer, the programme ran for 94 ºC 15 min followed by [35-45] cycles of: 94 ºC 20 s, [55-60 ºC] 60 s. The plates were read using a PHERAstar fluorescent microplate reader (BMG LABTECH). The results were then analysed using the KlusterCaller software (LGC Biosearch) and compiled using Microsoft Excel.

Table 4-1 List of additional KASP marker primers used to redefine the QTL region in chromosome 1 of Bd21xABR6 population.

QTL marker/ Bd position		**Primer**
Bd1-23900256	FwA	GAAGGTCGGAGTCAACGGATTGCTCTTTCCACTGTTCATTGTCCg
	FwB	GAAGGTGACCAAGTTCATGCTGCTCTTTCCACTGTTCATTGTCCa
	Rv	TGCTGTGAAGCTCCTAATGGCT
Bd1-24588073	FwA	GAAGGTCGGAGTCAACGGATTGACTCGATGCGTTGCTGTCCAc
	FwB	GAAGGTGACCAAGTTCATGCTGACTCGATGCGTTGCTGTCCAt
	Rv	CCCTTTTGCTCCACACGGCA
Bd1-24656925	FwA	GAAGGTCGGAGTCAACGGATTGGGAACACTGCTTCTTTGTTC
	FwB	GAAGGTGACCAAGTTCATGCTGGGAACACTGCTTCTTTGTTG
	Rv	GCAGTAGCCAGTAAGGCACA
Bd1-25026475	FwA	GAAGGTCGGAGTCAACGGATTGAGACAAGAGATCGAACGGC
	FwB	GAAGGTGACCAAGTTCATGCTGAGACAAGAGATCGAACGGT
	Rv	ACCCTGAACCAAACTAGGCG
Bd1-25264175	FwA	GAAGGTCGGAGTCAACGGATTCCATCCTGATGTCTTAGGATGAT
	FwB	GAAGGTGACCAAGTTCATGCTCCATCCTGATGTCTTAGGATGAC
	Rv	AGAGTACTTACCAGCTCCTGC
Bd1-25455677	FwA	GAAGGTCGGAGTCAACGGATTTCTGTCAGCACCCTTTCCTCG
	FwB	GAAGGTGACCAAGTTCATGCTTCTGTCAGCACCCTTTCCTCA
	Rv	CTGCCTGAAGCAACAGCCTC
Bd1-25466374	FwA	GAAGGTCGGAGTCAACGGATTGCTGTTGTGATTCCAAAGAGAACTA
	FwB	GAAGGTGACCAAGTTCATGCTGCTGTTGTGATTCCAAAGAGAACTC
	Rv	CATTCAGTTTAAAGCTTTCCTCCCTC
Bd1-25515933	FwA	GAAGGTCGGAGTCAACGGATTTTACTCCATCGCGGGGAATTAC
	FwB	GAAGGTGACCAAGTTCATGCTTTACTCCATCGCGGGGAATTAT
	Rv	TGTCCTCCGCCATGAACCTC
Bd1-26839250	FwA	GAAGGTCGGAGTCAACGGATTGCCGGCCACGAATAGATCG
	FwB	GAAGGTGACCAAGTTCATGCTGCCGGCCACGAATAGATCA
	Rv	CACAACAGCATGCAGGGCA

4.2.5 Bd21, ABR6 and wheat orthologue gene list:

The Bd21 gene list from the QTL region between Bd1-24656925 and 26839250 was obtained from Phytozome (https://phytozome.jgi.doe.gov/pz/portal.html#!info?alias=Org_Bdistachyon). The ABR6 region from pseudomolecule_1:23159527 to 25329589 was obtained through BLAST analysis using the Brachypan database (https://brachypan.jgi.doe.gov/). The Joint Genome Institute also performed their own analysis, attributing each ABR6 gene annotation to their most significant Bd21 gene homologue. This data was obtained from the Brachypan database and also compiled in the Bd21 and ABR6 gene lists. The Bd21 gene list was also BLASTed against ABR6 using the BLAST tool available in the bioinformatic tools of the John Innes Centre and was used to corroborate the ABR6-Bd21 gene attribution from Brachypan.

The list of wheat orthologue genes from the Bd21 QTL region between Bd1-24656925 and 26839250, was obtained using PlantEnsembl orthologue database search tool within BioMart (http://plants.ensembl.org/biomart/martview).

4.2.6 Protein domain analyses:

Protein domain analyses were performed using Phytozome database (https://phytozome.jgi.doe.gov/pz/portal.html#!info?alias=Org_Bdistachyon), InterProScan (https://www.ebi.ac.uk/interpro/search/sequence/) and Prosite (https://prosite.expasy.org/).

4.3 Results

4.3.1 QTL analyses of the overall death of the seedling on the ABR6xBd21 population

In the last chapter a large differential was observed between two accessions of *Bd*, Bd21 and ABR6, where ABR6 had a considerable delay in seedling death associated with FRR when compared to the more susceptible Bd21 line. A total of 100 lines including the parents were available from the F9 population from the crossing of ABR6xBd21 originating from the F8 population kindly donated by the Moscou group. Using a fresh inoculation of *Fusarium graminearum*, an average of 8 seedlings per line were inoculated and observed for

a maximum of 20 days for the progression of the complete death of the seedling. The highest differential between the two parents was observed at 11 and 14 dpi, where each seedling was scored between 0 and 3 using the scale introduced in the last chapter. An overall predicted mean for each line was calculated using the scores from the two different days and their distribution was analysed (Fig 4-1). Examination of the normal plot (Fig 4-1 B) and the histogram plot (Fig 4-1 A), reveals that the overall predicted mean of the score is normally distributed.

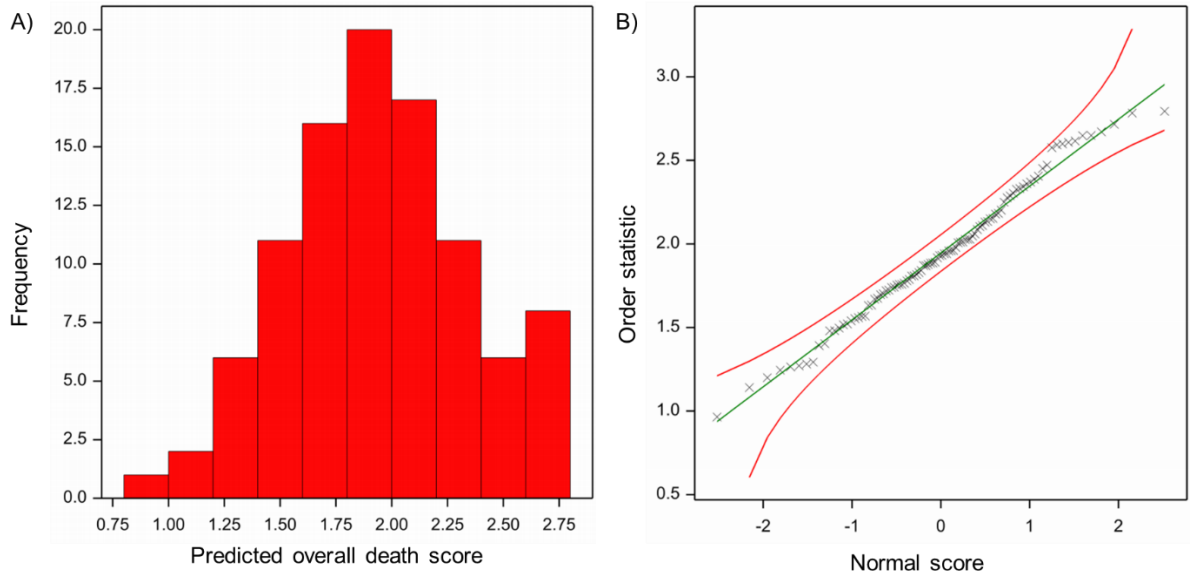

Figure 4-1 Overall death predicted mean scores statistics showing the distribution of the scores among the population. Both the histogram (A) and the normal plot (B) of the scores predict the data to be normality distributed.

The QTL analysis was performed using the F8 genetic and physical map provided by the Moscou group containing a total of 169 different KASP markers across all 5 chromosomes of *Bd* (Fig 4-2). By performing an initial SIM analysis of the data, a region between *Bd* genomic position markers Bd1-22268024 and Bd1-28686369, with a significant QTL peak on KASP marker and *Bd* genomic position Bd1-25478624, was observed on chromosome 1 (Fig 4-2).

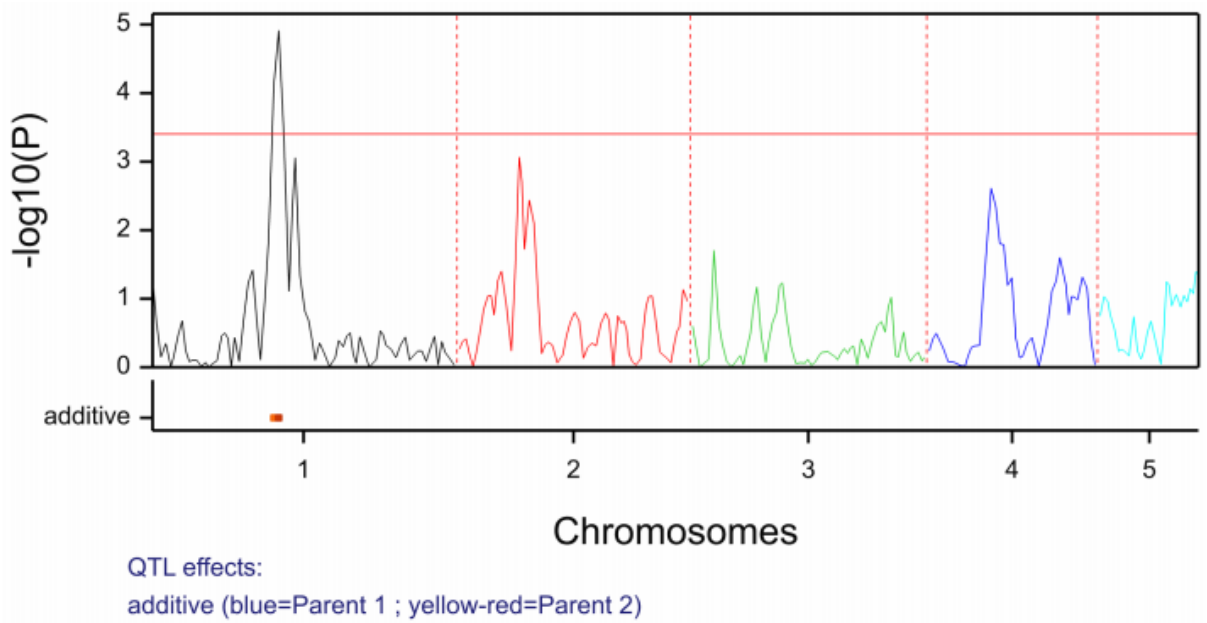

Figure 4-2 Representation of the SIM QTL analyses on the F9 population of ABR6xBd21 against the overall death phenotype of the seedlings by Fg. One significant QTL peak was obtained in chromosome 1 originating from the susceptible variety Bd21 (Parent 2).

By performing a CIM, using the KASP marker Bd1-25478624 as a co-factor, the final QTL analyses displays an increase in the LOD for marker Bd1-25478624, along with an additional marker showing significance from *Bd* genomic region Bd2-3624815 to Bd2-4620365 with a QTL peak originating from KASP marker and *Bd* genomic position Bd2-4214116, on chromosome 2. The final QTL test had KASP marker Bd1-25478624 explaining 27.6 % of the variance, along with the smaller peak on Bd2-4214116 accounting for only 12% (Fig 4-3). Both alleles associated with high scores originate from parent 2, Bd21, suggesting that the FRR resistance to 'overall death' of the plant originates from ABR6 as expected from the difference in resistance observed in the parent lines.

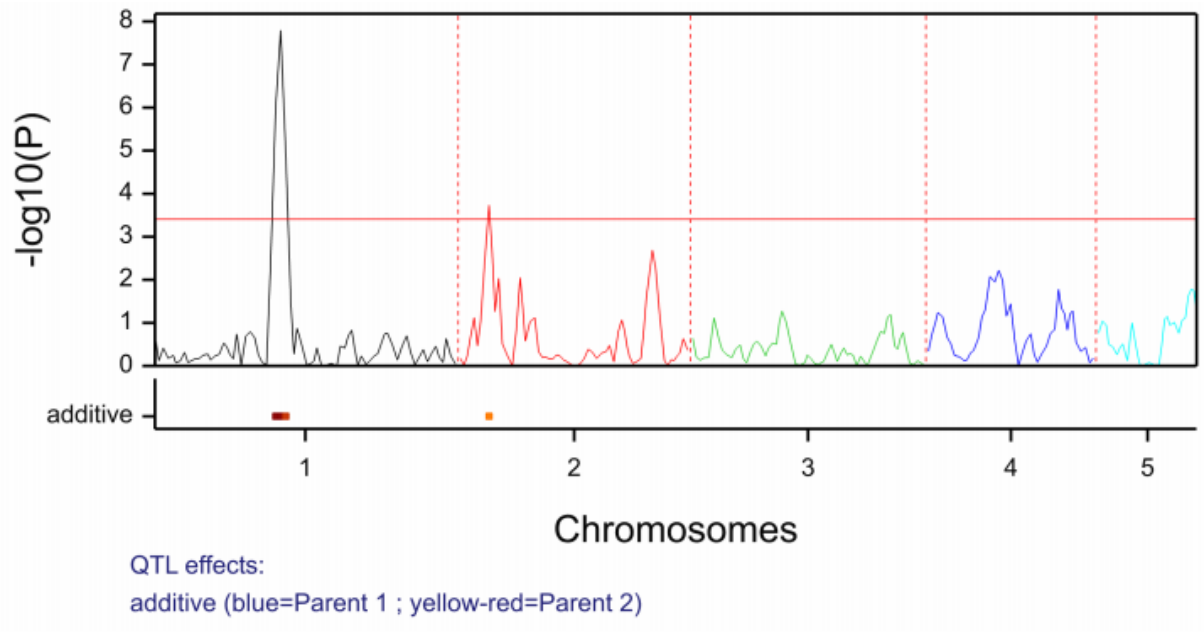

Figure 4-3 Representation of the CIM QTL analyses on the F9 population of ABR6xBd21 against the overall death phenotype of the seedlings by Fg. Two significant QTL peaks were obtained in chromosome 1 and chromosome 2 originating from the susceptible variety Bd21 (Parent 2).

4.3.2 QTL analyses of the number of lateral roots on the ABR6xBd21 population

When studying the spread of the fungus through the seedlings another phenotype was observed between the two lines where the development of more lateral roots upon infection of ABR6 was considerably higher when compared with Bd21 (Fig 4-4 A), a phenotype which is not observed between the two lines in normal conditions. In order to determine whether there is a correlation between the lateral root phenotype and overall death, a predicted mean for the total amount of lateral roots observed for each line in the two days of observation was calculated and a second QTL analysis was undertaken (Fig 4-4 B).

The QTL analysis resulted in two significant separate peaks, one on chromosome 2 (KASP marker and *Bd* genomic position Bd2-14991875, explaining 12.27% of the variance) and another on chromosome 3 (KASP marker and *Bd* genomic position Bd3-52074165, explaining 12.21% of the variance), both originating from parent1, ABR6 (Fig 4-4 B). The peaks from FRR resistance and lateral root QTLs both originate from ABR6 but, the peaks obtained from the two QTLs on chromosome 2 do not overlap, where the lateral root QTL is

10.7 Mbp (around 17% of the whole size of chromosome 2) downstream from the peak observed with FRR overall death.

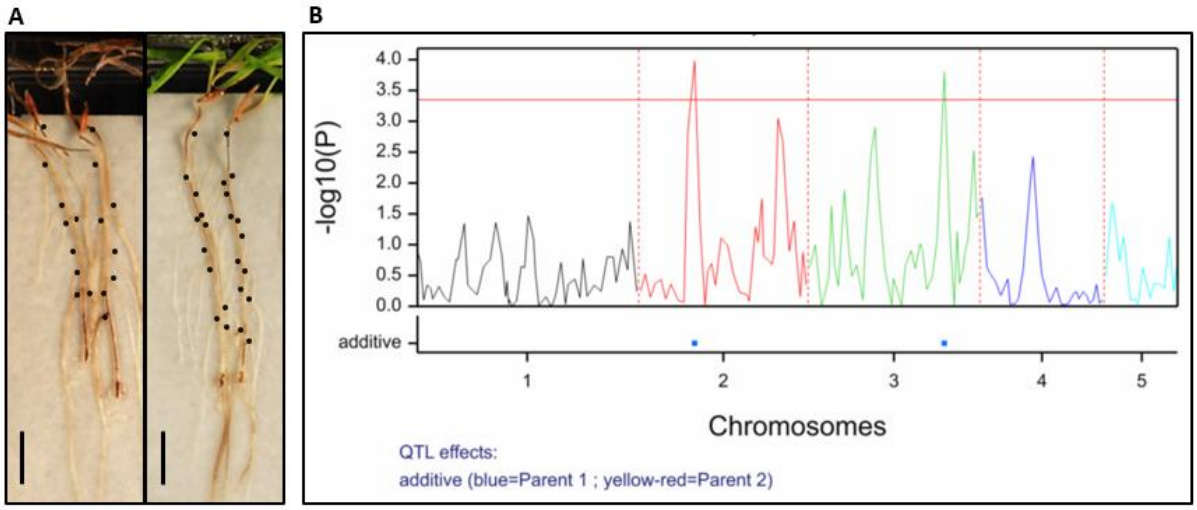

Figure 4-4 Lateral root characterization of the ABR6xBd21 population. A) number of lateral roots initiation sites (black dots) for Bd21 and ABR6, respectively. Black bar represents 1 cm. B) CIM QTL analyses on the F9 population of ABR6xBd21 against the number of lateral roots formed during 14 dpi. Two significant QTL peaks were obtained in chromosome 2 and chromosome 3 originating from the resistant variety ABR6 (Parent 1).

4.3.3 Re-mapping of the overall death of the seedling QTL in chromosome 1 with additional KASP markers

In order to refine the chromosome 1 QTL region, and narrow down the locus of interest, a further seven KASP markers were designed and characterized between the original left Moscou flanking marker Bd1-22268024 and the peak marker Bd1-25478624, as well as two markers between the peak marker and the original right flanking marker Bd1-28686369 (Fig 4-5). The discrepancy between the frequency of markers in the two flanking regions is due to two main reasons, the first is due to the QTL prediction analyses performed on the population, giving statistical preference to the left region of the peak marker as the main cause of the disease response. The second was the poor alignment between the Bd21 and ABR6 genomes in the right flanking region which led to the failure of three out of the five primers designed for the proximal region (three KASP primer sets that failed were not included in the primer list of Table 4-1).

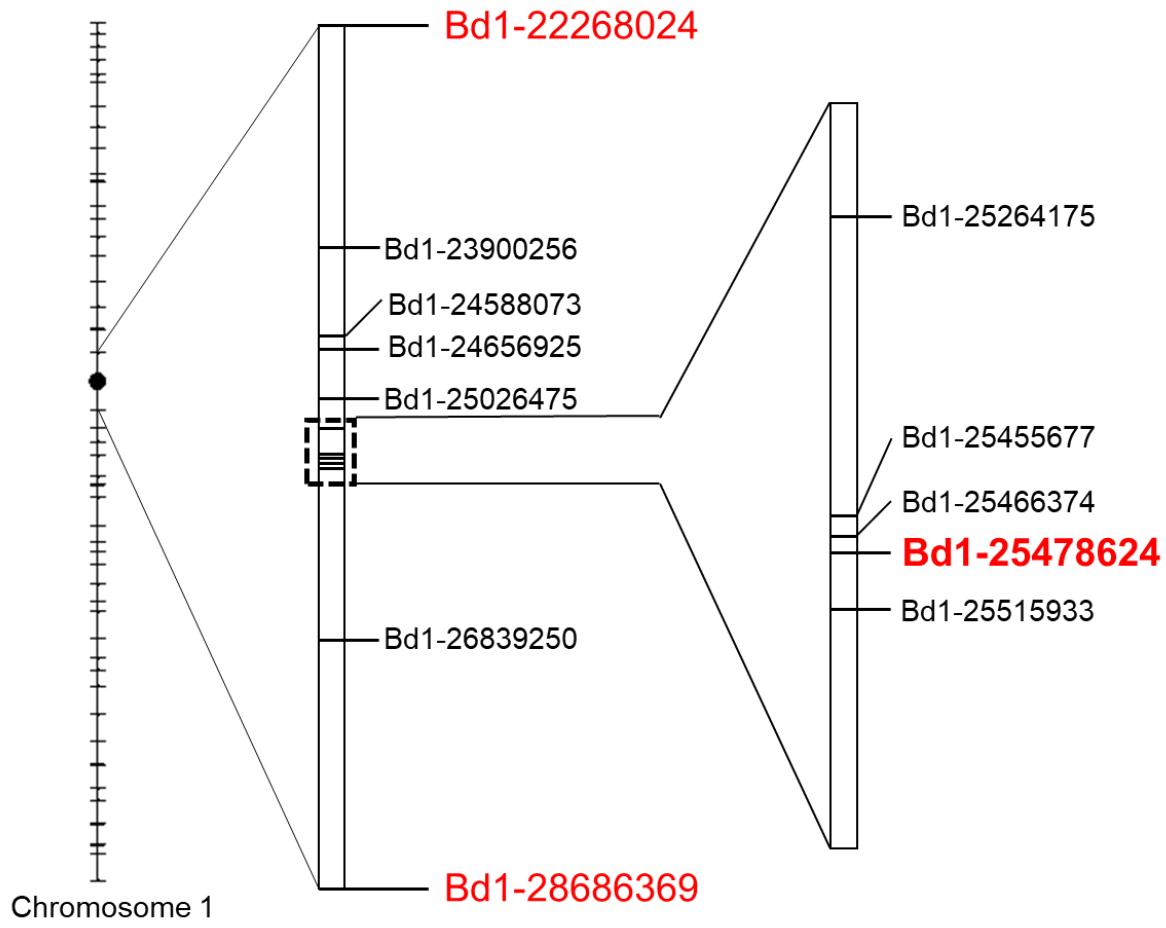

Figure 4-5 Genetic map with the location of the original Moscou KASP markers (highlighted in red) with the QTL peak marker further highlighted as black circle within chromosome 1. It is followed with the physical location of the newly designed KASP markers between the QTL region from KASP markers and Bd location Bd1-22268024 and Bd1-28686369. A total of seven KASP markers were designed between left flanking marker Bd1-2268024 and QTL peak marker Bd1-25478924, and two between Bd1-25478924 and the right flanking marker Bd1-28686369.

The same population was analysed using the new genetic map (Fig 4-6), minus four lines of the ABR6xBd21 original F9 population, due to their absence in the additional KASP marker analyses, in an attempt to minimise any errors analysing in the new region. The main CIM QTL peak extends from the original KASP marker Bd1-25478624 to the new KASP marker Bd1-26839250 (Fig 4-6), with a decrease of the overall variance to 15%. The QTL region remained largely unchanged between the SIM and CIM analyses (data not shown), unlike the first analyses were an enhancement in LOD was observed to peak marker in chromosome 1, which also reflected in the higher variance value in that experiment. During the QTL analyses, the peak on chromosome 2 observed in the previous experiment has also

lost its significance, making the region in chromosome 1 the main significant genetic response by the population to the disease in this experiment.

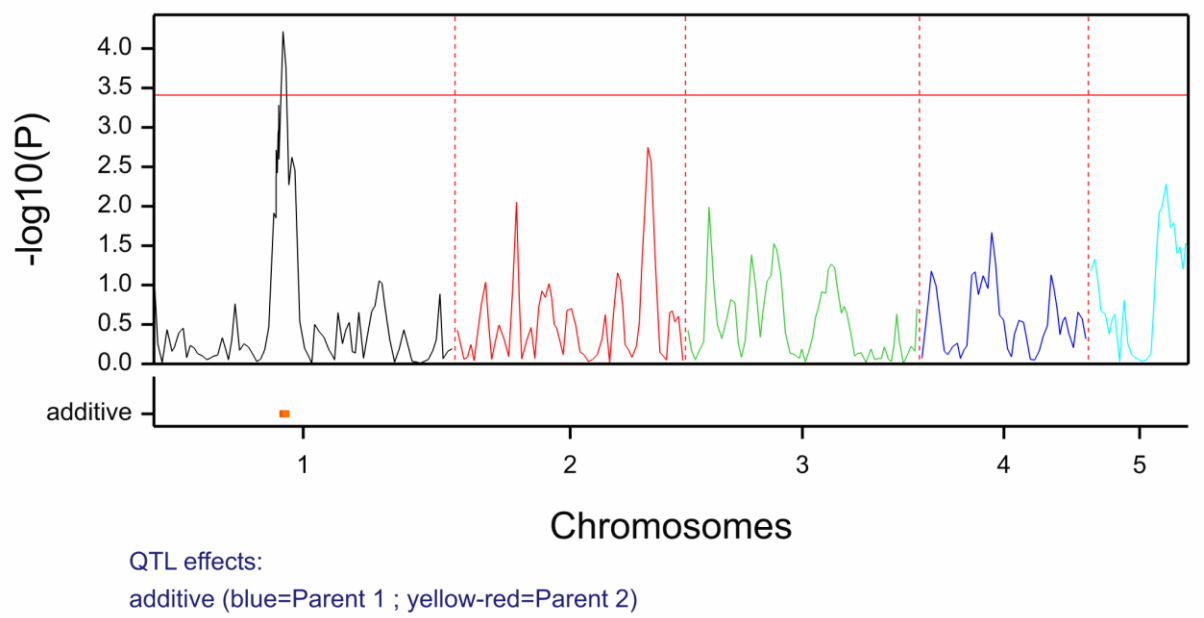

Figure 4-6 Re-analyses of the CIM QTL on the F9 population of ABR6xBd21 against the overall death phenotype of the seedlings by Fg, containing 9 additional KASP markers around the QTL KASP marker Bd1-25478624. Only one significant QTL peak is observed containing the region between KASP marker Bd1-25478624 and Bd1-26839250, originating from the susceptible parent Bd21 (Parent 2).

Since the region could not be further refined with the original data, two additional independent experiments where conducted. The first one contained 32 lines with 16 seedlings in each, including the parents, that represented all the different haplotypes observed within the QTL region between Bd1-22268024 and Bd1-28686369. The third one included a smaller set of 23 lines with an average of 22 seedlings each, that included recombinants in the QTL region between Bd1-24656925 and 26839250. The overall mean of the two scores showing the largest differential was calculated and correlated with the physical map to try to determine the most significant marker within the QTL region. Unfortunately, the new scores could not refine the region further (Supplemental Table 4-1). The best correlation was observed between the lines with the most extreme phenotypes, with the lines containing overall death scores above 3.5 or below 0.5 correlating to a Bd21 and an ABR6 haplotype, respectively, in the majority of the KASP markers analysed. The lines with intermediate phenotypes however did

not segregate to a specific KASP marker, making it difficult to narrow down the locus further to a specific set of candidate genes.

Even though the response of Bd21 and ABR6 to FRR could be directed by multiple factors, possibly a combination of multiple susceptibility/resistant factors of Bd21/ABR6 in chromosome 1 and other chromosomes, a series of tests can still be performed to try to narrow down possible candidates underlying the main susceptibility response found in chromosome 1. The first strategy was using the available predicted gene content from both parents and localize any significant differences between the chromosome 1 region in each parent. Using the combined scores of the three experiments the region between Bd1-24656925 and 26839250 was selected as the most significant region for the study of the transcriptome of both species. Using the genome database available from the Joint Genome Initiative (https://genome.jgi.doe.gov/), 311 predicted genes were identified in the region for Bd21, and 270 predicted for ABR6 (Supplemental Table 4-2). From the 311 Bd21 genes, 16 genes are characterised as potential errors in gene prediction by Phytozome and were excluded from the analyses (Supplemental Table 4-2 Red). By blasting the gene lists to each other, 239 genes were putative homologues between the two genomes with an average similarity above 99% (Supplemental Table 4-2). An additional 9 ABR6 genes also contained regions within the gene with an average similarity above 99%, that are represented by more than one gene in Bd21 (Supplemental Table 4-2). These were assumed to be due to errors in assembly of the ABR6 genome, which failed to properly identify the presence of multiple genes, combining multiple genes with highly similar sequences into one single gene, thus producing long sequences with several homologues in Bd21. The remaining genes comprise 47 genes from Bd21, and 31 from ABR6 that either do not BLAST to any gene in the other parent, or BLAST to a region in the genome outside the selected QTL region (Supplemental Table 4-2 Yellow). All the genes comprise hypothetical proteins, with no known significant orthologue in any species, indicating that they are specific to the Brachypodium accession. These genes range in size from 150bp to 8000bp, with ABR6 containing more short-sequence genes than Bd21.

It is possible that some of the ABR6 short-sequence genes could be due to an error during sequencing/assembly, generating small pseudo coding regions that might not be transcribed *in vivo*.

When analysing these genes for protein domains, the majority contain no protein domains, or only partial protein domains that might not be functional (information available on the Phytozome database). The only genes with full predicted protein domain are Bd21 genes Bradi1g30767 and Bradi1g30797, and ABR6 gene Brdisv1ABR6_r1004894m which contain a protein kinase domain, along with Bd21 gene Bradi1g30801 which contains a histidine protein kinase response regulator protein domain.

To unveil more about the resistance mechanism in the QTL region a search was made using the numerous studies in wheat to identify regions associated with resistance against *Fusarium*. In order to translate the region from Brachypodium to wheat all the *Bd* QTL genes of chromosome 1 were BLASTed against the latest version of wheat genome (Zhu et al. 2021). The majority of the genes (around 75.5 % of the total QTL) gave a top hit against the group 7 chromosomes of wheat (Fig 4-7, Supplemental Table 4-3). The rest were dispersed through the entire wheat chromosome with no further hotspot regions identified (chromosomes 1 - 3.1% of the overall genes: chromosomes 2 - 4.9%: chromosomes 3 - 5%: chromosomes 4 - 1.1%: chromosomes 5 - 1.5%: chromosomes 6 - 4.8%: undocumented - 3.9%) (Supplemental Table 4-3). The genes where equally dispersed between the most distal region of the long arms of the three group 7 chromosomes of wheat (chromosome A – 22.2%: chromosome B – 26.9%: and chromosome D – 23.8% (Supplemental Table 4-3). Most of the genes have an orthologue in each chromosome of wheat, with some genes undergoing an amplification from *Bd* to wheat, with a single *Bd* gene being represented by more than 40 duplications in the wheat orthologous region.

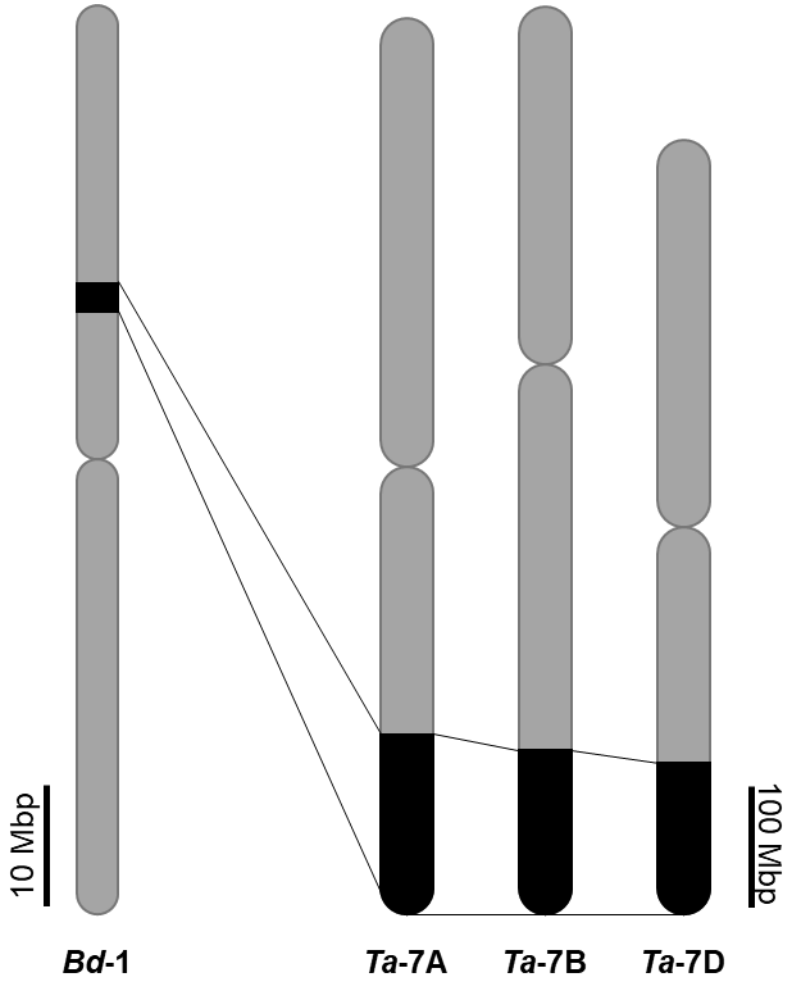

Figure 4-7 QTL region in chromosome 1 of Bd from KASP markers Bd1-24656925 to Bd1-26839250 and its corresponding orthologues region in the three chromosomes 7 in wheat (Triticum aestivum - Ta) using sequence annotation IWGSC RefSeq v2.

Although physically the QTL orthologue region in chromosome 7A is larger than the corresponding regions in chromosome 7B and 7D, the number of genes within the interval are very similar. Chromosome 7A has 216 orthologue genes that correspond to 163 *Bd* genes in the original *Bd* chromosome 1 QTL region; chromosome 7B 268 orthologues which correspond to 172 *Bd* QTL region genes, and chromosome 7D with 237 orthologues from 163 *Bd* QTL region genes. In order to study the relevance of the orthologue wheat genes, all the corresponding wheat genes in each region of chromosome 7 were compiled into a single list and compared to developed QTLs in the literature relating to wheat response to *Fusarium*, discussed ahead.

4.4 Discussion

The differential of the overall death of the seedling upon Fg infection was normally distributed in the population of ABR6xBd21 (Fig 4-1), reinforcing the large difference in the growth of the fungus between the two accessions. Upon analysing the fungal growth in the group of ABR6-like lines against the group of the Bd21-like lines in the population, there was a clear difference in the amount of external hyphal growth between the two groups, with Bd21-like lines exhibiting a considerable amount of hyphal growth around the root and leaves, compared to just isolated hyphal growth in the infection site of ABR6-like lines. This suggests that ABR6 could have a defence response that although incapable of preventing the fungus from penetrating the root, it can significantly affect and delay its growth. When performing the QTL analyses on the population, two significant peaks were obtained on chromosome 1 and chromosome 2 with KASP markers Bd1-25478624 and Bd2-4214116, respectively (Fig 4-3). When comparing the overall death QTL regions with the regions obtained in the population of ABR6xBd21 against wheat stripe rust (Bettgenhaeuser et al. 2018), *Yrr3* although in chromosome 2, does not coincide with QTL Bd2-4214116, having a distance of more than 45 Mb between them.

Another phenotype observed in the population is the formation of lateral roots, with Bd21-like line producing considerably fewer lateral roots than ABR6-like lines. This could suggest that upon infection, in order to bypass the disruption of the primary root growth, ABR6 tries to compensate by forming more lateral roots than Bd21, which in the long run could be helping the seedling remain alive longer. As discussed before, morphological traits have shown a significant contribution to the defence of the plant against *Fusarium*, however the data from the present work suggests that there is no correlation between the plant genetic response to the fungus and the morphological root differences of the two accessions. The two significant QTLs in chromosome 2 for the FRR resistance and root branching QTL do not overlap, with over 10 Mb distance between them. In addition, chromosome 1 does not appear to be involved in the differential between the lateral root formation (Fig 4-4), indicating that the main FRR

QTL peak in chromosome 1 in response to overall death phenotype is a specific response to the spread of the fungus. Although a minor role in resistance by the formation of more lateral roots by ABR6 cannot be discounted.

When reanalysing the same population with more KASP markers in the chromosome 1 QTL region, the QTL region continued to include KASP marker Bd1-25478624, extending to the new KASP marker Bd1-26839250 (Fig 4-6). The QTL in chromosome 2 relating to KASP marker Bd2-4214116 was completely lost. The loss of significance in chromosome 2 could be due to the loss of lines between the first and second QTL experiment, which in turn could have influenced the prediction of final CIM QTL model, as it was not included as a cofactor in the analyses. However, the reduction in the number of lines in the analysis and the re-genotyping of the QTL region between Bd1-22268024 and Bd1-28686369 is the most likely cause of the reducing of the impact of chromosome 1 in overall death from 27.6% of the variance to 15%, possibly to do with the transition between the SIM and CIM analyses not increasing the LOD associated with chromosome 1, as was observed in the first QTL analyses.

To try to study the region in more detail, two independent separate experiments were performed on lines with recombination points within the QTL interval. When comparing the regions to the phenotypical score, no correlation could be made between any single KASP marker and the disease score, possibly suggesting that other regions of the genome must be also playing a role in dictating the plants overall resistance / susceptibility. This is observed in the analyses with a variance of 15% associated to the region in chromosome 1, thus making 85% of the variance not accounted for by the region, reflecting in the difficulty in associating a phenotype to a specific region in the genome. The overall QTL analyses demonstrates that the host response to *Fusarium* can be complex and not dictated by a single major gene or gene cluster, as observed in many works to date. For example, as summarised by Bai and Shaner as early as 1994, when analysing the genetic sources of resistance in well-established resistant cultivars of wheat, the majority of resistance originates from several chromosomes instead of from a unique location in the genome (Bai and Shaner 1994). Wheat cultivar Sumai

3 for example, has its source of resistance originating from a combination of genes from chromosomes 1B, 2A, 5A, 6D and 7D (Yu 1982). Another cultivar, Wangshuibai, proved to contain resistance genes from 4A, 4D, 5A, 7A and 7B (Liao and Yu 1985). While resistant cultivar PHJZM, has predicted sources of resistance from 3B, 5B, 6B, 6D and 7A (Yu 1990). This pattern of scattered resistance factors to *Fusarium* related disease throughout the genome of wheat, has been repeatedly observed from studies as early as the 1980s all the way to the most recent QTL analyses, as can be observed later on in the discussion when addressing the reported QTLs that coincide with the orthologue *Bd* chromosome 1 QTL region in the group 7 chromosomes of wheat.

By analysing the differences in gene content and gene sequences within the QTL region from KASP marker Bd1-24656925 to 26839250, around 47 genes proved to be unique to Bd21, and 31 to ABR6. All the genes had no description, with no known orthologue found in other plant species. When analysing the protein domains present in the gene list three genes encoding proteins with protein kinase domains were identified, Bradi1g30767 and Bradi1g30797 in the Bd21 accession, and Brdisv1ABR6_r1004894m in the ABR6 accession. Another gene, Bradi1g30801, contained a histidine protein kinase response regulator protein domain, which is generally associated with receiving a high-energy phosphoryl group from a histidine protein kinase, itself activated from environment stimuli. Upon receiving the signal from the histidine kinase, it then autodephosphorylates of its own domain to transfer the stimuli response to an appropriate effector (West and Stock 2001). All the genes that have an identifiable protein domain, seem to be involved in intermediary steps where a kinase might be necessary to transfer a signal from upstream to downstream of its pathway, possibly in response to *Fusarium*. Proteins containing kinase domains or kinase functions have already been identified in having a role in responding to *Fusarium* diseases. An example is the characterization of wheat Leucine Rich Receptor Like Kinase *TaLRRK-6D* and its barley orthologue *HvLRRK-6H*, part of one of the largest family of genes involved in the recognition of pathogen-associated molecular patterns and thus modulate the response of the plant

against the pathogen (Thapa et al. 2018). Both genes seem to be involved in the early response to infection through a direct response to *Fusarium* virulence factor DON, working in the upstream induction of the hormone salicylic acid. Virus induced gene silencing (VIGS) of both genes, led to a substantial decrease in the production of salicylic acid and to an increase of disease development in the plant (Thapa et al. 2018). Another kinase with an important role in *Fusarium* resistance is the wheat sucrose non-fermenting-1 (SNF1)-related protein kinase 1 catalytic subunit α (SnRK1α), that has been shown to interact with TaFROG, a protein already proven to confer resistance to DON (Perochon et al. 2015; Perochon et al. 2019). Even though the expression of SnRK1α is not significantly affected by DON, DON is shown to increase the SnRK1α kinase activity and thus the amount of active SnRK1α in the cell (Perochon et al. 2019). By down-regulating SnRK1α expression in the cell using VIGS, an increase in susceptibility to DON is observed in the spikelet of wheat, demonstrating the positive role of SnRK1α along with TaFROG in DON and *Fusarium* resistance (Perochon et al. 2019). Another work performed in *Arabidopsis thaliana*, demonstrated that mutating the homoserine kinase gene *DRM1*, leads to an accumulation of homoserine in the cell along with delayed cell death which correlated to a positive role in disease resistance to *Fusarium* (Brewer, Hawkins, and Hammond-Kosack 2014). This demonstrates that kinases can play both beneficial and detrimental roles in conferring resistance to *Fusarium*, where in some scenarios *Fusarium* development is impaired by the downstream response caused by certain kinases, while in others *Fusarium* exploits the kinase regulatory pathway to its advantage. It could be that the previously mentioned QTL putative kinases present in Bd21, Bradi1g30767, Bradi1g30797 and Bradi1g30801 could be potential *Fusarium* susceptibility factors. This is unlikely however since all genes contain a perfect 100% similarity copy in the resistant ABR6 genome, even though the current ABR6 assembly places them outside the QTL region. The assembly of parts of the ABR6 genome has been found to be incorrect (E. Bankes-Jones, JIC, personal communication) making it likely that these genes are, in reality within the QTL interval. It is possible that the susceptibility/resistance observed in Bd21XABR6 population is

related to the function of remaining unknown genes, thus contributing with a novel system for resistance against *Fusarium*.

In order to compare the QTL region obtained in *Bd* to already published QTLs in wheat, a translation of the *Bd* region to wheat was performed. The most significant regions that displayed a high similarity between wheat and *Bd* chromosome 1 QTL region was found in the distal regions of the long arms of the three group 7 chromosomes of wheat (Fig 4-7). Only a small percentage of *Fusarium* resistance QTL regions colocalised into the long arms of the group 7 chromosomes in the QTLs published in the last two decades. A list has been produced of the main QTLs that are close or within the orthologous wheat QTL region produced from the overall death QTL. The selected QTL analyses mainly focus on identifying *Fusarium* type I and type II resistance in wheat. The main characteristics of both classes of disease resistance is that type I resistance comprises resistance to initial infection by *Fusarium*, while type II is characterized as resistance to the spread of infection (Mesterhazy et al. 1999).

Due to the nature of the analyses focusing on the overall death of the seedling, originating from *Fusarium* infection of the primary root, and not a strict FRR infection, the discussion of the selected QTL analyses will be divided in two parts. The first part will focus on QTL results deriving from FHB infection, giving insight into a more general resistance spectrum to *Fusarium*, independent from specific mechanisms involved in FRR resistance. This strategy will take into account the possibility of ABR6 being involved in fungal growth repression, as observed in the low levels of hyphal growth discussed in the previous chapter. It was also discovered that ABR6 is able to confer FHB resistance in *Bd* (E. Bankes-Jones, JIC, personal communication), making it more likely that ABR6 has a general resistance against *Fusarium* independent from the origin of infection. However specific tissue resistant mechanisms by ABR6 cannot be discounted. The second part will focus on QTLs performed on FCR infection. This *Fusarium* disease is more closely related to FRR, thus making a more focused analysis of the *Bd* chromosome 1 QTL region in connection with the origin of infection and primary source of overall death phenotype originating from the root system. This will enable the

correlation of more specific mechanisms of resistance to FRR by ABR6, rather than a more general approach.

One of the earliest analyses made use of the Chinese Spring Sumai 3 substitution lines, containing several lines with potential FHB resistant chromosomes regions. Positive substitution effects were found on chromosomes 2B, 3B, 6B, and 7A. Chromosome 7A showed the biggest effect to both DON accumulation and spread of FHB (Zhou et al. 2003). It was later discovered that the type II resistance to FHB conferred by 7A was additive to that of the more powerful chromosome 3BS gene *Fhb1* (Jayatilake, Bai, and Dong 2011). Even though both were identified in Sumai 3, the resistance of the 7A region was established to come from Sumai 3's parent Funo, while that of *Fhb1* originates from the other parent Tawain wheat (Jayatilake, Bai, and Dong 2011). A separate study used a cross between the tetraploid durum wheat Langdon and a disomic Langdon PI478742 chromosome 7A substitution line. The PI478742 insertion into durum wheat comes from the 7A chromosome from *Triticum turgidum* sp. *dicoccoides* accession PI478742, that has previously displayed significant levels of type II resistance against FHB (Miller, Stack, and Joppa 1998). Even though the study could not narrow down the region to a small interval it was able to correlate it with the 7A resistance from the Sumai 3 insertion lines mentioned earlier, demonstrating one of the first chromosome 7 overlaps obtained from two different studies using two different species of wheat, suggesting potential common ancestral inheritance of genes for resistance to *Fusarium* infection (Kumar et al. 2007).

Yang et al, 2005, followed this by demonstrating that chromosome 7B plays a role in response to FHB by using the double haploid population between the crossing of the resistant wheat line DH181 and susceptible cultivar AC Foremost (Yang et al. 2005). The population analyses identified different QTLs for Type I and Type II resistance, where the latter were associated with 2DS, 3BS, 6BS, and 7BL, where 6BS accounted for the most variance around 24%, while 7BL was only associated with a minor effect with less than 10% (Yang et al. 2005). In the same year a similar work was performed by using the population derived from crossing

Type II resistant cultivar Wangshuibai and Wheaton (Zhou et al. 2004). Two QTLs explaining most of the variance were localized to chromosome 3BS, followed by two less significant QTLs in chromosome 1BL and 7AL (Zhou et al. 2004). Another study using a cross between Wangshuibai and Alondra identified similar resistance conferred by chromosome 3B and 7A like the previous work, along with additional QTLs in chromosomes 2D, 4B and 5B (Jia et al. 2005). A third study used the crossing between Wangshibai and Sy95-7 that also identified QTL in chromosomes 1B, 2D, 3B and 7A, along with a new source of resistance in 6B (Zhang et al. 2010). A different population using a crossing between the moderately resistant cultivars Arina and NK93604, identified two resistance QTLs in chromosomes 1BL and 6BS originating from Arina, while another set of resistance QTLs were found in chromosomes 1AL and 7AL originating from NK93604. The resistance coming from chromosome 7AL correlated with the resistance regions from the previous three studies (Semagn et al. 2007). The same population was used in the comparison between FHB and anther extrusion and identified the overlap between the two traits in chromosome 1BL. Further anther extrusion QTLs in 1AL and 7AL were identified near the QTLs of resistance to FHB, however the regions did not overlap (Skinnes et al. 2010). Another study using the crossing between Shanghai-3/Catbird and Naxos also identified resistance in 7AL, along with DON tolerance and anther extrusion, however, general anther extrusion QTLs differed from Skinnes et al, 2010, suggesting that differences in anther extrusion is conferred through different genes between the two populations, with the overlap in chromosome 7AL being independent rather than linked to *Fusarium* response (Lu et al. 2013).

Another study focused on understanding the possible relationship between closed flowering (cleistogamy) and low incidence of FHB. The population between the crossing of the open-wide flower cultivar Patterson and Goldfield, a cultivar with closed florets, generated 4 different QTLs, 3 in chromosome 2B and 1 in chromosome 7B associated with low incidence of FHB (Gilsinger et al. 2005). Only the QTLs in chromosome 2B overlapped with the QTLs representing narrow flower opening, leaving chromosome 7B having a sole yet small role in

FHB resistance (Gilsinger et al. 2005). From another crossing between the moderately resistant cultivar Cansas and Ritmo seven QTLs were found, with a type I resistance in chromosome 1DS, and type II resistance in chromosomes 1BS, 3B, 3DL, 5BL, 7BS and 7AL. Although the majority of the FHB QTLs displayed a relationship to some extent to plant height and flowering date, only the QTLs for FHB in chromosome 5BL and 7AL showed consistent correlation to those two environmental traits, indicating a potential indirect role from those regions in FHB response through the manipulation of development traits (Klahr et al. 2007).

Using the crossing between the resistant Chinese cultivar Haiyanzhong with cultivar Wheaton, a major QTL was identified on 7DL, with minor QTLs being identified on 5AS, and 6BS. A further susceptibility factor was identified on chromosome 1AS coming from the resistant cultivar (Li et al. 2011). This demonstrates the complexity of *Fusarium* response, where some regions can contribute resistance while others could be potentially exploited by the fungus to infect more efficiently (Li et al. 2011). This is further complicated with the changes in environment that can severely affect the virulence of the fungus leading to differences in QTL variance between experiments, as also observed in this study. This was observed in a follow-up study to Li et al, 2011, when a section of the population was analysed using a different methodology that drastically reduced the effect of 7DL to that of a minor QTL, with 5AS increasing to be the major effect (Cai et al. 2016). The same group also performed QTL analyses using a population derived from another resistant Chinese cultivar Huangfangzhu and Wheaton, that display a major QTL in chromosome 3BS along with one on chromosome 7AL (Li et al. 2012). The resistance in 3BS colocalized with the *Fhb1* locus of Sumai 3, while the resistance in chromosome 7AL seems to colocalize with the previously mentioned independent Wangshuibai, NK93604 and Ritmo QTLs (Li et al. 2012).

Eckard et al, 2015, made use of pyramiding QTL to localize FHB resistance. This method makes use of different crossings between several cultivars known to be sources of resistance to *Fusarium* and then make use of identical-by-descent based linkage mapping to try and summarise the various resistance QTL regions (Eckard et al. 2015). In this study a total of 28

four-way crosses were performed between different Wesley-*Fhb1* lines with moderately resistant cultivars Lyman, Overland, Ernie and Freedom (Eckard et al. 2015). A total of 15 different QTLs were identified on chromosomes 1A, 1B, 2A, 3A, 3B, 4A, 4B, 4D, 5A, 6A, 6D, and 7D. Some of these QTLs overlapped with previously documented QTLs like *Fhb1*, *Fhb5*, and *Rht-B1.* The QTLs with the biggest effects where localized to chromosome 1A, 3B and 4A, followed by the smaller QTLs in chromosome 6A and 7D (Eckard et al. 2015). The same source of resistance on chromosome 7D was detected as a resistance QTL originating from cultivar Kenyon, from the crossing between the Canadian spring wheat Kenyon and cultivar 86ISMN 2137 (McCartney et al. 2016). In this study a total of 9 different QTLs where identified, with six coming from the more resistant cultivar Kenyon, where chromosome 7D displayed the major effect. The anthesis date and plant height was also studied, however only the FHB QTL in chromosome 2D seemed to correlate with the environmental QTLs, possibly due to the combined effect of anthesis related gene *Ppd-D1* and plant height related *Rht8*, that mapped to the same region (McCartney et al. 2016).

Another major QTL in chromosome 7DL was detected in the population from the crossing of resistant cultivar AQ24788-83 and susceptible cultivar Luke (Ren et al. 2019). Different environmental conditions were used, making use of single spikelet inoculations and spray inoculations in both greenhouse and field trials. Resistance coming from chromosome 7DL of AQ24788-83 was detected in all the different conditions. A crossing between AQ24788-83 with Aikang58, Jimai22 and Sumai 3 was also performed, and the resistance from 7DL was maintained, having a comparable and additive effect with *Fhb1* from Sumai 3 (Ren et al. 2019).

A unique work was performed to show a specific genetic response originating from the long arm of wheat's group 7 chromosomes (Brauer et al. 2020). Using transcriptional data from wheat upon infection with DON producing *Fusarium*, compared with that of wheat that was infected with a strain of *Fusarium* unable to produce DON, a single gene was highlighted due to its role in secondary metabolism, signalling, transport and stress response (Brauer et al. 2020). The wheat *Nuclear Transcription Factor, X-Box Binding Like 1* (*TaNFXL1*) is a DON-

responsive gene, that has been shown in other species to have a role in several biotic and abiotic stress responses, like promoting resilience against salt and osmotic stresses, along with sensitivity to T2-toxin and susceptibility to *Pseudmonas syringae* (Brauer et al. 2020). This study used VIGS and CRISPR/Cas9 techniques, to disrupt the expression of this gene. This caused increased resistance to *Fusarium* spread of infection, possibly due to its role in preventing salicylic acid accumulation, however the true mechanism remains unknown (Brauer et al. 2020). This study presents one of the first susceptibility phenotypes associated with distal region of the long arms of group 7 chromosomes. The three homeologous genes from 7AL, 7BL and 7DL interestingly do fall within the wheat orthologue QTL region, however its orthologue in *Bd*, Bradi1g44270, falls outside the Bd21 QTL region identified within this thesis. This is not unusual, since not all genes from the *Bd* QTL region have orthologues in the three group 7 chromosomes, the reverse is also applicable, where not all the genes in the distal regions of group 7 chromosomes necessarily have an orthologue within the *Bd* QTL region. The rearrangement events between the genomes of *Bd* and wheat are well documented, with *Bd* chromosome 1 being distributed to the distal regions of chromosome group 7, but also chromosome group 4, 5 and 2 (Chochois, Vogel, and Watt 2012). When looking in the wheat perspective, group 7 chromosomes have regions in common with *Bd* chromosome 1 but also to a large extent to chromosome 3 (Chochois, Vogel, and Watt 2012). Even though already outside of the *Bd* QTL region between Bd1-24656925 and Bd1-26839250, gene Bradi1g44270 is present on chromosome 1, which made it interesting in analysing regarding its similarity between Bd21 and ABR6 accession. When comparing the sequences between Bd21 and ABR6, there is 100% gene similarity between the two accessions, although Phytozome does not acknowledge it with a gene annotation in the ABR6 genome. Since most accessions in the Brachypan seem to have this gene conserved and annotated in their sequences, coupled with the 100% alignment between the Bd21 gene sequence and the right alignment within the predicted region in pseudomolecule 1 in the ABR6 genome, this indicates that the gene is not represented in ABR6 as part of an error during

annotation. However, it would be interesting to see if the expression profiles of these gene within the two accessions differ between ABR6 and Bd21.

Other QTL studies have been performed for FCR, a disease more related to FRR than FHB, which was the main focus of the above studies. Like FHB a large number of QTLs have been found, however only a small number localized to group 7 chromosomes. The first study made use of the pyramiding QTL technique mentioned earlier producing two different populations with selected few lines with moderate resistance to FCR (Rahman et al. 2020). A total of 23 different QTLs were identified in both populations with four QTLs localizing to chromosome 7A and one to chromosome 7B (Rahman et al. 2020). At the same time another study was being performed using genome-wide association study on 358 different Chinese wheat germplasms that demonstrated different seedling resistances to FCR originating from chromosomes 1BS, 1DS, 2AL, 5AL, 5DS, 5DL, 6BS and 7BL (Jin et al. 2020). Even though most of the resistances were novel, the major and more consistent FCR resistance seemed to originate from chromosome 5DL, where many genes related to TIR-NBS-LRR and DON detoxifying functions were upregulated in the resistant variety 04 Zhong 36 when compared to more susceptible variety Xinmai 26 (Jin et al. 2020).

Even though a relatively large number of studies has highlighted the group 7 chromosomes as having roles in *Fusarium* disease response, few have been able to pinpoint a specific cause for the resistance. This was mainly due to the fact that FHB and FCR are very difficult diseases to study, where small changes to the environment drastically changed the dynamics between the host and *Fusarium* response. This is easily seen from the numerous QTLs originating from a single experiment, demonstrating how broad the response can be in the host genome. Not only that, but some of the times the QTLs were influenced by environmental factors, further complicating the differentiation between genetic response to minimize *Fusarium* colonization and spread and the effects of environmental factors on these processes. In the present study a major QTL was observed on chromosome 1 of *Bd* against FRR phenotype of overall death of the seedling, even though not significant, some peaks were

observed in chromosome 2 and 4 that could be adding to the phenotype observed in the population. Only one physical trait was observed to be different within the population, which was the creation of lateral roots upon the disruption of growth of the primary root by *Fusarium*. Even though clear differences were observed between the two parents, the resulting QTL did not overlap with the *Fusarium* response, suggesting the resistance phenotype is not dependent on the ability of the plant to create lateral roots. In the overall comparison between the *Bd* QTL region with the selected studies discussed previously, all but one study, propose group 7 chromosome QTLs as sources of resistance, instead of susceptibility, which correlates with the theory of ABR6 having developed a specific mechanism which allows it to tolerate FRR and its subsequence overall death. It is possible that ABR6 could lack or have a modified susceptibility factor from the *Bd* QTL region that could lead to the plant being more resistant in comparable terms to Bd21. The one susceptibility factor found by Brauer et al, 2020, within the *Bd* QTL orthologue regions in group 7 chromosomes is *TaNFXL1*, although the *Bd* orthologue does not seem to reside within the *Bd* original QTL region, could be of interest since it does not seem to have a gene annotation in ABR6. It is also possible that a susceptibility factor from Bd21 resides within the set of the 41 unique genes found within the region, and its absence in ABR6 is enough to promote resistance against FRR. It could also be related to mutations within the common genes of Bd21 and ABR6, however that is unlikely since most of the genes in common have a similarity of more than 98% between the two parents. However, until expression studies are undertaken, it is not possible to exclude the possibility that differences in expression of one or more of these gene may be responsible for the effect on FRR at this locus. In all, the variance obtained with *Bd* QTL region, although small, could be providing a new source of resistance/susceptibility to *Fusarium*, establishing one of the first studies working with a successful protocol of root infection, providing a pioneer genetic study to FRR response by a cereal host. Hopefully by analysing this region in more detail in the future, the genetic basis and mechanism of resistance can be established to FRR and help breeders in creating more resistant cultivars, not only against FHB but also FRR in the field.

Chapter 5. RNA-sequence analyses of Bd21 response to DON

5.1 Introduction

One of the most described characteristics of *Fusarium* is the production of a group of toxins known as trichothecenes. Trichothecenes are complex molecules which can be divided in four distinct groups, from a combination of their chemical skeleton and the main fungi that produces them (Ueno et al. 1973). Under crop field conditions, the most prominent trichothecenes are part of the first two groups, A and B (Rocha, Ansari, and Doohan 2005). The other two groups, C and D, are mainly produced by *Myrothecium*, *Stachybotrys*, *Cylindrocarpon*, among other fungal genera. Although characterized as being more toxic than type A and B, they possibly possess a minor role in fungal infection as the majority are not quantifiable under normal field conditions (Rocha, Ansari, and Doohan 2005). The main trichothecenes found in cereals and other crops are type A, T-2 toxin and diacetoxyscirpenol; and type B, deoxynivalenol (DON) and nivalenol (NIV) (Ueno 1985). From these two classes, the most prominent trichothecene found in *Fusarium graminearum* and *Fusarium culmorum* infections is DON, which is characterized as one of the main indicators of the transition of the fungus from the biotrophic phase to its necrotrophic phase (Walter, Nicholson, and Doohan 2010). Its production normally starts in the first 24 hours of fungal growth in the tissue with a peak of production at 96 hours which correlates with the beginning of the necrotrophic phase in the spikes of wheat (Walter, Nicholson, and Doohan 2010). The amount of DON produced by the fungus is largely dependent on the environment, where high humidity and intensive rainfall around anthesis of the plant is known to lead to an increase in fungal growth and DON production, promoting a faster spread of the disease (Audenaert et al. 2014). The production of DON by the fungus is directly correlated to its aggressiveness, where *Fg* mutants with a disruption in the *TRI5* gene, an important gene in the biosynthesis of DON, causes a substantial decrease in the virulence of fungus in infecting and spreading within the rachis of wheat (Desjardins et al. 1996; Langevin, Eudes, and Comeau 2004; Jansen et al. 2005).

One of DON's known targets in the host cell is the 60S subunit of ribosomes causing major impairment to the subunit peptidyl transferase activity leading to the inhibition of initiation, elongation or termination in protein synthesis (Wei et al. 1974; Schindler 1974; McLaughlin et al. 1977; Christopher, Carter, and Cannon 1977). *Fusarium* species possess an altered ribosomal protein L3, that is not targeted by trichothecenes, and protects the fungi against the toxic effects of trichothecenes, thus continuing with a normal synthesis of proteins in their system (Fried and Warner 1981). The binding of DON to the large ribosomal subunit is known to promote a further mitogen-activated protein kinase (MAPK) cascade response leading to ribotoxic stress in mammalian cells (Shifrin and Anderson 1999; Zhou, Lau, and Pestka 2003). The triggering of the ribotoxic stress by DON, is attributed to two putative kinases, dsRNA-activated protein kinase R (PKR) and hematopoietic cell kinase (Hck) (Zhou, Lau, and Pestka 2003; Zhou, Jia, and Pestka 2005), which in turn regulate two distinct MAPK cascade responses involved in programmed cell death and a cytokine-induced inflammatory response (Zhou, Lau, and Pestka 2003; Moon and Pestka 2002).

Trichothecenes can also promote cell death by increasing the production of reactive oxygen species (ROS). T-2 toxin has been shown to promote an increase in the production of hydrogen peroxide (H_2O_2) in the cells of both tomato and Arabidopsis plants (Paciolla et al. 2004; Nishiuchi et al. 2006). In tomato this increase in ROS production led to severe wilting of the plant, accompanied by lipid peroxidation and eventual cell death (Paciolla et al. 2004; Paciolla et al. 2008). In DON-infiltrated wheat stem tissues the production of H_2O_2 was also observed in the first 6 hours, which led to cell death after 24 hours (Desmond et al. 2008). By treating the stem tissues with ascorbate, a known ROS scavenger, a reduction of DNA fragmentation and cell death was observed under the same DON conditions, further suggesting that DON can trigger programmed cell death in the plant through a ROS associated pathway (Desmond et al. 2008).

Another DON associated phenotype is the arrest of the normal cell cycle progression. During normal meiosis in mammalian cells, DON treatment interfered with microtubule

organization and distribution leading to impaired oocyte maturation (Schoevers et al. 2010). In humans, DON leads to G2/M phase cell cycle arrest, linked to the upregulation of p21WAF1/Cip1, a known negative regulator of cell cycle progression (Yang et al. 2008). In plants, DON is also capable of affecting cell-cycle leading to aberrations in the chromosomes, reduction in the mitotic index, increase of the G2/G1 index through the arrest of cells in the G2 stage, enlargement of the nucleoli and overall prevention of cell cycle progression (Linnainmaa, Sorsa, and Ilus 1979; Packa 1998; Packa and Sliwinska 2005).

If left unattended and used in animal and human food processing DON can cause feed refusal leading to severe weight loss and death (Eriksen and Pettersson 2004), as well as apoptotic lesions in the liver and lymphoid tissues (Mikami et al. 2010). Unlike plants, in mammalian cells the most toxic trichothecene is T-2 (SCF 2002). Apart from the aforementioned phenotypes, T-2 is known to cause severe pregnancy loss with mice, with the toxin being fatal to both embryos and developing foetus (Rousseaux, Schiefer, and Hancock 1986). Lymphocyte cells are also highly susceptible to T-2 leading to immunosuppression (Holladay et al. 1993), a trait also observed in mice that demonstrated more disease susceptibility while under a diet with high concentrations of DON (Reubel, Gareis, and Amselgruber 1987; Charoenpornsook, Fitzpatrick, and Smith 1998). DON can also lead to vomiting and delay gastric emptying, possibly mediated by its effect in serotinin receptors or serotinin stimulation of the central nervous system (SCF 1999). Due to the toxicity of DON for human and farm animals a set of acceptable levels of the toxin in grain has been set in many countries throughout the world, especially in the European Union (available information at https://eur-lex.europa.eu/) and the United States of America (available information at https://www.fda.gov/).

Studying the effects of the *Fusarium* infection in the root system is achievable but very variable as seen in the previous chapters. By studying the effects of a fixed amount of DON in the roots it could minimize complexity by focusing on the effects of just the toxin without the influence of the fungus itself. In addition, previous work has also established a toxic curve of

Bd root response to DON, which shows that low concentrations of DON promote root elongation before reaching a concentration that is toxic and inhibitory to primary root growth (Peraldi 2012). Low concentrations of DON have already been studied in *Arabidopsis thaliana*, wheat, and barley. In *Arabidopsis thaliana*, low concentrations of DON did not lead to cell death, but instead promoted protection against heat shock related programmed cell death (PCD) (Diamond et al. 2013). This phenomenon was light-dependent, with wheat and *Arabidopsis* cells demonstrating a higher PCD upon heat shock in the dark, when compared to the delay in heat shock PCD in cells grown under continuous light (Ansari et al. 2014). It was also suggested that low concentrations of DON are important during the initial biotrophic phase of the fungus, where DON is protecting the host cells against PCD, while the fungus grows and settles in the tissue. DON then either promotes or accompanies the switch to a necrotrophic phase where the high concentration of DON leads to an increase in ROS production and the activation of PCD (Diamond et al. 2013). In barley leaves, high concentrations of DON lead to a quick bleaching of the tissue. However, at low concentrations DON did not have any bleaching effects, leading to reduced senescence, with the leaves under DON remaining greener for a longer period of time than untreated barley leaves (Bushnell et al. 2010).

Although low concentrations of DON have demonstrated to promote a beneficial response in the plant, little is still known to its exact role within the cell. By trying to understand the effects of low concentrations of DON, it will minimize secondary effects on cell death resulting from use high concentrations, but also represent a pioneering study in the understanding of root response to DON at non-toxic levels. In this chapter, in order to document and characterize the full transcriptome from the *Bd* root response to low concentrations of DON, an initial RNA-seq analyses will be performed at two different time points in order to analyse the highest peak of expression during early exposure to DON. In the second part of the chapter a second RNA-seq will be performed with a focus in the characterization of the DON-ROS interaction within the root. This experiment will be conducted

to further categorise the general response of root tissues to DON through a ROS-independent mechanism, as well as the root response associated with a DON-mediated ROS pathway.

5.2 Materials and Methods

5.2.1 Brachypodium lines, seedling preparation and inoculation:

For the first RNA-seq experiment 20 sets of replicates containing 5 seedlings of Bd21 each, where stratified and grown as described in chapter 2. Each replicate set containing 7-day old seedlings where then split in to four groups and inoculated in the following way:

- 5 sets were submerged in a 9 cm Petri dish containing dH_20 for 6h in darkness in a growth chamber at 22ºC.
- 5 sets were submerged in a 9 cm Petri dish containing DON (5µM) for 6h in darkness in a growth chamber at 22ºC.
- 5 sets were submerged in a 9 cm Petri dish containing dH_20 for 24h in darkness in a growth chamber at 22ºC.
- 5 sets were submerged in a 9 cm Petri dish containing DON (5µM) for 24h in darkness in a growth chamber at 22ºC.

The seedlings of each set where then collected and severed in the crown region and their roots immediately frozen under liquid nitrogen. After all replicate sets where collected, the roots were ground to powder using a mortar and pestle and placed in a 1mL Eppendorf tube for RNA extraction.

For the second RNA-seq experiment 12 sets of replicates containing 5 seedlings of Bd21 each were grown as previously described and divided into the following groups:

- 4 sets were submerged in a 9 cm Petri dish containing dH_20 for 6h in darkness in a growth chamber at 22ºC.
- 4 sets were submerged in a 9 cm Petri dish containing DON (5µM) for 6h in darkness in a growth chamber at 22ºC.

- 4 sets were submerged in a 9 cm Petri dish containing H_2O_2 (1mM) for 6h in darkness in a growth chamber at 22ºC.

The seedlings where then collected, as described previously, before RNA extraction.

5.2.2 DON and ROS sensitivity assay:

For the analyses of the ROS response in the roots of *Bd* and how it correlates with the root response to DON, H_2O_2 along with three known ROS inducers will be used. Menadione is a well-known ROS inducer where the most characterized mode of action is described as its capability to release cytochrome c from the mitochondria which leads to an excessive production of H_20_2 (Loor et al. 2010). Alloxan also deregulates the mitochondria leading to a production of superoxide through the autoxidation of its reduced form dialuric acid (Ighodaro, Adeosun, and Akinloye 2017). Methyl viologen largely affects the chloroplast by being oxidized through the chloroplast's electron transport chain producing superoxide molecules that lead to an increase in ROS in the cells (Bus, Gibson, and Aust 1974).

Seeds of Bd21 were stratified as described in chapter 2 and placed in 1mL tubes containing 0.4% agar medium with the desired concentration of the test compound (DON (10 µM), H_2O_2 (0.5 mM), H_2O_2 (1 mM), H_2O_2 (2 mM), Methyl Viologen (1 nM), Methyl Viologen (10 nM), Methyl Viologen (50 nM), Alloxan (15 µM), Alloxan (150 µM), Alloxan (750 µM), Menadione (10 µM), Menadione (100 µM), Menadione (500 µM). The growth of the roots was recorded over the following 7 days.

5.2.3 RNA extraction and sequencing:

The RNA extraction was performed using the Qiagen RNA Miniprep kit with the RLT extraction buffer. No changes have been done to the protocol of the respective kits.

The cleaning of the samples with DNAse was done by using the Invitrogen Turbo DNAfree 50 Rxns kit. No changes have been done to the protocol. Previous to the second RNA-seq, 2µL of purified RNA was collected from each set for cDNA synthesis.

One replicate set from each condition was kept as a backup replicate, while the remaining replicates were sent for RNA library preparation and sequencing by GENEWIZ using the Illumina HiSeq, 2x150bp configuration, single index technology.

5.2.4 RNA-seq data analyses:

Upon receiving the raw data in fasta form from the company, the webtools in Galaxy were used to create the list of differentially expressed genes (DEG) for Bd21 under DON when compared to the control. The first step was performing a FastQC on all the raw files of each sample, where each sample has a separate sequencing file for its forward and reverse strand. This step includes a quality control assessment on the quality of the 150 bp reads inside the sequencing file, where each base is giving an overall quality score between 0 and 40 (low quality score between 0 and 20, medium quality score between 20 and 28, high quality score being between 28 and 40). All samples displayed an overall high quality, with only a few demonstrating medium quality in the edges of each read sequencing, where the quality is typically lower. For the quality optimising, the webtool Trimmomatic was used to trim the edges of each read as well as any other base with a quality bellow 28, along with the Illumina adapter used by Genewiz during the procedure. After each sequencing file has been properly trimmed, a second FastQC was performed on the data where all the samples displayed uniform high quality, but due to the trimming, the size of each read changed from a consistent 150 bp, to range from 50 bp to 150 bp.

In order to align the reads to the genome of Bd21, the webtool HiSat2 was used, which gave an overall mapping score for each sample set. StringTie was then used to associate each read to a gene coding sequence while compiling each replicate within each set and attributing it a general predicted gene read count within the set.

The following pipeline summarises the data analysis:

1. FastQC Galaxy Version 0.72 on the raw data files, for data quality control. No changes to the settings were performed.

2. Trimmomatic Galaxy Version 0.36.5 on the raw data files, to improve the quality of the samples for analyses. Settings: "*Paired-ended*" as "*collection data cluster*". Illuminaclip using Standard adapter sequences for TruSeq3 (2,30,10,8). Sliding window trimming (4,20). Leading trimming (3). Trailing trimming (3).

3. FastQC Galaxy Version 0.72 on the trimmomatic processed files. No changes to the settings were performed.

4. HiSat2 Galaxy version 2.1.0+galaxy4 was performed on the trimmomatic processed files using the FASTA genome file from Phytozome for Brachypodium Bd21v3.1. The library used was "*Paired-end*" using the forward and reverse sequencing for each sample. The rest of the settings were left in default.

5. StringTie Galaxy Version 1.3.4 was performed on the HiSat2 aligned reads BAM files. No changes to the settings were performed. The reference gene file used was Bd21 GFF3 file from Phytozome.

DESeq2 Galaxy Version 2.11.40.2 was performed on the StringTie gene count tabular files. The gene counts of each condition were grouped together, and each treatment was compared to the control condition. The program normalized the gene counts using default settings and produced the final variance graphics, sample pairing, dispersion estimates, p-value histogram, and MA plots. A separate table for gene log fold change and statistical significance was produced along with the additional normalized gene counts table.

5.2.5 GO enrichment analyses:

For the GO enrichment analyses, the Plant Transcriptional Regulatory Map webtool developed by the Centre for Bioinformatics from Peking University was used (http://plantregmap.gao-lab.org/go.php). A full analysis was performed on all the relevant DEG lists, including the analyses of enriched biological processes, molecular functions and cellular components. The threshold p-value used was <0.01.

5.3 Results

5.3.1 Overall RNAseq analyses of accession Bd21 response to low concentrations of DON

From the previous chapters one of the main conclusions was that *Fusarium*-host interactions can be very difficult to study, mainly due to the varying phenotypes and responses employed by both host and the fungus. The administration of a single concentration of DON to the roots of *Bd*, could bypass and solve the problem with the unpredictability of the fungus infection. To lower the cell death mechanisms attributed with high concentrations of DON, as well as minimise a strong resistance response from the host, an RNA-seq was performed on the roots of susceptible accession Bd21 with a low concentration of DON. For this experiment 5 replicate sets with 5 seedlings each were submerged in either a water control or DON 5 µM and incubated for either 6 h or 24 h. A total of 4 replicates were used in the RNA extraction and purification and sent to Genewiz for standardization, quality control, library preparation and RNA-sequencing. DeSeq2 was then used to compare each treatment to the control in order to calculate the magnitude in the difference in expression for each gene with an associated p-value. In order to get the most significant DEG, only the genes with a DeSeq2 statistical p-value lower than 0.01 were included. This showed a large response at 6h with 11,004 genes being differentially expressed (Fig 5-1, Supplemental Table 5-1), showing the powerful effect that just the toxin can have on the plant's response. At 24h the response was significantly lower, with only 2,254 DEG (Fig 5-1, Supplemental Table 5-1), most likely due to the acclimatization of the plant and the capacity for the plant to possibly be able to metabolize the low concentration of the toxin.

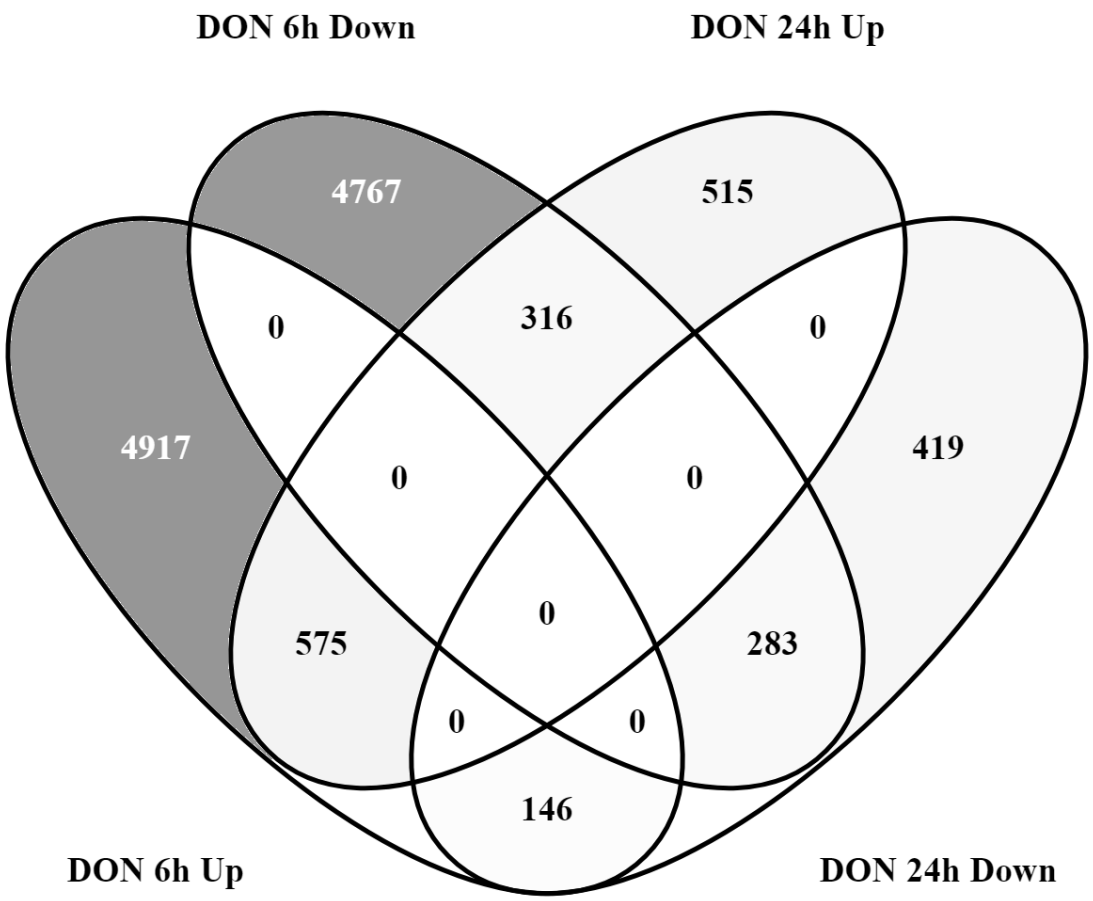

Figure 5-1 Overall response of Brachypodium roots to DON 5 µM at 6 h and 24 h. RNAseq DEGs were divided in four list corresponding to which time point they originated and if they were up or downregulated in relation to the control. The data was then inputted into Venny (https://bioinfogp.cnb.csic.es/tools/venny/) originating 8 distinct lists (4917 up-regulated DEGs exclusive to DON response at 6 h; 4767 down-regulated DEGs exclusive to DON response at 6 h; 515 up-regulated DEGs exclusive to DON response at 24 h; 419 down-regulated DEGs exclusive to DON response at 24 h; 575 up-regulated DEGs common to both 6 h and 24h; 283 down-regulated DEGs common to both 6h and 24 h; 316 DEGs down-regulated at 6 h and up-regulated at 24 h; and 146 DEGs up-regulated at 6 h and down-regulated at 24 h).

The total amount of up-regulated genes at 6h was then upload to PlantRegMap for GO enrichment analyses, with a total of 4477 genes having GO annotations and 635 GO terms being enriched. The majority of the most significantly enriched GO terms are well-known DON targets consisting of ribosome biosynthesis and subunit organization, as well as amino acid biosynthesis and gene silencing (Supplemental Table 5-2). One of the most relevant GO terms, *ribonucleoprotein complex biogenesis*, having 235 out of 355 annotated genes being up-regulated upon DON application. Another significantly affected GO process is *ribosomal*

large subunit biogenesis, with 64 out of 79 annotated genes being induced by DON, with the small subunit having 56 out of 80 genes induced.

Many processes associated with RNA are also affected, including processing, maturation, modification, splicing and transportation (Supplemental Table 5-2), with the most prominent GO term involving *RNA processing* having 315 out of 572 annotated genes being affected, which include mRNA, tRNA and rRNA processing.

Development processes are also disrupted, including the development of the embryo, reproduction system and lateral roots (Supplemental Table 5-2). Response to external stimuli, nitrogen, viruses, bacteria and fungi are also up-regulated along with the corresponding defence response (Supplemental Table 5-2).

When analysing the down-regulated genes at 6h, a total of 4121 genes have GO annotation and 494 GO terms are enriched. Another very important trait affected by DON is the maintenance of ROS, a trait well represented in the GO enrichment list with hydrogen peroxide metabolic process and reactive oxygen species metabolic process having half of its genes within the GO category being differentially expressed (Supplemental Table 5-3). Many other processes that lead to changes in ROS are also down-regulated by DON, including changes in expression in mitochondria and chloroplast proteins, including their corresponding electron transport chain (Supplemental Table 5-3). The cell wall and cytoskeleton are also affected, both in their biogenesis and structure. Several chemical transport, homeostasis and abiotic stress responses are also down-regulated, including water and ion transport, osmotic and salt stress response, and sugar transport and metabolic processes (Supplemental Table 5-3).

For the analyses of the plant response at 24 h, the GO enrichment analyses were divided in 2 parts, corresponding to up and down-regulated DEGs, with a total of 3 different lists each, according to the Venn diagram comparison between 6 h and 24 h (Fig 5-1).

The first analysis was performed on the 515 up-regulated DEGs exclusive to the 24 h expression profile with 356 genes having GO annotation and 67 GO terms being enriched. The most affected GO terms are mainly associated with photosynthesis and light stimulus and response (Supplemental Table 5-4). When analysing the 575 DEGs that are up-regulated at both 6 and 24 h, 412 genes have GO annotation and 125 GO terms are enriched, with the majority being associated with toxin response, glucuronidation and oxylipin biosynthesis (Supplemental Table 5-5). For the 316 DEGs that are down-regulated at 6 h and up-regulated at 24 h, 247 genes have GO annotation and 143 GO terms are enriched, which correspond to most of the genes involved in the ROS pathway and chemical transport, homeostasis and abiotic stress response (Supplemental Table 5-6).

The first list of the second part comprises the 419 down-regulated DEG exclusive to the 24 h response, with 324 genes having a GO annotation and 122 GO terms being enriched. The main GO terms affected relating to the cell cytokinesis and glycosylation (Supplemental Table 5-7). When it comes to the 283 common down-regulated DEGs at 6 and 24h, 230 genes have GO annotation and 105 terms are enriched, with the most significant terms being associated with cell wall and the ROS pathway (Supplemental Table 5-8). For the 146 DEGs that are up-regulated at 6h and down-regulated at 24 h, 125 genes have GO annotation and 183 are enriched, associated with RNA maturation and transportation and ribosome biosynthesis and subunit organization (Supplemental Table 5-9).

5.3.2 Comparison of the root growth of Bd21 between different ROS-inducers and DON

Among the various *Bd* responses to DON, one of the most represented at both times was the production, maintenance and detoxification of ROS. To understand if ROS can explain the response of DON in the roots a set of experiments were conducted using DON and a series of ROS inducers to observe the phenotype of the roots. In order to visualize the growth under the different conditions, 2-day old seedlings of Bd21 where place in a 1 mL tube containing 0.4% water agar amended with either 10 µM DON, or different concentrations of

four known ROS inducers and agents: hydrogen peroxide (H_20_2), menadione, alloxan and methyl viologen.

The concentration of DON used was based on the previous work by the group (Peraldi 2012), where after optimisation of the protocol, the most enhanced root growth phenotype was observed at 10 µM DON. The phenotypes of the roots where then recorded in the following days comparing their growth to the water control tubes.

In the water control the primary root displayed a general curvature alongside the walls of the tube (Fig 5-2), while under DON conditions the roots are longer and display a higher positive gravitropism displaying minimal curvature in growth (Fig 5-2). DON also promoted the growth of two coleoptile node axile roots in addition to the primary root in all replicates, which is not observed under control conditions at the same time point (Fig 5-2).

Figure 5-2 Roots of Bd21 at 3 days post stratification (dps) under control 0.4% foremedium agar (H_2O) and with DON 10 µM. White bar represents 1 cm.

No effect on root growth was able to be determined for menadione where all three concentrations proved to be highly toxic to the seedlings (Fig 5-3). Methyl viologen showed promising results in all three concentrations of 1 nM, 10 nM and 50 nM, with the roots showing a slight positive gravitropism reminiscent of the effects of DON (Fig 5-3). After 2 dpi however, the three concentrations proved to be toxic to the development of both the roots and shoots, where both tissues ceased growing.

Alloxan showed a similar tendency to the control at the lower concentration of 15 µM (Fig 5-4) but was capable to produce root elongation and positive gravitropism at the higher concentrations of 150 µM and 750 µM (Fig 5-4). Both concentrations, however, were highly toxic to the development of the shoots from the beginning of the experiment leading to their eventual death (Fig 5-4). This also affected the root development after 2 dpi with the plant ceasing to grow and dying. For H_20_2 a series of concentrations of 0.5 mM, 1 mM and 2 mM was applied, with the clearest phenotype observed at 1mM (Fig 5-4). The concentration of H_20_2 0.5 mM was similar to the control, while the concentration of H_20_2 2 mM was already showing signs of toxicity in the root development (Fig 5-4). When comparing H_20_2 (1 mM) and (DON 10 µM), similar phenotypes are observed, with loss of curvature and accentuated positive gravitropism. Although the phenotypes were similar, H_20_2 effect on the roots was more transient than DON, with the beforementioned phenotypes dissipating in some of the samples, with the root returning to exhibit a slight curvature similar to the control. The formation of coleoptile node axile roots was not observed in any of the ROS inducers and only partially observed in some replicates under the higher concentration of H_20_2 of 2 mM (Fig 5-4), remaining a trait mainly associated with DON.

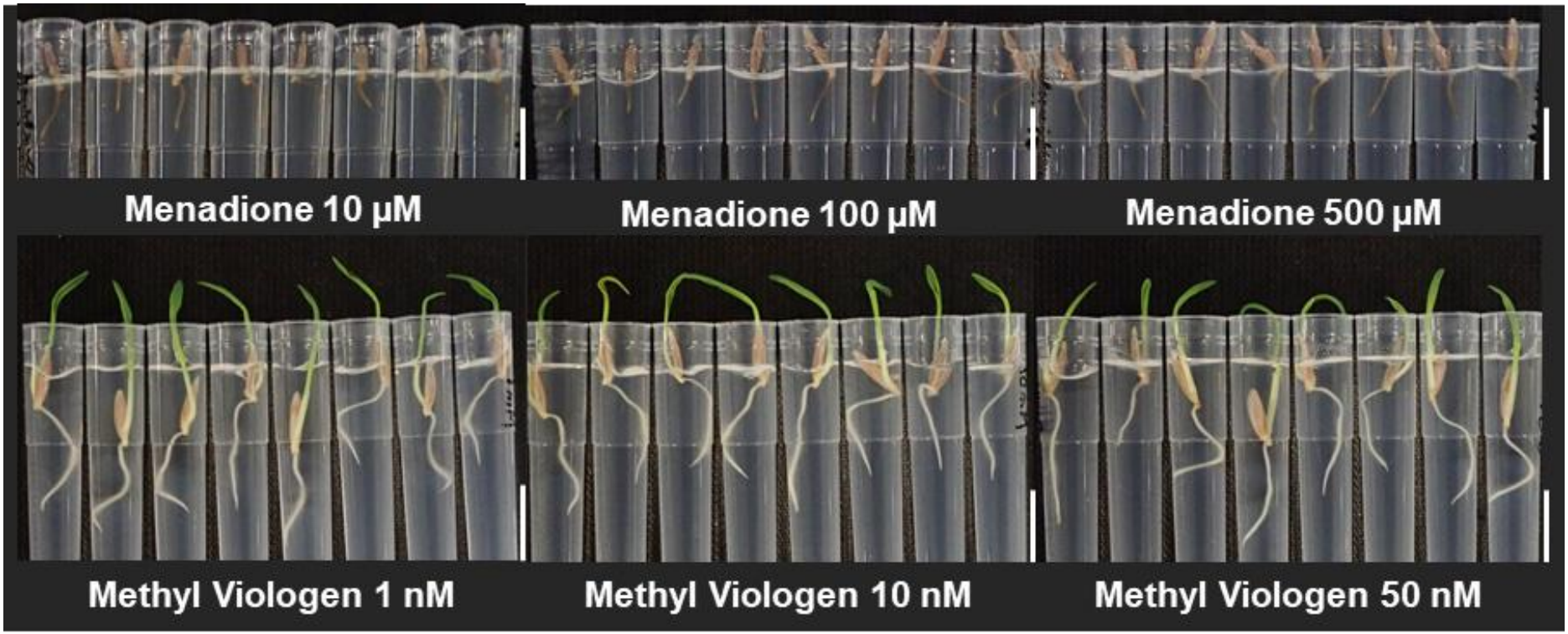

Figure 5-3 Roots of Bd21 at 3 dps under ROS inducers menadione and methyl viologen. White bar represents 1 cm.

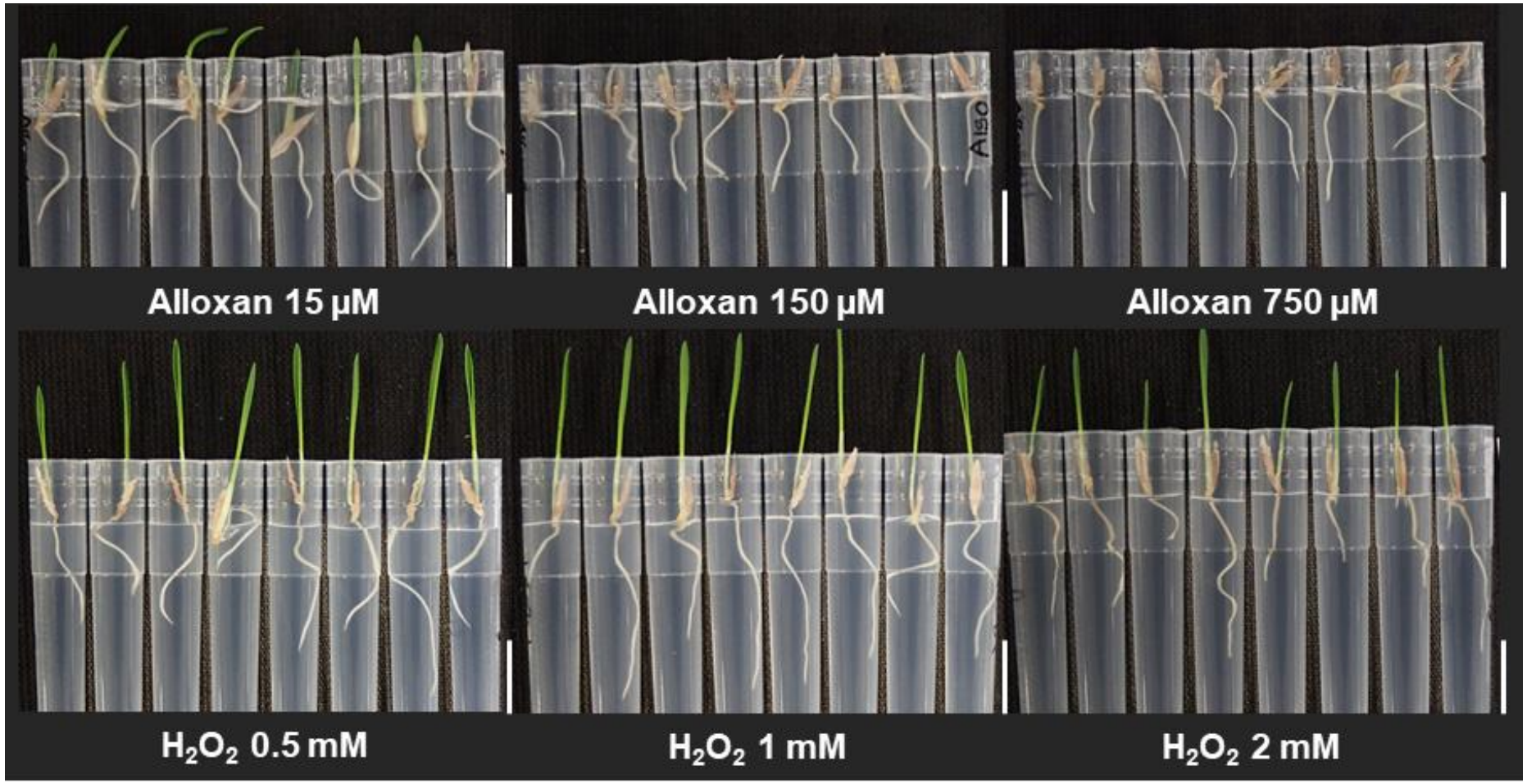

Figure 5-4 Roots of Bd21 at 3 dps under ROS inducer alloxan and the ROS H_2O_2. White bar represents 1 cm.

5.3.3 Comparison of Bd21 RNA-seq differential gene response under low concentrations of DON and ROS

To analyse the similarity in response between DON and H_20_2 a second RNAseq was performed using the same methodology as the previous RNAseq but focusing at 6 h as it was the highest response to DON by *Bd* (Supplemental Table 5-10). When comparing the response between DON and ROS, more than 50% of the ROS DEG response is also affected by DON (Fig 5-5 A), revealing that many of the pathways are affected by both molecules. Another observation that can be made is that there is no major indication of contrasting responses, with only around thirty genes being up regulated in response to one compound and down regulated in response to the other (Fig 5-5 A). For the analyses of the consistency of the *Bd* response to DON, the DEGs corresponding to the first DON RNAseq at 6h was compared to the second RNAseq (Fig 5-5 B). Although a complete overlap was not achieved, at least 50% of differential response was similar in both experiments. The up-regulated DEGs represented the best correlations between the two DON RNAseq experiments, as well as the highest magnitude of differential expression. There was again only a very low occurrence of contrasting expressions, with only a maximum of 18 genes being upregulated in one RNAseq experiment but down-regulated in the second RNAseq.

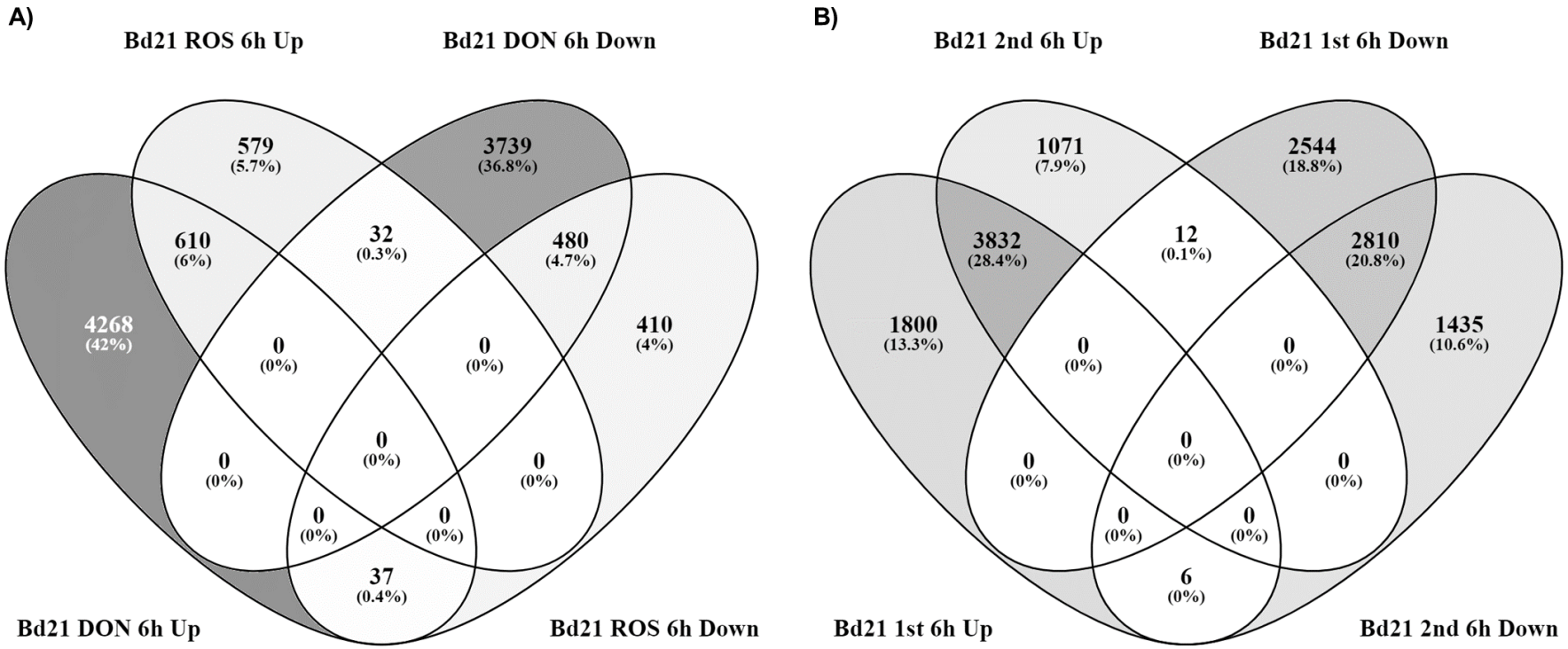

Figure 5-5 A) Second RNAseq comparison between DON 10 µM and H202 1mM (ROS) response in Bd21 plants at 6 h. Around fifty percent of the ROS response is accounted by DON, where 610 DEGs are up-regulated at 6 h in both DON and ROS response, and 480 DEGs are commonly down-regulated. Only 32 and 37 DEGs have contrasting expressions between the two responses. B) Comparison between the DON response at 6 h from the first and second RNAseq. The DON response was not fully conserved between the two RNAseq but displayed an overlap of 50% of its genetic response, with only 12 DEGs (0.1% of the entire differential gene response) having contradicting gene expressions.

In order to refine analyses between the interaction of ROS and DON response, the 'core' DON responsive DEGs (representing the genes that were differentially expressed in both DON RNAseq experiments), were compared to the ROS DEGs, separating the analyses between up-regulated (Fig 5-6 A) and down-regulated responses (Fig 5-6 B). The 3328 'core' DON up-regulated DEGs had 2605 genes with GO annotation and 561 GO terms enriched, with the most significant DEGs being those involved with the RNA and ribosome pathways as previously observed in the first DON RNAseq experiment (Supplemental Table 5-11). When examining the GO terms in common between ROS and DON up-regulated genes, 395 genes have GO annotation and 143 GO terms are enriched, on the great majority of which are involved in toxin and abiotic stress responses, along with glutathione, uronic acid and phytoalexin metabolic pathways (Supplemental Table 5-12). For the ROS specific up-regulated DEGs, 379 genes have GO annotations and 121 GO terms are enriched, with a focus on the ATP pathway along with metal ion homeostasis and ribonucleotide metabolic processes (Supplemental Table 5-13). In the down-regulated DEGs, of the common 2476 'core' DON DEGs, 2022 genes have GO annotation with 471 GO terms being enriched, mainly involved in cellular transport, microtubule-based movement and pigment biosynthesis including tetraterpenoid and carotenoid metabolic processes (Supplemental Table 5-14). In the analyses of the common down-regulated genes between the 'core' DON and ROS DEGs, 251 genes have GO annotation and 76 GO terms are enriched. The great majority being involved in ROS pathway and cell wall organisation and synthesis (Supplemental Table 5-15). The final list encompassed the down-regulated DEGs specific to the ROS response, with 253 genes having a GO annotation and 50 GO terms being enriched, involved in the transport of nitrate and ions as well as other pathways connected to the membrane integrity (Supplemental Table 5-16).

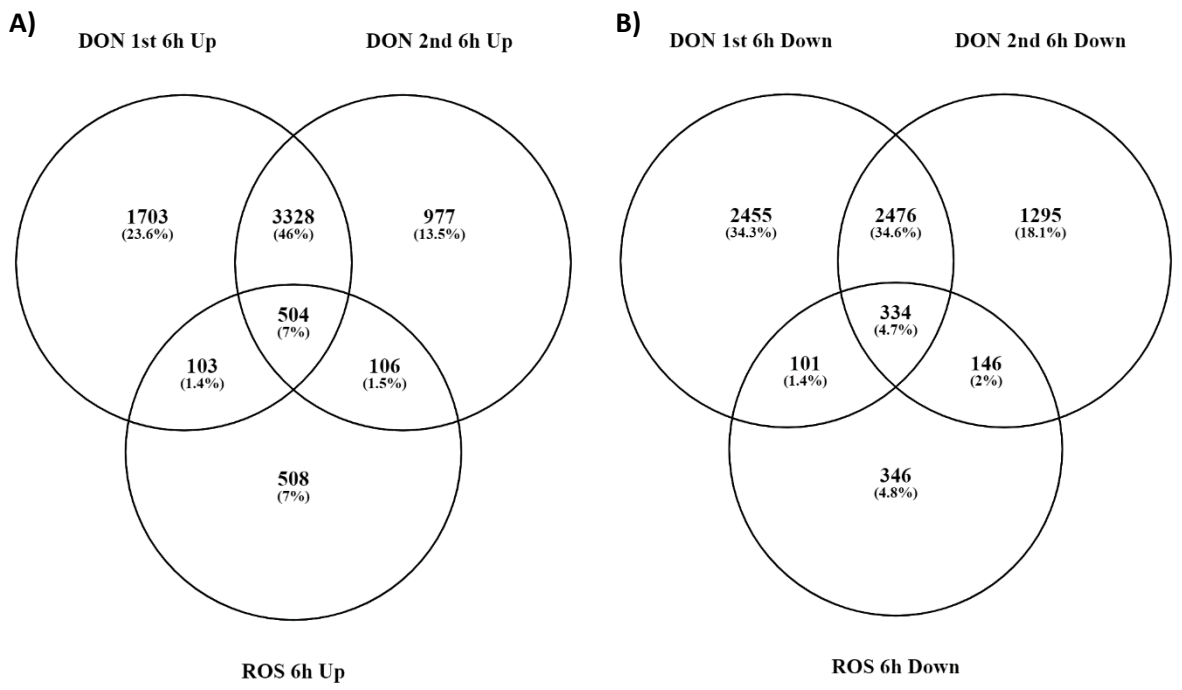

Figure 5-6 Overall DEG comparison between ROS and the two RNAseq DON responses at 6h A) Up-regulated response displaying the expression similarities between DON and ROS response, with a total of 504 DEGs common to both ROS and the core DON response (shared DEGs between the first and second RNAseq DON response at 6h). DON response still comprises the higher number of DEGs in the RNAseq experiment, with a total of 3328 DEGs being specific to the DON core response. B) Down-regulated response with a total of 334 DEGs common to both ROS and the core DON response. A total of 2476 DEGs being specific to the core DON gene response.

To try to reduce the number of genes and GO enrichment terms for consideration, a log2 expression fold change cut-off of “>2” or “<-2” was use on both the up-regulated and down-regulated DEG list of ROS and DON response at 6h (Fig 5-7). There was an overall reduction of 90% of the number of up-regulated DEG from ROS at 6h from 1221 to 122 genes (Fig 5-6A, Fig 5-7A). This reduction is also observed in the DEG lists shared between ROS and the core DON response and the DEG list specific to ROS, with a reduction between 87 to 91% (Fig 5-6A, Fig 5-7A). When examining the up-regulation in the DON response, the magnitude of expression cut-off affected the number of genes from the first RNAseq, more than the number genes from the second RNAseq, with the first RNAseq DEG list suffering a reduction of 90%, while the second RNAseq DEG list only suffering a reduction of 86% (Fig 5-6A, Fig 5-7A). When it comes to the specific core response of DON, it follows

the beforementioned trend of having a reduction of 90%, from 3328 genes to 338 genes (Fig 5-6A, Fig 5-7A).

The ROS down-regulation response had a higher reduction in the number of their DEG when subjected to a magnitude cut-off of "<-2", having a 97% reduction from 927 DEG to 26 (Fig 5-6B, Fig 5-7B). None of the 26 DEG is shared with the core DON response, with 21 being specific to the ROS response (Fig 5-7B). The discrepancy between the first and second RNAseq is still observed in the down-regulation response, with the overall DON response from the first RNAseq having a 93% reduction, while the second RNAseq having an 89% reduction in the number of their DEG (Fig 5-6B, Fig 5-7B). For the specific common core DON response, a reduction of 94% is observed, from 2476 to 132 DEG (Fig 5-6B, Fig 5-7B).

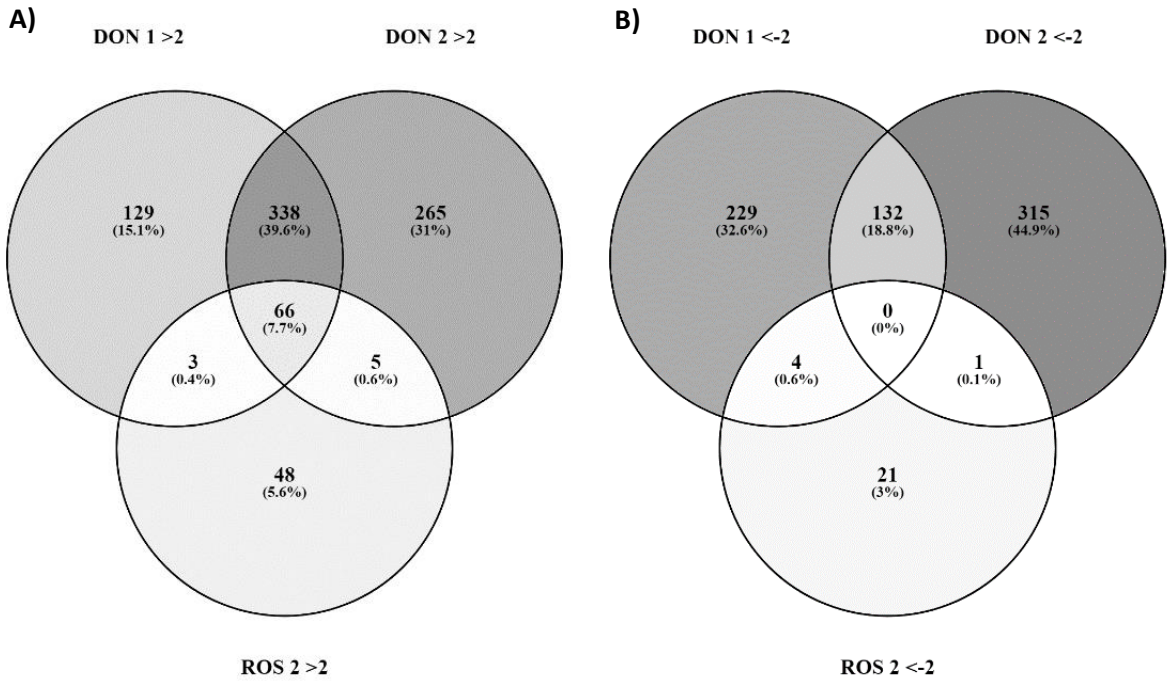

Figure 5-7 ROS and the core DON response with a threshold DEG log2 cut-off of >2 or <-2. The first RNAseq response to DON at 6h is represented as DON 1, while the DON and ROS response at 6h from the second RNAseq is represented as DON 2 and ROS 2, respectively.

When performing a GO enrichment analysis to the “>2” fold expression cut-off for the 338 specific core DON up-regulated DEGs the observation made in the initial analyses is affected with a large number of GO terms related to RNA and ribosome being lost (Supplemental Table 5-17). Terms like “oxoacid metabolic process”, “carboxylic acid metabolic process”, “glucuronate metabolic process”, “uronic acid metabolic process”, flavonoids, “drug transmembrane transport”; are among the most affected GO terms (Supplemental Table 5-17). For the 48 ROS-specific up-regulated DEGs, the GO terms related to oxidative stress remain highly represented, but now a more focused abiotic stress response related to heat stress, along with a more specific metal ion homeostasis involved in “cellular manganese ion homeostasis” is observed (Supplemental Table 5-18). When it comes to the 66 ROS and core DON common up-regulated DEGs the main focus becomes toxin catabolic and metabolic processes, along with glutathione and heat stress related pathways (Supplemental Table 5-19). It is important to note that the genes belonging to the ROS-specific up-regulation involved in heat stress were from a different group than the heat stress genes from the ROS and DON common response, suggesting different pathways being affected.

For the down-regulation analyses, when looking at the 132 down-regulated specific core DON DEGs, the pathways disrupted are mainly involved in the photosystem and thylakoid and cell wall organisation (Supplemental Table 5-20). Looking at the “<-2” fold expression cut-off for the 21 specific ROS DEG, the cell wall organisation is still one of the most significant GO terms affected (Supplemental Table 5-21). Transport pathways are also affected, specifically in the transport of sugars.

There are no common ROS and core DON related down-regulated genes with an expression cut-off of <-2, possibly indicating that the most significant shared pathways between the two are involved in the up-regulation response rather than a down-regulation in expression.

5.4 Discussion

One of the first described targets of DON in the plant cell is the inhibition of protein synthesis by causing a disruption to the initiation, elongation or termination of the chain elongation step due to its ability to bind to the 60S subunit of the ribosomal complex (Wei et al. 1974; Schindler 1974; McLaughlin et al. 1977; Christopher, Carter, and Cannon 1977). These findings corroborate with the RNAseq characterization of the DON response by *Bd*, where the most significant GO term enrichments observed in the up-regulated DEGs is involved in ribosome biosynthesis and subunit organisation. In mammalian cells DON has been shown to modify the structure of 28S rRNA (Zhou, Lau, and Pestka 2003; Gray et al. 2008), leading to the cleavage of the 28S rRNA and the activation of RNA-associated protein kinases (Gray et al. 2008; Li and Pestka 2008). This is also observed in the current analyses, with 28S and 60S subunits equivalents in Bd21 being affected upon DON exposure at 6h. DON has also been documented induce expression of a large number of microRNAs which possibly target ribosomal proteins on the basis of their complimentary sequence coinciding with several ribosomal subunit proteins (He and Pestka 2010). The GO terms involved in “microRNA production for gene silencing” are also enriched in the DON up-regulated DEGs, which might include the aforementioned ribosomal microRNA. It is probable that the cell increases expression of the synthesis of new ribosomal RNA to maintain protein synthesis in the cell in order to compensate the DON targeting of ribosomal RNA. This would explain the up-regulation of ribosomal biosynthesis in the RNAseq at 6 h. At 24 h, the GO terms involved in the ribosome pathway shift from their up-regulation at 6 h, to being down-regulated. This may reflect the ability of the plant to have acclimatized to the low concentrations of DON at 24 h, and no longer needs the compensatory up-regulation to cope with the toxic effects of DON. Apart from rRNA and microRNA, all pathways involved in mRNA modification and processing are also affected at 6 h. This could suggest that DON is not only involved in the ribosome binding to mRNA, but also in the disruption of other RNA binding systems, like the RNA transport proteins, RNA spliceosome and RNA maturation proteins. At 24 h, this response is

also down-regulated, possibly reflecting a reduction in DON content because of DON detoxification by the plant. This would reduce the number of DON molecules disrupting the connection between RNA binding sites and RNA, creating a similar compensatory-recycling effect from 6 h to 24 h, as observed in the ribosome pathway.

Apart from RNA, trichothecenes can also affect DNA synthesis and cell division. In mammalian cells, DON has proved to be able to cause changes in microtubule dynamics during cell division upon meiosis of porcine oocytes (Schoevers et al. 2010). It also affects mitosis, both in mammalian and plant cells, being capable of causing G2/M phase cell cycle arrest (Packa and Sliwinska 2005; Yang et al. 2008). In the roots of cereals, the arrest was partially caused due to the inhibition of the spindle formation (Packa and Sliwinska 2005). Other phenotypes like chromosomal malformations, along with enlarged nucleoli and micronuclei were also reported as mycotoxic phenotypes caused by DON in dividing cells in plants (Packa 1998; Packa and Sliwinska 2005). One of the two main processes down-regulated by DON at 6 h, is the maintenance and biogenesis of the cell wall. This disruption by DON during cell division could be related to the down-regulation of cell wall proteins and microtubules, disabling the capacity of the cell to divide efficiently.

DON also affects the hormone balance of the plant, where in wheat and barley an up-regulation of jasmonic acid biosynthesis genes occurs upon DON administration (Boddu, Cho, and Muehlbauer 2007; Walter and Doohan 2011). Apart from the hormone pathways, the abiotic stress response is also affected by DON, including drought and cold abiotic stress related genes (Ansari et al. 2007; Boddu, Cho, and Muehlbauer 2007). These processes are affected in the DON response at 6 h, with genes involved in oxylipin/jasmonic acid and abiotic stress responses being up-regulated.

Another well documented trichothecene function in the cell is the increase of production of ROS in the cell, where both T-2 and DON play the most significant roles. In both mammalian and plant cells, high concentrations of DON have shown to result in an increased production of H_20_2 in the cell, leading to cell death (Desmond et al. 2008; Costa et al. 2009).

ROS production and detoxification, along with oxidative stress related responses, are part of the other main group of pathways being down-regulated at 6 h, with the response to H_20_2 being the most significant ROS GO term represented in the list of DEGs. It is worth mentioning that separate detoxification responses are being triggered by DON and ROS, where complex detoxifiers, seem to be up-regulated, while more common detoxifiers, like peroxidases, are the main group being down-regulated.

In order to analyse the possible interaction between the DON and the ROS response, a series of tests were performed using known ROS and ROS inducers. All three ROS inducers, menadione, alloxan and methyl viologen, were found to be toxic to *Bd*, although displaying different initial development responses in the first two days of exposure. Menadione was toxic in all concentrations, possibly due to a high percentage of ethanol in the buffer where it was diluted, adding to the toxicity of the molecule. Methyl viologen and alloxan induced positive gravitropism in the roots of Bd21 but proved to be toxic to the seedling development. These compounds, unlike H_2O_2 and DON, may not be metabolised or degrade naturally and so continue to stimulate ROS production. If this is the case, it could suggest that production of ROS can lead to similar root phenotypes as observed with a low concentration of DON, but that the effect of prolonged exposure then becomes toxic with the increasing amount of ROS production induced by alloxan and methyl viologen.

The effects observed on administration of H_20_2, proved to be the most similar to those of the DON response, with the concentration of 1 mM producing both positive gravitropism and elongation of the primary root. Toxic effects were only observed under the higher concentration of H_20_2 at 2 mM, with 50% of the roots showing inhibition of the root growth. The long-term maintenance of growth under H_20_2, is possibly due to the capacity of the plant to more easily metabolize this compound, unlike the other ROS inducers. Desmond et al, have previously established that DON can cause the production of H_20_2, which in turn led to the PCD of the plant in later stages of exposure (Desmond et al. 2008). It seems some of the known phenotypes of DON can be explained by its associated production of H_20_2 within the

cell. This view is supported by findings that the addition of antioxidants to the cells affected by DON, decreases the occurrence of programmed cell death (Desmond et al. 2008). A similar relationship between low concentrations of DON and H_20_2 is observed in this study, where both compounds seem to lead to the same developmental phenotypes in the primary root of Bd21. This suggests that even under low concentrations, DON-mediated production of ROS still occurs, and is an important contributor for DON related phenotypes.

The internal production of H_20_2 has already been found as an important determent of root development in the plant. Production and balance of ROS in the root accumulates in the transition zone of cellular growth of the primary root of *Arabidopsis thaliana*, where H_20_2 seems to be present in the elongation zone, while superoxide ($O_{2^{\cdot}}^{-}$) accumulates in the meristematic zone (Tsukagoshi, Busch, and Benfey 2010). Disruption of the homeostasis between these two ROS species leads to abnormal elongation of the cells (Tsukagoshi, Busch, and Benfey 2010), which might explain the elongation of the roots under DON and H_20_2. Interestingly, Tsukagoshi et al 2010 suggests that H_20_2 over-production leads to cell differentiation, while $O_{2^{\cdot}}^{-}$ to cell proliferation. This is deduced by the supressing of the transcription factor UPBEAT1, which leads to an increase in peroxidases specific for H_20_2, leading to an increase of $O_{2^{\cdot}}^{-}$ as a plant mechanism in trying to maintain ROS homeostasis in the root system. This, in turn, leads to an increase in proliferation and thus root growth, but the specific mechanism in which this is controlled is not known (Tsukagoshi, Busch, and Benfey 2010). It is evident that destabilizing the homeostasis of ROS can affect the transition zone of the root, affecting cell elongation and proliferation, suggesting that the root elongation observed under the exogenous administration of DON and H_20_2, could be partly due to disrupting of this system. A similar observation in maize suggests a role of ROS in root cell development, where hydroxyl radicals interact with the plant cell wall, leading to loosening and cell elongation (Schopfer 2001). The detoxification of the hydroxyl radical and other ROS, leads to primary root inhibition and limited leaf growth in maize, linking ROS production with plant development (Rodriguez, Grunberg, and Taleisnik 2002; Liszkay, van der Zalm, and Schopfer 2004). The study of

apoplastic H_20_2 has also been studied, demonstrating that H_20_2 positively regulates the root cell production and elongation under well-watered conditions, but leads to root inhibition in water-depleted roots (Voothuluru et al. 2020). These studies suggest a strong link between the production of ROS and root growth and development, which coupled with the low concentration DON phenotypes in root growth, demonstrate DON as a potential up-stream regulator of ROS in the cell, and thus root development.

In order to understand what other mechanisms are shared between DON and ROS under low concentrations, a second RNA-seq was performed to compare the effects of H_20_2 and DON at 6 h on gene expression in the roots of Bd21. When looking at the most significant GO terms enriched in common between ROS and DON, most of the terms are involved in toxin metabolism, which is expected on the basis of the toxic characteristics of these two molecules. Other components shared between the two responses are those involved in glutathione, uronic acid and flavonoid metabolic pathways, all being involved in the production of, or acting as antioxidants against ROS production in the cell (Choudhary, Kumar, and Kaur 2020), further strengthening evidence for the potential of DON-related ROS production in the plant. When performing a GO analyses on the most highly expressed DEGs between the two responses, the toxin and antioxidants GO terms continue to be present, along with those for heat and temperature sensitivity, which could relate to increased free radical metabolism in the cell.

By analysing the specific DON up-regulated response, most of the pathways affected remain largely unchanged from the first RNAseq, most being involved in ribosome and RNA pathways. This agrees with the theory that DON affects the direct binding between ribosome subunits and other proteins to RNA. High concentrations of ROS have been shown to oxidise both deoxyribose and proteins, leading to DNA single strand breaks and amino acid fragmentation leading to proteolysis (Evans, Dizdaroglu, and Cooke 2004; Choudhary, Kumar, and Kaur 2020). No significant enrichment of these terms were found in the ROS response, suggesting that DON-mediated RNA and protein interactions are specific and possibly directly

controlled by DON, and not via a DON-mediated ROS interaction. Interestingly when analysing the most highly up-regulated DEGs among those specific to DON, most of the terms are involved with detoxification like flavonoid, uronic acid and glucuronidation, indicating a unique set of DEGs that are not involved in the antioxidation of ROS, but may reflect an attempt by the plant to try to modify the molecular structure of DON. Other terms related to ribosome and RNA pathways are still present, with a focus on tRNA modification and ribonucleotide binding, which agrees with the consequence of DON affecting the binding between the RNA molecules and the ribosome subunits.

When analysing the common DON and ROS down-regulation response, most of the pathways observed in the first RNAseq down-regulation response are shared between the two responses. As expected, most of the ROS response is similar between the two compounds, reinforcing the view that ROS-related effects are a component of the response of the plant to DON. Cell wall biosynthesis is the second most significant group in the analyses, follow by cell transport, possibly associated with the disruption of the cell wall. ROS has been associated with the maintenance of the cell wall by influencing the wall stiffness and wall loosening (Mhamdi and Van Breusegem 2018). In *Arabidopsis*, peroxidases involved in the production of $O_{2}^{\cdot -}$ lead to the breakdown of the cell wall polysaccharides and eventually to wall loosening (Muller et al. 2009). On the other hand, transcription factor KUODA1 is responsible for the control of peroxidases in the leaves of Arabidopsis (Lu et al. 2014). Disruption of the expression of KUODA1, led to accumulation of peroxidases, which affected the levels of H_20_2, leading to increased cell wall stiffness and smaller cells (Lu et al. 2014). Over-expression resulted in the opposite effect leading to larger leaves and bigger cells (Lu et al. 2014). It is possible that the down-regulation of genes involved in cell wall integrity and synthesis in the common DON-ROS RNAseq response reflects a component of the effect of DON on the ROS homeostasis in the cell and leading to modifications in the cell wall.

In the analyses of the genes showing the greatest reduction in expression in the core DON-specific response, the most highly represented GO terms are those involved in light

stimulus and chloroplasts. Involvement of DON in the chloroplast has already been documented, with one of the most important phenotypes associated being the bleaching of the heads, one of the most recognisable visual symptoms of FHB (Bushnell et al. 2003). *Fusarium* isolates with impaired DON production have a lower infection rate, normally correlated with low necrosis and bleaching in the plant, demonstrating the importance of DON production by the fungus (Boddu, Cho, and Muehlbauer 2007). Barley leaves exposed to high concentrations of DON entirely bleached after 48 to 72 h (Bushnell et al. 2010). This bleaching is linked to the decrease of chlorophyll a and b and carotenoids in the presence of light (Bushnell et al. 2010). Although pigment loss is directly connected with the presence of light, the stability of the plasmalemmas and tonoplasts, along with electrolyte leaking in the presence of DON is independent of light (Bushnell et al. 2010). Cycloheximide, a known protein synthesis inhibitor, was able to mimic the effect of DON, causing bleaching of barley leaves in high concentrations (Bushnell et al. 2010). This suggests that the direct role of DON in protein synthesis could be causing deleterious effects down-stream, creating instability to both cell membranes and chloroplasts. It is possible that the DON effect on chloroplast integrity could be the source of ROS production by DON, as chloroplast stress is known to increase the concentrations of $O_2^{\cdot -}$, which in turn is transformed to produce H_20_2 via the chloroplastic superoxide dismutase (Chang et al. 2009). Although not largely represented, auxin is the only hormone that displays a down-regulation in the core DON-specific response, which could correlate to the abnormal growth of the coleoptile node axile roots observed in all *Bd* replicates grown under low concentration of DON (Fig 5-4). As no development mechanism involving an interaction between DON and auxin has, to my knowledge, ever been described, this result would be novel within the role of DON in plant development. Other studies in wheat have shown that auxin production increases during the biotrophic phase of the fungus, leading to nutrient release and loosening of the cell walls promoting penetration and colonisation by *Fusarium* (Luo et al. 2021). It could be that under the absence of the fungus, DON perception by the roots could lead to the down-regulation of auxin genes, as an attempt by the plant to prevent fungal colonization.

In conclusion, DON is a complex molecule capable of producing several responses within the plant cell even at low concentrations. The primary target of DON is protein synthesis, with the majority of the pathways involved in ribosome and RNA being affected. It is hypothesised that DON directly links to the ribosome subunits and directly affects the linkage between mRNA and tRNA to the ribosome complex leading to compromised protein synthesis. This leads to organelle malformation, especially the chloroplasts of the plants, which may lead to an increase in ROS production. This increase in ROS production than leads to further effects in the plant, affecting cell membrane integrity, transport, proliferation and elongation. In order to cope with DON within the cell, the plant increases detoxification mechanisms, to maintain a homeostatic concentration of ROS. The return to homeostasis in response to a low concentration of DON is observed by 24 h, with almost all of the response observed at 6 h being significantly decreased, demonstrating the capacity of the early response to eliminate the effects of DON and allow the plant to return to equilibrium. The experiments in this chapter provide one of the first detailed studies into the specific responses to low concentrations of DON in the cell, with a dissection between its ROS and non-ROS mediated phenotypes.

Chapter 6. Candidate Gene Selection and Characterisation

6.1 Introduction

Just like *Fusarium*, DON resistance is very complex due to the multiple processes that the toxin affects. One of the most important resistances found in cereals against DON, is the synthesis of a family of UDP-glucosyltransferases (UGTs) by the host that are capable of converting DON to its less toxic form DON-3-O-glucoside (DON-3-G). The first example of UGT was observed in *Arabidopsis thaliana* where *DON-GLUCOSYLTRANSFERASE1* (*DOGT1*) showed an enhanced capacity to transform DON to DON-3-G (Poppenberger et al. 2003). Since this discovery similar UGTs have been found in barley (*HvUGT13248*) (Shin et al. 2012; Li et al. 2015), wheat (*TaUGT3*) (Lulin et al. 2010) and *Bd* (*Bradi5g02780*; *Bradi5g03300*) (Schweiger, Pasquet, et al. 2013; Pasquet et al. 2016), that can detoxify DON to DON-3-G promoting DON tolerance in the plant and decreasing FHB severity, although with different efficacies. A second class of detoxifiers were identified in *Sphingomonas* spp. where the cytochrome P450 encoded by the gene *Ddna* is capable of converting DON to 16-hydroxy-DON (16-HDON), a product incapable of reproducing the typical toxic DON phenotypes *in planta* (Ito et al. 2013).

Another family involved in DON tolerance are ABC transporters. The first one was identified in yeast, where the gene *PLEIOTROPIC DRUG RESISTANCE PROTEIN 5* (*PDR5*) when mutated resulted in an increase in DON related toxic effects, mainly growth inhibition (Mitterbauer and Adam 2002). When the gene was then transformed and expressed in tobacco leaves it increased DON resistance (Mitterbauer and Adam 2002). Similarly, the ATP-binding cassette (ABC) transporter in wheat *TaABCC3.1*, is associated with DON tolerance, where virus induced gene silencing (VIGS) of the gene increased bleaching and discoloration of the spikelets after toxin treatment (Walter et al. 2015). Although related to early response of the plant and response to jasmonic acid, little is known of the mechanism used by this

transporter, and whether it is directly targeting DON or one of the products from downstream affected pathways (Walter et al. 2015).

Another DON responsive gene is wheat methionyl-tRNA synthetase gene (TaMetRS), important in the synthesis of methionine, which although producing no significant effects when up-regulated in wheat when exposed to DON, was demonstrated to confer DON tolerance in transgenic Arabidopsis carrying the wheat gene (Zuo et al. 2016). The hormone pathways also display a role in the response to *Fusarium* and DON, where the *Reduced Height* (*Rht*) NIL lines, *Rht-B1b* and *Rht-B1c* which contain a gain of function of gibberellic acid sensitive DELLA proteins demonstrate increased resistance to FHB coupled with a significant reduction in DON-related phenotypes, showing reduced bleaching, smaller lesions and lower DON induced cell death (Saville et al. 2012). The silencing of the ethylene pathway gene *Ethylene Insensitive 2* (*EIN2*) was also demonstrated to decrease programmed cell death caused by DON in both Arabidopsis and wheat, as well as increased resistance to FHB (Chen et al. 2009).

A class of clade-specific genes, generally called orphan genes, also appear to play a prominent role in conferring DON resistance. Orphan genes are normally characterized as taxonomically restricted genes with strict homology within its plant family that confer lineage-specific adaptations which are coupled with the plant coping with various abiotic and biotic stresses. In wheat an orphan gene specific to the *Pooideae* was recently described as a major gene in DON tolerance (Perochon et al. 2015). Overexpression of *Triticum aestivum Fusarium Resistance Orphan Gene* (*TaFROG*) has been shown to increase plant tolerance of DON and resistance to FHB. In the opposite scenario where the expression of *TaFROG* is downregulated an increase in DON and FHB severity is observed (Perochon et al. 2015). Although the mechanism of *TaFROG*-related DON tolerance is not completely understood, it seems to interact with a central stress regulator *sucrose non-fermenting-1 (SNF1)-related protein kinase 1 catalytic subunit α* (*TaSnRK1α*), which leads to an increased kinase activity as well as a higher active phase upon DON application. Silencing of this gene was able to

mimic the silencing of *TaFROG* connecting the importance of both these genes in the plant tolerance to DON (Perochon et al. 2019).

The response to *Fusarium* and DON might be complex, but several studies have demonstrated that the plant can still adapt and create new mechanisms to acclimatize to or overcome the deleterious effects of the fungus. In chapter 3 and 4, it was demonstrated that *Bd* accessions differ markedly in their response to FRR. In chapter 5, it was also shown how DON induces a broad range of responses in accession Bd21. The two corresponding sets of data were able to refine the response of the plant to either specific regions of the genome, in case of the QTL analyses of *Bd* infection pattern to FRR; or to specific pathways that might play an important role in protecting the plant against DON, in case of the RNAseq data of Bd21 response to DON. However, no attempt was made to identify potential candidate genes in order to undertake further study of the FRR QTL interval and for potential translational studies of DON response.

In this chapter a candidate gene selection was performed using three different approaches. The fist approach makes use of the hypothesis from chapter 3 where ABR6 resistance is correlated with the restriction to the growth of *Fusarium* from the original point of infection in the roots. As previously discussed, DON as shown be important in *Fusarium* growth and infection, where mutations in the synthesis of DON lead to a severe reduction in virulence in the fungus. It is possible that ABR6 resistance could be connected with tolerance or a better detoxification of DON, leading to the reduction of the growth rate observed in *Fusarium*. Thus, a combination of Bd21 and ABR6 RNA-seq data, relating to each accession response to low concentrations of DON, was compared with the QTL interval from chapter 4, to look for potential QTL genes involved in the differential expression response to DON. The second approach was more focused in the Bd21 response to DON at 6 h and 24 h, where the genes with conserved high expression between the two time points were further characterised. The last approach focuses on the use of the available Bd21 RNA-seq data produced in the previous chapters, which was then compared with a another RNA-seq dataset from a

susceptible wheat variety, using similar low concentrations of DON. A candidate gene search was performed to identify genes that play a major role in the response of both *Bd* and wheat to DON. This latter approach enabled the creation of a conserved gene list between *Bd* and wheat. This list can then be use in the analyses of the potential role of the genes in resistance to DON and *Fusarium*, by using a single *Bd* candidate gene, bypassing the complications of working genome copies in tetraploid and hexaploid wheat. The gene of interested can then be used in a model-to-crop system to study if a similar role in resistance is conserved in wheat.

6.2 Materials and Methods

6.2.1 Wheat lines and seedling preparation:

The tetraploid durum wheat variety Kronos was used to reduce the effects of genome complexity in hexaploidy bread wheat. Kronos TILLING mutants, WKRON0198, WKRON1161, WKRON3714, WKRON2901, WKRON4096, WKRON2052, WKRON4211, WKRON2646, WKRON2065, WKRON3214 and WKRON2731, were obtained from the wheat TILLING seed bank (http://wheat-tilling.com/).

Seeds of Kronos were stratified in the same manner as *Bd*, described in chapter 2. After stratification they were either transferred to a 15 mL tube for DON response analyses, or to 96 well tray containing F2 compost, peat-based soil, and placed in a pre-vernalisation room at 20 ^{o}C day/ 17 ^{o}C night for 16 h / 8 h under fluorescent tube lights, until the emergence of the third leaf. Leaf samples were taken at this stage for all the seedlings that needed genotyping. Selected wheat plants were then placed in a 1 L pot containing cereal mix, John Innes No. 2, loam-based soil and placed in a speed breeding glasshouse (details below).

6.2.2 Wheat crossing and speed breeding:

The crossing between WKRON2901 (homozygous nonsense mutation in A genome) and WKRON2731 (heterozygous mutation removing start site in B genome) to produce a double mutant was performed by Andrew Steed. The subsequent populations were grown in

a speed breeding glasshouse at 22 ºC day/ 17 ºC night for 22 h / 2 h under a blend of metal halide and Valoya NS-1 LED (light-emitting diode) lights.

6.2.3 DON and ROS sensitivity assay:

Seeds of Kronos were stratified as described in chapter 2 and placed in 15 mL falcon tubes with 8 mL of 0.4% agar medium with the desired concentration of DON (3 µM, 5 µM and 7 µM). The growth of the roots was recorded over the following 7 days, generally quantifying the growth of the primary root. In the first analysis of Kronos parent, WKRON2605 and WKRON2901 a total of up to 15 seedlings per treatment per line were used. The same number of seedlings was used in the second analysis for Kronos parent, WKRON2901, WKRON2731-1, WKRON2731-2 and WKRON2731-3. In the third analysis a total up to 20 seedlings per treatment per line were used for WKRON2605, WKRON2901 and WKRON2731.

In the analyses of the double mutant, a total of 3 independent lines were used per genotype (Kronos WT, single mutant WKRON2901, single mutant WKRON2731, and double mutant 2731x2901), with a maximum of up to 5 seedlings per treatment. In the second analysis 2 independent lines for Kronos WT and double mutant 2731x2901 were used, with 10 seedlings of each. Only one independent line was used for the single mutants WKRON2731 and WKRON2901, with 10 seedlings per treatment each.

6.2.4 Double mutant KASP-like analysis:

For the DNA extraction of the F_2 population between WKRON2901 and WKRON2731, the third leaf of 14-day old seedlings were cut and followed the protocol used in the DNA extraction of Bd21 from chapter 4.

For the primer design for the mutations of WKRON2901 and WKRON2731 the sequences for genes TraesCS7A02G369500 and TraesCS7B02G259000 were obtained using the RefSeqv2.0 wheat genome reference from PlantEnsembl (http://plants.ensembl.org/Triticum_aestivum/Info/Index). The mutation location was obtained from the variant table for each gene in the database of PlantEnsembl. The primers were

designed by hand using the KASP primer design methodology from chapter 4 in order to differentiate between wild type and mutant sequences respectively. A full list of the primers is shown in Table 6-1.

Each line was analysed using the KASP methodology employed in chapter 4. Each line was characterized as being wild type, heterozygous or homozygous for the corresponding mutation in both of the genes.

Table 6-1 List of KASP marker primers used to identify the mutation homozygosity in the WKRON2731xWKRON2901 population.

QTL marker/ Bd position		**Primer**
7A02G369500Fw	FwA	GAAGGTCGGAGTCAACGGATTCGACGTGCGGGCGGCCATCC
	FwB	GAAGGTGACCAAGTTCATGCTCGACGTGCGGGCGGCCATCT
	Rv	TGGCTCCACCCTTTGGCCAC
7A02G369500Rv	FwA	GAAGGTCGGAGTCAACGGATTGGCCACGCGCGCCTTCTG
	FwB	GAAGGTGACCAAGTTCATGCTGGCCACGCGCGCCTTCTA
	Rv	TGGGCGGCGACGTGCGGG
7B02G259000Fw	FwA	GAAGGTCGGAGTCAACGGATTGAACAGAAGCGAAGGAGCAATG
	FwB	GAAGGTGACCAAGTTCATGCTGAACAGAAGCGAAGGAGCAATA
	Rv	TGATGTTGCCGCTCATCCTG
7B02G259000Rv	FwA	GAAGGTCGGAGTCAACGGATTGCCGCTCATCCTGCCCGTCGGC
	FwB	GAAGGTGACCAAGTTCATGCTGCCGCTCATCCTGCCCGTCGGT
	Rv	GCAGAGAGAACAGAAGCGAA

6.2.5 RNA-seq data analyses:

The RNA-seq data of *Bd* accession Bd21 was obtained in the previous chapter. RNA-seq data of *Bd* accession ABR6 followed the methodology employed in the second RNAseq experiment from the previous experiment. ABR6 was aligned to the *Bd* Bd21v3.1 genome because of the high quality of this assembly, and mapped using Bd21 GFF3, both obtained from Phytozome. ABR6 was also aligned to its own genome, the ABR6 genome (BdistachyonABR6_336_v1) and mapped using the ABR6 gene annotation (BdistachyonABR6_336_v1.ABR6_r.1.gene), also obtained from the Phytozome database.

The RNA-seq data of wheat (*Triticum aestivum* cultivar Hobbit 'sib') was performed using the RNA-seq raw data files obtained from the Genewiz data following the same settings as described in the previous chapter. Wheat seedling preparation and RNA extraction was performed by Lola González-Penadés following a similar pipeline as the previous chapter. The wheat genome RefSeqv2.0 from PlantEnsembl was used as a reference, along with the corresponding GFF3 gene list. The DEGs of the two datasets of Hobbit 'sib' response to DON at 6 h was kindly given by Lola González-Penadés for the purpose of comparing the response to DON between *Bd* and wheat. It should be noted that the Hobbit 'sib' RNA seq experiment was carried out as part of experiment 1 for Bd21 using identical approaches and materials to enhance the power of comparison of response between these hosts.

6.2.6 Data analysis:

For the analyses of the TILLING lines response to DON, the roots were measured from the crown to primary root tip for each day, to a maximum of 6 dpi.

All the data scores were analysed using a linear mixed model (REML), where each wheat line, date and treatment was characterized as fixed effects. The residual effect was also checked for normality and equal variance between the accessions and no further transformation was necessary. The final model was used for the calculation of the predicted means used in the final visual comparison between the lines. All analyses were carried out using Genstat 19th edition and RStudio with R version 3.5.0.

6.3 Results

6.3.1 QTL-based candidate gene selection

For the analyses of potential candidate genes involved in the response against FRR and DON three different strategies were employed. The first strategy involved combining the data obtained from the FRR QTL analysis of the population of ABR6 x Bd21 with the RNAseq data for response of the parent accessions to DON. To properly assess the two sets of data,

the ABR6 response to DON at 6 h was also assessed as part of the same experiment as the Bd21 response to DON and ROS at 6 h in the second RNAseq from the previous chapter (Supplemental Table 6-1). Since the sequencing and assembly of the ABR6 genome is not at the same high standard as that of Bd21, the RNAseq reads from the ABR6 response were aligned to both the ABR6 genome and Bd21 genome (Supplemental Table 6-1). The alignment of ABR6 to its own genome was used for the majority of the comparisons of the ABR6/Bd21 response to DON. The ABR6 alignment to the Bd21 genome was used as a quality control of the ABR6 data. The FRR resistance QTL region around the QTL peak marker Bd1-25478624 on chromosome 1 from chapter 4 was selected, spanning approximately 2.18 Mb, from region Bd1-24656925 to Bd1-26839250. This region was input into j-browse for Bd21 in the Phytozome database (https://phytozome-next.jgi.doe.gov/jbrowse/index.html?data=genomes%2FBdistachyon_v3_1), and 311 unique gene annotations were recovered (Supplemental Table 6-2). The flanking sequences of the region were BLASTed against the ABR6 genome, using the available BLAST tools of Phytozome, and a conserved region within ABR6 spanning around 2.17 Mb from pseudomolecule_1:23159527 to pseudomolecule_1:25329589 was obtained. This region was input into the corresponding ABR6 j-browse (https://phytozome-next.jgi.doe.gov/jbrowse/index.html?data=genomes%2FBdistachyonABR6_v1), following the same strategy employed for Bd21, and 270 unique ABR6 annotated genes were obtained (Supplemental Table 6-2). The corresponding log2 fold change from each RNAseq analysis of DON response was related to each gene obtained from the j-browse of Phytozome (two different log2 values corresponding to the first and second RNAseq of Bd21, and one single log2 fold value for the RNAseq performed on ABR6). Only a few genes within the respective regions displayed significantly differential expression in response to DON in the two parent genomes. Around 20% of the genes in the Bd21 interval showed significantly greater expression in response to DON and only 3 genes had a lower than -2 fold change in expression in one of the two RNAseqs (Supplemental Table 6-2). From the down regulated genes, Bradi1g30026 displayed a similar expression profile between Bd21 and ABR6, so it

was excluded from the final candidate gene list, leaving only genes Bradi1g29727 and Bradi1g30050 as differentially DON responsive (reduced expression) (Table 6-2). No gene in the QTL interval in Bd21 had a high fold change in expression that was consistent between the two RNAseq experiments performed in Bd21 response to DON at 6h (Supplemental Table 6-2). ABR6 on the other hand displayed differential expression of around 30% of its genes in the interval, with 4 genes displaying a differential lower than -2-fold change in expression and 10 displaying a differential higher than 2-fold change in expression (Supplemental Table 6-2). If the genes had around 1.5 times more expression between ABR6 and Bd21, they were included in the analyses. From these genes, one highly down-regulated gene Bradi1g29830, and two high up-regulated genes Bradi1g30610 and Bradi1g31060, were excluded due to their similarity in expression between Bd21 and ABR6, leaving 10 genes as potential candidate ABR6 FRR resistance genes (Table 6-2 *dark grey column*). Among these 10 highly differentially expressed genes from the ABR6 RNAseq alignment to the ABR6 genome, 8 also have a conserved high fold2 fold change in expression in the ABR6 RNAseq alignment to the Bd21 genome (Table 6-2 *light grey column*). A BLAST analysis was performed for each of the 13 candidate genes, and it was found that all had a corresponding gene represented in the other accession. All genes have a similarity between their sequences higher than 97%, apart from gene Brdisv1ABR6_r1004951m, for which the corresponding Bd21 Blast hit gene, Bradi1g29658, only shares around 90% of its DNA sequence (Supplemental Table 6-2). All QTL interval genes of pseudomolecule1 of ABR6 BLASTed to the corresponding chromosome 1 QTL interval Bd21 genes, apart from gene Brdisv1ABR6_r1004881m, which gave a top hit to chromosome 3 Bd21 gene, Bradi3g43660 (Table 6-2). Gene annotation of the 12 genes indicated that 7 of them are involved with cell division, gene expression and protein synthesis (Bradi1g29577, Bradi1g29740, Bradi1g30050, Bradi1g30290, Bradi1g30370, Bradi1g30580, Bradi1g30811). Two have a potential role in response to abiotic and biotic stresses (Bradi1g29658, Bradi1g30252). One gene is involved with chloroplast photosystem II (Bradi1g29500), while the remaining two genes lack precise gene descriptions, and therefore cannot be associated to a specific cell function (Bradi1g29727, Bradi1g30252).

Table 6-2 List of DON 6 h DEGs within the QTL region of Bd chromosome 1 related to FRR overall seedling death, in the genomes of accessions Bd21 and ABR6. Gene description was obtained from Phytozome and depicts predicted gene function. DEGs were filtered on the basis of their log2 (>2 or <-2, in any of the RNAseq analyses) and p-value (<0.01).

Accession Bd21	Description	Bd21 – 1st RNAseq		Bd21 – 2nd RNAseq		ABR6 - 2nd RNAseq [1]		Accession ABR6	ABR6 - 2nd RNAseq [2]	
		log2	p-value	log2	p-value	log2	p-value		log2	p-value
Bradi1g29500	PTHR32010:SF6 – Photosystem II stability/assembly factor HCF136, chloroplastic (1 of 1)	-1.065	2.27E-03	-1.829	7.76E-12	-3.084	4.13E-08	Brdisv1ABR6_r1004915m	-3.103	2.54E-08
Bradi1g29577	PTHR22891//PTHR22891:SF57 – Eukaryotic initiation factor 2C // subfamily not named (1 of 1)	-1.248	1.78E-11	-1.073	3.78E-04	2.399	3.43E-11	Brdisv1ABR6_r1004938m	2.400	3.10E-11
Bradi1g29658	PTHR23155//PTHR23155:SF637 – Leucine-rich repeat-containing protein // subfamily not named	-	-	-	-	-	-	Brdisv1ABR6_r1004951m	3.848	2.89E-06
Bradi1g29727	PF14309 - Domain of unknown function (DUF4378) (DUF4378) (1 of 24)	-2.307	7.58E-09	-	-	-1.650	2.98E-03	Brdisv1ABR6_r1004964m	-1.448	3.24E-03
Bradi1g29740	tRNA-intron endonuclease activity (Blast2GO)	0.891	1.26E-05	1.611	1.02E-11	2.385	7.58E-29	Brdisv1ABR6_r1004966m	2.371	9.69E-29
Bradi1g30050	PTHR31692:SF10 - Expansin-like B1 (1 of 1)	-3.619	6.47E-27	-	-	-	-	Brdisv1ABR6_r1005022m	-	-
Bradi1g30252	PTHR10641:SF483 – Transcription factor MYB44 (1 of 3)	1.436	1.38E-14	0.933	2.80E-03	1.200	2.63E-10	Brdisv1ABR6_r1005061m	2.410	5.92E-03
Bradi1g30290	K14797 - Essential nuclear protein 1 (ENP1, BYSL) (1 of 2)	1.755	6.96E-24	1.850	1.27E-11	2.389	1.32E-15	Brdisv1ABR6_r1005072m	2.700	3.30E-25
Bradi1g30370	H3/H4 histone acetyltransferase activity (Blast2GO)	1.234	7.75E-24	1.708	1.01E-27	2.311	7.15E-36	Brdisv1ABR6_r1005087m	2.308	9.69E-36
Bradi1g30580	Microtubule-severing ATPase activity (Blast2GO)	1.877	8.77E-27	1.997	1.61E-48	2.815	2.68E-15	Brdisv1ABR6_r1005129m	2.816	2.04E-15
Bradi1g30811	K02916 - Large subunit ribosomal protein L35 (RP-L35, MRPL35, rpmI) (1 of 1)	-0.735	3.90E-05	-1.207	8.75E-12	-1.547	2.22E-13	Brdisv1ABR6_r1005160m	-2.033	7.08E-14
Bradi3g43660	Manganese ion binding (Blast2GO)	-	-	-	-	2.900	7.73E-04	Brdisv1ABR6_r1004881m	2.915	7.35E-04

1 - ABR6 log2 value and p-value based on its mapping to the Bd21 genome. 2 - ABR6 log2 value and p-value based on its mapping to the ABR6 genome.

6.3.2 Identification of genes showing consistent high differential expression in response to DON.

The second approach for candidate gene selection made use of all three RNAseq data lists available for the Bd21 response to DON to identify those most highly responsive to DON. To observe if there were any highly expressed candidate genes between the different time points, the two lists of DEGs from the DON response at 6 h and the list of DEGs at 24 h were checked for common DEGs with an expression higher than 2 or lower than -2 (Fig. 6-1). By comparing the 404 genes highly up-regulated at 6 h to the 19 highly up regulated genes at 24 h, 17 genes proved to have a conserved high expression between the two time points (Fig. 6-1). None of the 132 highly down-regulated genes at 6 h, were the same as either of the two genes significantly down-regulated at 24 h (Fig. 6-1). A full characterization was performed on the 17 genes, taking into consideration available gene descriptions and orthologues in other cereals, such as wheat, barley and progenitors of wheat (*Aegilops tauchii* and *Triticum urartu*), obtained from the PlantEnsembl (https://plants.ensembl.org/index.html) database (Supplemental Table 6-3). If the DEGs were specific to the aforementioned cereal group, they were classified as Pooideae specific, characterizing them as potential orphan genes (Supplemental Table 6-3). For additional information, available tissue specific expression data from the Brachypodium eFP browser (http://bar.utoronto.ca/) was also included (Supplemental Table 6-3).

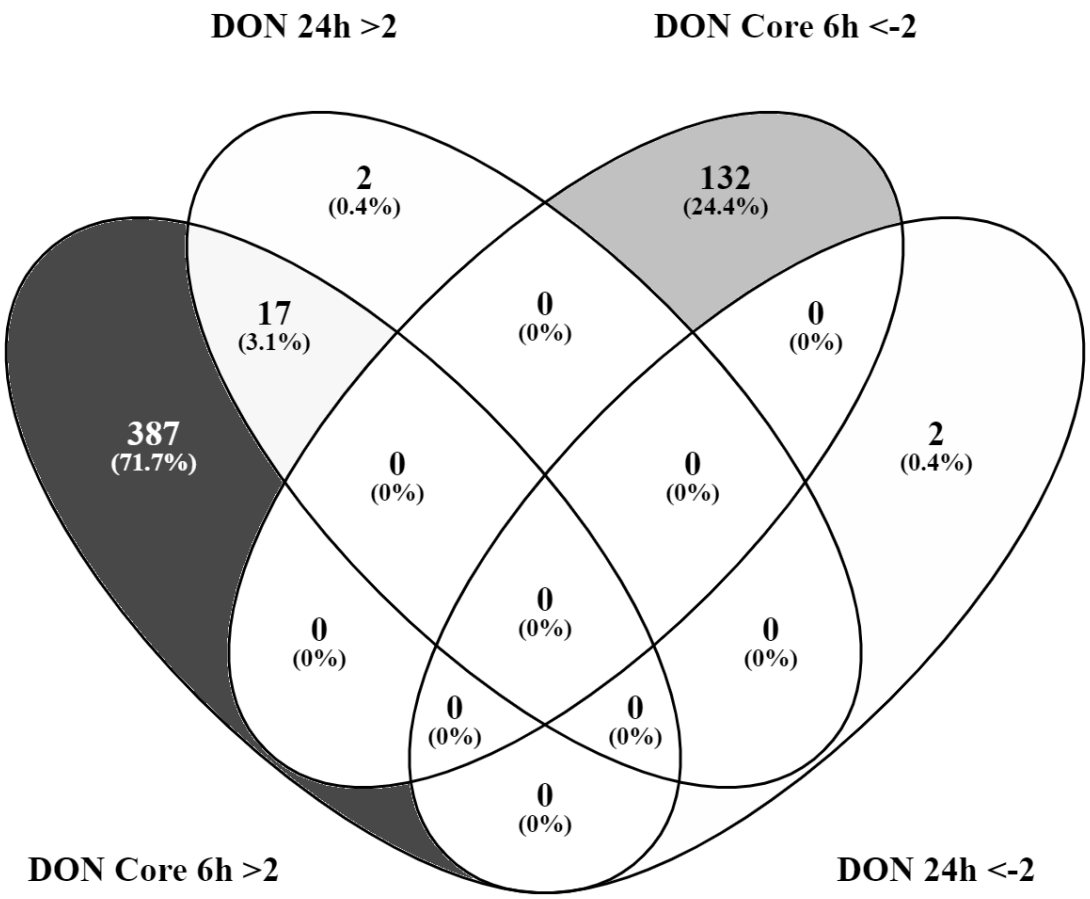

Figure 6-1 Venn diagram demonstrating the common DEG Bd21 response to DON from two different time points (6 h and 24 h). The DON core 6 h includes the common genes to both Bd21 RNAseq responses to DON. Only the significant DEGs with an expression higher than 1.5 or lower than -1.5 were included.

Taking into consideration all the data collected, 17 genes were identified as candidates for highly-DON responsive genes as they showed enhanced expression in all data sets (Table 6-3). These genes exhibited an expression fold change higher than 2 at both time points, and a very limited gene family expansion, not exceeding an average of 3 orthologues in diploid species (equivalent to 9 in hexaploid species), making them easier to study, as the risk of redundancy is reduced. In terms of tissue specific expression, some of the genes displayed highest expression in young tissues, including grain development, young root formation, young leaves, coleoptile emergence and development, along with primary internodes and the first root node (Supplemental Table 6-3). Older roots, leaves and floret and overall spikelet development, had a lower representation in the normal expression of these genes (Supplemental Table 6-3).

Table 6-3 Highly up-regulated DEGs with a log2 fold change in expression higher than 2 in both time points at 6 h and 24 h for all three different RNAseq datasets of Bd21 response to DON. All DEGs have a p-value <0.01.

GeneID	Description	log2 Bd21 1st RNAseq 6 h	log2 Bd21 2nd RNAseq 6 h	log2 Bd21 1st RNAseq 24 h
Bradi1g15252	#N/A	6.76	7.54	2.15
Bradi1g37080	Histone acetyltransferase activity (Blast2GO)	7.31	7.23	2.16
Bradi1g71630	PTHR12537//PTHR12537:SF68 - RNA binding protein pumilio-related // subfamily not named (1 of 3)	7.97	4.45	4.03
Bradi1g74980	#N/A	7.11	4.00	2.24
Bradi1g77491	#N/A	5.23	4.89	2.02
Bradi2g10857	PTHR10784//PTHR10784:SF1 – Eukaryotic translation initiation factor 6 // subfamily not named (1 of 1)	6.60	7.14	2.60
Bradi2g25440	F-Box	6.27	5.48	2.49
Bradi2g41010	#N/A	6.45	7.91	3.14
Bradi2g44200	Arachidonic acid binding (Blast2GO)	6.33	5.09	2.43
Bradi2g48540	#N/A	6.51	6.72	2.44
Bradi3g05960	PTHR31373:SF0 - EMB (1 of 3)	6.60	7.68	2.09
Bradi3g06330	Arachidonic acid epoxygenase activity (Blast2GO)	6.65	5.93	2.47
Bradi3g19390	K02941 - large subunit ribosomal protein LP0 (RP-LP0, RPLP0) (1 of 2)	8.07	9.83	2.37
Bradi3g31720	PTHR11260//PTHR11260:SF264 – Glutathione S-Transferase, GST, superfamily, GST domain containing // subfamily not named (1 of 4)	9.26	8.82	2.12
Bradi3g31727	PTHR11260//PTHR11260:SF269 - Glutathione S-Transferase, GST, superfamily, GST domain containing // subfamily not named (1 of 4)	8.37	7.97	2.47
Bradi3g38045	PTHR23024//PTHR23024:SF150 – Member of 'GDXG' family of lipolytic enzymes // subfamily not named (1 of 2)	8.67	8.14	3.24
Bradi4g22656	#N/A	6.58	2.96	2.43

This second approach identified 17 potential candidates, that much like the first analysis, have a relatively uninformative annotation for many of them. Four of the genes appear to be part of complexes involved in functions that need direct RNA and DNA binding (Bradi1g37080, Bradi1g71630, Bradi2g10857, Bradi3g19390). Three may be involved in the attempt to modify and detoxify DON (Bradi3g31720, Bradi3g31727, Bradi3g38045). Two genes (Bradi2g44200, Bradi3g06330) are involved with arachidonic acid related activity, with Bradi3g06330 function possibly being related to the cytochrome P450 arachidonic acid epoxygenase activity. The remaining 8 genes have no known function or are not described with a term sufficiently specific to narrow down to a particular role within the cell. Four of them, however, appear to be Pooideae specific (Bradi1g74980, Bradi1g77491, Bradi2g25440, Bradi4g22656), suggesting a potential role as an orphan gene within the plant.

6.3.3 Model-to-crop candidate gene selection

Another way to filter for potential genes of interest is to compare the *Bd* RNA-seq DON response dataset to the wheat RNA-seq DON response dataset. The wheat RNA-seq was developed by Lola González-Penadés and comprised two independent datasets. One was performed at the same time as the first Bd21 RNAseq response to DON, using the susceptible wheat cultivar Hobbit 'sib', with the same conditions and time-points, making a correlation between the two sets more reliable. The second used the same susceptible wheat cultivar Hobbit 'sib', with the same conditions to the second Bd21 and ABR6 RNAseq response to DON at 6 h. For the purpose of this chapter the main focus will be between the comparison of the first RNAseq of Bd21 and the first RNAseq of Hobbit ‘sib’ response to DON at 6h, using the data of the second RNAseq of both wheat and *Bd* to provide supplemental information. The ‘core’ DON response obtained from the consistent differential levels of expression at 6 h from the two Bd21 RNAseq was used as an initial step, to provide a robust list of DEGs in the comparison to the wheat response.

The list of the most highly up-regulated DEGS with a log2 fold change in expression higher than 2 in the core response of Bd21 to DON at 6 h was uploaded into PlantEnsembl in order to obtain the known orthologues of these genes in wheat. The following sequence of operations was performed to obtain and the characterize the common DON-induced DEGs between *Bd* and wheat:

1. Out of the 404 highly up-regulated Bd21 DEGs, a total of 1647 orthologues in wheat were identified.
2. The 1647 orthologues equivalent to the 404 Bd21 DEGs were then compared with the list of DEGs from the first RNAseq of Hobbit 'sib' experiment. This revealed a total of 781 genes that were also differentially expressed in the Hobbit 'sib' database.
3. The 781 wheat orthologues, corresponding to a total of 239 Bd21 DEGs were then combined in a single list, placing the Bd21 DEGs gene names in the head column with their corresponding Hobbit 'sib' orthologues and respective fold change (Supplemental Table 6-4).
4. When observing the correlation between the Bd21 genes and their corresponding wheat orthologues in the data, it was noted that several wheat DEGs related to a single Bd21 orthologue. In most instances this was due to the presence of the A, B and D genome homoeologues but evidence for gene expansion within wheat was also observed for some genes (Fig 6-2). This finding increases the potential importance of Bd21 in undertaking functional genomic study of the plant response to DON. This is significant for the genes that might play a role in the detoxification of DON, with the example from the candidate Glutathione S-Transferase gene (Bradi3g31720), obtained from the previous analysis, having 8 different DEGs orthologues in wheat.
5. When restricting the comparison to genes showing a log2 fold change higher than 2 in the wheat orthologues dataset, a total of 149 Bd21 genes with 441 orthologue genes of wheat were obtained (Supplemental Table 6-4 highlighted in dark grey). Most of the genes are potentially involved in an attempt by both plants to modify and detoxify DON

(Supplemental Table 6-4 highlighted in dark grey). Many genes are annotated as involved in energy transference, and cell membrane transporters are also highly represented (Supplemental Table 6-4 highlighted in dark grey).

6. Only 5 DEGs which were highly up-regulated in Bd21, were highly down-regulated in their corresponding 7 wheat DEG orthologues, demonstrating the high level of similarity in response between wheat and *Bd* to DON observed in these experiments (Supplemental Table 6-4 highlighted in light grey).

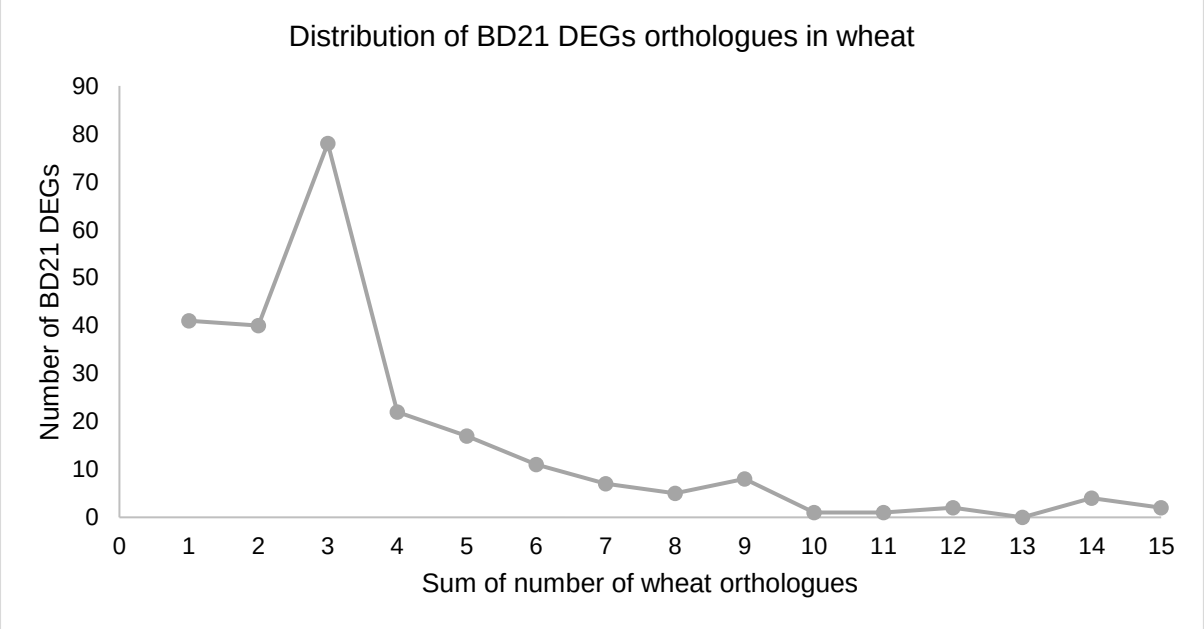

Figure 6-2 Correlation between the number of Bd21 up-regulated DEGs and the sum of their corresponding wheat DEG orthologues. The highest representation is observed with 78 Bd21 DEGs having a total of 3 wheat orthologues each, generally corresponding to wheat chromosome groups A, B and D.

The same approach was performed for the comparison between the most highly down-regulated genes in *Bd* and the response of their corresponding orthologue in wheat:

1. In the analyses of the down-regulated genes for correlation between the Bd21 and Hobbit 'sib' response to DON, a total of 502 orthologous wheat genes were obtained from the 132 highly down-regulated core DON DEGs.

2. From these 502, only 164 were significantly differentially expressed in the Hobbit 'sib' DON response, corresponding to a total of 66 Bd21 DEGs from the original 132 (Supplemental Table 6-5).
3. The distribution of the orthologues is similar to that for the genes showing significant up-regulation, with most of the Bd21 DEGs having only one to three orthologues in wheat (Fig 6-3). The most extreme exception is observed with *Bd* gene Bradi2g20850, which is represented by a total of 29 wheat DEG orthologues (Fig 6-3).
4. Out of the 66 Bd21 DEGs, 26 have a conserved Log2 down-regulation of -2 with their corresponding 60 highly down-regulated wheat DEG orthologues (Supplemental Table 6-4 highlighted in light grey). A very large proportion of the response is related to peroxidase activity (33 out of the 60 wheat DEG orthologues), with the orthologues of gene Bradi2g20850, accounting for 26 out of the 33 differentially expressed peroxidases in the wheat response (Supplemental Table 6-5 highlighted in light grey). The remaining 27 out of the 60 wheat orthologue DEGs are involved mainly in sugar hydrolysis and several were annotated as ion binding proteins (Supplemental Table 6-5 highlighted in light grey).
5. Only 2 genes are highly down-regulated in the Bd21 response but are highly up-regulated for their orthologues in wheat, consistent to the trend observed for the up-regulated genes in which the two species generally responded in a highly similar manner (Supplemental Table 6-5 highlighted in dark grey).

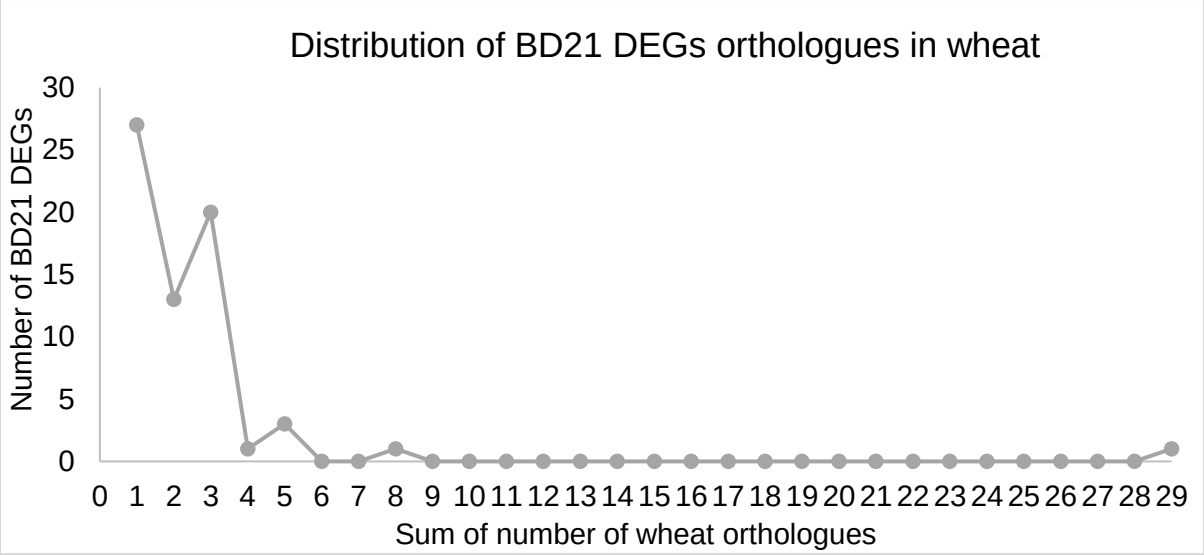

Figure 6-3 Correlation between the number of Bd21 down-regulated DEGs and the sum of their corresponding wheat DEG orthologues. The highest representation is observed with 27 Bd21 DEGs having only 1 wheat orthologue each.

To refine the list of candidates with a consistent response to DON in both *Bd* and wheat, a correlation was performed between the wheat orthologue list and the two previous analyses. The ABR6 corresponding Bd21 gene names were input into PlantEnsembl to obtain the corresponding wheat orthologues (data not shown). When analysing the log2 fold change in expression for all the orthologues, no orthologue displayed a log2 fold change higher than 2 or lower than -2 in the analyses. This resulted in no candidate gene from the QTL analyses being taken forward for translational study as none had a corresponding DEG orthologue in wheat with high differential expression in response to DON.

From the comparison with the highly expressed candidate genes at both 6 h and 24 h from the second approach, a total of 9 genes were in common with the highly expressed wheat orthologue genes (Table 6-4). Three of the potential orphan genes (Bradi1g74980, Bradi2g25440, Bradi4g22656), and the two arachidonic acid genes (Bradi2g44200, Bradi3g06330) were among the genes where the wheat orthologue was expressed in common (Table 6-4). The gene with the largest expansion observed in wheat corresponds to a potential DON detoxifier, Bradi3g31720, a predicted Glutathione S-Transferase (Table 6-4).

Table 6-4 Common DEGs between the third approach comprising of the wheat orthologue analyses and the second approach comprising of the candidate genes that were highly differentially expressed at both 6 h and 24 h.

***Bd* Gene stable ID**	**Description**	**log2 Bd21 1st RNAseq**	**log2 Bd21 2nd RNAseq**	***Ta* gene stable ID**	**log2 Hobbit 1st RNAseq**	**log2 Hobbit 2nd RNAseq**
Bradi1g37080	Histone acetyltransferase activity (Blast2GO)	7.3117	7.2317	TraesCS7B02G259000	4.657	1.631
				TraesCS7A02G369500	4.311	2.519
				TraesCS7D02G353800	4.168	1.679
Bradi1g74980	#N/A	7.1092	4.0016	TraesCS4D02G314100	3.615	1.270
				TraesCS4B02G317500	2.681	0.889
Bradi2g10857	PTHR10784//PTHR10784:SF1 – Eukaryotic translation initiation factor 6 // subfamily not named (1 of 1)	6.6025	7.1379	TraesCS3B02G220700	3.563	2.215
				TraesCS3A02G191100	2.646	1.653
Bradi2g25440	F-Box	6.2703	5.4774	TraesCS1D02G256900	1.742	#N/A
				TraesCS1D02G257000	5.293	1.877
				TraesCS1B02G268100	5.292	#N/A
				TraesCS1A02G257700	4.768	2.731
				TraesCSU02G003500	4.556	1.049
Bradi2g44200	Arachidonic acid binding (Blast2GO)	6.3317	5.0911	TraesCS3D02G225900	1.950	#N/A
				TraesCS3A02G228100	1.917	#N/A
				TraesCS3B02G256400	2.114	#N/A
Bradi3g05960	PTHR31373:SF0 - EMB (1 of 3)	6.6033	7.6765	TraesCS6A02G149200	6.008	#N/A
				TraesCS6B02G177100	4.160	2.373
				TraesCS6D02G138100	2.473	#N/A
				TraesCS6B02G176900	2.450	1.843
Bradi3g06330	Arachidonic acid epoxygenase activity (Blast2GO)	6.6505	5.9256	TraesCS6A02G181000	5.456	2.206
				TraesCS7B02G414300	4.234	#N/A
				TraesCS6B02G204500	2.691	#N/A

continuation of Table 6-4

***Bd* Gene stable ID**	**Description**	**log2 Bd21 1st RNAseq**	**log2 Bd21 2nd RNAseq**	***Ta* gene stable ID**	**log2 Hobbit 1st RNAseq**	**log2 Hobbit 2nd RNAseq**
Bradi3g31720	PTHR11260//PTHR11260:SF264 – Glutathione S-Transferase, GST, superfamily, GST domain containing // subfamily not named (1 of 4)	9.2604	8.8180	TraesCSU02G183000	3.351	#N/A
				TraesCSU02G184900	3.251	1.315
				TraesCS1A02G017400	3.197	1.140
				TraesCS1A02G017300	3.124	0.989
				TraesCS1D02G017000	2.956	1.240
				TraesCS1D02G014500	2.715	1.080
				TraesCS1A02G016800	2.669	#N/A
				TraesCS1B02G021100	2.309	0.971
Bradi4g22656	#N/A	6.5765	2.9650	TraesCS4A02G201900	3.685	1.477
				TraesCS4D02G102800	3.601	1.954
				TraesCS4B02G106100	3.448	2.421

From the final list of candidate genes obtained in Table 6-4, three genes were selected for consideration for a further analysis. The selection took into account genes that are highly differentially expressed, with at least a fold change of 3 in the first wheat RNAseq, and above 1.2 in the second wheat RNAseq. In order to allow functional validation in wheat only the *Bd* genes for which there were three or less orthologues in wheat, containing only one of the chromosome groups A, B and D represented, were considered This last step was chosen to improve the chances of obtaining an altered phenotype in lines carrying only a single chromosome A or B gene mutation in the tetraploid wheat cultivar Kronos, and also making it easier to generate double mutants through crossing.

The first selected gene corresponds to Bradi1g37080, a histone acetyltransferase activity protein, orthologue to the Arabidopsis gene AT3G24500, described in the TAIR database as MULTIPROTEIN BRIDGING FACTOR 1C (MBF1C), a highly conserved transcriptional coactivator. The other two genes correspond to the potential orphan genes Bradi1g74980 and Bradi4g22656, genes of unknown function restricted to the Pooideae subfamily, possibly arising from the need of the subfamily to adapt to certain environmental and/or biological stresses. Although gene Bradi2g10857, might also have been considered it was not investigated further. As a potential eukaryotic translation initiation factor, it may be essential for the plant, with the mutant possibly causing pleiotropic effects, making it difficult to interpret the results from study.

6.3.4 Selection of Kronos TILLING mutants for MBF orthologue genes

For the characterization of the candidate genes, the mutant TILLING genes available for tetraploid wheat cultivar Kronos were identified. The analyses of the Kronos lines were considered due to the fact that they only have two chromosome groups (A and B), making it less complicated than handling the hexaploid wheat genome. These lines will also provide phenotypic data for the model-to-crop translation between *Bd* and wheat, making it important for future crop research.

When analysing the three candidate genes in more detail, Bradi4g22656, was excluded, as the gene orthologues were already identified as *Fusarium* responsive orphan genes (TaFROG) able to confer DON tolerance to the plant (Perochon et al. 2015). When looking at the variant table of mutants from PlantEnsembl of the remaining two candidate genes, the Bradi1g37080 orthologues included several disruptive mutations, including a stop codon gain mutant in chromosome A (TraesCS7A02G369500), and a start codon loss mutant in chromosome B (TraesCS7B02G259000) (Fig 6-4). Other missense mutants were also available, including a synonymous variant in chromosome 7B, as a Kronos TILLING mutant control (Fig 6-4).

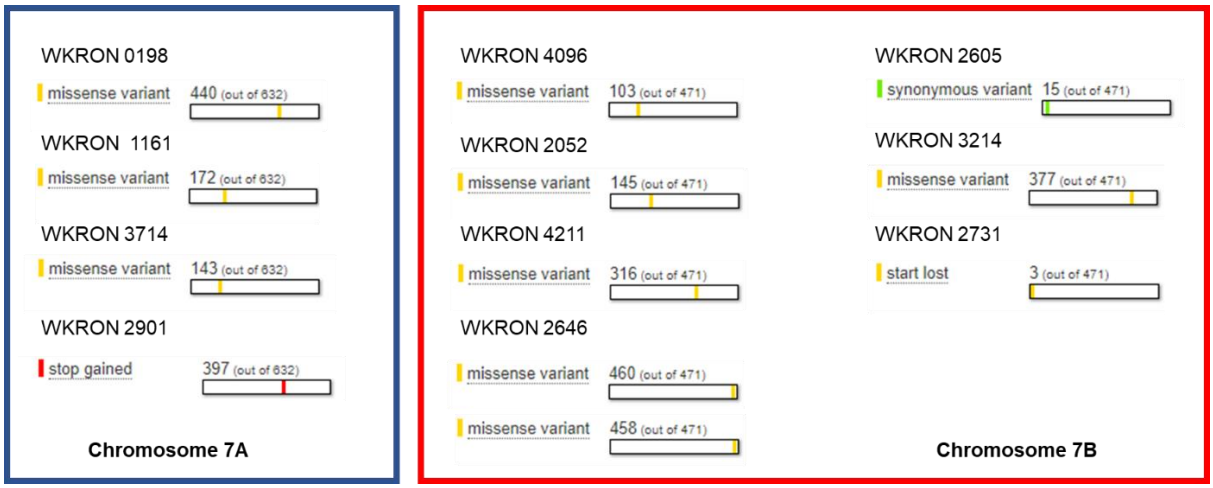

Figure 6-4 List of available Kronos TILLING mutants (WKRON) for the wheat orthologues of gene Bradi1g37080, TraesCS7A02G369500 and TraesCS7B02G259000. The effect of the mutation and their location were obtained from the variant table of mutants from PlantEnsembl.

Line WKRON2731, corresponding to the start loss mutation on chromosome 7B, was a heterozygous mutation, so it was grown and genotyped to obtain homozygous mutant plants. Lines WKRON0198, WKRON1161, WKRON3714, WKRON4096 and WKRON3214 did not produce viable seeds, so they could not be studied further. The remaining lines were subjected to a DON sensitivity assay, similar to the tests performed on Bd21.

6.3.5 Establishment of protocol for root growth analyses of Kronos under low concentrations of DON

The first step for the analyses of the Kronos TILLING mutants, is the adaptation of the protocol of Bd21 DON assay to Kronos. For this Kronos was subjected to three different

concentrations of DON, (3 µM, 5 µM and 7 µM). Roots of Kronos grew relatively slowly in the unamended agar and tended to grow in a spiral (Fig. 6-5). Growth was increased marginally in DON (3 µM) and DON (5 µM) but was similar to the untreated at 7 µM (Fig. 6-5). DON induced enhanced gravitropism in a dose dependent manner increasing with the DON concentration (Fig. 6-5).

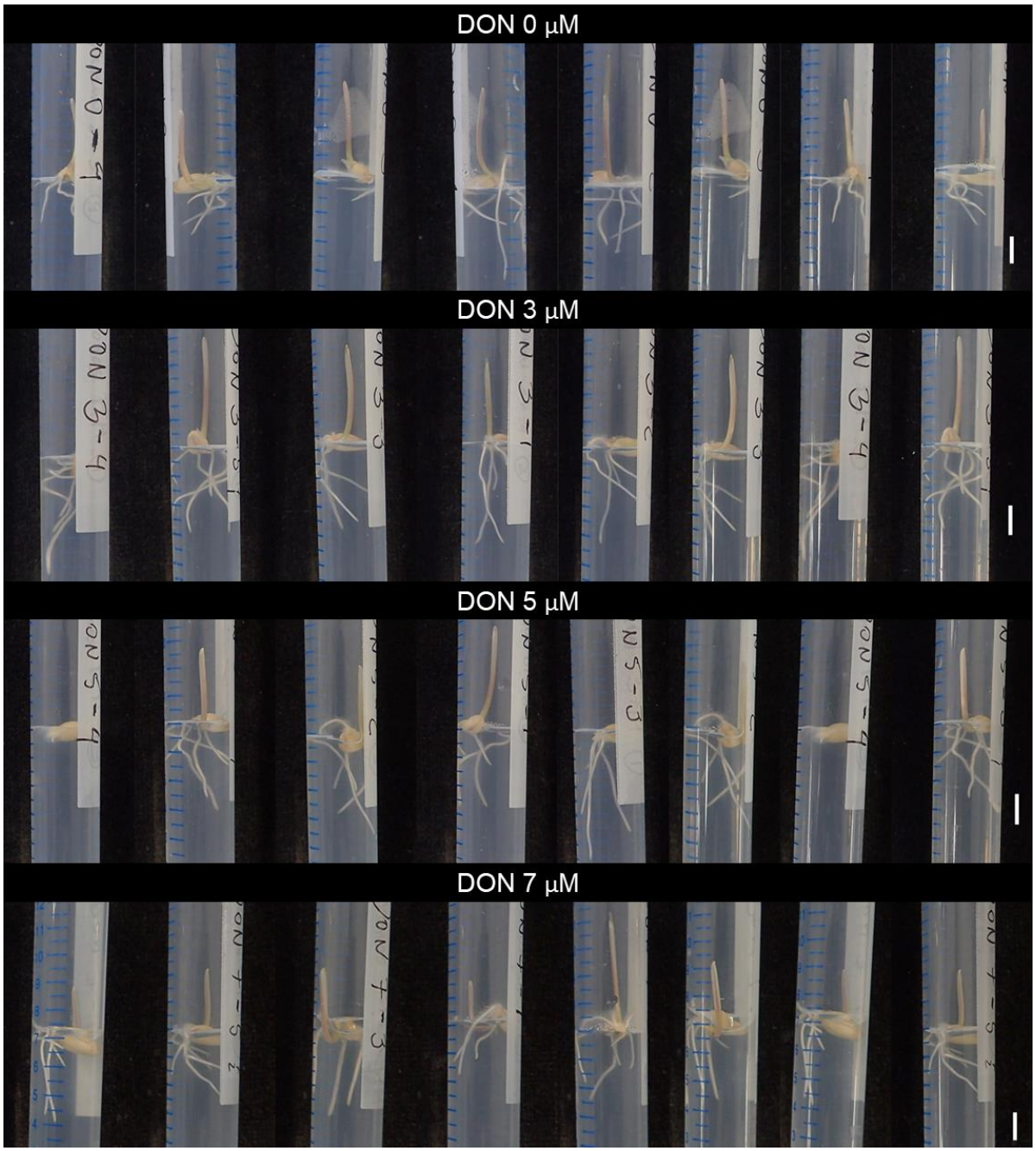

Figure 6-5 Kronos root growth under different concentrations of DON from 0 - 7 µM at 3 dpi. White bar represents 1 cm.

6.3.6 Characterization of Kronos TILLING lines root growth under DON

All the viable Kronos TILLING lines were assayed at 0 and DON 5 µM, and their root growth patterns were studied over the period of a week from the time they were placed in the DON tubes. The plants originating from the original Kronos seed stock used in the creation of the TILLING mutant lines, was used as the main control of the experiment, being renamed "Kronos parent". The "Kronos parent" exhibited a slight inhibition of root growth under DON 5 µM, but the growth rate and curvature were similar between the DON and water control (Fig. 6-6 A). The synonymous mutant WKRON2605 and the missense mutants WKRON2052 and WKRON2646 had similar growth patterns to that of the "Kronos parent", with no significant inhibition of the root growth in the presence of DON (Fig. 6-6 D-F). The root growth of missense mutant WKRON4211 in the water control was greater than any other line of the panel (Fig. 6-6 C). However, when comparing the root growth in 5 µM DON to the WKRON4211 control, a significant inhibition was observed, with the roots in DON being around half the length of the roots in the control (Fig. 6-6 C). The root growth of the only chromosome A mutant, consisting of the stop gain mutant WKRON2901, had a similar root growth in the water control to that of the "Kronos parent" (Fig. 6-6 B). The root growth in the presence of 5 µM DON was inhibited, although to a lesser extent than for WKRON4211, but still being greater than that for the "Kronos parent" (Fig. 6-6 B).

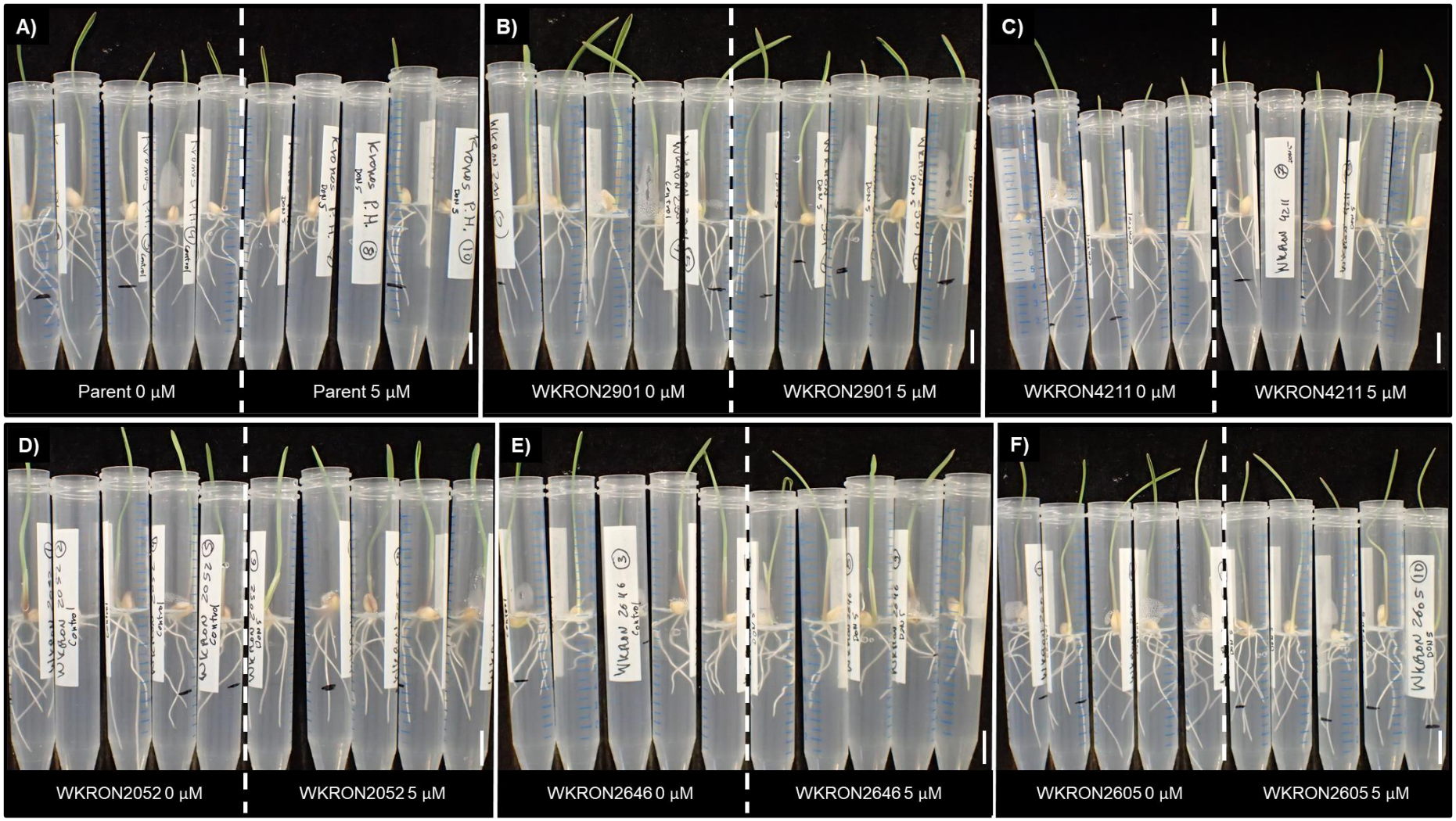

Figure 6-6 Kronos mutants screening against DON at 0 and 5 µM. A) Kronos parent, related to the original Kronos line that originated the TILLING population. B) WKRON2901 stop gain mutant on TraesCS7B02G259000. C-E) Missense mutation on TraesCS7A02G369500 (WKRON4211, WKRON2052 and WKRON2646). F) WKRON2605 synonymous mutation on TraesCS7A02G369500. White bar corresponds to 2 cm.

The growth of WKRON2901, was assessed at 3- and 4-days post inoculation (dpi), using synonymous mutant WKRON2605 and “Kronos parent” as controls to assess the levels of inhibition of root growth in response to DON. For this a maximum of 5 replicates for each treatment for each line was used. The growth in 5 µM DON was then compared to growth in the respective water control to determine the percentage stimulation/inhibition by DON (Fig 6-7). The percentage of root growth under DON for both “Kronos parent” and line WKRON2605, was close to 100% at both 3 and 4 dpi (Fig 6-7). The line WKRON2901 however was significantly inhibited, with the highest inhibition observed at 4 dpi, with the roots in 5 µM DON having an average 35% root growth when compared to the water control (Fig 6-7).

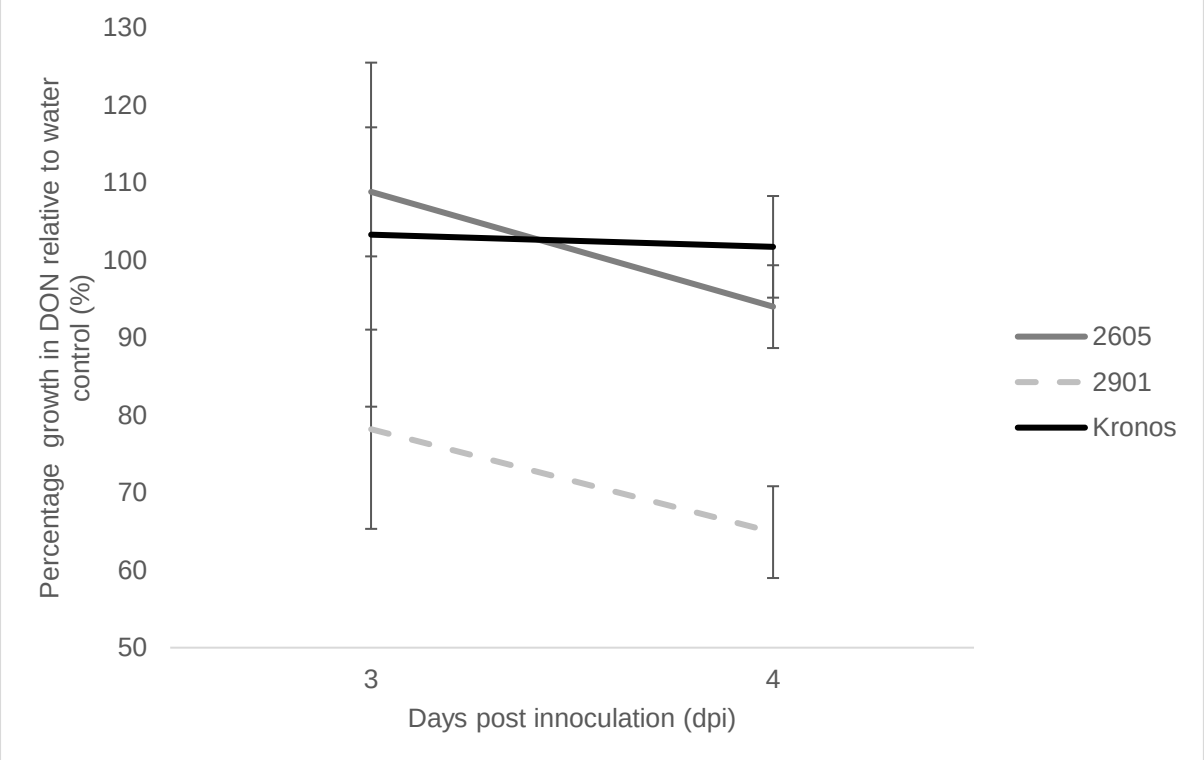

Figure 6-7 Percentage of root growth under DON compared to the growth of roots under the respective water control, for the “Kronos parent” and mutant lines WKRON2605 and WKRON2901. Error bars represent standard deviation.

For the analyses of the chromosome B start loss mutant WKRON2731, two homozygous mutant lines were included, WKRON2731-1 and WKRON2731-2, along with line WKRON2731-3 that was heterozygous for the mutation. The “Kronos parent” and line WKRON2901 were also retested (Fig 6-8).

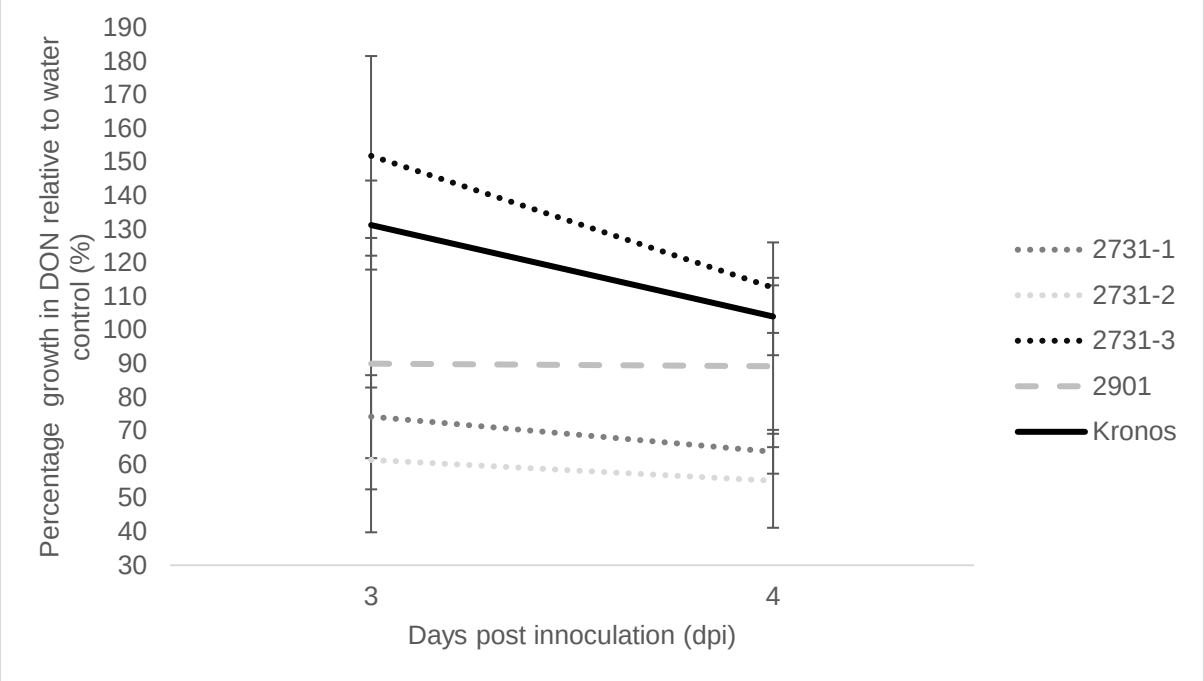

Figure 6-8 Percentage of root growth under DON compared to the growth of roots under the respective water control, for the Kronos parent and mutant lines WKRON2731 and WKRON2901. Three WKRON2731 sublines were tested, two homozygous lines (2731-1 and 2731-2) and one heterozygous line (2731-3). Error bars represent standard deviation.

When comparing the growth patterns from the second analysis of the “Kronos parent” and mutant line WKRON2901, the growth differential between the two sets again showed WKRON2901 to be more sensitive to DON (inhibited root growth) than the “Kronos parent” (Fig 6-8). The differential within the WKRON2901 response to DON was however lower than observed in the first trial, having only 10% inhibition in DON when compared to the water control (Fig 6-8). Both “Kronos parent” and WKRON2731-3, exhibited root elongation in 5 µM DON at 3 dpi, when compared to the water control being over 30% longer (Fig 6-8). In contrast, the roots of the two homozygous lines for mutant WKRON2731 were inhibited, with WKRON2731-1 having an inhibition between 37% to 25% under DON, and 2732-2 having 46% to 38% inhibition (Fig 6-8).

A third test was performed on lines WKRON2901 and WKRON2731-2, with WKRON2605 and “Kronos parent” being used as controls (Fig 6-9). Unfortunately, the “Kronos parent” line failed to grow because of fungal contamination so comparisons are made to WKRON2605 that carries a synonymous mutation. More additional time-points and replicates were included to increase the accuracy of the analyses.

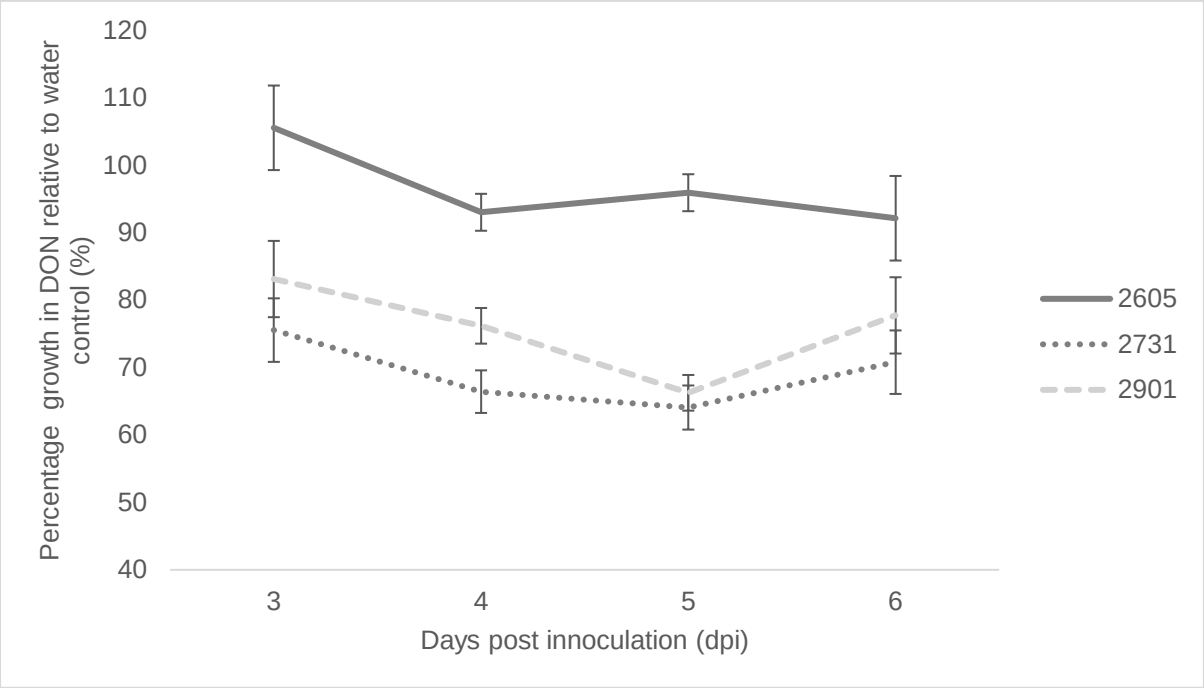

Figure 6-9 Percentage of root growth under DON compared to the growth of roots under the respective water control, for the Kronos parent and mutant lines WKRON2605, WKRON2731-1 and WKRON2901. Error bars represent standard deviation.

WKRON2605, had a similar growth rate in the water and DON treatments throughout the experiment (Fig 6-9). Both the A genome stop codon mutant (WKRON2901) and the B genome lost start codon mutant (WKRON2731), exhibited significant reduction in root growth in DON compared to growth in the control (Fig 6-9).

WKRON2901, exhibited enhanced sensitivity to DON as indicated by greater inhibition of root growth in all three experiments. The line WKRON2731 also demonstrated greater inhibition of root growth than the controls in both the second and third analyses. To analyse the effect of the combination of these mutations, a cross was made between line WKRON2901 and WKRON2731-2 to determine whether the inhibition of root growth in the presence of DON

is increased when the homoeologues on both chromosome groups are disrupted. During the genotyping of the F_2 population, several lines were selected on the basis of their genotype corresponding to presence of the mutation in the genes TraesCS7A02G369500 and TraesCS7B02G259000. At least three lines from the F_2 population were selected for each of the single homozygous mutant genotypes (WKRON2901 and WKRON2731), the wild type (WT), and the 2731x2901 (double mutant). The double mutant, along with the single mutants and the WT line were analysed for their response to DON (Fig. 6-10).

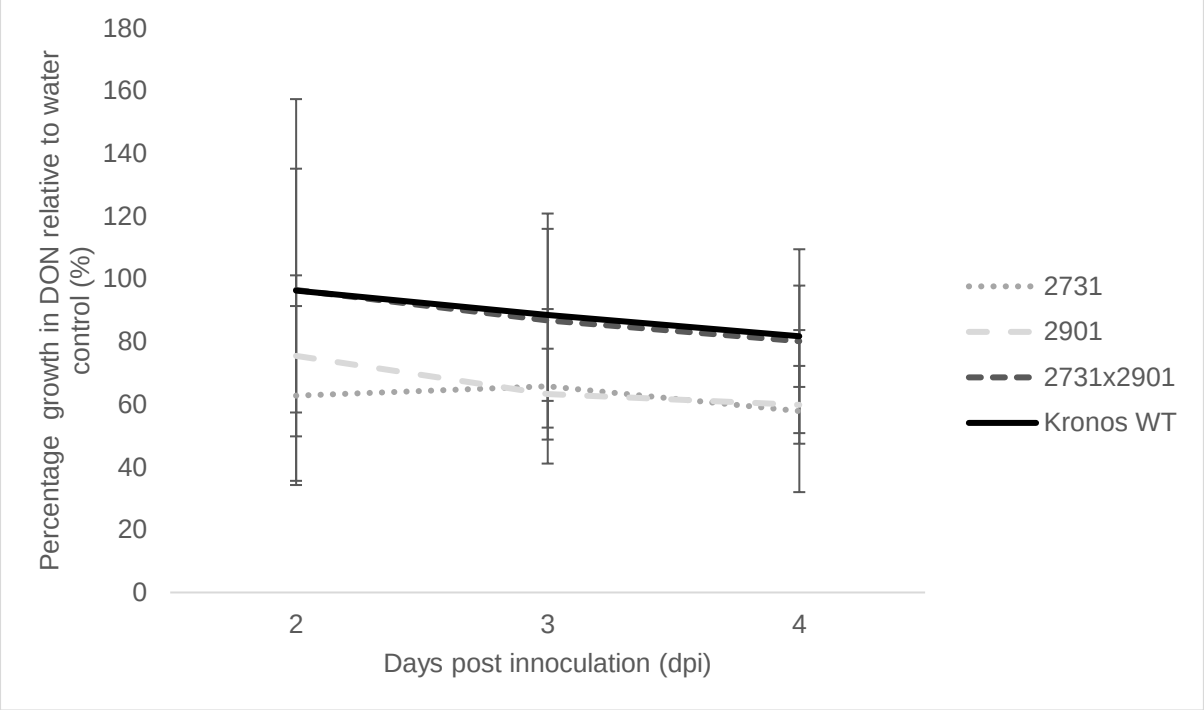

Figure 6-10 Percentage of root growth under DON compared to the growth of roots under the respective water control, for the Kronos WT and mutant lines WKRON2731, WKRON2901 and the double mutant WKRON2731xWKRON2901. Error bars represent standard deviation.

Both single mutants of WKRON2731 and WKRON2901 displayed a similar growth pattern to the previous experiment, with WKRON2731 having an inhibition between 38% and 24%, and WKRON2901 between 40% and 17% from the 2 dpi (Fig. 6-10). The double mutant on the other hand followed the growth pattern of the WT line, exhibiting very little to no inhibition under DON (Fig. 6-10).

In order to verify the results obtained from the first analyses of the double mutant, a new analysis was performed using both Kronos WT and the double mutant, with an increase in the number of replicates for each line. Only one line was used for each of the single mutants, with the same increased number of replicates as the WT and double mutant. All lines were accessed in the same time points, compiled, and compared to each respective control in order to obtain the respective percentage of inhibition (Fig. 6-11).

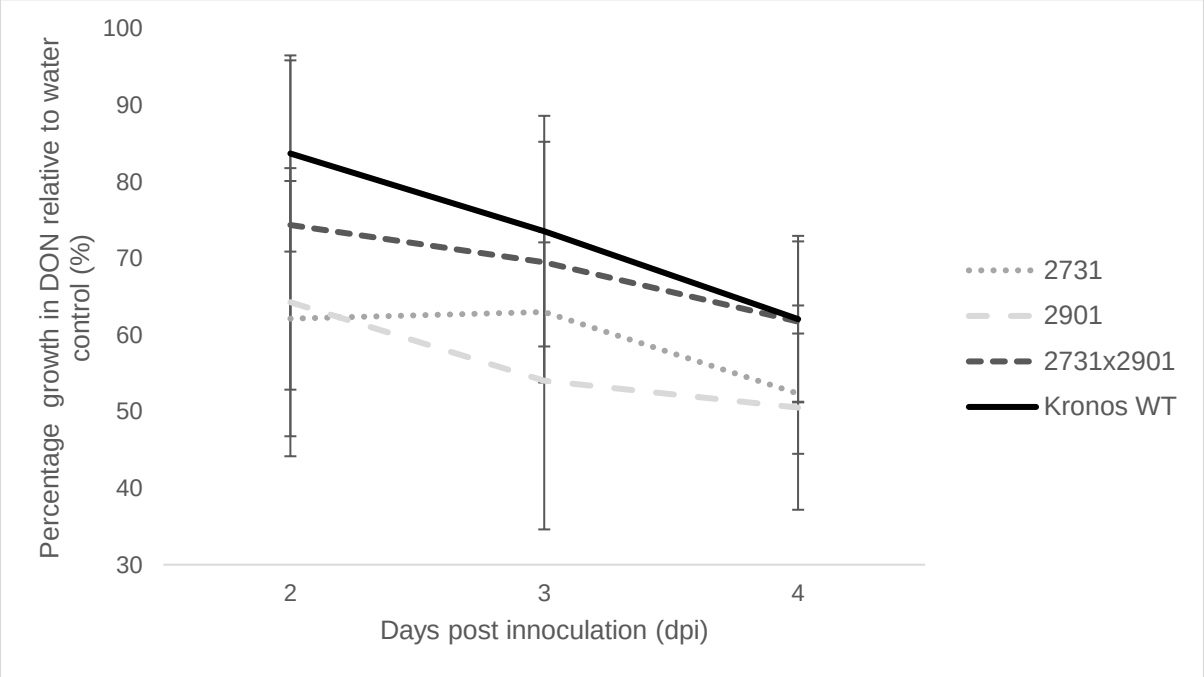

Figure 6-11 Percentage of root growth under DON compared to the growth of roots under the respective water control, for the second run with Kronos parent and mutant lines WKRON2731, WKRON2901 and the double mutant WKRON2731xWKRON2901. Error bars represent standard deviation.

When analysing the root growth in the second analyses, there is an overall inhibition of root growth in response to DON of all lines, with Kronos WT displaying an inhibition of between 38% and 16% (Fig. 6-11). It is closely followed by the double mutant, in similar profile to the first analyses, with an inhibition between 38% and 25% (Fig. 6-11). The single mutants remain the most susceptible lines, exhibiting an inhibition of root growth in the presence of 5 µM DON of between 50% to 36% (Fig. 6-11).

6.4 *Discussion*

In order to analyse the potential candidate genes involved in the ABR6 tolerance to FRR, (chapter 3), the genes within the QTL region of chromosome 1 (chapter 4) of Bd21 and ABR6 were compared to identify those showing differential expression in response to DON. For this the RNAseq Bd21 DON response from chapter 5 was compared to the RNAseq of ABR6 differential response to DON under the same conditions. The majority of the genes annotated in the region in both Bd21 and ABR6 did not show high differential in expression in response to DON. However, 12 genes were highly differentially expressed under DON with a significant contrasting response between ABR6 and Bd21 (Table 6-2). Two genes, Bradi1g29500 and Bradi1g30811, were highly down-regulated in response to DON in the ABR6 line, with only a small down-regulation in Bd21 (Table 6-2). Both genes are potentially involved in the most DON-affected processed identified in chapter 6, the ribosome and chloroplast. Interestingly in the wheat analyses of three different varieties for response to infection by mycotoxin producing *Fusarium* strains and DON, the most resistant lines displayed an up-regulation of expression of genes encoding ribosome proteins, while the most susceptible lines demonstrated a general down-regulation (Foroud et al. 2012). It was suggested that this up-regulation in the FHB wheat resistant varieties, contributes to a higher production of proteins to counterbalance the disruption in protein synthesis by DON, thus compensating for the toxic effects and providing resistance to both fungus and toxin (Foroud et al. 2012). In the case of *Bd*, however, the opposite is observed with Bradi1g30811, where the resistant line exhibited a greater downregulation than the susceptible line. It is possible that ABR6 might possess other ribosome proteins with better fitness against DON, and thus is prioritizing the expression of those proteins against ribosome proteins that are more heavily affected. That is partially observed with the increase in expression of Bradi1g29577, a eukaryotic initiation factor 2C protein, in ABR6 when compared to the down-regulation in Bd21 (Table 6-2). It is possible that overexpression of this crucial protein involved in translation initiation is related to the effects observed in Foroud et al, 2011, where the more resistant lines

are able to compensate or prevent the disruption in protein synthesis. Another ribosome related protein being over-expressed in ABR6 when compared to Bd21 is Bradi1g29740, that has a putative tRNA-intron endonuclease activity. Involved in the maturation of mRNA, little is known on its potential role with respect to DON tolerance. In wheat, DON is involved in the expression of a methionyl-tRNA synthetase (TaMetRS), a gene putatively involved in aminoacylation in the nucleus, rather than the cytoplasm (Zuo et al. 2016). Overexpression of this gene in Arabidopsis led to root tolerance to DON, and decreased infection spread in the florets (Zuo et al. 2016). It is hypothesised that these genes are expressed upon DON detection as an attempt by the plant to overcome the deregulation of protein synthesis by compensating with tRNA synthetase to increase the production of ribosomal RNA (Zuo et al. 2016). It is possible that Bradi1g29740 has a similar role to TaMetRS, where ABR6 is attempting to overcome the toxic effects of DON by overexpression of specific groups of tRNA and ribosome proteins.

The gene Bradi1g29658, a putative leucine-rich repeat-containing (LRR) protein was specifically up-regulated in ABR6 (Table 6-2). Specific LRR have largely been associated with pathogen detection and effector-triggered immunity. Several pathogens are recognised by surface-localized receptor-like kinases or receptor-like proteins, awakening a cascade of reactions within the cell leading to a specific immune response by the host. Very few LRR have been associated with *Fusarium* resistance or DON tolerance. The wheat gene *TaLRRK-6D* and its barley orthologue *HvLRRK-6H*, are LRRs with kinase motifs which are highly induced upon DON inoculation and during the biotrophic phase of *Fusarium* colonisation. Virus-induced gene silencing leads to increased disease rates both in resistant and susceptible varieties (Thapa et al. 2018). This increase of the LRR in response to *Fusarium* is correlated with the increase in expression of down-stream defence genes, possibly correlated with a ROS burst in the cell, that initiates the LRR cascade (Thapa et al. 2018). This cascade also controls the levels of salicylic acid in the cell, with the silencing of *TaLRRK-6D* in wheat cv. Remus leading to low concentration of salicylic acid, potentially contributing to the increase

in susceptibility of the plant to the fungus (Thapa et al. 2018). Another wheat LRR, *TaRCR1*, is involved in the defence mechanisms against *Rhizoctonia cerealis*, where disruption of the gene leads to increased susceptibility in the plant (Zhu et al. 2017). This protection by the LRR, is linked with its potential function in ROS homoeostasis, where the gene is over-expressed upon H_2O_2 exposure (Zhu et al. 2017). In the opposite scenario the over-expression of *TaRCR1* leads to reduced ROS accumulation upon *Rhizoctonia cerealis* infection (Zhu et al. 2017). Expression of several ROS scavengers are also highly correlated with the expression of *TaRCR1*, linking the function of this LRR closely with the role of ROS and associated defence genes in the cell (Zhu et al. 2017). It could be that this putative LRR over-expression in ABR6 is associated with the accession being more resistant to FRR than Bd21, with ABR6 being able to potentially create an early response to both the toxin and the fungus, leading to increased resistance. Since the over-expression of Bradi1g29658 is linked with DON tolerance, instead of overall FRR infection, it is also possible that the expression of this gene is correlated with the associated DON-mediated ROS response in the cell, in a similar mechanism to either *TaLRRK-6D* or *TaRCR1*.

A potentially more pronounced response to DON in ABR6 when compared to Bd21 also correlates with the expression of the putative MYB44 transcription factor, Bradi1g30252 (Table 6-2). MYB44 has been largely characterised in *Arabidopsis thaliana* as an important abiotic stress responsive gene (Jaradat et al. 2013). Upon an abiotic stress stimulus, a mitogen-activated protein kinase (MAPK) cascade is quickly promoted leading to the activation of MYB44 which in turn activates several stress responsive genes through promoter binding (Pitzschke, Schikora, and Hirt 2009). The gene is also involved in controlling the equilibrium between the salicylic acid and jasmonic acid pathways, demonstrating a positive regulation of salicylic acid leading to increased resistance to biotrophic pathogens, and a negative regulation of jasmonic acid leading to a decrease in resistance to necrotrophic pathogens (Shim et al. 2013). This gene is also involved in the negative regulation of ABA, with the overexpression of MYB44 leading to decreased levels of ABA in the cell which, in

turn, leads to reduced levels of chlorophyll loss and rate of senescence (Jaradat et al. 2013). It is possible that the higher expression of this transcription factor is contributing to the ability of ABR6 to remain green during infection with *Fusarium* when compared to Bd21. It is also possible that the greater expression of the MYB44 gene may be regulating genes that contribute to the protection of chlorophyll and chloroplasts from the effects of DON. Since Bd21 also displays an increase in expression of this gene in response to DON it is possible that ABR6 is responding to DON more rapidly than Bd21 leading to a faster increase in expression of several defence-related genes leading to a better tolerance by ABR6 to infection.

Overall, it appears that the greater resistance to FRR conferred by the ABR6 QTL interval may be related to a more rapid or pronounced response to DON, leading to up-regulation of essential genes involved in overcoming the toxic effects of DON. However, it is still an incomplete analysis as the response of ABR6 might be more complex upon FRR where the fungus may be producing many additional elicitors of host response. An analysis of potential DON tolerance genes from ABR6 from this study is still important since DON is essential for the full virulence of *Fusarium* infection in the plant.

In the analyses of the most highly differentially expressed DEG at both time points across the Bd21 response to DON, the most represented group was part of the glutathione S-transferase (GST) family of proteins, with Bradi3g31720 and Bradi3g31727, having the highest log2 fold change (Table 6-3). The role of GST in DON response has already been reported in the barley expression profile response to DON, where numerous GST were highly differentially expressed (Gardiner et al. 2010). It is proposed that DON leads to an increase of cysteine biosynthesis, which in turn increases glutathione levels in the cell, which is then used in a GSH-dependent detoxification of DON (Gardiner et al. 2010). The same up-regulation of GST proteins was observed in the characterization of resistant and susceptible wheat varieties in response to *Fusarium*, with an overall increase in the expression of GST proteins upon infection (Foroud et al. 2012). Foroud and colleagues suggested that GST proteins serve to

increase the level of antioxidants in the cell in an attempt by the plant to decrease the amounts of ROS induced by the fungal infection (Foroud et al. 2012). A similar over-expression of GST genes was also observed in the analyses of several wheat near-isogenic lines, with the most susceptible lines displaying a higher expression of GST genes, possibly associated with a more pronounced ROS burst in the cell resulting from the line's susceptibility (Hofstad et al. 2016). When looking at the specific characterization of the barley GST gene, *HvGST13*, it displayed a role in conferring tolerance to DON when over-expressed in Arabidopsis, by decreasing the levels of ROS induced by both DON and methyl viologen (Wahibah et al. 2018). It is highly likely that the high upregulation of the Bradi3g31720 and Bradi3g31727 GST genes at both time points is a consequence of increased concentrations of ROS caused by DON, and reflects an attempt by the cell to alleviate ROS accumulation and possibly decrease the toxic effects of DON.

Two other genes with a potential role in alleviating the toxicity of DON in the cell are the putative arachidonic acid pathway genes, Bradi2g44200 and Bradi3g06330 (Table 6-3). Arachidonic acid has been shown to serve several functions in pathogen defence, where in high concentrations it contributes to the accumulation of ROS species, leading to necrosis of the tissue, protecting the plant against biotrophic pathogens (Dedyukhina, Kamzolova, and Vainshtein 2014). In low concentrations it functions as an elicitor of systematic defence, mobilizing a series of defence genes, preparing the plant for a possible pathogen attack (Dedyukhina, Kamzolova, and Vainshtein 2014). Another pathway arachidonic acid is involved in is the cytochrome P450 pathway, which relies on the function of the arachidonic acid epoxygenase in order to create "arachidonic acid/P450" metabolites (Capdevila, Falck, and Harris 2000; Capdevila et al. 1993). The function of the P450 pathway has been frequently connected to the response of DON, being normally up-regulated upon DON inoculation or *Fusarium* infection (Walter et al. 2008; Gardiner et al. 2010; Li et al. 2010; Hofstad et al. 2016). The potential role of P450 in wheat upon *Fusarium* infection was associated with the corresponding expression profile of P450 gene, CYP709C1, due to its high expression in

resistant lines in both seedling and spike infection (Li et al. 2010). The FHB resistant line Sumai3 also exhibited a 7-fold change in expression in its P450 proteins when compared with the FHB susceptible line Annong8455 (Li et al. 2010). When analysing seedling blight, P450 remained linked with resistance, with an 84-fold change in expression in Annong8455 (resistant to seedling blight) when compared with Sumai3 which is susceptible to seedling blight (Li et al. 2010). The differential expression did not alter when using a DON-disrupted *Fusarium* strain, possibly suggesting that expression of P450 is unrelated with the presence or absence of DON (Li et al. 2010). The link between P450 and *Fusarium* defence mechanisms, rather than DON detoxification, is corroborated in the analyses of the response to DON of susceptible wheat lines. In these studies, the up-regulation of P450 was observed in both resistant and susceptible wheat lines in response to DON, indicating that they are part of general response to DON, rather than a specific DON detoxification mechanism used by resistant lines (Walter et al. 2008; Walter and Doohan 2011). Role of P450 proteins are diverse however, with some proteins being up-regulated in both pathological and mycotoxin systems, while other P450 proteins are exclusive to a DON response (Gardiner et al. 2010). Although hypothesised as being mainly involved in defence mechanisms rather than DON metabolism, another mechanism of detoxification of DON was found using *Sphingomonas* sp. strain KSM1, a bacteria capable of catabolizing DON into 16-HDON (Ito et al. 2013). The reaction is attributed to the combined action of three genes, between DdnA, Kdx and KdR (Ito et al. 2013). DdnA is the most relevant of the three genes, being part of the cytochrome P450 protein family, but demonstrating more affinity for mycotoxins DON, NIV, and 3-ADON than the normal target of P450, α-terpineol (Ito et al. 2013). DdnA is able of monooxygenate the allylic methyl group of DON, and this is followed by hydroxylation by Kdx and KdR, leading to the formation of 16-HDON, which proved to be less phytotoxic than DON when tested in wheat (Ito et al. 2013).

In the overall analyses of the second approach, most genes highly upregulated at both time points, are known genes associated with DON response and detoxification. This

validation of the data with other DON-related works, provide confirmation of the conserved mechanisms of response to DON across plant species.

In the analyses of the Bd21 DEGs to identify those with common differentially expressed orthologues in wheat, several genes were identified that showed conserved high differential expression in both species. The most represented class of genes observed in the common up-regulation between the two species are involved in glycosyl/glucuronosyl transferase activity (Supplemental Table 6-4). One of the most effective and commonly observed resistance methodologies developed by host plants, is the detoxification of DON, using UDP-glycosyltransferases (UGT), first found in Arabidopsis. *Arabidopsis thaliana* gene At2g36800, renamed from UGT73C5 to DOGT1 (deoxynivalenol-glucosyltransferase 1) is capable of transferring the glucose group from UDP-glucose to modify the hydroxyl group of carbon 3 of DON, creating the less toxic compound DON-3-G (Poppenberger et al. 2003). This transformed version of DON consists of inactivated aglycones, which make the hydroxyl group less reactive in the cell, leading to DON-3-G storage to the vacuole, or transport to the cell wall, minimizing the contact between the toxic molecules and the DNA/RNA-rich organelles of the cell (Poppenberger et al. 2003). The finding of this type of enzyme led to a search for UGTs of similar function in other plants. The next UGT found was wheat gene TaUGT3 (TraesCS3B02G144400), in which the corresponding protein amino-acid sequence was highly similar to DOGT1 (Lulin et al. 2010). Transformation of this protein into onion epidermal cells, demonstrated that it mainly localised to the nucleus and the plasma membrane (Lulin et al. 2010). When analysing its potential detoxifying ability, the protein was over-expressed in Arabidopsis cells, and was able to confer tolerance to DON (Lulin et al. 2010). This protein, however, was unable to confer DON tolerance in yeast (Schweiger et al. 2010), while another UGT identified in wheat, TaUGT12887, was able to confer tolerance to DON in *Saccharomyces cerevisiae* toxin-sensitive strains (Schweiger, Steiner, et al. 2013). The barley UGT, HvUGT13248, also confers DON tolerance in both yeast (Schweiger et al. 2010), and Arabidopsis, where it demonstrated an increased rate of conversion from DON to

DON-3-G than the Arabidopsis wild type (Shin et al. 2012). The barley gene was also transformed into wheat varieties cv. Bobwhite and cv. CBO37, where it increased the conversion of DON to DON-3-G, leading to an increase in resistance to FHB disease spread, both under greenhouse and field conditions (Li et al. 2015). The Arabidopsis DOGT1 and barley HvUGT13248 orthologues in *Brachypodium distachyon* were also characterized, with two out of eight *Bd* UGT genes with the highest similarity demonstrating tolerance to DON (Schweiger, Pasquet, et al. 2013). All eight genes were highly induced upon infection with a DON-producing strain of *Fusarium* when compared to a DON-deficient strain (Schweiger, Pasquet, et al. 2013). However, only genes Bradi5g02780 and Bradi5g03300, were able to withstand toxic concentrations of DON when transformed into a toxin-sensitive yeast strain, with Bradi5g03300 being able to withstand substantially higher concentrations of DON than its paralogue Bradi5g02780 (Schweiger, Pasquet, et al. 2013). A mutation in the gene Bradi5g03300 resulted in an increase in the sensitivity of *Bd* roots to DON, and *Bd* spikes to FHB spread, while the overexpression led to tolerance to DON and reduced disease spread, respectively (Pasquet et al. 2016). A transformation of wheat with Bradi5g03300, also led to a significant reduction of mycotoxin concentration in the plant, accompanied by reduced disease spread in wheat heads (Gatti et al. 2018).

Another important group represented in the up-regulated conserved response to DON between *Bd* and wheat, comprise of a series of membrane transporters. Membrane transporter also play a role in protecting the plant against the toxic effects of DON. One of the most studied transporters in response to DON and *Fusarium* comprise the multidrug resistance protein ABC transporters (Walter et al. 2008; Gardiner et al. 2010; Park et al. 2014; Hofstad et al. 2016). One of the first studies to identify a potential role for these proteins against *Fusarium* and DON, was encountered within the QTL resistance region in wheat chromosome 2DS, although no association between its possible transport of DON was established (Handa et al. 2008). ABC transporters also displayed considerable up-regulation in barley treated with DON, especially the class involved with the potential transport of DON and DON-like

molecules from the cytoplasm to internal vesicles, such as the vacuole (Gardiner et al. 2010) (Walter et al. 2015). In wheat an ABC transporter, *TaABCC3*, is expressed early in the host response to DON. By using virus induced gene-silencing (VIGS) targeting the chromosome 3A and 3B homoeologues, an increase in the bleaching of the spikelets upon DON inoculation was observed, leading also to enhanced head ripening and fewer grains when compared to the non-transformed variety (Walter et al. 2015). All three homoeologues of *TaABCC3* (TraesCS3B02G148100, TraesCS3D02G129900 and TraesCS3A02G129000), and its corresponding orthologue in Bradi2g04577, are substantially up-regulated, with the *Bd* gene having around a 6 fold change in expression. It would be interesting to see if disturbing these gene in *Bd*, along with other ABC transporters that show a significant differential expression could lead to a similar phenotype as the one observed in the study by Walter and colleagues.

Among the down regulated genes, a significant number of peroxidases are present, which contradicts the view of an excess production of ROS as a consequence of DON. This could reflect the plant adjusting the ROS concentration to maintain the ability to use ROS as part of a long-distance signalling response. It would be interesting to compare the levels of ROS in this study with the high levels of ROS normally observed under toxic concentrations, to determine if DON-induced production of ROS is dose dependent. Interestingly, when exposed to high concentrations of DON, peroxidases are substantially over-expressed (Desmond et al. 2008; Foroud et al. 2012), which corroborates the potential correlation between a toxic DON and its induction of ROS, suggesting that the amount of DON might also dictate the amount of ROS production.

When comparing the three strategies, the correlation between the second and third approaches led to the selection of three candidate genes for further characterization. One interesting fact that was observed, was that the fold change in expression was considerably lower in wheat than in *Bd*, for most of the orthologues in the list. This most probably reflects the higher number of copies in wheat (homoeologues and duplications), increasing the redundancy in expression. This increases the importance of using simple diploid models like

Bd as a preliminary study of pathogen response. By studying a system like *Bd* where the response triggers increased expression of individual genes rather than homoeologues and gene duplications it should be possible to highlight the most responsive genes without suffering a potential dilution in response that might lead to genes being lost to subsequent analysis as each homoeologue failed to pass an expression threshold for identifying DEGs. Although significant advances have been made in the characterization of wheat and its complex genome, wheat still remains a challenge, especially due to the dilution of the gene response through its genome, where most of the cases the role of a gene is only fully observed when deletions in all three homologues and corresponding duplications are achieved. This study proves how the expression in *Bd* can display a better response profile to DON, thus making it a more interesting model to work in before moving to the more complex organism that is wheat.

The first two candidate genes identified by both approaches, Bradi1g74980 and Bradi4g22656, are possible orphan genes, due to lack of known function and domains within their sequences, and more importantly, being specific to the Pooideae family. This specificity is important in the characterization of orphan genes, as their main characteristic is their lack of homologues in many other species, making the genes taxonomically restricted to a certain family, or even a species (Arendsee et al.,2014). By analysing the orthologs of Bradi1g74980 and Bradi4g22656 it is immediately obvious that the orthologues resembling these genes are all restricted to the Pooideae family, more specifically, to only *Hordeum vulgare, Triticum aestivum*, *Triticum turgidum* and *Aegilops tauchii*. When analysing the orthologues of Bradi4g22656 in *Triticum aestivum*, one orthologue in particular has already been characterised with respect to its role in DON tolerance and disease resistance against *Fusarium*. This is one of the most important orphan genes described against *Fusarium* diseases, especially in conferring DON tolerance and is termed *Fusarium* Resistance Orphan Gene (*TaFROG*) located in the chromosome 4 of wheat (Perochon et al. 2015). Upregulation of the gene enhances wheat tolerance to DON, while silencing of the gene leads to an increase

in susceptibility to both DON and *Fusarium* infection (Perochon et al. 2015). Expression of *TaFROG* seems to relate to the amount of DON present, being characterised as dose dependent, with correlation between expression of the gene between a series of DON producing and non-producing strains of *Fusarium* (Perochon et al. 2015). TaFROG is reported to interact with two different proteins, a kinase, TaSnRK1α, and a transcription factor, TaNACL-D, with the latter contributing to disease resistance when overexpressed, much like the phenotypes observed for the overexpression of *TaFROG* (Perochon et al. 2015; Perochon et al. 2019). It is possible that the other orphan gene Bradi1g74980, could have a similar role to *TaFROG*, interacting with key cell regulators and triggering a response to DON, potentially leading to DON tolerance in the plant.

Histone acetyltransferases are another important group dictating the activation of gene expression in the cell. The third candidate gene, Bradi1g37080, is part of the histone complex, and has already been described as multi-protein bridging factor 1c in Arabidopsis. There have been three major multi-protein bridging factors (MBFs) identified in *Arabidospis thaliana*: *MBF1a*, *MBF1b* and *MBF1c* (Tsuda and Yamazaki 2004). Even though *MBF1a* and *MBF1b* display no characterized function, the *MBF1c* displays an increase in expression upon pathogen infection or when exposed to a variety of abiotic stresses, including methyl viologen and hydrogen peroxide (Tsuda and Yamazaki 2004). Another abiotic stress associated with *MBF1c* is linked with its ability to promote tolerance to heat shock in Arabidopsis, partially through the activation of the ethylene signalling pathway (Suzuki et al. 2005; Suzuki et al. 2008). Constitutive expression of *MBF1c* in Arabidopsis led to an increase in tolerance to heat shock and osmotic stress, even when the two stresses were combined (Suzuki et al. 2005; Suzuki et al. 2011). The constitutive expression of the *MBF1c* also led to lower bacterial colony formation by *Pseudomonas syringae* cv tomato, possibly suggesting a role in pathogen resistance (Suzuki et al. 2005). Interestingly, following exposure to low concentrations of DON, Arabidopsis cell suspensions demonstrated increased tolerance to heat shock stress, and heat shock related cell death, in the present of light (Ansari et al. 2014). Since the *MBF1c* is

up-regulated upon exposure to DON, it suggests that the role of DON in heat stress tolerance could be conferred through the up-regulation of *MBF1c*, possibly by the DON-mediated effects on the ROS signalling pathway.

When analysing the single mutants in Kronos, for the tetraploid wheat orthologues of AtMBF1c, TraesCS7B02G259000 (WKRON2901) and TraesCS7A02G369500 (WKRON2731), a significant increase in susceptibility was observed to low concentrations of DON, with the single mutants displaying reduced root growth when compared to their corresponding controls. When analysing mutants in the Rpd3 histone deacetylase complex in yeast, an increase sensitivity to DON was observed (Kugler et al. 2016), similar to that observed with the single mutants of tetraploid wheat. The loss of sensitivity in the double mutant, may indicate that the disruption of all the orthologues of MBF1c, leads to the plant activating alternative pathways early in development that compensate the loss of both genes. In the single mutants, it is possible the plant can still detect the presence of at least one functional MBF1c, which is enough for the normal cell regulation. This regulation is disrupted when exposed to DON, leading to an overwhelming response from MBF1c to DON or to the DON-mediated ROS burst, leading to DON sensitivity.

In this chapter a specific analysis of the RNAseq data from Bd21 response to low concentrations of DON was performed. This demonstrated that low concentrations allow for a more sensitive analysis of the plant response, without the interference from cell death responses that would otherwise hide these responses. In the first instance it allowed study of the QTL region from chapter 4 in more depth, demonstrating the potential of ABR6 to be able to respond with a higher magnitude to DON when comparing to the susceptible Bd21 accession, which could account for its resistance phenotype. The second and third strategies for candidate gene selection, comprising the in-depth analyses of the highest differential expressed response at 6 h and 24 h, as well as the orthologue response in wheat, indicate that *Bd* is a powerful tool as a preliminary step before translating into a wheat genetic characterization. This is observed in the comparison between the strength in expression when

comparing *Bd* single gene log2 fold change and its corresponding wheat orthologues, where the expression of the latter seems to be diluted, most likely due to the redundancy of homeologues and duplicates in wheat. However, it is important to highlight that although the sensitivity of response in *Bd* seems to be greater than wheat, the synteny between the two species is highly conserved, with the two plants responding in a very similar manner to the same concentration of DON. This is observed in the analyses of the MBF1c putative genes, where a high up-regulation in both *Bd* and wheat, is translated into the Kronos TILLING mutant analyses, where a disruption of these genes seems to cause a higher sensitivity of the plant to DON. Although the single mutants seem to demonstrate a role of MBF1c in wheat response to DON, the same effect is not observed in the double mutant, suggesting that, at least in some instances, gene dosage may be important in DON response in wheat.

Chapter 7. General Discussion

Wheat is one of the most important sources of food in the world, leading to the production of bread, biscuits and pasta. For this purpose, protection of wheat against external stress is extremely important. The genome of wheat is highly complex, mainly due to the hybridisation of three different genomes over thousands of years, which led to an hexaploid genome of around 17 Gbp containing a large variety of redundant and duplicated genes (Brenchley et al. 2012; Krasileva et al. 2013). Although the wheat genome has been sequenced with an estimate coverage of 94%, studies on wheat are still complex and time consuming, making advances in improving wheat against adverse stress a very slow process (Zhu et al. 2021).

To bypass the difficulty of working with complex or unknown genomes, scientists have resorted into studying simpler plants, that can provide answers to certain biological questions in a more time friendly manner. One of the most studied model plants is *Arabidopsis thaliana*, a small, annual, diploid species, which has served has a powerful tool in understanding many pathways employed by angiosperm plants (Kramer 2015). Although a good model in establishing a variety of resources in the study of other dicotyledon plants, especially in the Brassicaceae group, like oilseed crops, various types of cabbages, garden radish and mustard (Kramer 2015), it can only provide limited information for the full understanding of other plants, like monocotyledon crops such as wheat, barley and rye. For this endeavour other plants have been proposed as potential model system for the study of monocots, the two strongest ones being rice and maize (Brkljacic et al. 2011). These two species are studied by a large research community, which continuously provide more genetic resources to complement their well sequenced genomes. Limitations occur however, when it comes to the practical use of these species, which occupy a substantial amount of space to grow, coupled with demanding growth requirements and with long generation times (Brkljacic et al. 2011). Since it was first proposed as model system in 2001 (Draper et al. 2001), *Brachypodium distachion* (Bd), a small diploid

monocot species, has proved to blend the needed characteristics of rice and maize with *Arabidopsis thaliana*, to become established as a strong model for the study of C_3 temperate cereals. Similar to *Arabidopsis*, *Bd* has a small stature, short life cycle, with undemanding growth conditions and a small genome of 272 Mbp (IBI 2010). The most studied accession of *Bd*, Bd21, is a fully sequence line, with a predicted strong syntenic relationship with wheat and other cereals (Huo et al. 2009; IBI 2010). Just like rice and maize, *Bd* also has a good library of genetic resources, ranging from EMS and T-DNA mutant libraries (Vain et al. 2008; Bragg et al. 2012; Collier et al. 2016), a fully-sequence database of 54 different accessions from across Europe and the Middle-East (Gordon et al. 2017), along with several gene network analyses and gene expression data. In the past decade, *Bd* has been an important tool in the characterization of important crop diseases, demonstrating similar symptoms to wheat, in response to FHB and eyespot (Peraldi et al. 2011), rice blast (Routledge et al. 2004; Wang, Wang, Chen, et al. 2012), and Ramularia leaf spot (Peraldi et al. 2014). In this study a full characterization of *Bd* has been made in its abilities to mimic the symptoms of disease progression of another set of diseases, take-all and *Fusarium* root rot, and its important role in serving as an important preliminary step in understanding disease resistance to these two diseases before translating findings into wheat. These two diseases were of special interest due to the difficulty in assessing root disease progression in the complex root system of wheat, which generally is coupled with destructive time-point measurements, rather than a progressive infection timeline of the disease in the roots of the same plant.

In the analyses of take-all infection in the roots of *Bd* using the most frequently studied accessions, Bd21 and Bd3-1, disease progression was efficiently quantified in real time, with timepoints of necrotic lesion progression in the same plant being recorded and analysed. These methodologies expanded and corroborated the works performed previously using *Bd* as a general model for disease quantification, specifically on the studies working with FRR, take-all and Rhizoctonia root rot (Peraldi et al. 2011; Sandoya and Buanafina 2014; Schneebeli, Mathesius, and Watt 2015). A total of 58 different accessions, with the majority

being already fully sequenced and incorporated into the pangenome of *Bd* (Brachypan) (Gordon et al. 2017; Gordon et al. 2020), were used to explore the potential of *Bd* in the characterization of potential sources of disease resistance to take-all. Disease progression varied from accessions that displayed a very high tolerance to necrotic lesion progression to accessions in which seedlings were killed by high disease pressure. This represents the first step in establishing *Bd* as a model for root disease characterization since, to date, most hexaploid wheat cultivars display high susceptibility to take-all, with very limited resistance against *Ggt* infection (Palma-Guerrero et al. 2021). Other members of the Pooideae sub-family have been characterized in their potential to tolerate and be resistant against take-all, either through the production of specific compounds, like the production of specific hydroxamic acids by rye (Wilkes, Marshall, and Copeland 1999) and avenacin by oats (Papadopoulou et al. 1999), to specific genome adaptations like the intrinsic resistance of *Triticum monococcum* (McMillan, Gutteridge, and Hammond-Kosack 2014) and *Haynaldia villosa* (Ren et al. 2003). Since the production of specific compounds are normally associated with a bimodal model of response, where the fungus either is resistant to the chemical and is capable of infecting, or is completely inhibited by the compound, it is unlikely that this is the strategy employed by more resistant accessions of *Bd*, since the infection profile observed in Brachypan is normally distributed. The infection profile of the Brachypan panel is more closely associated with the analyses performed in the introduction of resistance-conferring chromosomes into wheat from *Triticum monococcum* and *Haynaldia villosa*, where a normal distribution of disease resistance is observed (Huang et al. 2007; McMillan, Gutteridge, and Hammond-Kosack 2014). Understanding the resistance mechanism conferred by these crosses is difficult however, since their genome is not fully sequenced, making the characterisation of resistance, highly complex and time consuming. By observing a similar pattern in *Bd*, a more promising study can be performed, since the majority of the accessions have already been sequenced, and due to the synteny with wheat, it is possible to translate the findings into wheat without the need for inter-species crossing.

Among the populations already developed for *Bd*, the parents that showed the most promising differential to *Ggt* strain T5-2, was between resistant parent Jer1, and susceptible parent Luc1. This proved to an interesting result, since in the characterization of the pangenome, Gordon and colleagues, annotated these two accessions as genetically very similar, both originating from the same geographical location in northeast Spain (Gordon et al. 2017). Although highly similar, these two lines have already proved to differ in their response to pathogens, where Bettgenhaeuser and colleagues, identified a putative NB-LRR, that could be responsible for the resistance observed in Jer1 to wheat stripe rust (Bettgenhaeuser et al. 2018). The differential in take-all symptoms between the two accessions was unstable however, with Jer1 having inconsistent necrotic lesion progression with strain *Ggt* T5-2, and being as susceptible as Luc1, with strains *Ggt* 18e and *Ggt* 1d. This may reflect the virulence of each strain, where *Ggt* 18e and *Ggt* 1d display greater virulence than *Ggt* T5-2, which results in collapse of the differential between the two accessions. Differences in virulence between strains of *Ggt* to wheat have already been reported, obtained from the isolation of different strains of *Ggt* from contaminated soils (Kwak et al. 2009).

Another study using take-all analysed the potential role of the 9-LOX pathway jasmonates in their potential role in disease resistance. Unfortunately, there was not enough evidence to suggest that the single mutants in the two potential 9-LOX *Bd* genes, *BdLOX1a* and *BdLOX1b*¸ play a role in resistance. By analysing the concentrations of the 9-LOX metabolites, there is no significant decrease in the mutant line of *BdLOX1a*, suggesting that in order to fully analyse the effect of the 9-LOX in disease resistance, a double mutant is needed. Although not conclusive, this study proved another promising role of *Bd* in the preliminary study of potential sources of resistance. The analyses of all the single mutants of the 9-LOX pathway in wheat would have taken a substantial amount of space, coupled with the subsequent complete disrupting of all the 9-LOX genes in wheat taking a considerable amount of time. In this study the amount of time and space needed for *Bd* analyses of the single mutants was significantly reduced, leading to consider the analyses of the double

mutant in a potentially smaller time frame than working with wheat directly. If the complete disruption of 9-LOX pathway proves to play a role in the disease resistance against take-all, this work in *Bd* can then be translated into wheat, in establishing whether the same orthologue pathway can be exploited in the protection of wheat against *Ggt* infection in the field. If successful, this strategy will further establish *Bd* as a power tool for functional validation of candidate genes.

The same methodology was employed to identify potential sources of resistance to FRR. The same infection differential was observed in the Brachypan response to the necrotic lesion progression of *Fg*. In initial comparisons of FRR resistance from infection in the middle section of root, the best differential in the parents of established populations of *Bd*, was observed between the resistant accession Foz1 and the susceptible accession Luc1. Unfortunately, upon re-analysing the parents Foz1 and Luc1 using a revised 'slurry' methodology, the differential collapsed, with the necrotic lesion progression in the root not been statistically different between the two accessions. This illustrates the importance of protocol optimisation, where simple changes can increase the accuracy of the results considerably. Using the simple root architecture of *Bd*, the optimisation is relatively simpler when compared to crops. The experiment also benefits from being substantially more compact, where all 58 available accessions of *Bd* and its respective replicate sets were able to be analysed in a single experiment in a 4 m^2 area. If the same experimental settings were transferred into studies in wheat, or even barley, the amount of space needed to study the same number of lines and replicates would be considerable and require a much longer time.

The same experimental setup also allowed for the characterization of 'overall death of the seedling' phenotype across the Brachypan panel. The differential across the panel was very considerable, with accessions displaying no symptoms of premature death to accessions completely overtaken by the fungus. The overall death also displayed interesting phenotypes, where the infection in the crown and cotyledons and first leaves of *Bd* was not directly connected with the internal growth of the fungus from the original infection area within the

primary root, assumed to reflect new infection attempts following growth of the fungus along the outside of the root. A clear differential was observed between the available population parents, resistant accession ABR6 and the susceptible Bd21. The available F9 population was characterized for FRR resistance/susceptibility by performing a CIS QTL analyses. The generation of the F9 population of ABR6xBd21, also demonstrated the benefits of using *Bd* as a model, with the nine generations being collectively generated in less than 5 years, which is considerably quicker than producing the same generation in crops. The further characterization of the 100 different lines of the population also follows up from the aforementioned benefits of *Bd* in studying a high number of lines in a short timescale and considerably smaller space.

It was also observed that ABR6 infected seedlings, also produced a higher number of lateral roots when compared to Bd21. This phenotype was not present in non-infected roots. Increased growth rate and formation of more lateral roots have been described previously as a potential mechanism of resistance in some crops, where for example the intrinsic resistance of rye to take-all and other roots diseases is described as a combined effect of production hydroxamic acids and new roots (Skou 1975; Palma-Guerrero et al. 2021). The QTL analyses of the overall death of the seedling did not, however, overlap with the QTL results obtained from the lateral root number, suggesting that the lateral roots are not the main cause of resistance controlled by ABR6.

In the initial QTL analyses, two regions were statistically significant, with the region in chromosome 1 contributing to 27.6% of the total variance, and the region in chromosome 2 with an additional 12%. These findings are consistent to those for wheat with known sources of resistance to *Fusarium* diseases normally being dictated by numerous resistant factors scattered among the genome of the host. Upon translating the *Bd* QTL region to wheat, the orthologue region was mainly localized on the distal region of the chromosome group 7. Analyses of FHB and FCR resistance in wheat have regularly identified QTL in these regions and it is conceivable that similar genes in *Bd* and wheat are responsible. This proved to be

one of the first QTL performed in the direct consequences of FRR infection, being able to robustly characterize a strong phenotype in *Bd*. These findings increase the importance of *Bd* as a model, presenting a new approach in the dissection of resistance against root diseases, contributing to a better understanding of global resistance to *Fusarium*, with the possibility of being translated into the field.

In the analysis of the chromosome 1 region QTL region in Bd21 and its corresponding region in ABR6, a total of 311 predicted genes were found in Bd21 and 270 in ABR6. From the 311 genes, 16 genes are characterised as potential errors in gene prediction by Phytozome, and 239 genes have a similarity higher than 99% between the two accessions. In the ABR6 genome, 9 genes also have a similarity higher than 99% but BLAST to regions outside the QTL chromosome 1 in Bd21. These may reflect errors in the assembly and annotation of the ABR6 genome, which has not been proofread to the same extent as Bd21. A total of 47 genes in Bd21 and 31 genes in ABR6 appeared to be specific to the accession, or have an homologue outside the QTL region selected in this study. Genes Bradi1g30767, Bradi1g30797 and Brdisv1ABR6_r1004894m contained predicated kinase domains. Kinases have proved to be involved in signal cascades in response to *Fusarium* and DON, with wheat gene *TaLRRK-6D* and *TaSnRK1α*, along with barley gene *HvLRRK-6H*, proving a role in the response to *Fusarium*, being essential in conferring partial resistance to *Fusarium* and DON, with the complete disruption of their expression leading to increased disease development and sensitivity to DON (Thapa et al. 2018; Perochon et al. 2019). Interestingly the expression profile of these genes in Bd21 and ABR6 to DON, did not show a significantly increase in their expression as observed in the aforementioned wheat and barley kinases. This suggests that the three genes are unlikely to be responsible for the resistance differential between these two accessions. However, gene expression upon *Fusarium* infection and exposure to higher concentrations of DON must be performed in order to test this hypothesis. When comparing the remaining genes in their response to DON, twelve genes showed a differential response between Bd21 and ABR6, with Bd21 having two significantly down-regulated genes; and

ABR6 having two significant down-regulated genes and eight significant up-regulated genes. Among these, two predicted genes involved in protein translation have contrasting expression, with Bradi1g30811, a putative large subunit ribosomal protein being down-regulated in ABR6, and Bradi1g29577, a putative eukaryotic initiation factor, being up-regulated. If involved in the resistance phenotype of ABR6, it suggests that ABR6 might have the ability to change its protein translation mechanism to cope with the adverse effects of DON, to maintain protein synthesis. Another gene that might contribute to this system in ABR6 is Bradi1g29740, a putative tRNA-intron endonuclease potentially involved in mRNA maturation, that is also up-regulated. It is conceivable that ABR6 is able to up-regulate specific genes involved in protein synthesis that are capable of bypassing the direct disruption by DON, coupling the ABR6 resistance strategy with that observed in the wheat resistant cultivars analysed by Foroud and colleagues (Foroud et al. 2012), and the methionyl-tRNA synthetase role in resistance to DON in *Arabidopsis thaliana* (Zuo et al. 2016).

Other strategies employed by ABR6 could depend in the expression of specific LRR proteins, or transcription factors, as observed in the up-regulation of putative LRR gene Bradi1g29658, and the MYB44 transcription factor Bradi1g30252. Function of LRR is largely associated with effector-triggered immunity, with the example of LRR wheat genes, TaLRRK-6D displaying a positive role in disease resistance against *Fusarium* (Thapa et al. 2018). Another LRR, TaRCR1, is involved in the reduction of ROS accumulation, an effect of DON (Zhu et al. 2017). MYB44, although proving to play a negative role in resistance to necrotrophic pathogens in *Arabidopsis thaliana*, has a positive role in reducing chlorophyll loss and delaying senescence, processes commonly accelerated by DON (Shim et al. 2013; Jaradat et al. 2013). It would be interesting to examine the consequences of disruption and over-expression of these two genes in ABR6 and study the effects on resistance to the overall death of the seedling as a consequence of FRR and *Fg* infection.

In the general analyses of Bd21 response to low concentrations of DON, the most significant GO terms observed in the unfiltered up-regulation response, are mainly involved in

protein synthesis and RNA maintenance. This global up-regulation of genes involved in the normal gene transcription and translation pathway in the cell are most likely associated with the need to compensate the disruption of essential ribosomal and RNA proteins by DON. DON disruption of ribosomal and other important proteins involved in protein synthesis has already been documented, with studies demonstrating the binding of DON to ribosomal subunits and disrupting the initiation, elongation or termination of the chain elongation step (Christopher, Carter, and Cannon 1977; McLaughlin et al. 1977; Schindler 1974; Wei et al. 1974). Other pathways which possess RNA binding sites, like RNA transport proteins, RNA maturation and the spliceosome, are also highly affected by DON, suggesting that DON binds to several RNA-binding sites, thus explaining the very broad effects of DON in the plant. Interestingly, no significant expression of genes involved in PCD were detected when exposing the plant to low concentrations of DON and by 24h post exposure, Bd21 down-regulated the aforementioned pathways involved in protein synthesis. This indicates that the low concentration of DON used was still able to deregulate its common targets but was not high enough to create a toxic effect within the cell to initiate PCD. *Bd* was able to establish homeostasis indicating that the plant was able to manage and detoxify DON, allowing the cell to return to normal levels of expression. Other documented effects of DON were also observed at 6 h, with the disruption of cell wall biogenesis and maintenance, induction of general abiotic stress responses, and ROS oxidative stress and detoxification pathways. Desmond and colleagues demonstrated that high levels of DON increase production of H_20_2 in the cell and concluded that this was the main cause for DON associated PCD within the cell. The absence of evidence for induction of PCD in the current study allowed an investigation of the effects of DON on ROS associated genes without the interference of expression of ROS genes involved in this process. By establishing this system, the complex role of DON could be further characterised, by dissecting the pathways that are affected by DON, in a ROS and non-ROS mediated action.

The first step in this process was to identify ROS-inducing compounds that phenocopied the effects of low concentrations of DON on root growth and elongation in *Bd*.

Exposure of roots to H_2O_2 produced a similar phenotype to exposure to low concentrations of DON. Both DON and H_2O_2 promoted elongation of the root growth and enhanced gravitropism.

After demonstrating the phenotypic similarities of DON and H_2O_2 at low concentrations, an RNA-seq was performed in both Bd21 exposed to low concentrations of DON or H_2O_2. The general response of the plant to H_2O_2, was considerably weaker than the response to DON, with relatively few genes altering expression beyond 2-fold change threshold. However, the comparison between the two responses demonstrated that DON was able to account to more than half of the response observed under H_2O_2. The reverse is not observed, with DON sharing less than 10% of its response with H_2O_2. Many of the up-regulated genes in common between the two compounds were involved in abiotic stress responses and toxin metabolism, especially toxin detoxification including genes involved in the glutathione, uronic acid and phytoalexin pathways, which are known antioxidants (Choudhary, Kumar, and Kaur 2020). The common down-regulated genes were mainly involved in the ROS pathway and the cell wall biogenesis and organisation. Both findings correlate with expected responses of the cell to oxidative bursts, with the cell trying to employ detoxifiers to control ROS levels. Interestingly peroxidases which are also known detoxifiers of ROS, are down regulated, suggesting the cell is responding to DON and H_2O_2 by employing more complex antioxidants like glutathione and phytoalexins, rather than direct protein modifiers like peroxidases. It could be that active radicals in the cell are not direct targets of peroxidases, and the cell is trying to maintain levels of signalling ROS molecules by down-regulating peroxidases, while trying to detoxify more complex free radical molecules by producing more specific antioxidants.

The cell wall integrity is another commonly reported target of both ROS and DON, suggesting that the effect of DON on this pathway may be indirect, through its interaction with H_2O_2. Although the great majority of GO terms in the down-regulated response are shared between DON and H_2O_2, no highly down-regulated gene is shared between H_2O_2 and the core DON response. This indicates that similarity in effects of these agents on the down-regulation of these processes are only minor, with the greatest similarity in response being mainly

directed to an up-regulation of selected genes in *Bd*. This similarity in the effects of DON and H_2O_2 is evident in the common phenotype of root elongation observed upon inoculation with low concentrations of both compounds. It has been established that H_2O_2 plays an important role in the development of the root of *Arabidopsis thaliana*, where the balance between H_2O_2 in the elongation zone and $O_2^{\cdot -}$ in the meristematic zone is crucial for root development (Tsukagoshi, Busch, and Benfey 2010). In maize, H_2O_2 is the main regulator of elongation in the roots, where in well-watered conditions, an increase in H_2O_2 led to cell elongation and growth, while the opposite was observed in water-stressed plants (Voothuluru et al. 2020). Studies in the role of H_2O_2 in root elongation has also been observed upon dysregulation of the ROS balance in the root of sweet potato seedlings, where low concentrations of H_2O_2 led to increased development of adventitious roots, while high concentrations led to the global inhibition of root and plant growth (Deng et al. 2012). High concentrations of H_2O_2 also led to disruption in cell elongation and root growth in tomato (Ivanchenko et al. 2013). This is highly reminiscent of the role of DON in the root growth of the plant where low concentrations stimulate root elongation and growth, and high concentrations repress root growth and development (Peraldi 2012). High production of H_2O_2 and DON is also associated with the transition of *Fusarium* between its biotrophic and necrotrophic phase (Audenaert et al. 2014). Production of DON in the biotrophic phase of the fungus is relatively low with a substantial increase only observed upon the fungus entering its necrotrophic infection phase (Walter, Nicholson, and Doohan 2010). This increase in DON correlates to a similar increase of H_2O_2 in the cell (Audenaert et al. 2014). Interestingly H_2O_2 as proved to be an efficient inducer of DON production, with exogenous application in the early stages leading to an increase in DON production by the fungus (Ponts et al. 2006; Ponts et al. 2007; Audenaert et al. 2010). This is hypothesized to create a positive feed-back loop between the both molecules leading to a mutual increase in the production of H_2O_2 by the plant and DON by the fungus (Audenaert et al. 2014). These findings display the importance in the balance of DON and H_2O_2 in the relationship between host and *Fusarium*, where its possible disruption could be one of the major causes that leads the fungus to switch between its biotrophic to its necrotrophic phase.

In the DON-specific response by *Bd*, the main up-regulated pathways are still involved in protein synthesis, such as ribosome and RNA maintenance. These findings suggest that instability in protein synthesis caused by DON is not correlated with an increase in ROS, reinforcing the hypothesis of DON functions as a direct target of these proteins, destabilising their binding to RNA molecules. In the analyses of the specific down-regulated genes to DON, interestingly the most affected pathways are involved in light stimulus and chloroplasts. DON has been documented in decreasing levels of chlorophyl and carotenoids in the cell in the presence of light, leading to the eventual bleaching of the tissue (Bushnell et al. 2003). As oxidative bursts and ROS production is often associated with disruption to the mitochondria and chloroplasts (Chang et al. 2009), it may be that the ROS production in the presence of DON is an indirect consequence of DON's effects on the stability of chloroplast and its components. By coupling all the aforementioned scenarios together, the final hypothetical scenario for the effects of DON within the cell involves the interaction between RNA binding proteins and RNA, severely affecting the normal protein synthesis of the cell (Fig 7-1). This dysregulation may lead to instability within the cell, specifically affecting the normal integrity of cellular transports, chloroplast and other organelles, leading to the production of ROS and other free radicals, coupled with an increase in antioxidants and detoxifiers within the cell, along with general stress response mechanisms (Fig 7-1). At low concentrations, *Bd* may be able to adjust to this, mainly affecting cell division and elongation, explaining the rapid elongation of the primary to both low concentrations of DON and H_20_2. At high concentrations, the DON disruption of protein synthesis along with cell stability is more accentuated, leading to a higher production of ROS (perhaps including OH^- and O_2^- radicals), culminating in the activation of programmed cell death, bleaching of the tissue and the eventual the death of the plant.

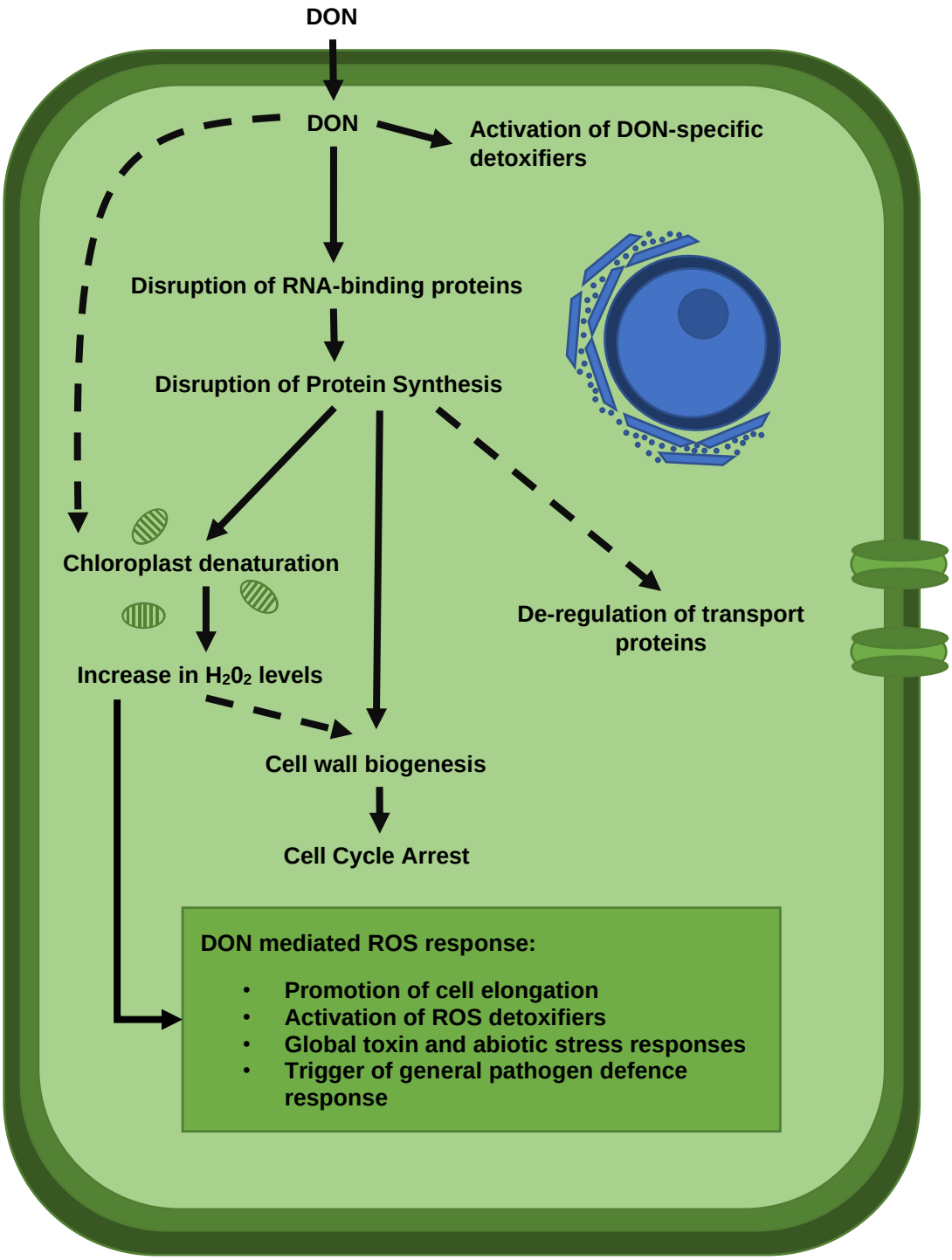

Figure 7-1 Hypothetical model for the effects on the plant cell of exposure to low concentrations of DON. Full lines represent putative direct mode of action. Dashed lines represent a possible indirect role.

The DON triggered response seems to be shared between *Bd* and wheat, where the analyses of the common most highly differential expression between the two species displayed a consistent response. Interestingly the most represented differentially expressed groups affected in both species are associated with putative detoxifiers, transporters and peroxidases. The most common were part of the glutathione S-transferase and glycosyl/glucuronosyl transferase family of proteins, a class of proteins already reported as prominent detoxifiers of ROS and DON, respectively (Foroud et al. 2012; Shin et al. 2012; Wahibah et al. 2018). Interestingly a cluster of UDP-glycosyltransferases on chromosome 5, from gene Bradi5g03300 to Bradi5g03380, display prominent up-regulation upon DON exposure, with Bradi5g03300 displaying the highest fold change of 8.6. This is concordant with the previous findings where Bradi5g03300 displays an important role in detoxifying DON to its less toxic form DON-3-G, leading to plant tolerance to the toxin and subsequently the fungus infection (Schweiger, Pasquet, et al. 2013; Pasquet et al. 2016). It is possible that over-expression of this class of protein is one of the main contributors to the plant homeostasis evident at 24 h.

To explore the similarity in response of *Bd* and wheat to DON and find other sources of resistance to DON, a candidate gene selection was performed between the most highly differentially expressed genes observed at both 6 h and 24 h with the common orthologue gene differential expression of wheat to DON. It was noticed that the expression of genes in *Bd* was generally relatively higher than their corresponding orthologues in wheat. One example is the aforementioned UGT Bradi5g03300, where the log2 fold-change in *Bd* is over 8, while its corresponding four orthologues in wheat display an expression between 3.2 and 3.4. This may be due to the effects of gene redundancy in wheat where, due to the multiple copies of the same gene, expression is diluted through the different homoeologues and duplications of the gene. If true, this contributes to *Bd* playing an important role as a preliminary model plant for the study of gene response to certain factors. By analysing the expression profile in *Bd*, it is possible to highlight genes with a significant differential expression to certain

external stimuli, among others, in a more efficient manner than in wheat, where the response is diluted among all the homoeologues, making it more difficult to dissect. This proved to be an important asset in the selection of candidate genes, where the *Bd* database and its high expression profile, was fundamental in filtering the large list of homoeologue and duplicate genes in the wheat response to DON. In the final list of candidate genes produced by the datasets from the two species, a putative GST and arachidonic acid metabolic pathway gene were among the genes highlighted, all already previously discussed as playing a potential role in maintenance of ROS and DON levels within the cell. Another pair of genes highlighted in the final analyses, Bradi1g74980 and Bradi4g22656, belong to a set of genes referred to as orphan genes, due to their poor annotation and restriction to the Pooideae family. The latter is the orthologue of *TaFROG*, an important orphan gene described as capable of increasing the tolerance of wheat to DON and FHB (Perochon et al. 2015). Another gene, Bradi1g37080, an hypothetical histone protein, described in *Arabidopsis thaliana* as multi-protein bridging factor 1c (MBF1c), was of particular interest, since it displayed a high up-regulation in *Bd* and in its corresponding three orthologue genes in wheat. Apart from the high up-regulation in both species, no work to date, as far as I am aware, has been reported for this as a potential DON resistance gene. It has been previously reported in *Arabidopsis thaliana*, that these genes play an important role in the plant response to heat shock, possibly through an ethylene-mediated pathway (Suzuki et al. 2005). Low concentrations of DON have also been reported as conferring heat tolerance in Arabidopsis cell suspensions (Ansari et al. 2014), and it is possible that this reflects the up-regulation of the MBF protein by DON that, in turn, subsequently provides enhanced heat tolerance. This gene also seems to play a potential role in ROS response, where exposure to methyl viologen and hydrogen peroxide was able to promote an up-regulation of these genes (Tsuda and Yamazaki 2004). Expression of Bradi1g37080 was also highly upregulated in the present study of Bd21 response to H_2O_2, corroborating the aforementioned findings in *Arabidospis*. Interestingly, Bradi4g22656, the orthologue of *TaFROG*, described as being DON-specific, in this study does not display a significant up-regulation in the ROS response, although having a high up-regulation upon DON exposure.

Again, this corroboration of similarities in interspecies gene expression is an important finding, which not only validates the consistency in expression between *Bd* and other species, but it also makes it possible to conduct the separation between DON and ROS responsive genes, allowing for the identification of pathways that are directly or indirectly affected by DON through either a ROS (H_2O_2) or non-ROS mediated pathways.

. For the characterization of Bradi1g37080 role in DON resistance, Kronos TILLING mutants in the orthologue wheat genes TraesCS7B02G259000 and TraesCS7A02G369500, where analysed for their response to low concentrations of DON. KRONOS proved to be less tolerant to DON than *Bd*, and root elongation of the primary root was not evident although accentuated positive gravitropism was still observed. In the analyses of the single A and B genome mutants to the DON, both mutants displayed increased sensitivity to DON in comparison to their respective controls. The WT accession of KRONOS and the synonymous mutation in WKRON2605 showed little inhibition upon inoculation with DON when compared to their respective control, reinforcing the potential role of MBF in DON response. Surprisingly, the double mutant did not exhibit increased DON sensitivity It is possible that the complete disruption of MBF1c leads to disruption of multiple pathways within the cell and that these acts to buffer the effect of the loss of MBF1c function. The wheat mutants identified and produced in this study can also be examined to establish how they affect heat tolerance. It would be interesting to analyse the effects of constitutive over-expression of MBF1c in Kronos to analyse if its early up-regulation leads to tolerance to DON and, perhaps, also to heat stress.

Unfortunately, it was not possible to obtain the corresponding MBF1c mutant in *Bd* in the duration of these studies. It would also be interesting in the future to study the effects of the disruption and over-expression of Bradi1g37080 in response to DON and heat stress to observe whether more pronounced DON sensibility/tolerance by *Bd* is observed, thereby contributing to a better understanding of the findings of Kronos.

In conclusion, the majority of the main project goals have been met, demonstrating the use of *Bd* as a crop model in the understanding of disease resistance to take-all and FRR,

and how *Bd* can serve as a powerful tool in the preliminary study of gene response before translation to more complex systems, like wheat. In this study, the Brachypan panel revealed high levels of genetic variability in *Bd* to both take-all and FRR. This makes *Bd* a good source of genetic variability for future studies to unravel disease resistance to these two diseases, something that has been difficult to access in wheat, especially since wheat displays high susceptibility to both diseases in most of the cultivars currently used. The response of *Bd* to DON was also considerably more 'condensed' than wheat, displaying much more pronounced gene expression responses than wheat. These responses to DON were however highly conserved between *Bd* and wheat.

Most studies reported to date evaluate the role of DON using high concentrations. In the current study it was possible to create a profile of expression in response to low concentrations of DON, providing a new insight to the role of DON in the plant, as well as enabling dissection of the pathways disrupted by DON in a ROS (H_2O_2) and non-ROS mediated response. This study also provided evidence for the potential for model-to-crop translation using *Bd*, where the study of MBF provided a promising target for examination of its role in DON tolerance with the disruption of the single mutants in Kronos displaying enhanced sensibility to the toxin. Overall, even though the resources to wheat are continuously increasing, the complexity of its hexaploid genome and its high gene redundancy is still a characteristic that hinders wheat gene research. *Bd* is potentially a powerful tool in the dissection of this complexity, by providing simpler and more rapid gene response analyses that can then be translated into wheat.

Chapter 8. References

Ameye, M., K. Audenaert, N. De Zutter, K. Steppe, L. Van Meulebroek, L. Vanhaecke, D. De Vleesschauwer, G. Haesaert, and G. Smagghe. 2015. 'Priming of wheat with the green leaf volatile Z-3-hexenyl acetate enhances defense against Fusarium graminearum but boosts deoxynivalenol production', *Plant Physiology*, 167: 1671-84.

Ansari, K. I., S. M. Doyle, J. Kacprzyk, M. R. Khan, S. Walter, J. M. Brennan, C. S. Arunachalam, P. F. McCabe, and F. M. Doohan. 2014. 'Light Influences How the Fungal Toxin Deoxynivalenol Affects Plant Cell Death and Defense Responses', *Toxins*, 6: 679-92.

Ansari, K. I., S. Walter, J. M. Brennan, M. Lemmens, S. Kessans, A. McGahern, D. Egan, and F. M. Doohan. 2007. 'Retrotransposon and gene activation in wheat in response to mycotoxigenic and non-mycotoxigenic-associated Fusarium stress', *Theoretical and Applied Genetics*, 114: 927-37.

Audenaert, K., E. Callewaert, M. Hofte, S. De Saeger, and G. Haesaert. 2010. 'Hydrogen peroxide induced by the fungicide prothioconazole triggers deoxynivalenol (DON) production by Fusarium graminearum', *Bmc Microbiology*, 10.

Audenaert, K., A. Vanheule, M. Hofte, and G. Haesaert. 2014. 'Deoxynivalenol: A Major Player in the Multifaceted Response of Fusarium to Its Environment', *Toxins*, 6: 1-19.

Ayliffe, M., D. Singh, R. Park, M. Moscou, and T. Pryor. 2013. 'Infection of Brachypodium distachyon with Selected Grass Rust Pathogens', *Molecular Plant-Microbe Interactions*, 26: 946-57.

Bai, G. H., and G. Shaner. 1994. 'Scab of Wheat - Prospects for Control', *Plant Disease*, 78: 760-66.

Bai, S. S., F. P. Yuan, H. B. Zhang, Z. Y. Zhang, J. X. Zhao, Q. H. Yang, J. Wu, and X. H. Chen. 2020. 'Characterization of the Wheat-Psathyrostachys huashania Keng 2Ns/2D Substitution Line H139: A Novel Germplasm With Enhanced Resistance to Wheat Take-All', *Frontiers in Plant Science*, 11.

Barbieri, M., T. C. Marcel, R. E. Niks, E. Francia, M. Pasquariello, V. Mazzamurro, D. F. Garvin, and N. Pecchioni. 2012. 'QTLs for resistance to the false brome rust Puccinia brachypodii in the model grass Brachypodium distachyon L.', *Genome*, 55: 152-63.

Beccari, G., L. Covarelli, and P. Nicholson. 2011. 'Infection processes and soft wheat response to root rot and crown rot caused by Fusarium culmorum', *Plant Pathology*, 60: 671-84.

Bettgenhaeuser, J., F. M. K. Corke, M. Opanowicz, P. Green, I. Hernandez-Pinzon, J. H. Doonan, and M. J. Moscou. 2017. 'Natural Variation in Brachypodium Links Vernalization and Flowering Time Loci as Major Flowering Determinants', *Plant Physiology*, 173: 256-68.

Bettgenhaeuser, J., M. Gardiner, R. Spanner, P. Green, I. Hernandez-Pinzon, A. Hubbard, M. Ayliffe, and M. J. Moscou. 2018. 'The genetic architecture of colonization resistance in Brachypodium distachyon to non-adapted stripe rust (Puccinia striiformis) isolates', *Plos Genetics*, 14.

Boddu, J., S. Cho, and G. J. Muehlbauer. 2007. 'Transcriptome analysis of trichothecene-induced gene expression in barley', *Mol Plant Microbe Interact*, 20: 1364-75.

Borrill, P., N. Adamski, and C. Uauy. 2015. 'Genomics as the key to unlocking the polyploid potential of wheat', *New Phytologist*, 208: 1008-22.

Bowyer, P., B. R. Clarke, P. Lunness, M. J. Daniels, and A. E. Osbourn. 1995. 'Host-Range of a Plant-Pathogenic Fungus Determined by a Saponin Detoxifying Enzyme', *Science*, 267: 371-74.

Bragg, J. N., J. J. Wu, S. P. Gordon, M. E. Guttman, R. Thilmony, G. R. Lazo, Y. Q. Gu, and J. P. Vogel. 2012. 'Generation and Characterization of the Western Regional Research Center Brachypodium T-DNA Insertional Mutant Collection', *Plos One*, 7.

Brauer, E. K., M. Balcerzak, H. Rocheleau, W. Leung, J. Schernthaner, R. Subramaniam, and T. Ouellet. 2020. 'Genome Editing of a Deoxynivalenol-Induced Transcription Factor Confers Resistance to Fusarium graminearum in Wheat', *Molecular Plant-Microbe Interactions*, 33: 553-60.

Brenchley, R., M. Spannagl, M. Pfeifer, G. L. A. Barker, R. D'Amore, A. M. Allen, N. McKenzie, M. Kramer, A. Kerhornou, D. Bolser, S. Kay, D. Waite, M. Trick, I. Bancroft, Y. Gu, N. Huo, M. C. Luo, S. Sehgal, B. Gill, S. Kianian, O. Anderson, P. Kersey, J. Dvorak, W. R. McCombie, A. Hall, K. F. X. Mayer, K. J. Edwards, M. W. Bevan, and N. Hall. 2012. 'Analysis of the breadwheat genome using whole-genome shotgun sequencing', *Nature*, 491: 705-10.

Brewer, H. C., N. D. Hawkins, and K. E. Hammond-Kosack. 2014. 'Mutations in the Arabidopsis homoserine kinase gene DMR1 confer enhanced resistance to Fusarium culmorum and F-graminearum', *Bmc Plant Biology*, 14.

Brkljacic, J., E. Grotewold, R. Scholl, T. Mockler, D. F. Garvin, P. Vain, T. Brutnell, R. Sibout, M. Bevan, H. Budak, A. L. Caicedo, C. X. Gao, Y. Gu, S. P. Hazen, B. F. Holt, S. Y. Hong, M. Jordan, A. J. Manzaneda, T. Mitchell-Olds, K. Mochida, L. A. J. Mur, C. M. Park, J. Sedbrook, M. Watt, S. J. Zheng, and J. P. Vogel. 2011. 'Brachypodium as a Model for the Grasses: Today and the Future', *Plant Physiology*, 157: 3-13.

Brown, N. A., C. Bass, T. K. Baldwin, H. Chen, F. Massot, P. W. Carion, M. Urban, A. M. van de Meene, and K. E. Hammond-Kosack. 2011. 'Characterisation of the Fusarium graminearum-Wheat Floral Interaction', *J Pathog*, 2011: 626345.

Brown, N. A., M. Urban, A. M. van de Meene, and K. E. Hammond-Kosack. 2010. 'The infection biology of Fusarium graminearum: defining the pathways of spikelet to spikelet colonisation in wheat ears', *Fungal Biol*, 114: 555-71.

Buerstmayr, Maria, Barbara Steiner, and Hermann Buerstmayr. 2020. 'Breeding for Fusarium head blight resistance in wheat—Progress and challenges', *Plant Breeding*, 139: 429-54.

Bus, J. S., J. E. Gibson, and S. D. Aust. 1974. 'Superoxide-Catalyzed and Singlet Oxygen-Catalyzed Lipid Peroxidation as a Possible Mechanism for Paraquat (Methyl Viologen) Toxicity', *Biochemical and Biophysical Research Communications*, 58: 749-55.

Bushnell, W. R., B. E. Hazen, C. Pritsch, and K. Leonard. 2003. 'Histology and physiology of Fusarium head blight.' in K. J. Leonard and W. R. Bushnell (eds.), *Fusarium Head Blight ofWheat and Barley* (APS Press: St. Paul, MN).

Bushnell, W. R., P. Perkins-Veazie, V. M. Russo, J. Collins, and T. M. Seeland. 2010. 'Effects of Deoxynivalenol on Content of Chloroplast Pigments in Barley Leaf Tissues', *Phytopathology*, 100: 33-41.

Cacas, J. L., F. Vailleau, C. Davoine, N. Ennar, J. P. Agnel, M. Tronchet, M. Ponchet, J. P. Blein, D. Roby, C. Triantaphylides, and J. L. Montillet. 2005. 'The combined action of 9 lipoxygenase and galactolipase is sufficient to bring about programmed cell death during tobacco hypersensitive response', *Plant Cell and Environment*, 28: 1367-78.

Cai, J., S. Wang, T. Li, G. R. Zhang, and G. H. Bai. 2016. 'Multiple Minor QTLs Are Responsible for Fusarium Head Blight Resistance in Chinese Wheat Landrace Haiyanzhong', *Plos One*, 11.

Capdevila, J. H., J. R. Falck, and R. C. Harris. 2000. 'Cytochrome P450 and arachidonic acid bioactivation: molecular and functional properties of the arachidonate monooxygenase', *Journal of Lipid Research*, 41: 163-81.

Capdevila, J. H., Y. Jin, A. Karara, and J. R. Falck. 1993. 'Cytochrome-P-450 Epoxygenase Dependent Formation of Novel Endogenous Epoxyeicosatrienoyl-Phospholipids', *Eicosanoids and Other Bioactive Lipids in Cancer, Inflammation and Radiation-Injury*, 71: 11-15.

Chang, C. C. C., I. Slesak, L. Jorda, A. Sotnikov, M. Melzer, Z. Miszalski, P. M. Mullineaux, J. E. Parker, B. Karpinska, and S. Karpinski. 2009. 'Arabidopsis Chloroplastic Glutathione Peroxidases Play a Role in Cross Talk between Photooxidative Stress and Immune Responses', *Plant Physiology*, 150: 670-83.

Charoenpornsook, K., J. L. Fitzpatrick, and J. E. Smith. 1998. 'The effects of four mycotoxins on the mitogen stimulated proliferation of bovine peripheral blood mononuclear cells in vitro', *Mycopathologia*, 143: 105-11.

Chekali, S., S. Gargouri, T. Paulitz, J. M. Nicol, M. Rezgui, and B. Nasraoui. 2011. 'Effects of Fusarium culmorum and water stress on durum wheat in Tunisia', *Crop Protection*, 30: 718-25.

Chen, P. D., L. L. Qi, B. Zhou, S. Z. Zhang, and D. J. Liu. 1995. 'Development and Molecular Cytogenetic Analysis of Wheat-Haynaldia Villosa 6vs/6al Translocation Lines Specifying Resistance to Powdery Mildew', *Theoretical and Applied Genetics*, 91: 1125-28.

Chen, X., A. Steed, S. Travella, B. Keller, and P. Nicholson. 2009. 'Fusarium graminearum exploits ethylene signalling to colonize dicotyledonous and monocotyledonous plants', *New Phytologist*, 182: 975-83.

Chen, Y. C., C. L. Wong, F. Muzzi, I. Vlaardingerbroek, B. N. Kidd, and P. M. Schenk. 2014. 'Root defense analysis against Fusarium oxysporum reveals new regulators to confer resistance', *Scientific Reports*, 4.

Chochois, V., J. P. Vogel, and M. Watt. 2012. 'Application of Brachypodium to the genetic improvement of wheat roots', *Journal of Experimental Botany*, 63: 3467-74.

Choudhary, A., A. Kumar, and N. Kaur. 2020. 'ROS and oxidative burst: Roots in plant development', *Plant Diversity*, 42: 33-43.

Christensen, S. A., A. Huffaker, F. Kaplan, J. Sims, S. Ziemann, G. Doehlemann, L. X. Ji, R. J. Schmitz, M. V. Kolomiets, H. T. Alborn, N. Mori, G. Jander, X. Z. Ni, R. C. Sartor, S. Byers, Z. Abdo, and E. A. Schmelz. 2015. 'Maize death acids, 9-lipoxygenase-derived cyclopente(a)nones, display activity as cytotoxic phytoalexins and transcriptional mediators', *Proceedings of the National Academy of Sciences of the United States of America*, 112: 11407-12.

Christensen, S. A., A. Nemchenko, Y. S. Park, E. Borrego, P. C. Huang, E. A. Schmelz, S. Kunze, I. Feussner, N. Yalpani, R. Meeley, and M. V. Kolomiets. 2014. 'The Novel Monocot-Specific 9-Lipoxygenase ZmLOX12 Is Required to Mount an Effective Jasmonate-Mediated Defense Against Fusarium verticillioides in Maize', *Molecular Plant-Microbe Interactions*, 27: 1263-76.

Christopher, J., C. Carter, and M. Cannon. 1977. 'Structural Requirements for Inhibitory Action of 12,13-Epoxytrichothecenes on Protein-Synthesis in Eukaryotes', *Biochemical Journal*, 166: 399-409.

Clavijo, B. J., L. Venturini, C. Schudoma, G. G. Accinelli, G. Kaithakottil, J. Wright, P. Borrill, G. Kettleborough, D. Heavens, H. Chapman, J. Lipscombe, T. Barker, F. H. Lu, N. McKenzie, D. Raats, R. H. Ramirez-Gonzalez, A. Coince, N. Peel, L. Percival-Alwyn, O. Duncan, J. Trosch, G. T. Yu, D. M. Bolser, G. Namaati, A. Kerhornou, M. Spannagl, H. Gundlach, G. Haberer, R. P. Davey, C. Fosker, F. Di Palma, A. L. Phillips, A. H. Millar, P. J. Kersey, C. Uauy, K. V. Krasileva, D. Swarbreck, M. W. Bevan, and M. D. Clark. 2017. 'An improved assembly and annotation of the allohexaploid wheat genome identifies complete families of agronomic genes and provides genomic evidence for chromosomal translocations', *Genome Research*, 27: 885-96.

Cole, S. J., A. J. Yoon, K. F. Faull, and A. C. Diener. 2014. 'Host perception of jasmonates promotes infection by Fusarium oxysporum formae speciales that produce isoleucine- and leucine-conjugated jasmonates', *Molecular Plant Pathology*, 15: 589-600.

Collier, R., J. Bragg, B. T. Hernandez, J. P. Vogel, and R. Thilmony. 2016. 'Use of Agrobacterium rhizogenes Strain 18r12v and Paromomycin Selection for Transformation of Brachypodium distachyon and Brachypodium sylvaticum', *Frontiers in Plant Science*, 7.

Cook, R. J. 2003. 'Take-all of wheat', *Physiological and Molecular Plant Pathology*, 62: 73-86.

———. 2007. 'Take-all decline: model system in the science of biological control and clue to the success of intensive cropping.' in C. Vincent, M. S. Goettel and G. Lazarovits (eds.), *Biological control: a global perspective* (Cabi: Wallingford).

Costa, S., S. Schwaiger, R. Cervellati, H. Stuppner, E. Speroni, and M. C. Guerra. 2009. 'In vitro evaluation of the chemoprotective action mechanisms of leontopodic acid against aflatoxin B1 and deoxynivalenol-induced cell damage', *Journal of Applied Toxicology*, 29: 7-14.

Covarelli, L., G. Beccari, A. Steed, and P. Nicholson. 2012. 'Colonization of soft wheat following infection of the stem base by Fusarium culmorum and translocation of deoxynivalenol to the head', *Plant Pathology*, 61: 1121-29.

Coyne, C. J., L. D. Porter, G. Boutet, Y. Ma, R. J. McGee, A. Lesne, A. Baranger, and M. L. Pilet-Nayel. 2019. 'Confirmation of Fusarium root rot resistance QTL Fsp-Ps 2.1 of pea under controlled conditions', *Bmc Plant Biology*, 19.

De Pace, C., D. Snidaro, M. Ciaffi, D. Vittori, A. Ciofo, A. Cenci, O. A. Tanzarella, C. O. Qualset, and G. T. Scarascia Mugnozza. 2001. 'Introgression of Dasypyrum villosum chromatin into common wheat improves grain protein quality', *Euphytica*, 117: 67-75.

Deacon, J. W. 1973. '*Phialophora radicicola* and *Gaeumannomyces graminis* on roots of grasses and cereals.', *Trans. Br. Mycol. Soc.*, 61: 471-85.

Dedyukhina, Emiliya G., Svetlana V. Kamzolova, and Mikhail B. Vainshtein. 2014. 'Arachidonic acid as an elicitor of the plant defense response to phytopathogens', *Chemical and Biological Technologies in Agriculture*, 1: 18.

Deng, Xi-Ping, Yu-Jie Cheng, Xiao-Bing Wu, Sang-Soo Kwak, Wei Chen, and Anthony Egrinya Eneji. 2012. 'Exogenous hydrogen peroxide positively influences root growth and metabolism in leaves of sweet potato seedlings', *Australian Journal of Crop Science*, 6: 1572–78.

Desjardins, A. E., and T. M. Hohn. 1997. 'Mycotoxins in plant pathogenesis', *Molecular Plant-Microbe Interactions*, 10: 147-52.

Desjardins, A. E., R. H. Proctor, G. H. Bai, S. P. McCormick, G. Shaner, G. Buechley, and T. M. Hohn. 1996. 'Reduced virulence of trichothecene-nonproducing mutants of Gibberella zeae in wheat field tests', *Molecular Plant-Microbe Interactions*, 9: 775-81.

Desmond, O. J., J. M. Manners, A. E. Stephens, D. J. MaClean, P. M. Schenk, D. M. Gardiner, A. L. Munn, and K. Kazan. 2008. 'The Fusarium mycotoxin deoxynivalenol elicits hydrogen peroxide production, programmed cell death and defence responses in wheat', *Molecular Plant Pathology*, 9: 435-45.

Diamond, M., T. J. Reape, O. Rocha, S. M. Doyle, J. Kacprzyk, F. M. Doohan, and P. F. McCabe. 2013. 'The fusarium mycotoxin deoxynivalenol can inhibit plant apoptosis-like programmed cell death', *Plos One*, 8: e69542.

Ding, L., H. Xu, H. Yi, L. Yang, Z. Kong, L. Zhang, S. Xue, H. Jia, and Z. Ma. 2011. 'Resistance to hemi-biotrophic F. graminearum infection is associated with coordinated and ordered expression of diverse defense signaling pathways', *Plos One*, 6: e19008.

Dodman, R. L., and R. L. Flentje. 1970. "The mechanism and physiology of plant penetration by Rhizoctonia solani." In *Rhizoctonia Solani, Biology and Pathology*, edited by J.R. Parmeter Jr. (Ed.), pp. 149–60. University of California Press, Berkeley/Los Angeles/London.

Draper, J., L. A. J. Mur, G. Jenkins, G. C. Ghosh-Biswas, P. Bablak, R. Hasterok, and A. P. M. Routledge. 2001. 'Brachypodium distachyon. A new model system for functional genomics in grasses', *Plant Physiology*, 127: 1539-55.

Eckard, J. T., J. L. Gonzalez-Hernandez, M. Caffe, W. Berzonsky, W. W. Bockus, G. F. Marais, and P. S. Baenziger. 2015. 'Native Fusarium head blight resistance from winter wheat cultivars 'Lyman,' 'Overland,' 'Ernie,' and 'Freedom' mapped and pyramided onto 'Wesley'-Fhb1 backgrounds', *Molecular Breeding*, 35.

Eriksen, G. S., and H. Pettersson. 2004. 'Toxicological evaluation of trichothecenes in animal feed', *Animal Feed Science and Technology*, 114: 205-39.

Evans, M. D., M. Dizdaroglu, and M. S. Cooke. 2004. 'Oxidative DNA damage and disease: induction, repair and significance', *Mutation Research-Reviews in Mutation Research*, 567: 1-61.

Figueroa, M., K. E. Hammond-Kosack, and P. S. Solomon. 2018. 'A review of wheat diseases-a field perspective', *Molecular Plant Pathology*, 19: 1523-36.

Foroud, N. A., T. Ouellet, A. Laroche, B. Oosterveen, M. C. Jordan, B. E. Ellis, and F. Eudes. 2012. 'Differential transcriptome analyses of three wheat genotypes reveal different host response pathways associated with Fusarium head blight and trichothecene resistance', *Plant Pathology*, 61: 296-314.

Fried, H. M., and J. R. Warner. 1981. 'Cloning of Yeast Gene for Trichodermin Resistance and Ribosomal Protein-L3', *Proceedings of the National Academy of Sciences of the United States of America-Biological Sciences*, 78: 238-42.

Fung, F., and R. F. Clark. 2004. 'Health effects of mycotoxins: A toxicological overview', *Journal of Toxicology-Clinical Toxicology*, 42: 217-34.

Gao, X. Q., W. B. Shim, C. Gobel, S. Kunze, I. Feussner, R. Meeley, P. Balint-Kurti, and M. Kolomiets. 2007. 'Disruption of a maize 9-lipoxygenase results in increased resistance to fungal pathogens and reduced levels of contamination with mycotoxin fumonisin', *Molecular Plant-Microbe Interactions*, 20: 922-33.

Gao, X. Q., J. Starr, C. Gobel, J. Engelberth, I. Feussner, J. Tumlinson, and M. Kolomiets. 2008. 'Maize 9-lipoxygenase ZmLOX3 controls development, root-specific expression of defense genes, and resistance to root-knot nematodes', *Molecular Plant-Microbe Interactions*, 21: 98-109.

Gardiner, S. A., J. Boddu, F. Berthiller, C. Hametner, R. M. Stupar, G. Adam, and G. J. Muehlbauer. 2010. 'Transcriptome Analysis of the Barley-Deoxynivalenol Interaction: Evidence for a Role of Glutathione in Deoxynivalenol Detoxification', *Molecular Plant-Microbe Interactions*, 23: 962-76.

Garvin, D. F., Y. Q. Gu, R. Hasterok, S. P. Hazen, G. Jenkins, T. C. Mockler, L. A. J. Mur, and J. P. Vogel. 2008. 'Development of genetic and genomic research resources for Brachypodium distachyon, a new model system for grass crop research', *Crop Science*, 48: S69-S84.

Gatti, M., F. Choulet, C. Macadre, F. Guerard, J. M. Seng, T. Langin, and M. Dufresne. 2018. 'Identification, Molecular Cloning, and Functional Characterization of a Wheat UDP-Glucosyltransferase Involved in Resistance to Fusarium Head Blight and to Mycotoxin Accumulation', *Frontiers in Plant Science*, 9: 1853.

Geisler, K., R. K. Hughes, F. Sainsbury, G. P. Lomonossoff, M. Rejzek, S. Fairhurst, C. E. Olsen, M. S. Motawia, R. E. Melton, A. M. Hemmings, S. Bak, and A. Osbourn. 2013. 'Biochemical analysis of a multifunctional cytochrome P450 (CYP51) enzyme required for synthesis of antimicrobial triterpenes in plants', *Proceedings of the National Academy of Sciences of the United States of America*, 110: E3360-E67.

Gilsinger, J., L. Kong, X. Shen, and H. Ohm. 2005. 'DNA markers associated with low Fusarium head blight incidence and narrow flower opening in wheat', *Theoretical and Applied Genetics*, 110: 1218-25.

Gordon, S. P., B. Contreras-Moreira, J. J. Levy, A. Djamei, A. Czedik-Eysenberg, V. S. Tartaglio, A. Session, J. Martin, A. Cartwright, A. Katz, V. R. Singan, E. Goltsman, K. Barry, H. D. T. Vinh, B. Chalhoub, A. Diaz-Perez, R. Sancho, J. Lusinska, E. Wolny, C. Nibau, J. H. Doonan, L. A. J. Mur, C. Plott, J. Jenkins, S. P. Hazen, S. J. Lee, S. Q. Shu, D. Goodstein, D. Rokhsar, J. Schmutz, R. Hasterok, P. Catalan, and J. P. Vogel. 2020. 'Gradual polyploid genome evolution revealed by pan-genomic analysis of Brachypodium hybridum and its diploid progenitors', *Nature Communications*, 11.

Gordon, S. P., B. Contreras-Moreira, D. P. Woods, D. L. D. Marais, D. Burgess, S. Q. Shu, C. Stritt, A. C. Roulin, W. Schackwitz, L. Tyler, J. Martin, A. Lipzen, N. Dochy, J. Phillips, K. Barry, K. Geuten, H. Budak, T. E. Juenger, R. Amasino, A. L. Caicedo, D. Goodstein, P. Davidson, L. A. J. Mur, M. Figueroa, M. Freeling, P. Catalan, and J. P. Vogel. 2017. 'Extensive gene content variation in the Brachypodium distachyon pan-genome correlates with population structure', *Nature Communications*, 8.

Gray, J. S., H. K. Bae, J. C. B. Li, A. S. Lau, and J. J. Pestka. 2008. 'Double-stranded RNA-activated protein kinase mediates induction of interleukin-8 expression by deoxynivalenol, Shiga toxin 1, and ricin in monocytes', *Toxicological Sciences*, 105: 322-30.

Griffiths, S., R. Sharp, T. N. Foote, I. Bertin, M. Wanous, S. Reader, I. Colas, and G. Moore. 2006. 'Molecular characterization of Ph1 as a major chromosome pairing locus in polyploid wheat', *Nature*, 439: 749-52.

Guenther, J. C., and F. Trail. 2005. 'The development and differentiation of Gibberella zeae (anamorph : Fusarium graminearum) during colonization of wheat', *Mycologia*, 97: 229-37.

Gutteridge, R. J., G. L. Bateman, and A. D. Todd. 2003. 'Variation in the effects of take-all disease on grain yield and quality of winter cereals in field experiments', *Pest Management Science*, 59: 215-24.

Haidoulis, J F., and P. Nicholson. 2020. 'Different effects of phytohormones on Fusarium head blight and Fusarium root rot resistance in Brachypodium distachyon', *bioRxiv*: 2020.06.26.173385.

Handa, H., N. Namiki, D. Xu, and T. Ban. 2008. 'Dissecting of the FHB resistance QTL on the short arm of wheat chromosome 2D using a comparative genomic approach: from QTL to candidate gene', *Molecular Breeding*, 22: 71-84.

Haralampidis, K., G. Bryan, X. Qi, K. Papadopoulou, S. Bakht, R. Melton, and A. Osbourn. 2001. 'A new class of oxidosqualene cyclases directs synthesis of antimicrobial phytoprotectants in monocots', *Proceedings of the National Academy of Sciences of the United States of America*, 98: 13431-36.

He, K., and J. J. Pestka. 2010. 'Deoxynivalenol-induced modulation of microRNA expression in RAW 264.7 macrophages—a potential novel mechanism for translational inhibition.', *The Toxicologist (Toxicological Sciences Supplement)*, 114: 310.

Heil, M., and J. Ton. 2008. 'Long-distance signalling in plant defence', *Trends in Plant Science*, 13: 264-72.

Heslop-Harrison, J.S. 2001. 'Three pieces: C.D. Darlington (pp. 512-513); Chromosome Bridge (pp. 350-351); and Polyploidy (pp. 1509-1511).' in Miller JH Brenner S (ed.), *Encyclopedia of Genetics* (Academic Press: San Diego).

Hofstad, A. N., T. Nussbaumer, E. Akhunov, S. Shin, K. G. Kugler, H. C. Kistler, K. F. X. Mayer, and G. J. Muehlbauer. 2016. 'Examining the Transcriptional Response in Wheat Fhb1 Near-Isogenic Lines to Fusarium graminearum Infection and Deoxynivalenol Treatment', *Plant Genome*, 9.

Holladay, S. D., B. L. Blaylock, C. E. Comment, J. J. Heindel, and M. I. Luster. 1993. 'Fetal Thymic Atrophy after Exposure to T-2 Toxin - Selectivity for Lymphoid Progenitor Cells', *Toxicology and Applied Pharmacology*, 121: 8-14.

Hornby, D., G.L. Bateman, R.J. Gutteridge, P. Lucas, A.E. Osbourn, E. Ward., and D.J. Yarham. 1998. *Take-all Disease of Cereals* (CAB International: University of Wisconsin - Madison).

Howe, G. A., and A. L. Schilmiller. 2002. 'Oxylipin metabolism in response to stress', *Current Opinion in Plant Biology*, 5: 230-36.

Huang, Da-hui, Zhi-shan Lin, Xiao Chen, Zeng-yan Zhang, Cai-ceng Chen, Shun-he Cheng, and Zhi-yong Xin. 2007. 'Molecular Characterization of a Triticum durum-Haynaldia villosa Amphiploid and Its Derivatives for Resistance to Gaeumannomyces graminis var. tritici', *Agricultural Sciences in China*, 6: 513-21.

Huo, N. X., J. P. Vogel, G. R. Lazo, F. M. You, Y. Q. Ma, S. McMahon, J. Dvorak, O. D. Anderson, M. C. Luo, and Y. Q. Gu. 2009. 'Structural characterization of Brachypodium genome and its syntenic relationship with rice and wheat', *Plant Molecular Biology*, 70: 47-61.

Hwang, I. S., and B. K. Hwang. 2010. 'The Pepper 9-Lipoxygenase Gene CaLOX1 Functions in Defense and Cell Death Responses to Microbial Pathogens', *Plant Physiology*, 152: 948-67.

IBI, International Brachypodium Initiative. 2010. 'Genome sequencing and analysis of the model grass Brachypodium distachyon', *Nature*, 463: 763-8.

Ighodaro, O. M., A. M. Adeosun, and O. A. Akinloye. 2017. 'Alloxan-induced diabetes, a common model for evaluating the glycemic-control potential of therapeutic compounds and plants extracts in experimental studies', *Medicina-Lithuania*, 53: 365-74.

Ito, M., I. Sato, M. Ishizaka, S. Yoshida, M. Koitabashi, S. Yoshida, and S. Tsushima. 2013. 'Bacterial Cytochrome P450 System Catabolizing the Fusarium Toxin Deoxynivalenol', *Applied and Environmental Microbiology*, 79: 1619-28.

Ivanchenko, M. G., D. den Os, G. B. Monshausen, J. G. Dubrovsky, A. Bednarova, and N. Krishnan. 2013. 'Auxin increases the hydrogen peroxide (H2O2) concentration in tomato (Solanum lycopersicum) root tips while inhibiting root growth', *Annals of Botany*, 112: 1107-16.

IWGSC. 2018. 'Shifting the limits in wheat research and breeding using a fully annotated reference genome', *Science*, 361: 661-+.

Jansen, C., D. von Wettstein, W. Schafer, K. H. Kogel, A. Felk, and F. J. Maier. 2005. 'Infection patterns in barley and wheat spikes inoculated with wild-type and trichodiene synthase gene disrupted Fusarium graminearum', *Proceedings of the National Academy of Sciences of the United States of America*, 102: 16892-97.

Jaradat, M. R., J. A. Feurtado, D. Q. Huang, Y. Q. Lu, and A. J. Cutler. 2013. 'Multiple roles of the transcription factor AtMYBR1/AtMYB44 in ABA signaling, stress responses, and leaf senescence', *Bmc Plant Biology*, 13.

Jayatilake, D., G. Bai, and Y. Dong. 2011. 'A novel quantitative trait locus for Fusarium head blight resistance in chromosome 7A of wheat', *Theoretical and Applied Genetics*, 122: 1189-98.

Jia, G., P. D. Chen, G. J. Qin, G. H. Bai, X. Wang, S. L. Wang, B. Zhou, S. H. Zhang, and D. J. Liu. 2005. 'QTLs for Fusarium head blight response in a wheat DH population of Wangshuibai/Alondra's'', *Euphytica*, 146: 183-91.

Jia, H. Y., J. Y. Zhou, S. L. Xue, G. Q. Li, H. S. Yan, C. F. Ran, Y. D. Zhang, J. X. Shi, L. Jia, X. Wang, J. Luo, and Z. Q. Ma. 2018. 'A journey to understand wheat Fusarium head blight resistance in the Chinese wheat landrace Wangshuibai', *Crop Journal*, 6: 48-59.

Jin, J. J., S. N. Duan, Y. Z. Qi, S. H. Yan, W. Li, B. Y. Li, C. J. Xie, W. C. Zhen, and J. Ma. 2020. 'Identification of a novel genomic region associated with resistance to Fusarium crown rot in wheat', *Theoretical and Applied Genetics*, 133: 2063-73.

Jones, J. D. G., and J. L. Dangl. 2006. 'The plant immune system', *Nature*, 444: 323-29.

Kang, Xingxing, Lanhua Wang, Yu Guo, Muhammad Zain ul Arifeen, Xunchao Cai, Yarong Xue, Yuanqin Bu, Gang Wang, and Changhong Liu. 2019. 'A Comparative Transcriptomic and Proteomic Analysis of Hexaploid Wheat's Responses to Colonization by Bacillus velezensis and Gaeumannomyces graminis, Both Separately and Combined', *Molecular Plant-Microbe Interactions®*, 32: 1336-47.

Kang, Z. S., and H. Buchenauer. 2000. 'Cytology and ultrastructure of the infection of wheat spikes by Fusarium culmorum', *Mycological Research*, 104: 1083-93.

Klahr, A., G. Zimmermann, G. Wenzel, and V. Mohler. 2007. 'Effects of environment, disease progress, plant height and heading date on the detection of QTLs for resistance to Fusarium head blight in an European winter wheat cross', *Euphytica*, 154: 17-28.

Kouzai, Y., M. Kimura, M. Watanabe, K. Kusunoki, D. Osaka, T. Suzuki, H. Matsui, M. Yamamoto, Y. Ichinose, K. Toyoda, T. Matsuura, I. C. Mori, T. Hirayama, E. Minami, Y. Nishizawa, K. Inoue, Y. Onda, K. Mochida, and Y. Noutoshi. 2018. 'Salicylic acid-dependent immunity contributes to resistance against Rhizoctonia solani, a necrotrophic fungal agent of sheath blight, in rice and Brachypodium distachyon', *New Phytologist*, 217: 771-83.

Kramer, U. 2015. 'Planting molecular functions in an ecological context with Arabidopsis thaliana', *Elife*, 4.

Krasileva, K. V., V. Buffalo, P. Bailey, S. Pearce, S. Ayling, F. Tabbita, M. Soria, S. C. Wang, E. Akhunov, C. Uauy, J. Dubcovsky, and IWGS Consortium. 2013. 'Separating homeologs by phasing in the tetraploid wheat transcriptome', *Genome Biology*, 14.

Kugler, K. G., Z. Jandric, R. Beyer, E. Klopf, W. Glaser, M. Lemmens, M. Shams, K. Mayer, G. Adam, and C. Schuller. 2016. 'Ribosome quality control is a central protection mechanism for yeast exposed to deoxynivalenol and trichothecin', *Bmc Genomics*, 17.

Kumar, S., R. W. Stack, T. L. Friesen, and J. D. Faris. 2007. 'Identification of a novel fusarium head blight resistance quantitative trait locus on chromosome 7A in tetraploid wheat', *Phytopathology*, 97: 592-97.

Kwak, Y. S., P. A. H. M. Bakker, D. C. M. Glandorf, J. T. Rice, T. C. Paulitz, and D. M. Weller. 2009. 'Diversity, Virulence, and 2,4-Diacetylphloroglucinol Sensitivity of Gaeumannomyces graminis var. tritici Isolates from Washington State', *Phytopathology*, 99: 472-79.

Lagudah, E. S., and S. G. Krattinger. 2019. 'A new player contributing to durable Fusarium resistance', *Nature Genetics*, 51: 1070-71.

Langevin, F., F. Eudes, and A. Comeau. 2004. 'Effect of trichothecenes produced by Fusarium graminearum during Fusarium head blight development in six cereal species', *European Journal of Plant Pathology*, 110: 735-46.

Lemmens, M., U. Scholz, F. Berthiller, C. Dall'Asta, A. Koutnik, R. Schuhmacher, G. Adam, H. Buerstmayr, A. Mesterhazy, R. Krska, and P. Ruckenbauer. 2005. 'The ability to detoxify the mycotoxin deoxynivalenol colocalizes with a major quantitative trait locus for fusarium head blight resistance in wheat', *Molecular Plant-Microbe Interactions*, 18: 1318-24.

Leveau, A., J. Reed, X. Qiao, M. J. Stephenson, S. T. Mugford, R. E. Melton, J. C. Rant, R. Vickerstaff, T. Langdon, and A. Osbourn. 2019. 'Towards take-all control: a C-21 beta oxidase required for acylation of triterpene defence compounds in oat', *New Phytologist*, 221: 1544-55.

Li, G. Q., J. Y. Zhou, H. Y. Jia, Z. X. Gao, M. Fan, Y. J. Luo, P. T. Zhao, S. L. Xue, N. Li, Y. Yuan, S. W. Ma, Z. X. Kong, L. Jia, X. An, G. Jiang, W. X. Liu, W. J. Cao, R. R. Zhang, J. C. Fan, X. W. Xu, Y. F. Liu, Q. Q. Kong, S. H. Zheng, Y. Wang, B. Qin, S. Y. Cao, Y. X. Ding, J. X. Shi, H. S. Yan, X. Wang, C. F. Ran, and Z. Q. Ma. 2019. 'Mutation of a histidine-rich calcium-binding-protein gene in wheat confers resistance to Fusarium head blight', *Nature Genetics*, 51: 1106-+.

Li, H. J., R. L. Conner, Q. Chen, X. Jia, H. Li, R. J. Graf, A. Laroche, and A. D. Kuzyk. 2002. 'Different reactions to the wheat curl mite and Wheat streak mosaic virus in various wheat-Haynaldia villosa 6V and 6VS lines', *Plant Disease*, 86: 423-28.

Li, M. X., and J. J. Pestka. 2008. 'Comparative induction of 28S ribosomal RNA cleavage by ricin and the trichothecenes deoxynivalenol and T-2 toxin in the macrophage', *Toxicological Sciences*, 105: 67-78.

Li, T., G. H. Bai, S. Y. Wu, and S. L. Gu. 2011. 'Quantitative trait loci for resistance to fusarium head blight in a Chinese wheat landrace Haiyanzhong', *Theoretical and Applied Genetics*, 122: 1497-502.

———. 2012. 'Quantitative trait loci for resistance to Fusarium head blight in the Chinese wheat landrace Huangfangzhu', *Euphytica*, 185: 93-102.

Li, X., S. Shin, S. Heinen, R. Dill-Macky, F. Berthiller, N. Nersesian, T. Clemente, S. McCormick, and G. J. Muehlbauer. 2015. 'Transgenic Wheat Expressing a Barley UDP-Glucosyltransferase Detoxifies Deoxynivalenol and Provides High Levels of Resistance to Fusarium graminearum', *Molecular Plant-Microbe Interactions*, 28: 1237-46.

Li, X., J. B. Zhang, B. Song, H. P. Li, H. Q. Xu, B. Qu, F. J. Dang, and Y. C. Liao. 2010. 'Resistance to Fusarium Head Blight and Seedling Blight in Wheat Is Associated with Activation of a Cytochrome P450 Gene', *Phytopathology*, 100: 183-91.

Liao, Y.C., and Y.J. Yu. 1985. 'Genetic analysis of scab resistance in the local wheat variety Wang-Shui-Bai', *Journal of Huazhong Agricultural College*, 4: 6-14.

Lim, G. H., R. Singhal, A. Kachroo, and P. Kachroo. 2017. 'Fatty Acid- and Lipid-Mediated Signaling in Plant Defense', *Annual Review of Phytopathology, Vol 55*, 55: 505-36.

Linnainmaa, K., M. Sorsa, and T. Ilus. 1979. 'Epoxytrichothecene Mycotoxins as C-Mitotic Agents in Allium', *Hereditas*, 90: 151-56.

Liszkay, A., E. van der Zalm, and P. Schopfer. 2004. 'Production of reactive oxygen intermediates (O-2(center dot-), H2O2, and (OH)-O-center dot) by maize roots and their role in wall loosening and elongation growth', *Plant Physiology*, 136: 3114-23.

Liu, C. J., and F. C. Ogbonnaya. 2015. 'Resistance to Fusarium crown rot in wheat and barley: a review', *Plant Breeding*, 134: 365-72.
Liu, X. L., and C. J. Liu. 2016. 'Effects of Drought-Stress on Fusarium Crown Rot Development in Barley', *Plos One*, 11.
Loor, G., J. Kondapalli, J. M. Schriewer, N. S. Chandel, T. L. Vanden Hoek, and P. T. Schumacker. 2010. 'Menadione triggers cell death through ROS-dependent mechanisms involving PARP activation without requiring apoptosis', *Free Radical Biology and Medicine*, 49: 1925-36.
Lu, D., T. Wang, S. Persson, B. Mueller-Roeber, and J. H. M. Schippers. 2014. 'Transcriptional control of ROS homeostasis by KUODA1 regulates cell expansion during leaf development', *Nature Communications*, 5.
Lu, Q. X., M. Lillemo, H. Skinnes, X. Y. He, J. R. Shi, F. Ji, Y. H. Dong, and A. Bjornstad. 2013. 'Anther extrusion and plant height are associated with Type I resistance to Fusarium head blight in bread wheat line 'Shanghai-3/Catbird'', *Theoretical and Applied Genetics*, 126: 317-34.
Lulin, M., S. Yi, C. Aizhong, Q. Zengjun, X. Liping, C. Peidu, L. Dajun, and E. W. Xiu. 2010. 'Molecular cloning and characterization of an up-regulated UDP-glucosyltransferase gene induced by DON from Triticum aestivum L. cv. Wangshuibai', *Molecular Biology Reports*, 37: 785-95.
Luo, K., T. Ouellet, H. Zhao, X. Wang, and Z. Kang. 2021. 'Wheat-Fusarium graminearum Interactions Under Sitobion avenae Influence: From Nutrients and Hormone Signals', *Front Nutr*, 8: 703293.
Makandar, R., V. Nalam, R. Chaturvedi, R. Jeannotte, A. A. Sparks, and J. Shah. 2010. 'Involvement of salicylate and jasmonate signaling pathways in Arabidopsis interaction with Fusarium graminearum', *Mol Plant Microbe Interact*, 23: 861-70.
Marcos, R., Y. Izquierdo, T. Vellosillo, S. Kulasekaran, T. Cascon, M. Hamberg, and C. Castresana. 2015. '9-Lipoxygenase-Derived Oxylipins Activate Brassinosteroid Signaling to Promote Cell Wall-Based Defense and Limit Pathogen Infection', *Plant Physiology*, 169: 2324-34.
Markell, S. G., and L. J. Francl. 2003. 'Fusarium head blight inoculum: Species prevalence and Gibberella zeae spore type', *Plant Disease*, 87: 814-20.
Martin, F. N., and J. E. Loper. 1999. 'Soilborne plant diseases caused by Pythium spp: Ecology, epidemiology, and prospects for biological control', *Critical Reviews in Plant Sciences*, 18: 111-81.
McCartney, C. A., A. L. Brule-Babel, G. Fedak, R. A. Martin, B. D. McCallum, J. Gilbert, C. W. Hiebert, and C. J. Pozniak. 2016. 'Fusarium Head Blight Resistance QTL in the Spring Wheat Cross Kenyon/86ISMN 2137', *Frontiers in Microbiology*, 7.
McLaughlin, C.S., M.H. Vaughan, I.M. Campbell, C.M. Wei, M.E. Stafford, and B.S. Hansen. 1977. 'Inhibition of protein synthesis by trichothecenes.' in J.V. Rodericks, C.W. Hesseltine and M.A. Mehlman (eds.), *Mycotoxins in human and health.* (Pathotox: Park Forest South, IL).
McMillan, V. E., G. Canning, J. Moughan, R. P. White, R. J. Gutteridge, and K. E. Hammond-Kosack. 2018. 'Exploring the resilience of wheat crops grown in short rotations through minimising the build-up of an important soil-borne fungal pathogen', *Scientific Reports*, 8.
McMillan, V. E., R. J. Gutteridge, and K. E. Hammond-Kosack. 2014. 'Identifying variation in resistance to the take-all fungus, Gaeumannomyces graminis var. tritici, between different ancestral and modern wheat species', *Bmc Plant Biology*, 14.
McMillan, V. E., K. E. Hammond-Kosack, and R. J. Gutteridge. 2011. 'Evidence that wheat cultivars differ in their ability to build up inoculum of the take-all fungus, Gaeumannomyces graminis var. tritici, under a first wheat crop', *Plant Pathology*, 60: 200-06.
McMullen, M., G. Bergstrom, E. De Wolf, R. Dill-Macky, D. Hershman, G. Shaner, and D. Van Sanford. 2012. 'A Unified Effort to Fight an Enemy of Wheat and Barley: Fusarium Head Blight', *Plant Disease*, 96: 1712-28.

Mesterhazy, A., T. Bartok, C. G. Mirocha, and R. Komoroczy. 1999. 'Nature of wheat resistance to Fusarium head blight and the role of deoxynivalenol for breeding', *Plant Breeding*, 118: 97-110.
Mhamdi, A., and F. Van Breusegem. 2018. 'Reactive oxygen species in plant development', *Development*, 145.
Mikami, O., H. Yamaguchi, H. Murata, Y. Nakajima, and S. Miyazaki. 2010. 'Induction of apoptotic lesions in liver and lymphoid tissues and modulation of cytokine mRNA expression by acute exposure to deoxynivalenol in piglets', *Journal of Veterinary Science*, 11: 107-13.
Miller, J. D., and M. A. Ewen. 1997. 'Toxic effects of deoxynivalenol on ribosomes and tissues of the spring wheat cultivars Frontana and Casavant', *Nat Toxins*, 5: 234-7.
Miller, J. D., R. W. Stack, and L. R. Joppa. 1998. 'Evaluation of Triticum turgidum L. var. dicoccoides for resistance to Fusarium head blight and stem rust in', *Proc. 9th Int. Wheat Genetics Symp, ed. A. E. Slinkard (Saskatoon, SK: University of Saskatoon)*: 292–93.
Minati, Mohammed Hussein. 2020. 'First record of nine Fusarium spp. causing root rot on wheat (Triticum aestivum L.) in Iraq', *AIP Conference Proceedings*, 2290: 020009.
Mitterbauer, R., and G. Adam. 2002. 'Saccharomyces cerevisae and Arabidopsis thaliana: Useful model systems for the identification of molecular mechanisms involved in resistance of plants to toxins', *European Journal of Plant Pathology*, 108: 699-703.
Moon, Y., and J. J. Pestka. 2002. 'Vomitoxin-induced cyclooxygenase-2 gene expression in macrophages mediated by activation of ERK and p38 but not JNK mitogen-activated protein kinases', *Toxicological Sciences*, 69: 373-82.
Mugford, S. T., T. Louveau, R. Melton, X. Qi, S. Bakht, L. Hill, T. Tsurushima, S. Honkanen, S. J. Rosser, G. P. Lomonossoff, and A. Osbourn. 2013. 'Modularity of plant metabolic gene clusters: A trio of linked genes that are collectively required for acylation of triterpenes in oat (vol 25, pg 1078, 2013)', *Plant Cell*, 25: 3632-32.
Muller, K., A. Linkies, R. A. M. Vreeburg, S. C. Fry, A. Krieger-Liszkay, and G. Leubner-Metzger. 2009. 'In Vivo Cell Wall Loosening by Hydroxyl Radicals during Cress Seed Germination and Elongation Growth', *Plant Physiology*, 150: 1855-65.
Murray, G. M., and J. P. Brennan. 2009. 'Estimating disease losses to the Australian wheat industry', *Australasian Plant Pathology*, 38: 558-70.
Nishiuchi, T., D. Masuda, H. Nakashita, K. Ichimura, K. Shinozaki, S. Yoshida, M. Kimura, I. Yamaguchi, and K. Yamaguchi. 2006. 'Fusarium phytotoxin trichothecenes have an elicitor-like activity in Arabidopsis thaliana, but the activity differed significantly among their molecular species', *Molecular Plant-Microbe Interactions*, 19: 512-20.
Niwa, S., K. Kubo, J. Lewis, R. Kikuchi, M. Alagu, and T. Ban. 2014. 'Variations for Fusarium head blight resistance associated with genomic diversity in different sources of the resistant wheat cultivar 'Sumai 3'', *Breeding Science*, 64: 90-96.
O'Driscoll, Aoife, Fiona Doohan, and Ewen Mullins. 2015. 'Exploring the utility of Brachypodium distachyon as a model pathosystem for the wheat pathogen Zymoseptoria tritici', *BMC research notes*, 8: 132-32.
Okubara, P. A., M. B. Dickman, and A. E. Blechl. 2014. 'Molecular and genetic aspects of controlling the soilborne necrotrophic pathogens Rhizoctonia and Pythium', *Plant Science*, 228: 61-70.
Osbourn, A. E., B. R. Clarke, P. Lunness, P. R. Scott, and M. J. Daniels. 1994. 'An Oat Species Lacking Avenacin Is Susceptible to Infection by Gaeumannomyces-Graminis Var Tritici', *Physiological and Molecular Plant Pathology*, 45: 457-67.
Paciolla, C., N. Dipierro, G. Mule, A. Logrieco, and S. Dipierro. 2004. 'The mycotoxins beauvericin and T-2 induce cell death and alteration to the ascorbate metabolism in tomato protoplasts', *Physiological and Molecular Plant Pathology*, 65: 49-56.
Paciolla, C., M. P. Ippolito, A. Logrieco, N. Dipierro, G. Mule, and S. Dipierro. 2008. 'A different trend of antioxidant defence responses makes tomato plants less susceptible to beauvericin than to T-2 mycotoxin phytotoxicity', *Physiological and Molecular Plant Pathology*, 72: 3-9.

Packa, D. 1997. 'Cytogenetic effects of Fusarium mycotoxins on root tip cells of rye [Secale cereale L.], wheat [Triticum aestivum L.] and field bean [Vicia faba L.var.minor]', *Journal of Applied Genetics*, 38: 259-72.

———. 1998. 'Potential genotoxicity of Fusarium mycotoxins in *Vicia* and *Pisum* cytogenetic tests', *Journal of Applied Genetics*, 39: 171-92.

Packa, Danuta, and Elwira Sliwinska. 2005. 'Trichothecene fusarial toxins perturb the cell cycle in meristem-atic cells of Secale cereale L., Triticum aestivum L. and Vicia faba L', *Caryologia -Firenze-*, 58: 86-93.

Palma-Guerrero, J., T. Chancellor, J. Spong, G. Canning, J. Hammond, V. E. McMillan, and K. E. Hammond-Kosack. 2021. 'Take-All Disease: New Insights into an Important Wheat Root Pathogen', *Trends in Plant Science*.

Papadopoulou, K., R. E. Melton, M. Leggett, M. J. Daniels, and A. E. Osbourn. 1999. 'Compromised disease resistance in saponin-deficient plants', *Proceedings of the National Academy of Sciences of the United States of America*, 96: 12923-28.

Park, J., H. H. Lee, K. Youn, S. Kim, B. Jung, J. Lee, and Y. S. Seo. 2014. 'Transcriptome analyses to understand effects of the Fusarium deoxynivalenol and nivalenol mycotoxins on Escherichia coli', *J Biotechnol*, 192 Pt A: 231-9.

Park, Y. S., S. Kunze, X. Z. Ni, I. Feussner, and M. V. Kolomiets. 2010. 'Comparative molecular and biochemical characterization of segmentally duplicated 9-lipoxygenase genes ZmLOX4 and ZmLOX5 of maize', *Planta*, 231: 1425-37.

Parry, D. W., P. Jenkinson, and L. Mcleod. 1995. 'Fusarium Ear Blight (Scab) in Small-Grain Cereals - a Review', *Plant Pathology*, 44: 207-38.

Pasquariello, M., J. Ham, C. Burt, J. Jahier, S. Paillard, C. Uauy, and P. Nicholson. 2017. 'The eyespot resistance genes Pch1 and Pch2 of wheat are not homoeoloci', *Theoretical and Applied Genetics*, 130: 91-107.

Pasquet, J. C., V. Changenet, C. Macadre, E. Boex-Fontvieille, C. Soulhat, O. Bouchabke-Coussa, M. Dalmais, V. Atanasova-Penichon, A. Bendahmane, P. Saindrenan, and M. Dufresne. 2016. 'A Brachypodium UDP-Glycosyltransferase Confers Root Tolerance to Deoxynivalenol and Resistance to Fusarium Infection', *Plant Physiology*, 172: 559-74.

Peraldi, A. 2012. 'Brachypodium distachyon as a genetic model pathosystem to study resistance against fungal pathogens of small grain cereals', University of East Anglia.

Peraldi, A., G. Beccari, A. Steed, and P. Nicholson. 2011. 'Brachypodium distachyon: a new pathosystem to study Fusarium head blight and other Fusarium diseases of wheat', *Bmc Plant Biology*, 11.

Peraldi, A., L. L. Griffe, C. Burt, G. R. D. McGrann, and P. Nicholson. 2014. 'Brachypodium distachyon exhibits compatible interactions with Oculimacula spp. and Ramularia collo-cygni, providing the first pathosystem model to study eyespot and ramularia leaf spot diseases', *Plant Pathology*, 63: 554-62.

Perochon, A., J. G. Jia, A. Kahla, C. Arunachalam, S. R. Scofield, S. Bowden, E. Wallington, and F. M. Doohan. 2015. 'TaFROG Encodes a Pooideae Orphan Protein That Interacts with SnRK1 and Enhances Resistance to the Mycotoxigenic Fungus Fusarium graminearum', *Plant Physiology*, 169: 2895-906.

Perochon, A., Z. Vary, K. B. Malla, N. G. Halford, M. J. Paul, and F. M. Doohan. 2019. 'The wheat SnRK1 alpha family and its contribution to Fusarium toxin tolerance', *Plant Science*, 288.

Pilgeram, A. L., and J. M. Henson. 1992. 'Sexual crosses of the homothallic fungus *Gaeumannomyces graminis* var. *tritici* based on use of an auxotroph obtained by transformation.', *Exp. Mycol.*, 16: 35-43.

Pitzschke, A., A. Schikora, and H. Hirt. 2009. 'MAPK cascade signalling networks in plant defence', *Current Opinion in Plant Biology*, 12: 421-26.

Ponts, N., L. Pinson-Gadais, C. Barreau, F. Richard-Forget, and T. Ouellet. 2007. 'Exogenous H2O2 and catalase treatments interfere with Tri genes expression in liquid cultures of Fusarium graminearum', *Febs Letters*, 581: 443-47.

Ponts, N., L. Pinson-Gadais, M. N. Verdal-Bonnin, C. Barreau, and F. Richard-Forget. 2006. 'Accumulation of deoxynivalenol and its 15-acetylated form is significantly modulated by oxidative stress in liquid cultures of Fusarium graminearum', *Fems Microbiology Letters*, 258: 102-07.

Poppenberger, B., F. Berthiller, D. Lucyshyn, T. Sieberer, R. Schuhmacher, R. Krska, K. Kuchler, J. Glossl, C. Luschnig, and G. Adam. 2003. 'Detoxification of the Fusarium mycotoxin deoxynivalenol by a UDP-glucosyltransferase from Arabidopsis thaliana', *Journal of Biological Chemistry*, 278: 47905-14.

Powell, J. J., J. Carere, G. Sablok, T. L. Fitzgerald, J. Stiller, M. L. Colgrave, D. M. Gardiner, J. M. Manners, J. P. Vogel, R. J. Henry, and K. Kazan. 2017. 'Transcriptome analysis of Brachypodium during fungal pathogen infection reveals both shared and distinct defense responses with wheat', *Scientific Reports*, 7.

Qi, X., S. Bakht, M. Leggett, C. Maxwell, R. Melton, and A. Osbourn. 2004. 'A gene cluster for secondary metabolism in oat: Implications for the evolution of metabolic diversity in plants', *Proceedings of the National Academy of Sciences of the United States of America*, 101: 8233-38.

Qi, X., S. Bakht, B. Qin, M. Leggett, A. Hemmings, F. Mellon, J. Eagles, D. Werck-Reichhart, H. Schaller, A. Lesot, R. Melton, and A. Osbourn. 2006. 'A different function for a member of an ancient and highly conserved cytochrome P450 family: From essential sterols to plant defense', *Proceedings of the National Academy of Sciences of the United States of America*, 103: 18848-53.

Rahman, M., P. Davies, U. Bansal, R. Pasam, M. Hayden, and R. Trethowan. 2020. 'Marker-assisted recurrent selection improves the crown rot resistance of bread wheat', *Molecular Breeding*, 40.

Rance, I., J. Fournier, and M. T. Esquerre-Tugaye. 1998. 'The incompatible interaction between Phytophthora parasitica var. nicotianae race 0 and tobacco is suppressed in transgenic plants expressing antisense lipoxygenase sequences', *Proceedings of the National Academy of Sciences of the United States of America*, 95: 6554-59.

Rawat, N., M. O. Pumphrey, S. X. Liu, X. F. Zhang, V. K. Tiwari, K. Ando, H. N. Trick, W. W. Bockus, E. Akhunov, J. A. Anderson, and B. S. Gill. 2016. 'Wheat Fhb1 encodes a chimeric lectin with agglutinin domains and a pore-forming toxin-like domain conferring resistance to Fusarium head blight', *Nature Genetics*, 48: 1576-80.

Reilly, A., S. J. Karki, A. Twamley, A. M. M. Tiley, S. Kildea, and A. Feechan. 2020. 'Isolate specific responses of the non-host grass Brachypodium distachyon to the fungal pathogen Zymoseptoria tritici, compared to wheat', *Phytopathology*.

Ren, J. D., Z. Wang, Z. Y. Du, M. Z. Che, Y. B. Zhang, W. Quan, Y. J. Wang, X. Jiang, and Z. J. Zhang. 2019. 'Detection and validation of a novel major QTL for resistance to Fusarium head blight from Triticum aestivum in the terminal region of chromosome 7DL', *Theoretical and Applied Genetics*, 132: 241-55.

Ren, X., D.G. Yang, X.Y. Zhang, J.D. Wang, and J.L. Dong. 2003. 'Transfer of take-all resistant gene into wheat.', *Crops*, 1: 15-17.

Reubel, G. H., M. Gareis, and W. M. Amselgruber. 1987. 'Cytotoxicity Evaluation of Mycotoxins by an MTT-Bioassay', *Mycotoxin Res*, 3: 85-96.

Robert-Seilaniantz, A., L. Navarro, R. Bari, and J. D. Jones. 2007. 'Pathological hormone imbalances', *Current Opinion in Plant Biology*, 10: 372-79.

Rocha, O., K. Ansari, and F. M. Doohan. 2005. 'Effects of trichothecene mycotoxins on eukaryotic cells: A review', *Food Additives and Contaminants Part a-Chemistry Analysis Control Exposure & Risk Assessment*, 22: 369-78.

Rodriguez, A. A., K. A. Grunberg, and E. L. Taleisnik. 2002. 'Reactive oxygen species in the elongation zone of maize leaves are necessary for leaf extension', *Plant Physiology*, 129: 1627-32.

Rousseaux, C. G., H. B. Schiefer, and D. S. Hancock. 1986. 'Reproductive and Teratological Effects of Continuous Low-Level Dietary T-2 Toxin in Female Cd-1 Mice for 2 Generations', *Journal of Applied Toxicology*, 6: 179-84.

Routledge, A. P. M., G. Shelley, J. V. Smith, N. J. Talbot, J. Draper, and L. A. J. Mur. 2004. 'Magnaporthe grisea interactions with the model grass Brachypodium distachyon closely resemble those with rice (Oryza sativa)', *Molecular Plant Pathology*, 5: 253-65.

Sandoya, G. V., and M. M. D. Buanafina. 2014. 'Differential responses of Brachypodium distachyon genotypes to insect and fungal pathogens', *Physiological and Molecular Plant Pathology*, 85: 53-64.

Saville, R. J., N. Gosman, C. J. Burt, J. Makepeace, A. Steed, M. Corbitt, E. Chandler, J. K. M. Brown, M. I. Boulton, and P. Nicholson. 2012. 'The 'Green Revolution' dwarfing genes play a role in disease resistance in Triticum aestivum and Hordeum vulgare', *Journal of Experimental Botany*, 63: 1271-83.

SCF, (Scientific Committee for Food). 1999. "Opinion on Fusarium toxins. Part 1: Deoxynivalenol (DON)." In. http://www.europa.eu.int/comm/food/fs/sc/scf/out44_en.pdf.

———. 2002. "Opinion on Fusarium toxins. Part 6: Group evaluation of T-2 toxin, HT-2 toxin, nivalenol and deoxynivalenol." In. http://www.europa.eu.int/comm/food/fs/sc/scf/out123_en.pdf.

Scherm, B., V. Balmas, F. Spanu, G. Pani, G. Delogu, M. Pasquali, and Q. Migheli. 2013. 'Fusarium culmorum: causal agent of foot and root rot and head blight on wheat', *Molecular Plant Pathology*, 14: 323-41.

Schindler, D. 1974. '2 Classes of Inhibitors of Peptidyl Transferase-Activity in Eukaryotes', *Nature*, 249: 38-41.

Schneebeli, K., U. Mathesius, and M. Watt. 2015. 'Brachypodium distachyon is a pathosystem model for the study of the wheat disease rhizoctonia root rot', *Plant Pathology*, 64: 91-100.

Schneebeli, K., U. Mathesius, A. B. Zwart, J. N. Bragg, J. P. Vogel, and M. Watt. 2016. 'Brachypodium distachyon genotypes vary in resistance to Rhizoctonia solani AG8', *Functional Plant Biology*, 43: 189-98.

Schoevers, E. J., J. Fink-Gremmels, B. Colenbrander, and B. A. J. Roelen. 2010. 'Porcine oocytes are most vulnerable to the mycotoxin deoxynivalenol during formation of the meiotic spindle', *Theriogenology*, 74: 968-78.

Schopfer, P. 2001. 'Hydroxyl radical-induced cell-wall loosening in vitro and in vivo: implications for the control of elongation growth', *Plant Journal*, 28: 679-88.

Schweiger, W., J. Boddu, S. Shin, B. Poppenberger, F. Berthiller, M. Lemmens, G. J. Muehlbauer, and G. Adam. 2010. 'Validation of a candidate deoxynivalenol-inactivating UDP-glucosyltransferase from barley by heterologous expression in yeast', *Mol Plant Microbe Interact*, 23: 977-86.

Schweiger, W., J. C. Pasquet, T. Nussbaumer, M. P. K. Paris, G. Wiesenberger, C. Macadre, C. Ametz, F. Berthiller, M. Lemmens, P. Saindrenan, H. W. Mewes, K. F. X. Mayer, M. Dufresne, and G. Adam. 2013. 'Functional Characterization of Two Clusters of Brachypodium distachyon UDP-Glycosyltransferases Encoding Putative Deoxynivalenol Detoxification Genes', *Molecular Plant-Microbe Interactions*, 26: 781-92.

Schweiger, W., B. Steiner, C. Ametz, G. Siegwart, G. Wiesenberger, F. Berthiller, M. Lemmens, H. Jia, G. Adam, G. J. Muehlbauer, D. P. Kreil, and H. Buerstmayr. 2013. 'Transcriptomic characterization of two major Fusarium resistance quantitative trait loci (QTLs), Fhb1 and Qfhs.ifa-5A, identifies novel candidate genes', *Molecular Plant Pathology*, 14: 772-85.

Semagn, K., H. Skinnes, A. Bjornstad, A. G. Maroy, and Y. Tarkegne. 2007. 'Quantitative trait loci controlling Fusarium head blight resistance and low deoxynivalenol content in hexaploid wheat population from 'Arina' and NK93604', *Crop Science*, 47: 294-303.

Shifrin, V. I., and P. Anderson. 1999. 'Trichothecene mycotoxins trigger a ribotoxic stress response that activates c-Jun N-terminal kinase and p38 mitogen-activated protein kinase and induces apoptosis', *Journal of Biological Chemistry*, 274: 13985-92.

Shim, J. S., C. Jung, S. Lee, K. Min, Y. W. Lee, Y. Choi, J. S. Lee, J. T. Song, J. K. Kim, and Y. D. Choi. 2013. 'AtMYB44 regulates WRKY70 expression and modulates

antagonistic interaction between salicylic acid and jasmonic acid signaling', *Plant Journal*, 73: 483-95.
Shin, S., J. A. Torres-Acosta, S. J. Heinen, S. McCormick, M. Lemmens, M. P. K. Paris, F. Berthiller, G. Adam, and G. J. Muehlbauer. 2012. 'Transgenic Arabidopsis thaliana expressing a barley UDP-glucosyltransferase exhibit resistance to the mycotoxin deoxynivalenol', *Journal of Experimental Botany*, 63: 4731-40.
Skinnes, H., K. Semagn, Y. Tarkegne, A. G. Maroy, and A. Bjornstad. 2010. 'The inheritance of anther extrusion in hexaploid wheat and its relationship to Fusarium head blight resistance and deoxynivalenol content', *Plant Breeding*, 129: 149-55.
Skou, J.P. 1975. 'Development and regeneration of roots in cereal species during the attack.', *Studies on the Take-All Fungus Gaeumannomyces graminis*: 142–60.
———. 1981. 'Morphology and cytology of the infection process.' in P.J. Shipton M.J.C. Asher (ed.), *Biology and Control of Take-all* (Academic Press: London).
Smiley, R. W., J. A. Gourlie, S. A. Easley, and L. M. Patterson. 2005. 'Pathogenicity of fungi associated with the wheat crown rot complex in oregon and Washington', *Plant Disease*, 89: 949-57.
Spoel, S. H., and X. N. Dong. 2012. 'How do plants achieve immunity? Defence without specialized immune cells', *Nature Reviews Immunology*, 12: 89-100.
Srinivasachary, N. Gosman, A. Steed, T. W. Hollins, R. Bayles, P. Jennings, and P. Nicholson. 2009. 'Semi-dwarfing Rht-B1 and Rht-D1 loci of wheat differ significantly in their influence on resistance to Fusarium head blight', *Theoretical and Applied Genetics*, 118: 695-702.
Srinivasachary, N. Gosman, A. Steed, J. Simmonds, M. Leverington-Waite, Y. Wang, J. Snape, and P. Nicholson. 2008. 'Susceptibility to Fusarium head blight is associated with the Rht-D1b semi-dwarfing allele in wheat', *Theoretical and Applied Genetics*, 116: 1145-53.
Stark, R., M. Grzelak, and J. Hadfield. 2019. 'RNA sequencing: the teenage years', *Nat Rev Genet*, 20: 631-56.
Steiner, B., M. Buerstmayr, C. Wagner, A. Danler, B. Eshonkulov, M. Ehn, and H. Buerstmayr. 2019. 'Fine-mapping of the Fusarium head blight resistance QTL Qfhs.ifa-5A identifies two resistance QTL associated with anther extrusion', *Theoretical and Applied Genetics*, 132: 2039-53.
Su, Jun, Jiaojie Zhao, Shuqing Zhao, Mengyu Li, Shuyong Pang, Shisheng Chen, Feng Chen, Wenchao Zhen, Zhensheng Kang, and Xiaodong Wang. 2021. 'Genetics of resistance to common root rot (spot blotch), Fusarium crown rot, and sharp eyespot in wheat', *bioRxiv*: 2020.07.30.228932.
Su, Z. Q., A. Bernardo, B. Tian, H. Chen, S. Wang, H. X. Ma, S. B. Cai, D. T. Liu, D. D. Zhang, T. Li, H. Trick, P. St Amand, J. M. Yu, Z. Y. Zhang, and G. H. Bai. 2019. 'A deletion mutation in TaHRC confers Fhb1 resistance to Fusarium head blight in wheat', *Nature Genetics*, 51: 1099-+.
Suzuki, N., S. Bajad, J. Shuman, V. Shulaev, and R. Mittler. 2008. 'The transcriptional co-activator MBF1c is a key regulator of thermotolerance in Arabidopsis thaliana', *Journal of Biological Chemistry*, 283: 9269-75.
Suzuki, N., L. Rizhsky, H. J. Liang, J. Shuman, V. Shulaev, and R. Mittler. 2005. 'Enhanced tolerance to environmental stress in transgenic plants expressing the transcriptional coactivator multiprotein bridging factor 1c', *Plant Physiology*, 139: 1313-22.
Suzuki, N., H. Sejima, R. Tam, K. Schlauch, and R. Mittler. 2011. 'Identification of the MBF1 heat-response regulon of Arabidopsis thaliana', *Plant Journal*, 66: 844-51.
Thapa, G., L. R. Gunupuru, J. G. Hehir, A. Kahla, E. Mullins, and F. M. Doohan. 2018. 'A Pathogen-Responsive Leucine Rich Receptor Like Kinase Contributes to Fusarium Resistance in Cereals', *Frontiers in Plant Science*, 9.
Thole, V., A. Peraldi, B. Worland, P. Nicholson, J. H. Doonan, and P. Vain. 2012. 'T-DNA mutagenesis in Brachypodium distachyon', *Journal of Experimental Botany*, 63: 567-76.

Thomma, B. P. H. J., K. Eggermont, I. A. M. A. Penninckx, B. Mauch-Mani, R. Vogelsang, B. P. A. Cammue, and W. F. Broekaert. 1998. 'Separate jasmonate-dependent and salicylate-dependent defense-response pathways in Arabidopsis are essential for resistance to distinct microbial pathogens', *Proceedings of the National Academy of Sciences of the United States of America*, 95: 15107-11.

Tolley, Jordan P., Yukihiro Nagashima, Zachary Gorman, Michael V. Kolomiets, and Hisashi Koiwa. 2018. 'Isoform-specific subcellular localization of Zea mays lipoxygenases and oxo-phytodienoate reductase 2', *Plant Gene*, 13: 36-41.

Trail, F. 2009. 'For Blighted Waves of Grain: Fusarium graminearum in the Postgenomics Era', *Plant Physiology*, 149: 103-10.

Tsuda, K., and K. Yamazaki. 2004. 'Structure and expression analysis of three subtypes of Arabidopsis MBF1 genes', *Biochimica Et Biophysica Acta-Gene Structure and Expression*, 1680: 1-10.

Tsukagoshi, H., W. Busch, and P. N. Benfey. 2010. 'Transcriptional Regulation of ROS Controls Transition from Proliferation to Differentiation in the Root', *Cell*, 143: 606-16.

Tufan, F., C. Ucarli, B. Tunali, and F. Gurel. 2017. 'Analysis of early events in barley (Hordeum vulgare L.) roots in response to Fusarium culmorum infection', *European Journal of Plant Pathology*, 148: 343-55.

Ueno, Y. 1985. 'The toxicology of mycotoxins', *Crit Rev Toxicol*, 14: 99-132.

Ueno, Y., K. Ishii, N. Sato, N. Shimada, H. Tsunoda, M. Sawano, and M. Enomoto. 1973. 'Screening of Trichothecene-Producing Fungi and Comparative Toxicity of Isolated Mycotoxins', *Japanese Journal of Pharmacology*, 23: 133-33.

US FDA, US Food and Drug Administration. 2010. "Guidance for industry and FDA: advisory levels for Deoxynivalenol (DON) in finished wheat products for human consumption and grains and grain by-products used for animal feed." In. Washington, DC.

Vain, P., B. Worland, V. Thole, N. McKenzie, S. C. Alves, M. Opanowicz, L. J. Fish, M. W. Bevan, and J. W. Snape. 2008. 'Agrobacterium-mediated transformation of the temperate grass Brachypodium distachyon (genotype Bd21) for T-DNA insertional mutagenesis (vol 6, pg 236, 2008)', *Plant Biotechnology Journal*, 6: 941-41.

Vellosillo, T., M. Martinez, M. A. Lopez, J. Vicente, T. Cascon, L. Dolan, M. Hamberg, and C. Castresana. 2007. 'Oxylipins produced by the 9-lipoxygenase pathway in Arabidopsis regulate lateral root development and defense responses through a specific signaling cascade', *Plant Cell*, 19: 831-46.

Vergne, E., X. Grand, E. Ballini, V. Chalvon, P. Saindrenan, D. Tharreau, J. L. Notteghem, and J. B. Morel. 2010. 'Preformed expression of defense is a hallmark of partial resistance to rice blast fungal pathogen Magnaporthe oryzae', *Bmc Plant Biology*, 10.

Vicente, J., T. Cascon, B. Vicedo, P. Garcia-Agustin, M. Hamberg, and C. Castresana. 2012. 'Role of 9-Lipoxygenase and alpha-Dioxygenase Oxylipin Pathways as Modulators of Local and Systemic Defense', *Molecular Plant*, 5: 914-28.

Voothuluru, P., P. Makela, J. M. Zhu, M. Yamaguchi, I. J. Cho, M. J. Oliver, J. Simmonds, and R. E. Sharp. 2020. 'Apoplastic Hydrogen Peroxide in the Growth Zone of the Maize Primary Root. Increased Levels Differentially Modulate Root Elongation Under Well-Watered and Water-Stressed Conditions', *Frontiers in Plant Science*, 11.

Wahibah, N. N., T. Tsutsup, D. Tamaoki, K. Sato, and T. Nishiuchi. 2018. 'Expression of barley Glutathione S-Transferase13 gene reduces accumulation of reactive oxygen species by trichothecenes and paraquat in Arabidopsis plants', *Plant Biotechnology*, 35: 71-79.

Walter, S., J. M. Brennan, C. Arunachalam, K. I. Ansari, X. J. Hu, M. R. Khan, F. Trognitz, B. Trognitz, G. Leonard, D. Egan, and F. M. Doohan. 2008. 'Components of the gene network associated with genotype-dependent response of wheat to the Fusarium mycotoxin deoxynivalenol', *Functional & Integrative Genomics*, 8: 421-27.

Walter, S., and F. Doohan. 2011. 'Transcript profiling of the phytotoxic response of wheat to the Fusarium mycotoxin deoxynivalenol', *Mycotoxin Res*, 27: 221-30.

Walter, S., A. Kahla, C. Arunachalam, A. Perochon, M. R. Khan, S. R. Scofield, and F. M. Doohan. 2015. 'A wheat ABC transporter contributes to both grain formation and mycotoxin tolerance', *Journal of Experimental Botany*, 66: 2583-93.

Walter, S., P. Nicholson, and F. M. Doohan. 2010. 'Action and reaction of host and pathogen during Fusarium head blight disease', *New Phytologist*, 185: 54-66.
Wang, Jiao-yu, Xiao-yan Wang, Ling Li, Xin Zhang, Yan-li Wang, Rong-yao Chai, and Guo-chang Sun. 2012. 'Pathogenicity of Rice Blast Fungus Magnaporthe oryzae on Brachypodium distachyon', *Rice Science*, 19: 252-58.
Wang, Q., S. V. Buxa, A. Furch, W. Friedt, and S. Gottwald. 2015. 'Insights Into Triticum aestivum Seedling Root Rot Caused by Fusarium graminearum', *Molecular Plant-Microbe Interactions*, 28: 1288-303.
Wang, S. L., K. Wang, G. X. Chen, D. W. Lv, X. F. Han, Z. T. Yu, X. H. Li, X. G. Ye, S. L. K. Hsam, W. J. Ma, R. Appels, and Y. M. Yan. 2012. 'Molecular characterization of LMW-GS genes in Brachypodium distachyon L. reveals highly conserved Glu-3 loci in Triticum and related species', *Bmc Plant Biology*, 12.
Wang, Z., M. Gerstein, and M. Snyder. 2009. 'RNA-Seq: a revolutionary tool for transcriptomics', *Nat Rev Genet*, 10: 57-63.
Wasternack, C., and B. Hause. 2013. 'Jasmonates: biosynthesis, perception, signal transduction and action in plant stress response, growth and development. An update to the 2007 review in Annals of Botany', *Annals of Botany*, 111: 1021-58.
Wei, C. M., I. M. Campbell, C. S. Mclaughlin, and M. H. Vaughan. 1974. 'Binding of Trichodermin to Mammalian Ribosomes and Its Inhibition by Other 12,13-Epoxytrichothecenes', *Molecular and Cellular Biochemistry*, 3: 215-19.
Weller, D. M., B. B. Landa, O. V. Mavrodi, K. L. Schroeder, L. De La Fuente, S. B. Bankhead, R. A. Molar, R. F. Bonsall, D. V. Mavrodi, and L. S. Thomashow. 2007. 'Role of 2,4-diacetylphloroglucinol-producing fluorescent Pseudomonas spp. in the defense of plant roots', *Plant Biology*, 9: 4-20.
West, A. H., and A. M. Stock. 2001. 'Histidine kinases and response regulator proteins in two-component signaling systems', *Trends in Biochemical Sciences*, 26: 369-76.
Wilkes, M. A., D. R. Marshall, and L. Copeland. 1999. 'Hydroxamic acids in cereal roots inhibit the growth of take-all', *Soil Biology & Biochemistry*, 31: 1831-36.
Winter, M., P. L. Samuels, L. K. Otto-Hanson, R. Dill-Macky, and L. L. Kinkel. 2019. 'Biological Control of Fusarium Crown and Root Rot of Wheat by Streptomyces Isolates It's Complicated', *Phytobiomes Journal*, 3: 52-60.
Woods, D., Y. X. Dong, F. Bouche, R. Bednarek, M. Rowe, T. Ream, and R. Amasino. 2019. 'A florigen paralog is required for short-day vernalization in a pooid grass', *Elife*, 8.
Yan, C., and D. X. Xie. 2015. 'Jasmonate in plant defence: sentinel or double agent?', *Plant Biotechnology Journal*, 13: 1233-40.
Yang, H., D. H. Chung, Y. B. Kim, Y. H. Choi, and Y. Moon. 2008. 'Ribotoxic mycotoxin deoxynivalenol induces G(2)/M cell cycle arrest via P21(Cip/WAF1) mRNA stabilization in human epithelial cells', *Toxicology*, 243: 145-54.
Yang, Z. P., J. Gilbert, G. Fedak, and D. J. Somers. 2005. 'Genetic characterization of QTL associated with resistance to Fusarium head blight in a doubled-haploid spring wheat population', *Genome*, 48: 187-96.
Yildirim, A., S. S. Jones, T. D. Murray, and R. F. Line. 2000. 'Evaluation of Dasypyrum villosum populations for resistance to cereal eyespot and stripe rust pathogens', *Plant Disease*, 84: 40-44.
Yu, Y.J. 1990. 'Genetic analysis for scab resistance in four wheat cultivars PHJZM, HHDTB, CYHM and YGFZ.' in L.-H. Zhu (ed.), *Advances in Researches on Inheritance to Diseases in Major Crops* (Jiangsu Sci-Tech. Pulishing House.: Nanjing, China).
Yu, Yu-Jun. 1982. 'Monosomic Analysis for Scab Resistance and Yield Components in the Wheat Cultivar Soo-mo 3', *Cereal Research Communications*, 10: 185-89.
Zhang, J., H. Yan, M. Xia, X. Han, L. Xie, P. H. Goodwin, X. Quan, R. Sun, C. Wu, and L. Yang. 2020. 'Wheat root transcriptional responses against *Gaeumannomyces graminis* var. *tritici*.', *Phytopathol Res*, 2: 23.
Zhang, M., R. Zhang, J. Z. Yang, and P. G. Luo. 2010. 'Identification of a new QTL for Fusarium head blight resistance in the wheat genotype "Wang shui-bai"', *Molecular Biology Reports*, 37: 1031-35.

Zhou, H. R., Q. S. Jia, and J. J. Pestka. 2005. 'Ribotoxic stress response to the trichothecene deoxynivalenol in the macrophage involves the Src family kinase Hck', *Toxicological Sciences*, 85: 916-26.

Zhou, H. R., A. S. Lau, and J. J. Pestka. 2003. 'Role of double-stranded RNA-activated protein kinase R (PKR) in deoxynivalenol-induced ribotoxic stress response', *Toxicological Sciences*, 74: 335-44.

Zhou, W. C., F. L. Kolb, G. H. Bai, L. L. Domier, L. K. Boze, and N. J. Smith. 2003. 'Validation of a major QTL for scab resistance with SSR markers and use of marker-assisted selection in wheat', *Plant Breeding*, 122: 40-46.

Zhou, W. C., F. L. Kolb, J. B. Yu, G. H. Bai, L. K. Boze, and L. L. Domier. 2004. 'Molecular characterization of Fusarium head blight resistance in Wangshuibai with simple sequence repeat and amplified fragment length polymorphism markers', *Genome*, 47: 1137-43.

Zhu, T., L. Wang, H. Rimbert, J. C. Rodriguez, K. R. Deal, R. De Oliveira, F. Choulet, G. Keeble-Gagnere, J. Tibbits, J. Rogers, K. Eversole, R. Appels, Y. Q. Gu, M. Mascher, J. Dvorak, and M. C. Luo. 2021. 'Optical maps refine the bread wheat Triticum aestivum cv Chinese Spring genome assembly', *Plant J*.

Zhu, X. L., C. G. Lu, L. P. Du, X. G. Ye, X. Liu, A. Coules, and Z. Y. Zhang. 2017. 'The wheat NB-LRR gene TaRCR1 is required for host defence response to the necrotrophic fungal pathogen Rhizoctonia cerealis', *Plant Biotechnology Journal*, 15: 674-87.

Zuo, D. Y., S. Y. Yi, R. J. Liu, B. Qu, T. Huang, W. J. He, C. Li, H. P. Li, and Y. C. Liao. 2016. 'A Deoxynivalenol-Activated Methionyl-tRNA Synthetase Gene from Wheat Encodes a Nuclear Localized Protein and Protects Plants Against Fusarium Pathogens and Mycotoxins', *Phytopathology*, 106: 614-23.